Faculdade de Engenharia da Universidade do Porto

Biofilm control approaches: alternative biocides and shear stress

Doctoral Program in Chemical and Biological Engineering

Madalena Barbosa Pereira de Lemos

Supervisor: Professor Manuel Simões (Universidade do Porto)

Co-advisors: Professor Luís de Melo (Universidade do Porto)

Professor Ian Wilson (University of Cambridge)

2016

FCT Fundação para a Ciência e a Tecnologia
MINISTÉRIO DA EDUCAÇÃO E CIÊNCIA

GOVERNO DA REPÚBLICA PORTUGUESA
UNIÃO EUROPEIA Fundo Social Europeu
QREN QUADRO DE REFERÊNCIA ESTRATÉGICO NACIONAL
COMPETE PROGRAMA OPERACIONAL FACTORES DE COMPETITIVIDADE
POPH

“If I have seen further it is by standing on the shoulders of giants.”

Isaac Newton, letter to Robert Hooke, 1676

Acknowledgements

This thesis could not be accomplished without the help of some important persons that I would like to acknowledge:

First and foremost I would like to thank Dr Manuel Simões, my main supervisor, for his patience, motivation, and immense knowledge. Most of all, I am grateful for his support and guidance, as he always had a kind word to help and comfort me. He was a fundamental mentor throughout all this work.

I want to express my gratitude to Prof Luís de Melo who was an inspiration and a great example. I am very glad I had his invaluable contributions to my work. His insightful comments and encouragements were very important for my motivation during all the time of research and writing of this thesis.

I would like to express my appreciation to Prof Ian Wilson for receiving me and supervising me at the University of Cambridge. I was extremely lucky for the time, knowledge and opportunities he offered me. I lived memorable times both academically and personally in Cambridge, and that was only possible with his help. I will never forget his generosity, friendship and support.

I am truly grateful to my 'giant' supervisors, for sharing their knowledge with me and for guiding me on this journey.

A word of appreciation for Dr Filipe Mergulhão for his helpful contribution and for Dr Nuno Azevedo, as they always gave me valuable comments and encouragement. Equally, to Dr Bart Hallmark, a big thank you for the cheering words and for the help with some of the computational fluid dynamics work.

This work was supported by Programa Operacional Factores de Competitividade – COMPETE and by FCT – Fundação para a Ciência e Tecnologia de Portugal through my PhD grant (SFRH/BD/79396/2011) and through the Project UID/EQU/00511/2013-LEPABE (Laboratory for Process Engineering, Environment, Biotechnology and Energy – EQU/00511) by FEDER funds through Programa Operacional Competitividade e Internacionalização – COMPETE2020.

I also want to thank the Faculty of Engineering of University of Porto, especially the LEPABE - Laboratory for Process Engineering, Environment, Biotechnology and Energy, for

providing excellent working conditions. I am equally grateful to the Department of Chemical Engineering and Biotechnology (CEB) of the University of Cambridge for welcoming me within the Paste, Particle and Polymer Processing group (P^4G) and for the possibility to develop my work in their excellent facilities.

I want to express my appreciation to the administrative and technical staff from FEUP and from the University of Cambridge that always helped me whenever I needed. Thanks to Sílvia Faia and Paula Pinheiro for their assistance and sympathy. I must leave a special note of gratitude to Gary Chapman, Lee Pratt and Andy Hubbard, my friends from the workshop at CEB, for the long hours of constructions, brainstorming, therapy and friendship.

A big thank you to all the colleagues that were and are a part of the 007lab, former 303, for all the great times. I learned a great deal with them and their help was fundamental for this work, especially from Carla Ferreira, Anabela, Ana Luísa and Catarina. Equally my aM1gos in Cambridge were vital for me, all of them. The times spent at the M1 were wonderful and I will always carry those memories with great love. For all the great work we did and fun moments we had, I want to thank Shiyao Wang, my 'partner in business', co-author and great friend.

To my friends that supported through this journey, my warmest gratitude and love. We lived a lot together throughout these years, some of us scattered around the world. But it was in the moments when we were together that it was all worth it. Thank you all for being there for me.

Finally, I am very grateful to my family for their love, help and care. I want to dedicate this work to my parents, my sister and to Vóvó Dina.

You are my safe harbour and I own what I am to you.

Abstract

Biofouling is a costly challenge for many industries as it causes major losses in energy, equipment damage, compromises the product quality and can even lead to unscheduled downtime. Biofilms are also potential harbours for pathogenic microorganisms and can represent a threat to public health due to the dissemination of infectious agents. The biofilm's complex physical structure and resistance to antimicrobials reduces the efficacy of the contemporary cleaning processes and justifies the need for novel control strategies, more efficient and sustainable.

The global objective for this work was to study the behaviour of *Bacillus cereus* and *Pseudomonas fluorescens* biofilms when exposed to chemical and mechanical control strategies.

Initial screening tests were performed with selected phytochemicals, ferulic (FA) and salicylic acids (SA), alone and in combination (FSA), as their antimicrobial properties and sustainable sources could present a promising alternative to conventional chemicals used for cleaning and disinfection. Prevention tests showed that the *B. cereus* and *P. fluorescens* single and dual-species biofilms were able to grow in the presence of the phytochemicals. Nevertheless, dual-species biofilms formed in the presence of the phytochemicals were highly susceptible to a second exposure. Their minimum inhibitory concentration (MIC) was 500 µg/mL for both bacterial species. The biocide benzyldimethyldodecyl ammonium chloride (BDMDAC) was also used in this stage as a positive control. BDMDAC's MIC for *B. cereus* was 5 µg/mL and 15 µg/mL for *P. fluorescens.* Due to its high efficiency compared to the phytochemicals, BDMDAC was selected for further studies.

B. cereus and *P. fluorescens* mature biofilms (single and dual-species) were formed on a rotating cylinder reactor (RCR), which provided mild shear stress conditions similar to those found on industrial settings. The effects of the substratum type on biofilm formation and control with BDMDAC and hydrodynamic stress were assessed. The biofilms were formed on AISI316 stainless steel (SS) and polymethyl methacrylate (PMMA), and presented distinct phenotypical characteristics (mass, cell density and content of matrix proteins and polysaccharides), both dependent on the microorganism and the adhesion surface. After exposure to BDMDAC and to hydrodynamic stress, alone and combined, *P. fluorescens* biofilms were the most resistant to removal. The biofilms were more easily cleaned from SS surfaces, however, biofilm-free surfaces were not obtained even after the combined chemical and hydrodynamic treatments.

In the case of *B. cereus* biofilms formed on SS surfaces, the influence of the hydrodynamic conditions on its susceptibility to removal when exposed to chemical and mechanical stresses was also investigated. The biofilm volumetric density increased significantly with the shear stress while the thickness decreased. Biofilms formed under low shear stress were more resistant to treatment with BDMDAC whereas those formed under higher shear stress were more resistant to the combination of the biocide with high shear stress (up to 22.84 Pa).

B. cereus and *P. fluorescens* biofilms were also formed on high-density-polyethylene (HDPE) to ascertain their resistance to removal due to BDMDAC combined with increasing shear stress pulses. Dual-species biofilms, which were the thickest, were the most affected by the BDMDAC exposure. *P. fluorescens* biofilms were the most resistant to shear stress (up to 17.7 Pa) even after treatment with BDMDAC. The results suggested a stratification of the biofilm based on its mechanical stability, with detachment observed when low shear stress (1.46 Pa) was applied followed by apparent compression caused by higher shear stress (> 1.46 Pa).

Due to the lack of available equipment for *in situ* and in real time biofilm monitoring without compromising its physical structure, a cylindrical zero-discharge Fluid Dynamic Gauging (czFDG) was created. This device was designed to measure the thickness and the shear stress needed to remove the biofilms formed on cylindrical surfaces in aseptic conditions. The device was designed and commissioned at the University of Cambridge, and computational fluid dynamics simulations were performed, which agree well with the calibrations tests. *P. fluorescens* biofilms formed on HDPE and SS cylinders using the RCR were analysed with this device that allows local measurements (12 different points) and therefore an approximation of the topography of the biofilm. The biofilms formed on HDPE were thicker than those formed on SS, however, the biofilm thickness for both materials was not uniform, ranging from effectively zero to 300 µm.

Resumo

O *biofouling* é um problema dispendioso para muitas indústrias, uma vez que provoca grandes perdas de energia, causa danos nos equipamentos, deterioração da qualidade do produto final e pode até levar a paragens não programadas. Os biofilmes são também potenciais focos de microrganismos patogénicos e podem representar uma ameaça para a saúde pública devido à disseminação de agentes infeciosos. A estrutura física complexa do biofilme e a resistência a agentes antimicrobianos reduz a eficácia dos processos de limpeza atuais e justifica a necessidade de novas estratégias de controlo, mais eficientes e sustentáveis.

O objetivo global para este trabalho foi estudar o comportamento de biofilmes de *Bacillus cereus* e *Pseudomonas fluorescens* quando expostos a métodos de limpeza e desinfeção, particularmente com exposição a agentes químicos e a condições de stress hidrodinâmico.

Dois novos biocidas, ácidos ferrúlico (FA) e salicílico (AS), conhecidos como produtos secundários do metabolismo de plantas (fitoquímicos) foram testados no controlo do crescimento bacteriano planctónico e em biofilme. Esses biocidas foram testados individualmente e em combinação (FSA) pois têm a vantagem de serem obtidos de forma sustentável e poderiam apresentar uma alternativa promissora aos produtos químicos convencionais utilizados para o controlo dos biofilmes. Os testes de prevenção mostraram que os biofilmes simples e mistos de *B. cereus* e *P. fluorescens* foram capazes de crescer na presença dos produtos fitoquímicos. No entanto, os biofilmes mistos formados na presença desses produtos demonstraram suscetibilidade significativa a uma segunda exposição. A concentração mínima inibitória (MIC) de FA e SA foi de 500 µg/mL para ambas as espécies. O biocida cloreto de benzil-dimetil-dodecil-amónio (BDMDAC) foi usado como controlo positivo, tendo uma MIC de 5 µg/mL para *B. cereus* e de 15 µg/mL para *P. fluorescens*. Dado que o biocida BDMDAC demonstrou uma ação antimicrobiana substancialmente superior aos produtos fitoquímicos, este foi selecionado para ensaios posteriores de controlo de biofilmes.

Biofilmes simples e mistos de *B. cereus* e *P. fluorescens* foram formados num reator de cilindros rotativos, que proporcionou condições com tensões de corte baixas, semelhantes às encontradas em determinados ambientes industriais. Inicialmente foi avaliado o efeito do tipo de superfície de adesão na formação de biofilmes e na sua suscetibilidade ao BDMDAC e à exposição a tensões de corte superiores à usada para formar o biofilme. Os biofilmes foram formados em aço inoxidável AISI316 (SS) e polimetil-metacrilato (PMMA), e apresentaram caraterísticas fenotípicas distintas (massa, densidade celular e quantidade de proteínas e polissacarídeos na matriz), dependentes do microrganismo e da superfície de adesão. Os

biofilmes de *P. fluorescens* foram mais resistentes à remoção por exposição ao BDMDAC e ao stresse hidrodinâmico (tratamentos individuais e combinados). Os biofilmes foram mais facilmente removidos de superfícies de SS, porém não se obtiveram superfícies livres de biofilme, nem mesmo após a combinação do BDMDAC e da ação mecânica.

Também foi investigada a influência das condições hidrodinâmicas (0.20, 1.46 e 2.14 Pa) na formação de biofilmes de *B. cereus* em SS e na sua suscetibilidade a tratamentos químicos e mecânicos. A formação de biofilmes em condições de tensão de corte mais elevadas originou biofilmes com maior densidade volumétrica e menor espessura. Os biofilmes formados a baixas tensões de corte foram os mais resistentes ao tratamento com BDMDAC, enquanto que aqueles formados a tensões de corte mais altas foram os mais resistentes à combinação do biocida com a exposição a tensões de corte significativamente mais altas do que as usadas na sua formação (até 22,84 Pa).

Biofilmes simples e mistos de *B. cereus* e *P. fluorescens* formados em polietileno de elevada densidade (HDPE) foram utilizados para estudar a sua estabilidade mecânica numa estratégia de remoção baseada no tratamento com BDMDAC combinado com pulsos de tensão de corte crescente. Os biofilmes mistos, que foram os mais espessos, foram os mais afetados pela ação do BDMDAC. Os biofilmes de *P. fluorescens* foram os mais resistentes à exposição ao tratamento hidrodinâmico (até 17.7 Pa), mesmo após a prévia exposição ao BDMDAC. Os resultados sugeriram uma estratificação do biofilme, de acordo com a sua estabilidade mecânica, com remoção de camadas superficiais a ocorrer a baixa tensão de corte (1.46 Pa), ocorrendo compressão das camadas basais quando expostas a tensão de corte > 1.46 Pa.

Dada a inexistência de equipamentos que permitam a monitorização de biofilmes *in situ* e em tempo real, sem comprometer a sua estrutura física, foi desenvolvido o *cylindrical zero-discharge Fluid Dynamic Gauging* (czFDG). O czFDG foi concebido com a finalidade de medir a espessura e tensão de corte necessária para a remoção dos biofilmes formados em superfícies curvas e em condições de assepsia. O dispositivo foi projetado e testado na Universidade de Cambridge. Foram realizadas simulações de dinâmica de fluidos computacional que demonstraram concordância com os testes de calibração. Biofilmes de *P. fluorescens* formados no RCR em cilindros de HDPE e SS foram analisados com o czFDG, que permitiu fazer medições em 12 pontos diferentes, obtendo-se assim uma aproximação da topografia do biofilme. Os resultados demonstraram que os biofilmes formados em HDPE eram mais espessos do que os formadas em SS, no entanto, a espessura do biofilme para ambos os materiais não era uniforme, variando entre zero e 300 µm.

Contents

List of Figures

List of Tables

Nomenclature

Roman

a	arc length (m)
C_d	discharge coefficient (-)
D	dilution rate (1/s)
$\mathrm{D_a}$	diameter of the cylinder
d	inner diameter of dynamic gauging tube (m)
d_t	nozzle throat diameter (m)
$\Delta \mathrm{G_{1w1}}$	free energy of interaction between two entities of that material (1), when immersed in water (w) (mJ/m^2)
$\Delta \mathrm{G_{1w2}^{Tot}}$	Free energy of adhesion between surface 1 (bacterium) and 2 (substratum) that are immersed or dissolved in water (mJ/m^2)
f	Fanning friction factor (-)
h	clearance between nozzle and gauging surface (m)
h_0	clearance between nozzle and gauging surface (m)
$\dot{m}$	tube discharge mass flow rate (kg/s)
$\mathbf{n}$	normal vector of the relevant plane (-)
N	rotation speed (Hz)
N_e	number of mesh elements (-)
p_i	pressure (Pa)
ΔP	pressure drop (Pa)
Q	volumetric flow rate (m^3/s)
r	radial co-ordinate (m)
Re_A	Reynolds number of agitation (-)
Re_t	Reynolds number at the throat of the nozzle (-)
s	lip width (m)
u_m	mean bulk velocity (m/s)
V	volume of the reactor (m^3)
$\mathbf{v}$	velocity vector (m/s)
v	velocity (m/s)
v_max	centreline velocity (m/s)
v_y	velocity in *y* direction (m/s)
v_z	velocity in *z* direction (m/s)
x	horizontal coordinate (m)
X_biofilm	wet mass of the biofilm (kg)
y	vertical coordinate

Greek

α	Internal divergent angle (˚)
γ^{LW}	Lifshitz-van der Waals component of the surface free energy (mJ/m^2)
γ^{AB}	Lewis acid-base component of the surface free energy (mJ/m^2)
γ^{+}	electron acceptor parameter of γ^{AB} (mJ/m^2)
γ^{-}	electron donor parameter of γ^{AB} (mJ/m^2)
δ	thickness of measured layer (m)
ζ	zeta potential (mV)
Θ	nozzle angle (–)
λ	nozzle entry length (m)
μ	fluid viscosity (Pa s)
ρ	fluid density (kg/m^3)
τ_w	wall shear stress (Pa)
τ_{rz}	wall shear stress on *x*-plane in the *y*-direction (Pa)
$\tau_{\mathrm{r\theta}}$	wall shear stress on *x*-plane in the *a*-direction (Pa)
Ψ	contact angles of the liquid with the surface (˚)

Acronyms

16S rRNA	16S ribosomal ribonucleic acid
AISI	American Iron and Steel Institute
APHA	American Public Health Association
ATCC	American Type Culture Collection
ATR	attenuated total reflectance
AWWA	American Water Works Association
BAC	benzalkonium chloride
BCDDMH	bromo-chloro-dimethyl-hydantoin
BDMDAC	benzyldimethyldodecyl ammonium chloride
CCR	concentric cylinder reactor
CCTR	conical Couette-Taylor reactor
CDC	Centre for Disease Control and Prevention
CFD	computational fluid dynamics
CFSTR	continuous flow stirred tank reactor
CFU	colony forming units
CIP	cleaning-in-place
CLSM	confocal laser scanning microscopy
CNM	concentrated nutrient medium

CPC	cetylpyridinium chloride
CTAB	cetrimonium bromide (CTAB)
CTC	5-cyano-2,3-di-4-tolyl-tetrazolium chloride
czFDG	cylindrical zero-discharge fluid dynamic gauging
DAPI	4`, 6–diamidino–2–phenylindole
DMSO	dimethyl sulfoxide
DNM	diluted nutrient medium
EPS	extracellular polymeric substance
FA	ferulic acid
FDG	fluid dynamic gauging
FEM	finite element method
FSA	combination (1:1) of FA and SA
FTIR	Fourier transform infrared spectroscopy
GTA	glutaraldehyde
HAI	healthcare-associated infection
HDPE	high density polyethylene
LB	lysogeny broth
MBEC	minimal biofilm eradication concentration
MDD	modified Robbins device
MIC	minimum inhibitory concentration
NMR	nuclear magnetic resonance
OD_{610}	optical density measured at 610 nm
OPA	*o*-phthalaldehyde
OPP	*o*-phenylphenol
PAA	peracetic acid
PB	phosphate buffer
PCMC	4-chloro-3-methylphenol
PCMX	4-chloro-3,5-dimethylphenol
PE	polyethylene
PEX	cross-linked polyethylene
PFR	plug flow reactor
PMMA	poly(methyl methacrylate)
PP	polypropylene
PS	polystyrene
PSU	polyesterurethane
PTAP	4-(2-methylbutyl)phenol
PTFE	polytetrafluoroethylene (teflon)
QAC	quaternary ammonium compounds

QSI	quorum sensing inhibition
RAR	rotating annular reactor
RCR	rotating cylinder reactor
RDR	rotating disc biofilm reactor
SA	salicylic acid
SDS	sodium dodecyl sulphate
SEM	scanning electron microscopy
SGR	specific growth rate (1/s)
TSV	total volatile solids
WPCF	Water Pollution Control Federation

Chapter 1

Objectives and work outline

1. Objectives and work outline

Biofouling in industrial systems is an undesirable consequence of processing aqueous chemical and biological liquids. In the food industry, biofilms can be a critical source of recalcitrant contamination, causing food spoilage and public health problems due to the spread of foodborne pathogens. Moreover, it is known that biofilm formation in drinking water distribution systems is common even with the implementation of preventive measures, such as the continuous presence of a disinfectant residual. These complex structures present resistance mechanisms to antimicrobials that render the current disinfection practices ineffective. This inherent resistance of biofilms is related to their phenotypes. Hence, one goal of this work was to understand some of the phenomena responsible for biofilm resistance to biocides, through the study of alterations in some of their phenotypic aspects under diverse conditions. As it will be discussed in detail, effective strategies for biofilm control must be holistic in the sense that there are many factors that can affect the development of those structures. Chemical and mechanical treatments were selected for this work as it is not possible to study all available strategies in detail. It was also a goal of this study to present results regarding the mechanical stability of mature biofilms after those chemical and mechanical treatments.

This work constitutes one output of the research project *Bioresist - The influence of biofilm phenotype on its resilience and resistance* (PTDC/EBB-EBI/105085/2008). It was also supported by a PhD grant awarded to the author (SFRH/BD/79396/2011). Both were funded by the Operational Programme for Competitiveness Factors – COMPETE and by the Fundação para a Ciência e a Tecnologia (FCT).

This chapter presents the main objectives and context for this work, as well as a brief description of the tasks and milestones.

The projected research path had the following objectives:

a) Assessment of the most suitable antimicrobials to control bacteria in different states
b) Characterization of single and dual-species biofilms, formed in a rotating cylinder reactor (RCR) under diverse conditions similar to those found in real systems
c) Biofilms treatment with a selected antimicrobial in order to assess their mechanical stability after chemical exposure.

d) Real-time measurement of biofilm response to the selected antimicrobial in a rotating bioreactor and simulation of results to link to (c).

The experimental work started in the facilities of the LEPABE - Laboratory for Process Engineering, Environment, Biotechnology and Energy, at the Department of Chemical Engineering of the Faculty of Engineering of the University of Porto. Tests were performed regarding objective a), through screening of selected phytochemicals (ferulic and salicylic acids) for their antimicrobial activity against *B. cereus* and *P. fluorescens*, two contaminant microorganisms of concern in the food industry. The effectiveness of ferulic and salicylic acids on the control of *B. cereus* and *P. fluorescens* biofilms was tested. The results showed that application of these phytochemicals to *B. cereus* and *P. fluorescens* biofilms caused low to moderate inactivation and removal. Objective a) was then considered closed; for further studies preference was given to another biocide – benzyldimethyldodecyl ammonium chloride (BDMDAC) due to its high antimicrobial activity. The work of objectives b) and c), was developed at LEPABE, and included much work regarding the improvement and commissioning of the RCR. The RCR allowed single and dual-species biofilms of *B. cereus* and *P. fluorescens* to be formed under different environmental conditions; these were then subjected to the chemical and mechanical treatments.

The work concerning objective d) was performed at the laboratory of the Paste, Particle and Polymer Processing group (P^4G) at the Department of Chemical Engineering and Biotechnology of the University of Cambridge. This stage evolved commissioning a new fluid dynamic gauging (FDG) probe specially built for this purpose: the cylindrical zero-discharge FDG (czFDG), as well as additional refurbishing of the RCR, as the two tools were meant to be used together. After a time-consuming process, it was possible to acquire the first results using the biofilms formed in the RCR and measure biofilm properties with the czFDG.

This thesis is organized in nine main chapters:

Chapter 2 is a literature review, mainly focused on the problematic of industrial biofouling and its control. After some generic concepts about this topic (definition, context and location), biofouling is presented as a phenomenon to control in industries. Its undesirable consequences are listed, as well as the main factors that affect its development. Current anti-biofouling measures are listed. Laboratory-scale reactors as well as methods to study biofilms are described.

Chapter 3 describes all the materials and methods used during the experimental work reported in this thesis. For each of the five following chapters, reference to subsections of this chapter will be made regarding the experimental methodologies employed.

Chapter 4 reports the work obtained during the stage of screening of the best antimicrobials to control microbial growth, and it is adapted from the manuscript: Lemos, M., Borges, A., Teodósio, J., Araújo, P., Mergulhão, F., Melo, L. and Simões, M. (2013). The effects of ferulic and salicylic acids on *Bacillus cereus* and *Pseudomonas fluorescens* single- and dual-species biofilms. International Biodeterioration & Biodegradation 86(Part A), 42-51.

Chapter 5 relates to the study of different surface materials on the behaviour of biofilms formed on the RCR after chemical and mechanical treatments, and it is adapted from the manuscript: Lemos, M., Gomes, I., Mergulhão, F., Melo, L. and Simões, M. (2015) The effects of surface type on the removal of *Bacillus cereus* and *Pseudomonas fluorescens* single and dual species biofilms. Food and Bioproducts Processing 93(0), 234-241.

Chapter 6 relates to the study about the effect of different hydrodynamic conditions used in the RCR on the behaviour of biofilms exposed to chemical and mechanical treatment. The chapter is adapted from the manuscript: Lemos, M., Mergulhão, F., Melo, L. and Simões, M. (2015). The effect of shear stress on the formation and removal of *Bacillus cereus* biofilms. Food and Bioproducts Processing 93(0), 242-248.

Chapter 7 is based on the analysis of different phenotypical characteristics of *Bacillus cereus* and *Pseudomonas fluorescens* single- and dual-species biofilms formed on high density polyethylene using the RCR and the effects of benzyldimethyldodecyl ammonium chloride on their removal. The results are in the process of submission to an international peer-reviewed journal.

Chapter 8 describes the proof of concept of the cylindrical zero-discharge Fluid Dynamic Gauging device developed in the University of Cambridge to measure biofilm thickness on cylindrical surfaces, and it is adapted from the manuscript: Lemos, M., S. Wang, A. Ali, M. Simões, and D.I. Wilson, A fluid dynamic gauging device for measuring biofilm thickness on cylindrical surfaces. Biochem. Eng. J., 2016. 106: 48-60.

The conclusions gathered from those studies are outlined in Chapter 9 as well as suggestions of future work.

Besides the manuscripts referred to above, results obtained during the work presented in this thesis were also presented to the scientific community in the following conferences:

Lemos, M., Wang, S., Ali, A., Simões, M. and Wilson, D. I. 2015. A fluid dynamic gauging device for measuring biofilm thickness on cylindrical surfaces. Heat Exchanger Fouling and Cleaning XI – 2015. Enfield (Dublin), Ireland (oral presentation)

Lemos, M., Mergulhão, F., Melo, L. and Simões, M. 2014. The effect of shear stress on the formation and removal of *Bacillus cereus* biofilms. Fouling and Cleaning in Food Processing 2014: 'Green Cleaning' Cambridge, United Kingdom (oral presentation)

Lemos, M., Gomes, I., Mergulhão, F., Melo, L. and Simões, M. 2014. The effects of surface type on the removal of *Bacillus cereus* and *Pseudomonas fluorescens* single and dual species biofilms. Fouling and Cleaning in Food Processing 2014: 'Green Cleaning' Cambridge, United Kingdom (poster)

Lemos, M., Mergulhão, F., Melo, L. and Simões, M. 2013. A rotatory cylinder reactor to assess the mechanical stability of *Bacillus cereus* and *Pseudomonas fluorescens* single and dual biofilms on stainless steel and high density polyethylene. IWA 9th International Conference on Biofilm Reactors, 28 - 31 May, Paris, France (poster)

Lemos, M., Mergulhão, F., Melo, L. and Simões, M. 2012. Resistance of single and dual biofilms of *Bacillus cereus* and *Pseudomonas fluorescens* to chemical and mechanical stresses. Biofilms 5, 10 - 12 December, Paris, France (poster)

Chapter 2

Literature review

2. Literature review

2.1. History, definition and formation steps of biofilms

Antoni van Leeuwenhoek, who lived in Delft, Dutch Republic (1632–1723), performed the first observations of bacteria using his own handmade microscopes. In 1684, he provided the first scientific report on biofilms to the Royal Society of London, where he said “The number of these animalcules in the scurf of a man's teeth are so many that I believe they exceed the number of men in a kingdom”.

Later, during the XIX century great advances were made in clinical microbiology. Louis Pasteur was the first to recognize variability in virulence, discovered that microorganisms cause fermentation and disease and created the process of pasteurization. Robert Koch, discovered the anthrax disease cycle and the bacteria responsible for tuberculosis and cholera. It was only in 1933 that Henrici reported for the first time observations of non-free floating bacteria [1] and later in 1940 Heukelekian and Heller described bacterial development in diluted substrates ”either as bacterial slime or colonial growth attached to surfaces” [1, 2]. Research on biofilms continued with key scientists like William Characklis and J. W. (Bill) Costerton. In fact, Costerton [3] defined biofilms as “matrix-enclosed bacterial populations adherent to each other and/or to surfaces or interfaces” including “microbial aggregates and floccules and also adherent populations within the pore spaces of porous media”. Microbial adhesion to surfaces and consequent biofilm formation is a survival strategy that has been studied and documented in recent decades [4]. It is widely accepted now that biofilms are complex structures composed of microbial cells adhered to a surface and enclosed in a matrix of hydrated extracellular polymeric substances (EPS) [5].

The initial adhesion of bacterial cells frequently involves preconditioning of the surfaces with macromolecules (proteins, DNA and humic acids) suspended in fluids. Passive transport, i.e., convection and diffusion approximates planktonic (free-floating) cells to the surface [6]. The cells produce signalling molecules and detect their presence in the bulk fluid when its concentration increases, so that they can sense the proximity of a surface as the diffusion of the signalling molecules is limited in that area [7]. This communication mechanism triggers active forms of bacterial motility like swarming and twitching, facilitates the contact of the cells with the surface and also allows reversible adhesion [8]. The EPS secretion is initiated and the adhesion becomes irreversible. Specific alterations in the genetic traits occur in biofilms. [9]. As

the bacteria multiply, microcolonies are formed and more EPS are produced. The EPS components – polysaccharides, proteins and DNA, are distributed among the cells in a heterogeneous configuration, with weak physicochemical interactions and entanglement between the biopolymers. This generates diverse regions in the matrix in terms of structural features with a porous architecture [10]. Dissemination of sessile cells occurs naturally, by detachment of clumps of biofilms due to hydrodynamic shearing [11, 12]. Sudden alterations in nutrient availability, including starvation, may also cause dispersion of cells. Those alterations trigger quorum sensing and motility mechanisms, promoting enzymatic action and the modification of the matrix, and therefore the liberation of cells into the surrounding fluid [10].

2.2. Factors influencing biofilm development

Biofilms tend to grow in the presence of water and nutrients under certain conditions. However, there are several factors affecting the events at the surface.

2.2.1. Biological aspects

The microorganisms' nature, the dynamics and the diversity of the microbial community can be considered the first factors influencing the biofilms composition and structure [13]. Natural biofilms (as opposed to those formed in the laboratory) are multispecies microbial communities, complex and highly differentiated [14, 15]. Studies have demonstrated that in these multispecies biofilms, synergistic interactions exist that affect their entire behaviour and enhance their resistance to stress conditions [16].

For bacteria in the planktonic state, swimming motility is the individual movement of cells in liquid environments, caused by rotation of flagella. Swarming motility is also powered by rotating flagella. However this is a collective rapid movement, used by coordinated groups of bacteria to approach surfaces, and is involved in the early stages of biofilm formation. Another important motility mechanism in bacterial attachment is twitching, a slow surface motility powered by the extension and retraction of type IV pili [17-19].

Bacteria possess cell-cell communication that happens by secreting signalling molecules into the environment as messages to be sensed by other cells of the community. By this quorum sensing mechanism the bacterial community is able to control its cell density accordingly to the

surrounding conditions. Recently 'sociomicrobiology' studies have been showing that quorum sensing mechanisms are highly related to biofilm formation [8, 20].

New genetic traits are generated as a consequence of adhesion [21] as well as alterations in the bacterial phenotype [3, 22]. One of the main phenotypic alterations is the secretion of EPS. These biopolymers are mainly polysaccharides, proteins and nucleic acids although phospholipids and humic acids have also been reported in EPS composition studies [23]. The EPS are fundamental for the biofilm mechanical stability; promote the adhesion to surfaces; facilitate the aggregation of bacterial cells and cohesion of cell clusters within the biofilm and act as a barrier that protects those cells against aggressions (specific or nonspecific) [24]. Furthermore, the EPS matrix maintains the biofilms in a highly hydrated state and permits the sorption of exogenous organic compounds and inorganic ions, accumulation of important nutrients for metabolism and facilitates enzymatic activities. EPS components also act as electron donors or acceptors and their DNA molecules also facilitate horizontal gene transfer between biofilm cells [23].

2.2.2. Suspended solids and nutrient availability

Particle deposition, controlled essentially by mass transfer, shear stress and thermal effects, conditions the surface and facilitates the attachment of bacteria. The flow velocity affects the mass transfer of nutrients to the biofilm and consequently its diffusion to the cells, therefore influencing their metabolic growth, the production of EPS and ultimately the structure of the biofilm [25, 26].

In industrial settings, nutrient limitation is the main variable affecting biofilm formation [27]. Sessile cells exist in a variety of metabolic states within biofilms and as the EPS matrix offers resistance to diffusion, these structures present gradients in the concentration of oxygen, nutrients, metabolites and signalling molecules. Meanwhile, bacteria adapt to the local depletion of nutrients and oxygen, and consequently biofilms' physiology grow very heterogeneous [28].

2.2.3. Surface

The type of surface has a strong influence on bacterial adhesion, due to physicochemical interactions and roughness, notwithstanding the biological aspects described above. There is a large variety of materials applied in industrial settings, therefore many studies have been

performed to investigate bacterial adhesion and biofilm formation on the most commonly used surfaces. Table 2.1 describes materials used in industrial equipments and water distribution systems which were investigated for biofilm formation, including the type of test preformed, the main focus of the study and the microorganisms found or used in those studies.

Surface charge is one of the aspects that influences adhesion, due to the electrostatic interactions with bacteria. Under normal physiological conditions the surface of bacterial cells is negatively charged, so they are attracted to positively charged surfaces, whereas electrostatic repulsion disfavours contact with negatively charged surfaces [29]. Hydrophobic interactions stabilize the interfacial phenomena that lead to bacterial attachment [30]. For a cell immersed in water to attach to a surface, it is necessary to remove the water film existent between them, hence the importance of the affinity of both entities to water. These hydrophobic forces are the strongest of long-range non-covalent interactions present in biological systems and are governed by the hydrogen bonding energy of cohesion between the surrounding water molecules [31, 32]. Even though thermodynamic predictions of surface energies can give some information about forces involved in the adhesion process, their influence on bacterial adhesion still lacks detailed understanding and therefore they may not always correspond to what happens in real systems [29]. The topography of the surface also plays an important role in the attachment of bacteria, which is highly dependent on the bacteria dimensions and the roughness height and width. Materials with roughness that provides gaps bigger than the cells naturally offer better conditions than smooth materials, because they offer physical protection against shear forces of flowing liquids. Hence, adhesion is also the result of the favourable combinations of size, position and orientation of the cells with their surface properties [33].

Table 2.1 - Materials used in industrial equipments and water distribution systems, which were investigated for biofilm formation, including the type of test preformed, the main focus of the study and the microorganisms found or used in those studies.
FT: test with biofilm obtained at the field or with experimental set-ups at pilot scale. LT: test with biofilm produced in the laboratory at small scale.

Material	Type of test: main objective of the study	Microorganisms	ref.
Metals			
Austenitic stainless steel AISI 304	FT: long term study on the effect of materials on biofilm development in drinking water distribution systems (SS 304L	*Enterobacteria*, Nitrifying bacteria (not specified)	[34]
	FT: effect of engineered changes on stainless steel surfaces on biofilm formation (2B mill or electropolished finish)	not specified (bacterial suspensions from saline rinses of poultry carcasses from a commercial broiler processing plant)	[35]
	FT: effect of attachment of common *Salmonella* serovars to materials used in a poultry processing plant	*Salmonella* Infantis, *Salmonella* Sofia, *Salmonella* Typhimurium, *Salmonella* Virchow	[36]
	FT: effect of pipe materials on biofilm and drinking water quality	*Arthrobacter* spp., *Bacillus* spp., *Methylobacterium* spp., *Micrococcus* spp., *Novoshingobium* spp., *Paenobacillus* spp., *Sphingomonas* spp., drinking water bacterium, uncultured bacterium	[37]
	LT: effect of materials on biofilm removal in cleaning procedures applied in closed dairy and brewery equipment	*Bacillus thuringiensis* ATCC 10792, *Pseudomonas fragi* ATCC 4973, *Pantoea agglomerans* isolated from brewery sample, *Pantoea inopinatus* isolated from brewery sample	[38]
	LT: effect of materials on the biofilm formation by isolates from meat tables in a municipal abattoir in Nigeria	*Listeria monocytogenes* isolates (SLM 14) and *Listeria* spp. (SLS 6)	[39]
Austenitic stainless steel AISI 316	FT: long term study on the effect of materials on biofilm development in drinking water distribution systems (SS 316L and SS 316LN grades)	*Enterobacteria* , Nitrifying bacteria (not specified)	[34]
	LT: effect of materials on the adhesion of bacteria isolated from drinking water.	*Acinetobacter calcoaceticus, Methylobacterium* spp. *Staphylococcus sp.*	[40]
	FT: effect of materials on biofilm development in model warm water distribution systems	not specified	[41]
Cast iron	LT: effect of materials on biofilm formation using potable water	not specified	[42]

Table 2.1 - (continued)

Material	Type of test: main objective of the study	Microorganisms	ref.
Copper	FT: long term study on the effect of materials on biofilm development in drinking water distribution systems	Nitrifying bacteria (not specified)	[34]
	FT: effect of pipe materials on biofilm and drinking water quality	*Arthrobacter* spp., *Bacillus* spp., *Brevundimonas* spp., *Methylobacterium* spp., *Paenobacillus* spp., *Sphingomonas* spp., *Tetrasphaera* spp., agricultural soil bacterium, drinking water bacterium, uncultured bacterium	[37]
	FT: effect of pipe materials on UV- and chlorine disinfection in drinking water and biofilms.	not specified	[43]
	LT: effect of materials on biofilm formation with drinking water, mixed water (inoculated with 10% v/v of river water) and drinking water inoculated with a representative coliform bacterium	*Cytophagales* sp., *Dechloromonas* sp., *Escherichia coli* JM109, *Mycobacterium* sp., species belonging to actinobacteria group, uncultured bacterium detected from a hydropower plant reservoir	[44]
Ductile iron (lined and unlined)	FT: effect of blending different source waters on distribution systems water quality (ground water, surface water and brackish water).	not specified	[45]
Duplex stainless steel	FT: long term study on the effect of materials on biofilm development in drinking water distribution systems (duplex SS UR 2304 and UR 2205 grades)	*Enterobacteria* , Nitrifying bacteria (not specified)	[34]
Ferritic stainless steel	FT: long term study on the effect of materials on biofilm development in drinking water distribution systems (444 grade)	*Enterobacteria* , Nitrifying bacteria (not specified)	[34]
Galvanized iron	FT: effect of pipe materials on the viable but nonculturable state and bacterial numbers in drinking water.	not specified	[46]
Galvanized steel	FT: long term study on the effect of materials on biofilm development in drinking water distribution systems	*Enterobacteria* , Nitrifying bacteria (not specified)	[34]
	FT: effect of blending different source waters on distribution systems water quality (ground water, surface water and brackish water).	not specified	[45]
Grey iron	FT: effect of pipe materials on the densities of fixed bacteria from drinking water from underground and surface waters.	not specified	[47]

Table 2.1 - (continued)

Material	Type of test: main objective of the study	Microorganisms	ref.
Steel	FT: effect of pipe materials on biofilm and drinking water quality	*Brevundimonas* spp., *Methylobacterium* spp., *Mycobacterium* spp., *Novoshingobium* spp., *Sphingomonas* spp. *Staphylococcus* spp., *Tetrasphaera* spp., agricultural soil bacterium, drinking water bacterium, uncultured bacterium	[37]
Steel coated with zinc	LT: effect of materials on biofilm formation with drinking water, mixed water (inoculated with 10% v/v of river water) and drinking water inoculated with a representative coliform bacterium	*Cytophagales* sp., *Dechloromonas* sp., *Escherichia coli* JM109, *Pandoraea* sp., species belonging to actinobacteria group, uncultured bacterium detected from a hydropower plant reservoir	[44]
Plastics			
Chlorinated polyvinyl chloride –CPVC	LT: effect of materials on biofilm formation with drinking water, mixed water (inoculated with 10% v/v of river water) and drinking water inoculated with a representative coliform bacterium	*Dechloromonas* sp., *Escherichia coli* JM109) species belonging to actinobacteria group, uncultured bacterium detected from a hydropower plant reservoir	[44]
Cross-linked polyethylene – PEX	LT: effect of materials on drinking water biofilm formation in flow/non flow conditions: high-density polyethylene (HDPE)	not specified	[48]
	FT: effect of materials on biofilm development in model warm water distribution systems	not specified	[41]
Formica-type plastic laminate	LT: development of methods for fluorescence image-based optical detection of biofilms	*E. coli* O157:H7, *Salmonella enterica* serotype Poona	[49]
Poly(vinyl chloride) – PVC	FT: effect of blending different source waters on distribution systems water quality (ground water, surface water and brackish water)	not specified	[45]
	FT: effect of pipe materials on biofilm and drinking water quality	*Brevundimonas* spp, *Caulobacter* spp., *Deftia* spp., *Methylobacterium* spp., *Moraxella* spp., *Mycobacterium* spp., *Ornithinimicrobium* spp., *Sphingomonas* spp., *Staphylococcus* spp., drinking water bacterium, uncultured bacterium	[37]
	LT: effect of materials on biofilm formation using potable water (unplasticized PVC)	not specified	[42]

Table 2.1 - (continued)

Material	Type of test: main objective of the study	Microorganisms	ref.
Poly(vinyl chloride) – PVC	FT: effect of pipe materials on the viable but nonculturable state and bacterial numbers in drinking water	not specified	[46]
	LT: effect of materials on drinking water biofilm formation in flow/non flow conditions	not specified	[48]
	LT: effect of pH and surface on EPS production and biofilm formation	*P. fluorescens* isolated from a river water	[50]
	LT: effect of materials on the adhesion of bacteria isolated from drinking water	*A. calcoaceticus, Sphingomonas capsulata* sp., *Staphylococcus* sp., *Stenotrophomonas maltophilia*	[40]
Polybutylene –PB	LT: effect of materials on biofilm formation with drinking water, mixed water (inoculated with 10% v/v of river water) and drinking water inoculated with a representative coliform bacterium	*Cytophagales* sp., *Dechloromonas* sp., *Escherichia coli* JM109, *Methylophilus* sp., species belonging to actinobacteria group, uncultured bacterium detected from a hydropower plant reservoir	[44]
Polyethylene – PE	FT: long term study on the effect of materials on biofilm development in drinking water distribution systems	*Enterobacteria* , Nitrifying bacteria (not specified)	[34]
	LT: development of methods for fluorescence image-based optical detection of biofilms: high-density polyethylene (HDPE)	*E. coli* O157:H7, *S. enterica* serotype Poona	[49]
	LT: effect of materials on biofilm formation using potable water: (medium-density polyethylene – MDPE)	not specified	[42]
	FT: effect of pipe materials on UV- and chlorine disinfection in drinking water and biofilms.	not specified	[43]
	LT: effect of materials on drinking water biofilm formation in flow/non flow conditions (high-density polyethylene – HDPE)	not specified	[48]
	LT: effect of pH and surface on EPS production and biofilm formation	*P. fluorescens* isolated from a river water	[50]
	LT: effect of materials on the adhesion of bacteria isolated from drinking water	*A. calcoaceticus, Burkholderia cepacia, Mycobacterium mucogenicum, S. capsulata* sp., *Staphylococcus sp., S. maltophilia*	[40]

Table 2.1 - (continued)

Material	Type of test: main objective of the study	Microorganisms	ref.
Polyethylene – PE	LT: effect of materials on biofilm formation with drinking water, mixed water (inoculated with 10% v/v of river water) and drinking water inoculated with a representative coliform bacterium	*Brevundimonas intermedia, Cytophagales* sp., *Dechloromonas* sp., *Escherichia coli* JM109, *Methylophilus* sp., species belonging to actinobacteria group, uncultured bacterium detected from a hydropower plant reservoir	[44]
Polypropylene – PP	LT: effect of materials on drinking water biofilm formation in flow/non flow conditions	not specified	[48]
	LT: effect of pH and surface on EPS production and biofilm formation	*P. fluorescens* isolated from a river water	[50]
Polystyrene – PS	LT: effect of pH and surface on EPS production and biofilm formation	*P. fluorescens* isolated from a river water	[50]
Polytetrafluoroethylene – PTFE (Teflon™)	LT: effect of the cell surface hydrophobicity on the adhesion	*Corynebactenium* DSM 44016, *Corynebacterium* DSM 6688, Coryneform bacteria with type B peptidoglycan DSM 6685, *Gordona* 1775/15, *Rhodococcus* spp. C125	[51]
	FT: effect of attachment of common *Salmonella* serovars to materials used in a poultry processing plant	*Salmonella* Infantis , *Salmonella* Sofia , *Salmonella* Typhimurium, *Salmonella* Virchow	[36]
	LT: effect of materials on biofilm removal in cleaning procedures applied in closed dairy and brewery equipment	*P. agglomerans* isolated from brewery sample, *P. inopinatus* isolated from brewery sample	[38]
Elastomers			
Ethylene propylene diene monomer rubber – EPDM	LT: effect of materials on biofilm removal in cleaning procedures applied in closed dairy and brewery equipment	*B. thuringiensis* ATCC 10792, *P. fragi* ATCC 4973, *P. agglomerans* isolated from brewery sample, *P. inopinatus* isolated from brewery sample	[38]
	FT: effect of materials on biofilm development in model warm water distribution systems	not specified	[41]
Fluoroelastomer (Viton®)	LT: effect of materials on biofilm removal in cleaning procedures applied in closed dairy and brewery equipment	*B. thuringiensis* ATCC 10792, *P. fragi* ATCC 4973, *P. agglomerans* isolated from brewery sample, *P. inopinatus* isolated from brewery sample	[38]

Table 2.1 - (continued)

Material	Type of test: main objective of the study	Microorganisms	ref.
Nitrile butyl rubber – Buna-N rubber	FT: effect of attachment of common *Salmonella* serovars to materials used in a poultry processing plant	*Salmonella* Infantis , *Salmonella* Sofia , *Salmonella* Typhimurium, *Salmonella* Virchow	[36]
	FT: model for heat inactivation of biofilms	*L. monocytogenes, P. agglomerans, Pseudomonas* spp	[52]
	LT: effect of materials on biofilm removal in cleaning procedures applied in closed dairy and brewery equipment	*B. thuringiensis* ATCC 10792, *P. fragi* ATCC 4973	[38]
Polyesterurethane – PSU	LT: effect of conveyor belt surface roughness on the biofilm formation, in a chicken meat plant in Thailand	*L. monocytogenes* ATCC19114 and ATCC51782.	[53]
Polyurethane	FT: effect of attachment of common *Salmonella* serovars to materials used in a poultry processing plant	*Salmonella* Infantis , *Salmonella* Sofia , *Salmonella* Typhimurium, *Salmonella* Virchow	[36]
Others			
Cement	FT: long term study on the effect of materials on biofilm development in drinking water distribution systems	*Enterobacteria,* Nitrifying bacteria (not specified)	[34]
Cemented cast iron and cemented steel	FT: effect of pipe materials on the densities of fixed bacteria from drinking water from underground and surface waters	not specified	[47]
Glass	LT: effect of the cell surface hydrophobicity on the adhesion	*Corynebactenium* sp. DSM 44016, *Corynebacterium* sp. DSM 6688, Coryneform bacteria with type B peptidoglycan DSM 6685, *Rhodococcus* spp. C125	[51]
	FT: effect of attachment of common *Salmonella* serovars to materials used in a poultry processing plant	*Salmonella* Infantis , *Salmonella* Sofia , *Salmonella* Typhimurium, *Salmonella* Virchow	[36]
	LT: effect of materials on the biofilm formation by isolates from meat tables in a municipal abattoir in Nigeria	*L. monocytogenes* isolates (SLM 14) and *Listeria spp* (SLS 6)	[39]
Granite	LT: development of methods for fluorescence image-based optical detection of biofilms	*E. coli* O157:H7, *S. enterica* serotype Poona	[49]
Tarred steel	FT: effect of pipe materials on the densities of fixed bacteria from drinking water from underground and surface waters	not specified	[47]

2.2.4. Hydrodynamics

Biofilms adopt complex structures, with viscoelastic properties, that are resilient to physical stress and chemical agents [54, 55]. The hydrodynamic conditions in the bulk fluid influence the biofilm formation process.

The shear stress at the surface is dependent on the flow velocity of the surrounding fluid and therefore it affects the boundary layers where the adhesion is occurring. High shear stress conditions lead to thin fluid boundary layers that facilitate mass transfer [56]. This increases particle deposition at the surface and defines the transport of the cells, oxygen and nutrients from the bulk fluid to the microbial film [57-59]. On the other hand, high flow velocities tend to enhance turbulent burst phenomena close to the surface, thereby creating forces that dislodge the cells from the surface. Therefore, since bacteria are known to attach to surfaces even at high shear stresses, it appears that they develop adaptive mechanisms (such as EPS production) to overcome (at least, partially) the detachment effects promoted by shear stress [60, 61].

Throughout the maturation of the biofilms, this effect of the hydrodynamic environment in mass transfer promotes nutrient and density gradients and affect the biofilm thickness. The signalling molecules, when diffusing to the bulk fluid, may be washed away and therefore quorum sensing mechanisms may also be affected [62]. The species in the biofilm may have different physiological adaptation mechanisms to this change [63] and their aggregation properties may be altered under high shear stress conditions leading to more cohesive biofilms [64, 65]. On the other hand, an increase in flow velocity leads to increased shear stress that also affects the biofilm structure [66-68]. Studies have shown that biofilms grown under low shear stress conditions present uneven clumps, whereas high shear stress conditions leads to dense planar biofilms with filamentous consistency [57]. The detachment of the biofilm will thus be determined by the ratio between the hydrodynamic forces that contribute to the mass transport of nutrients and the limit breaking strength that is inherent in the internal cohesion of the biofilm.

2.2.5. Temperature and pH

The environment where biofouling occurs is generally an aqueous solution. Temperature variations affect the physicochemical properties of the fluid, including the density and viscosity, thus influencing the flow conditions [69]. Moreover, all microorganisms have optimal conditions for growth and so temperature and pH changes also affect biofilm formation.

As biofilms offer additional protection and survival chances to cells compared to those in planktonic state, sessile cells can survive and even multiply in conditions that otherwise would be unfavourable. This has been seen particularly in food industries, where biofilms grow at the otherwise unfavourable temperatures used in the processing areas. Dourou et al. [70] noted that *E. coli* O 157:H7 attachment to beef-contact surfaces occurred not only at temperatures representative of non-production periods (15 °C), but also at cold storage (4 °C) temperatures. Meira et al. [71] performed a study using *Staphylococcus aureus* strains isolated from food services cultivated in a vegetable-based broth at 7 and 28 °C. This author studied the adhesion of those cells on stainless steel and polypropylene surfaces and found that the isolates adhered over 4 Log CFU/cm^2 regardless of the surface type and incubation temperature. Biofilms have been reported in dairy industries in several areas (gaskets, conveyor belts, dead legs of pipelines) including plate-heat exchangers and the pasteurized milk holding section where during the pasteurization the temperature is held at 76 ± 3 °C for 15-20 s [72].

Large variations in pH have importance on biofilm formation and composition [73]. Bacteria have a transmembrane electrochemical gradient due to cytoplasmic and membrane-bound proton pumps. Hence regulation of the cytoplasmic pH is sensitive to the inflow of protons. Even though bacteria can adapt to the environmental conditions, some of their metabolic processes, like excretion of exopolymeric substances, are not that flexible to pH variations and generally require a neutral pH [74]. The relationship between polysaccharide production and biofilm formation by *P. fluorescens* at different pH conditions was studied by Oliveira et al. [50], who found that the maximum EPS amount and biomass production occurred in pH 7 phosphate buffer.

2.3. Context

Biofilms can develop on almost all natural and synthetic surfaces [75, 76]. In fact, there are evidences of biofilm formation in natural environments [76-78], including early biofilm findings in the fossil records [79, 80]. Despite the incessant application of disinfection measures, biofilms continue to be found in drinking water distribution systems (DWDS), threatening the microbial safety and organoleptic quality of the distributed water [65, 81, 82]. Biofilms in DWDS can act as potential harbours for pathogenic microorganisms. Drinking water is contaminated when there is detachment of those biofilms and dispersal of the cells, ultimately leading to public health issues due to infections caused by waterborne pathogens [83].

Water-based industries are likely to be affected by the presence of detrimental biofilms. This happens particularly in crevices, corners, dead zones, valves or areas where the mixing rate is low. Stagnation promotes biofilm formation and accumulation, which in industrial context is called biofouling [84]. The main industries where biofouling causes significant detrimental consequences are summarized in Table 2.2 alongside the critical aspects that promote biofilm formation and the main colonizer bacteria found.

Biofilm contamination can also occur in household sites like cutting surfaces, washing machines and dishwashers, scourers and bath cloths, water taps and shower heads, drains, sanitary bowls, air conditioning devices, swimming pools, saunas and domestic plumbing systems, amongst others [85-92]. Biofilms are often present in areas like bathrooms and kitchens that present moist conditions with poor ventilation and may have areas of difficult access where there is accumulation of organic residues and deposits of cleaning products (phosphate based detergents, shampoos, tooth paste, etc.) [93-95].

Biofilms have also been identified as root of many persistent and chronic bacterial infections like otitis media, pneumonia in cystic fibrosis patients, osteomyelitis, peptic ulcers, infections of the biliary and of the urinary tracts, bacterial prostatitis, diabetic foot ulcers, endocarditis, caries, gingivitis and periodontitis, etc. [95, 96]. Contaminated catheters and implanted devices often are ideal surfaces for biofilm growth. These infections persist despite the immune and inflammatory responses of the host and are resistant to conventional antibiotic therapy [97]. A point prevalence survey from the European Centre for Disease Prevention and Control [98] reported that between 2011 and 2012, on any given day, 5.7% of patients in European hospitals have at least one healthcare-associated infection (HAI).

About 80% of the HAIs are biofilm-related [99], which translates in Europe to about 64 000 hospitalized patients who have at least one HAI caused by biofilms on any given day. The HAI most frequently reported were respiratory tract infections (pneumonia and lower respiratory tract infections), surgical site infections, urinary tract infections, bloodstream infections and gastro-intestinal infections. According to this survey the most frequently isolated microorganisms in HAIs were: *E. coli*, *S. aureus*, *Enterococcus* species, *P. aeruginosa*, *Klebsiella* species, coagulase-negative staphylococci, *Candida* species, *Clostridium difficile*, *Enterobacter* species, *Proteus* species and *Acinetobacter* species.

Table 2.2 – Main industries affected by biofouling, critical aspects that facilitate biofilm formation and bacterial species regularly found in those biofilms

Industry/ references	Critical aspects	Main bacteria found
Beverages/ [96-100]	Microorganisms used for fermentation processes often form biofilms that can harbour spoiling organisms. This is critical in some industries where there is no filtration or pasteurization, like microbreweries.	*Brettanomyces bruxellensis* *Lactobacillus brevis* *Lactobacillus lindneri* *Pediococcus pentosaceus*
Dairy/ [101-104]	Cleaning-in-place (CIP) is not effective for microbial inactivation due to dead spaces (bends in pipes, rubber seals, gaskets) in pasteurization lines, plate heat exchangers air handling systems, milk transfer lines, conveyors, packaging machines, ultra-filtration surfaces, mixers, tanks and other equipment.	*B. cereus* *Bacillus subtilis* *E. coli* *Enterobacter aerogenes* *Klebsiella* spp. *Listeria* spp. *S. aureus* *Shigella* spp.
Fish and seafood/ [105-109]	Cross-contamination with microflora present in the environment, which may be directly transferred to the raw materials or to the surfaces, namely when seawater is used. Water storage tanks, water pipes and larval tanks are prone to biofilm formation.	*Aeromonas* spp. *Bacillus* spp. *L. monocytogenes* *Neisseriaceae* spp. *Pseudomonas* spp. *Salmonella* spp. *Serratia liquefaciens* *Vibrio* spp.
Meat/ [110-113]	Despite the low temperatures, organic residues on surfaces lead to resident biofilms that persist after ineffective cleaning procedures facilitating the growth of pathogenic microorganisms. The lack of heat treatments allows the contamination of final products.	*A. calcoaceticus* *Bacillus* spp. *Corynebacterium* spp. *E. coli* O157:H7 *L. monocytogenes* *Micrococcus* spp. *Pseudomonas* spp. *Staphylococcus* spp.
Poultry/ [36, 114-117]	Cross-contamination between dust, surfaces, faeces, feed, transportation systems and processing units.	*Campylobacter jejuni* *Salmonella sofia* *Salmonella typhimurium*
Produce/ [118-121]	Cross-contamination with microorganisms present internally in the plant tissue and the equipments and products used for cutting, trimming, washing, rinsing, dewatering and packaging. Sanitation cannot affect the final product qualities of fresh-cut produce so often the microbial activity is not totally eradicated.	*E. coli* O157:H7 *L. monocytogenes* *S. enterica* Typhimurium

Table 2.2 – (continued)

Industry/ references	Critical aspects	Main bacteria found
Cooling towers/ [122-126]	High aeration, possible contamination from the atmosphere, favourable temperatures, high residence time and high ratio of surface area to the volume. Production of aerosols.	*Desulfococcus* spp. *Desulfomicrobium* spp. *Desulfonema* spp. *Desulfosarcina* spp. *Desulfotomaculum* spp. *Desulfovibrio* spp. *Flavobacterium* sp. *Klebsiella pneumoniae* *Legionella* spp. *Pseudomonas aeruginosa*
Oil/ [127-132]	Contamination and biofilm formation on the injection systems and reservoirs due to the injection of untreated water (often seawater), for pressure maintenance and secondary oil recovery.	*Acetobacterium* spp. *Anaerophaga* spp. *Clostridium* spp. *Desulfomicrobium* spp. *Desulfovibrio* spp. *Methanobacterium* spp. *Methanococcus aeolicus* *Methanococcus maripaludis* *Methanoplanus limicola* *Tindallia* spp.
Paper manufacture/ [116-119	Cross contamination (nutrients and microorganisms) from raw materials and additives. Closed water cycles. Acid-free processes and chlorine-free bleaching that increases 'pink slime' (which stains the paper).	*B. cepacia* *Bacillus* spp. *Chryseiobacterium* spp. *Brevundimonas* spp. *Deinococcus geothermalis* *Rubellimicrobium thermophilum*

2.4. Biofouling – a common occurrence with detrimental consequences

Biofouling, caused by the accumulation of biofilms, is dependent on the process where it occurs, i.e. the type of microrganisms that form the biofilms and the environmental conditions under which they are formed [133]. Despite particular technical aspects that will be described further in this section, there are some detrimental consequences caused by biofouling in virtually all the industries using non-sterile water (summarized in Fig. 2.1). Biofilm accumulation in pipelines causes a reduced flow area, requiring more work to pump liquids, reduced heat transfer rates, increased energy consumption, additional maintenance and operational costs [81, 134]. Biofilms interact with their surroundings, both the liquid environment and the surfaces around them, and the products of sessile cell metabolism can cause microbially induced corrosion [13, 135]. When compared to their planktonic forms, biofilm bacteria exhibit increased resistance to

antimicrobials [136]. The reasons for this are not completely understood, and the mechanisms hypothesized include: direct interaction between EPS and antimicrobials, affecting diffusion and availability; an altered microenvironment within the biofilm, leading to areas of reduced or no growth; the development of biofilm/attachment-specific phenotypes; and the possibility of programmed cell death of damaged bacterial cells and persistent cells [137]. Biofilm elimination is difficult because of the evolution of resistant phenotypes, to the extent that control strategies that rely mainly on biocide action often fail against biofilms, as total inactivation of the microbial cells is rarely achieved.

Moreover, when the biomass is not completely removed from the surface, there is a greater dispersion of persister cells, causing rapid growth of recidivist biofilms [138, 139]. The final product may be contaminated by planktonic cells and their metabolites, eventually promoting the spread of pathogens and resistant infectious diseases [140-142].

For example, heat exchangers are widely used in industries and are subjected to chronic fouling, which has been estimated to cost 0.25% of the gross national product of industrialized countries [143]. Biofilms have much lower (30 to 300 times less) thermal conductivity than metals, and their accumulation in heat exchanger tubes causes high pressure drop, reduces the surface area available and decreases the heat transfer rate [144, 145]. Consequently, these units are frequently designed with excess capacity to match the decrease of efficacy of heat transfer caused by biofouling [133]. This preventive dimensioning of equipments increases the capital costs of manufacturing plants, and these implications occur in all industries using heat exchangers, including food, paper manufacturing and oil production.

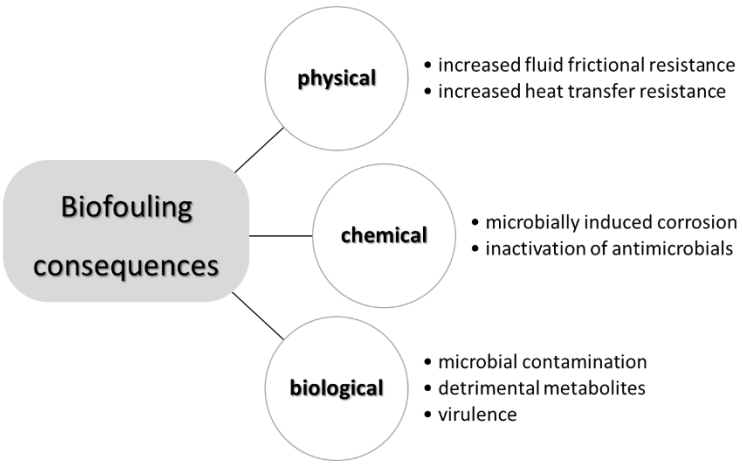

Fig. 2.1 – Detrimental consequences of biofouling.

Downtime may be necessary for maintenance of fouled equipment and sometimes premature replacement of damaged equipment due to microbially induced corrosion. Ultimately biofouling can increase safety problems and unscheduled turnarounds [143, 146].

In food processing plants there is a biotransfer potential, as foodborne microorganisms adhere to typical food contact surfaces [147-149]. Food processing evolves intermittent use of water and generates organic residues that are favourable for microbial growth. On the other hand, the cleaning cycles employed may be insufficient for removal and eradication of biofilms, allowing regrowth and the evolution of mechanisms of antimicrobial resistance. Bacteria can directly colonize the equipment in the processing line or cross-contamination may occur when they are present in other surfaces like drains, walls, floors, washrooms, etc. [140, 147, 150]. The presence of moisture, nutrients and microorganisms in the raw material are inherent to food industries and these are also favourable factors to biofilm formation.

In paper manufacturing, slime sloughing onto the equipment and paper sheets leads to defects (holes, spots, and blotches) and discoloration of pigments, decreasing the product quality. Microbial contamination also produces dangerous bio-aerosols, malodours and the formation of methane and hydrogen, eventually promoting explosive conditions [151, 152].

Souring is one of the main consequence of biofilm formation in the oil industry, due to hydrogen sulphide (H_2S) generated by sulphate-reducing bacteria that contaminate oil and water. H_2S is toxic, corrosive and reduces the quality of oil and gas. Microbial contamination in the water injection systems results in downstream biofouling in the pipelines and consequent corrosion of the tubing and casing alloys. This bacterial contamination can propagate through the flow line and oil storage, leading to microbial corrosion of the onshore crude oil tank, the refinery and even contamination of the ship and aviation fuel. Microbial corrosion and fouling also severely affects heat exchangers and the desalinization plant and reverse osmosis plant. Biofouling in the oil field has serious impact on the functioning of equipment, increasing the maintenance cost and downtime of the refineries [129].

2.5. Control of industrial biofilms

The detrimental consequences of biofouling described above can lead to prohibitive costs resulting from losses in energy and goods, maintenance of equipment and related operating costs, as well as eventual opportunity costs due to unscheduled downtime. Therefore, biofilm control is of utmost importance for industries in order to avoid such problems. In theory

one can consider that biofilm growth can be controlled by the removal of those deposits from the surfaces or by the inactivation of the biofilm microorganisms. The use of mechanical forces is preferred for the former whereas the latter would be achieved by application of biocides. Removing the nutrients from the environment or elevating the temperatures would also be an option, although this is not so feasible for the majority of industrial settings. The chemical and physical control methods are the most commonly employed against biofilms formed in industrial settings and are thus described in greater detail.

2.5.1. Chemical control

Chemical control of biofilms is widely performed in industries and is achieved through the usage of biocides, which are active substances that aim to make harmless, stop the growth, destroy or avoid the action of pathogenic organisms by means of chemical processes [153]. Unlike the antibiotics used to treat clinical infections, biocides do not act on a specific cellular target, but cause damages varying from sub-lethal damage to cell death [154]. The selection of a biocide must take in consideration the nature of microorganisms to be killed so that the mechanism of action and spectrum of activity ensures the results wanted. The possible effects of the biocide on the processing line and final product must be accessed as well as the application mode and health risks for the operators. Finally, the effects of its activity on the environment, including the management of wastes and the cost/efficacy relationship must also be considerated. The information in Table 2.3 is a summary of the biocides used in industry, their mechanism of action, advantages and limitations [27, 154-157].

The most common classification distinguishes between oxidising and non-oxidising biocides. Oxidising biocides promote radical-mediated reaction oxidizing organic material, and include the halogenated agents, ozone and peroxygens. Non-oxidising agents can include a rather large range of biocides like electrophilic agents, surface active agents and weak acids [157].

Table 2.3 – Biocides commonly used for controlling industrial biofilms

Biocide/ reference	Mode of action	Advantages and applications	Limitations
Aldehydes			
Glutaraldehyde (GTA)/ [158-160]	Cross-linking with the amines from the outer layers of bacterial cells, inhibiting transport and enzyme activity and eventually preventing the cell to undertake its functions.	Effective against bacteria and spores, fungi and virus. Low-temperature disinfection in oil fields, cooling towers, farm animal housing and metal working fluids. High materials compatibility.	Pungent and irritating odour Dangerous handling: can cause allergic contact dermatitis and respiratory irritation (vapour).
O-phthalaldehyde (OPA)/ [161-163]	Cross-linking with amino acids and proteins in a smaller degreed compared with GTA but potentiated by its aromatic ring, that helps penetration in the outer layers of cells.	High-level disinfection in medical field.	
Halogens			
Bromide based agents: Bromide/ [164, 165] Bromide chlorine/ [165] Bromo-chloro-dimethyl-hydantoin (BCDMH)/ [164-166]	Production of hypobromous acid, a potent oxidising agent that inactivates the activity of cellular proteins and DNA.	Has been used in substitution of chlorine due to its powerful antimicrobial properties and lack of restrictions from the Environmental Protection Agency.	

Table 2.3 – (continued)

Biocide/ reference	Mode of action	Advantages and applications	Limitations
Chlorine based agents: Chlorine [167] chlorine dioxide [168, 169] sodium hypochlorite [170, 171] Chloramine-T	Production of hypochlorous acid, a potent oxidising agent that inactivates cellular proteins and DNA.	Very powerful biocides with wide spectrum, used for bleaching and hard-surface disinfection. Sporicidal and virucidal at high concentrations.	Their reaction with organic material produces toxic or carcinogenic compounds that are dangerous for the environment. Maximum activity occurs at low pH.
Ozone/ [120, 172, 173]	Disruption of the microbial cell membrane and leakage of the cell components.	Potent antimicrobial against bacteria, fungi, viruses, protozoa, and bacterial and fungal spores used for water disinfection (for CIP, sanitizing treatments and cooling water circuits).	High cost. At pH 8 or higher it decomposes to form hydroxyl radicals, which are stronger oxidising agents than molecular ozone itself.
Peroxygens			
hydrogen peroxide (H_2O_2) [174, 175] peracetic acid (PAA) [176, 177]	Production of hydroxyl free radicals that attack sulfhydryl (-SH) and sulphur (S-S) bonds and therefore oxidising lipids, proteins and DNA.	Effective against bacteria and spores, yeasts and virus. Prevention of biofilm formation, disinfection, and sterilization in clinical settings. Environmentally friendly: hydrogen peroxide decomposes to oxygen and water; peracetic acid decomposes to oxygen and acetic acid.	High transportation costs because are available in solution. Bacteria can increase resistance to low concentration of H_2O_2 if in the presence of peroxidases, however PAA will not be degraded and will remain active. Dangerous handling (eye and skin damage). Material compatibility concerns (brass, zinc, copper).

Table 2.3 – (continued)

Biocide/ reference	Mode of action	Advantages and applications	Limitations
Phenolics/ [178-182]			
o-Phenylphenol (OPP) 4-(2-Methylbutyl)phenol (PTAP) 4-Chloro-3-methylphenol (PCMC) 4-Chloro-3,5-dimethylphenol, (PCMX) 2-Benzyl-4-chlorophenol, (chlorophene) 5-Chloro-2-(2,4-dichlorophenoxy)-phenol (Triclosan)	Progressive leakage of intracellular components with coagulation.	Effective against bacteria, yeast, fungi and lipophilic viruses. OPP and PCMC are used for disinfection, post-harvest treatment of fruit, as canned preservatives, etc. Chlorophene is mainly used combined with OPP, PTAP, and/or PCMX. Triclosan is widely used as antiseptic in consumer goods, for antimicrobial treatments of textiles and plastics.	Not effective against bacterial spores and non-enveloped viruses.
Surfactants			
Anionic agents: Sodium dodecyl sulphate (SDS) [183]	Induce membrane-protein solubilization in the outer and cytoplasmic membranes.	Strong detergent Used in detergent formulations.	Weak antimicrobial properties. Less toxic than oxidising chemicals.
Amphoteric agents: Dodecyl-di(aminoethyl)-glycine derivatives: Tego 51 ® [184]	Disorganization of the plasmatic membrane interfering with its functions and leading to metabolites loss.	Clinical disinfection and sanitization (skin and surgical instruments). Sanitizers and disinfectants in food industry.	Combine the detergent properties of anionic with the antimicrobial properties of the cationic compounds.

Table 2.3 – (continued)

Biocide/ reference	Mode of action	Advantages and applications	Limitations
Cationic surfactants: quaternary ammonium compounds (QAC): [170, 185-187] Benzalkonium chloride (BAC) and its derivatives Cetrimonium bromide (CTAB) Cetylpyridinium chloride (CPC)	Penetration in the cell wall and reaction with the cytoplasmic membrane. General damage in the cell due to loss of structural organization and integrity of the cytoplasmic membrane, leakage of low-weight intracellular material and degradation of proteins and nucleic acids	They are active against enveloped viruses and are sporostatic but not sporicidal, and fungistatic but not fungicidal. Used for clinical disinfection, preservatives in consumer goods (domestic cleaners, cosmetics, ophthalmic and oral antiseptics). Non-specific action due to multi-target nature, which hinders the development of resistance mechanisms. Low toxicity.	Weak detergent properties. Heavy organic loads may require high concentrations.

2.5.2. Physical control

Mechanical cleaning of the surfaces where biofilm is formed is essential to remove the biomass, whether a previous disinfection step was employed or not. The most commonly used techniques to remove industrial biofilms are presented below.

Hydrodynamic stress

The mechanical stability of biofilms is highly dependent on the EPS matrix structure and composition. It is expected that biofilms formed under high shear stress conditions are more dense and thin than the ones formed under low shear stress conditions [57]. When the flow velocity is increased so that the hydrodynamic forces exerted at the surface are superior to the limit of the biofilm's internal cohesive forces, detachment occurs. This phenomenon is used to intentionally remove the biofilms from surfaces when the operators use water turbulence or flushing, i.e., sudden increase of the fluid flow rate to exert a higher shear stress on the surface [65].

The flushing method is frequently used in DWDS. However, studies have shown that even though the shear stress induced with this procedure may be 1000 times higher than what is normally observed in normal conditions in those pipelines, it is not possible to obtain total cleaning of the pipe surfaces [188, 189]. The design of the equipment is important for this method as it alters the distribution of wall shear stress.

Studies have been performed to assess the variation of the mean wall shear stress and its associated fluctuation rate on biofilm removal in different sections of equipment items [190]. It was noted that in gradual expansions the wall shear stress values were quite low and non-uniform and therefore these areas were considered poorly cleanable. Lelièvre et al. [190] also showed that cleaning is also achieved when high turbulence levels, and therefore high fluctuation rate, counterbalance the low wall shear stress observed in some areas. Paul et al. [191] also performed erosion tests, where they exposed biofilms to different values of shear stress, and concluded that mature biofilms present stratified layers of increased cohesiveness closer to the surface and that they always present a strong basal layer, which is denser and more cohesive than the other layers.

Ultrasonication

Ultrasonication is the application of ultrasound (waves with a frequency of 20 kHz to 10 MHz) to induce vibrations on the deposits, causing their breakage and dislodge from the surface. The intensity of application and frequency are the important factors to consider in this technique, and it would be recommended using many treatments of single pulses (30 s per instance) with high ultrasound amplitudes rather than less treatments of multiple pulses (3 × 30 s per instance).

Food industries use this technique for some operations including processing (freezing, cutting, drying, tempering, bleaching, etc.), preservation and extraction [192]. This method presents good results for removal; however, like other mechanical removal methods, it is not very efficient for inactivating bacteria. Nevertheless, it presents more potential for bacterial inactivation when used in combination with other physical methods in thermosonic (heat plus sonication), manosonic (pressure plus sonication), and manothermosonic (heat and pressure plus sonication) treatments [193]. Oulahal-Lagsir et al. [194] recreated an industrial meat process in the laboratory to conduct tests using ultrasonic treatments of 10 s at 40 kHz and obtained 4 times more biofilm removal when compared with wiping methods. Even though electric power is needed for this method, it does not require water or chemical products and it does not generate unwanted by-products, so it is very attractive from the environmental point of view. However, the devices and their installation are very expensive and therefore may not be a cost-effective solution for all industries [69, 195].

Pigging

Pigging is the use of temporary inserts (‘pigs’) to perform maintenance operations in pipelines without dismantling the system or stopping the flow. Pigs of different configurations can be used for cleaning purposes. One of the most common systems is the Taprogge System™ that uses sponge rubber balls slightly larger than the tubes that are pushed through the system with water and wipe their surface [196].

The brush and cage system is another pigging method used for straight pipelines, where the pig is a brush projected and is collected in the end of the pipe in a “cage”. The flow of the brush is repeated reversed according to the amount of biofilm to be removed. This technique implies complex equipment for pumping the fluid, automated control of the brush, and is mainly used for heat exchangers [69, 195].

Ice pigging is a technique similar to flushing, in which a semi-solid pig is used. A saline ice slurry is pumped into the pipe and forced by the upstream pressure of the water to circulate, removing the sediments that are adhered on the surfaces of the pipes. This system presents several advantages facing normal flushing as it requires far less amount of water and presents higher effectiveness. Moreover, the ice slurry pig has non-Newtonian flow that allows it to flow in atypical pipeline configurations and easily assume plug flow. Also, there are no problems of blockage, waiting for it to reach the room temperature will be sufficient to melt the slurry and allow its normal flow [197, 198].

Air or gas injection

The injection of air or other suitable gas has the same objective of the brush and cage, and is based on the principle that the high turbulence caused by the air bubbles will erode and dislodge the biofilm. The accessibility is always a question to be considered, as well as the energy needed for the injection of air. Good results have been obtained using this technique for spiral wound membrane elements [199].

2.5.3. Design of control strategies

Even though biofilm prevention is possible in a short temporary scale, due to all the above described mechanisms it is not feasible in an industrial context [200]. Therefore, the control of industrial biofilms involves essentially cleaning methods, in dedicated stages. CIP systems are frequently used, as they allow the cleaning of complete items of plant or circuits, without disassembly and little or no manual effort. However, the variability in CIP effectiveness, particularly in eliminating surface adherent bacteria, is a major disadvantage because residual microorganisms on equipment surfaces promote the rapid re-establishment of biofilms, increasing the biotransfer potential as well as the presence of persistant biofilms and the evolution of the mechanisms of cross-resistance to antimicrobials [149, 201, 202].

Every industry will present a set of specific characteristics that contribute to the biofilms behaviour, as described in section 2.3., which must be taken in consideration when planning the strategy for control. The identification of the microorganism forming the biofilms and the surface where these are would ideally be the first step on the design of a biofilm control strategy [203] (Fig. 2.2). With this information the most appropriate methods must be selected considering the final level of eradication desired, the process, the layout and equipments used, the cost and the environmental burden of its application. For instance, food industries have very

specific legislations for the presence of microbial contaminants due to public health issues [204, 205]. Afterwards, it is necessary to determine the frequency and dosage of the treatment, and this will naturally vary according to the scenario. Even in the same facility, different locations may present biofilms with different thickness and stages of maturation that will respond differently to the control strategy, and this should be taken into account in the initial sampling plan as well.

Once the control strategy is established and the methods are defined, constant monitoring is necessary to assure its efficacy. The first instance of monitoring is by analysis of the final product in the laboratory, which is critic for all the food grade industries, and consequent analysis of the data obtained. The limitation of this is not only the delay between the sampling of the products and the results of the analysis but also the fact that it is not possible to identify the origin of the problem within the process or layout [133]. Many industries limit these monitoring activities to water samples, analysing the number of colony counts, which only indicates the number of bacteria that are able to replicate but neglect viable cells that are non-cultivable or in a dormant state [193]. This is why online monitoring devices are important. Those can be installed in aqueous systems and provide real time data specific for the monitoring of the surface, i.e. excluding signal from the particles in the bulk fluid [133].

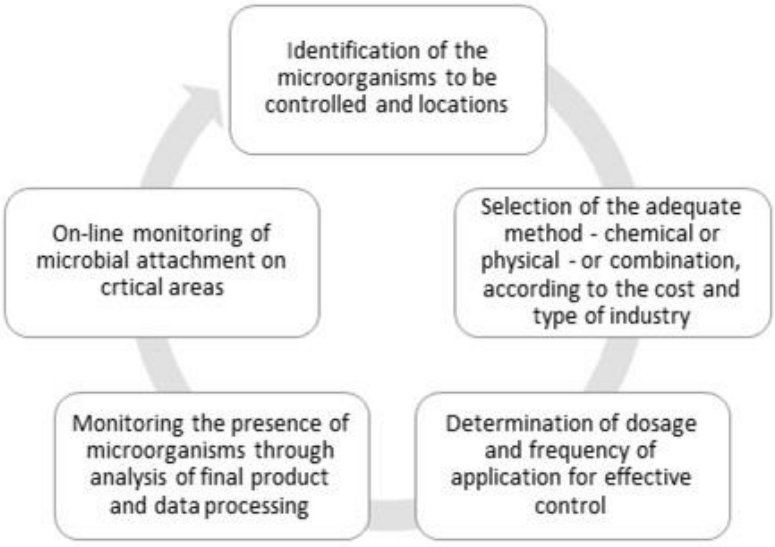

Fig. 2.2 – Steps to consider when planning a strategy for industrial biofilm control.

Many techniques may be employed for this purpose and their monitoring complexity increases from detecting the deposit and its thickness variation, to distinguish biomolecules from the deposit inorganic compounds and finally to assess its chemical composition. On the first category some examples include for instance the Rotoscope [206] that measures the deposits using light absorption or the Mechatronic Surface Sensor [207] that monitors the deposit by measuring a vibration response on the analysed surface. To detect biomass in systems that usually do not present biomolecules, like cooling water systems, it is possible to use attenuated total reflectance Fourier transform infrared spectroscopy (ATR-FTIR) spectroscopy specific for amid bands in a bypass pipe transparent IR. [208] Nuclear magnetic resonance imaging of deposits in pipes allows to map the spatial distribution of biofilm and provides some details about its chemical composition [209].

2.6. Laboratory scale reactors for biofilm control studies

At the laboratory scale, many systems may be used to study biofilm formation and control. These reactor systems are built in order to permit the control and measure a number of important experimental variables [210, 211], as described in Table 2.4.

Table 2.4 – Experimental variables that may be controlled in bioreactors (based on [210, 211])

Chemical	Physical	Biological
	Controlled variables	
Nutrients in the influent pH of the influent Oxygen concentration	Hydraulic residence time Reactor volume Recycle ratio Shear stress on the clean surface Surface area available for growth Surface composition and texture Temperature Volumetric flow rate	Organism type (pure culture, defined consortium or microcosm) Organism concentration entering the reactor
	Measured variables	
Dissolved oxygen Nutrients in the effluent pH of the effluent Growth inhibitors (antimetabolites, antimicrobials)	Pressure drop Shear stress on the biofilm surface	Biofilm thickness Biofilm density Cellular density per surface area Biofilm structure

Biofilm reactors provide multiple and consistent samples that can be used for different studies, including measurements of parameters as biofilm mass, thickness, metabolic activity, cell density, resistance and resilience to chemical or physical stresses and spatial distribution of cells, among others [212]. Regarding the operation mode of the reactor, it can be either continuous or discontinuous. Three general types will be consider in the following description: the batch reactor, the plug flow reactor (PFR) and the continuous flow stirred tank reactor (CFSTR) [210] (Table 2.5) and described in detail in the following sections.

The batch reactor is a closed system, therefore discontinuous, with optional mixing. It may have gases input/output, and the addition of substances for pH control. The main advantage of this configuration is the control of aseptic conditions and the efficient sterilization, as well as the flexibility of operation, as the same reactor can be used to produce different products each time it is used. This mode of operation, has low risk of contamination. However, product accumulation or low substrate concentrations may cause growth inhibition. Batch reactors for biofilm formation will generally have a large number of planktonic cells co-existing with the biofilm, and they are not fit to support stable biofilms for long periods of time [210].

The PFR is a continuous system, where the fluid moves along the reactor so there is minimum mixture in the axial direction, i.e. any differential fluid element will behave like a very small agitated batch reactor, with perfect mixture in the radial direction, moving along the reactor without mixing with the previous or following differential fluid elements. In this arrangement, the nutrients and optionally the microbial culture are introduced to the reactor, and move along its length like a 'plug'. In a biofilm reactor with plug flow, the biofilm metabolic activity will cause gradients on the constituents of the reactor along the axis due to consumption of nutrients and elimination of waste products, so the system should include a second reactor where the nutritional conditions remain stable, with proper mixing and aeration if needed, to recycle the nutrients and microorganisms to the PFR. This configuration is often used to operate as a biofilm reactor because it has radial velocity gradient and along the walls the fluid velocity is low, so cells adhere to the wall of the reactor and therefore to its coupons [213].

A CFSTR is a continuous system where mixing is provided in order to assure that there is no variation or concentration gradients within the reactor volume. A CFSTR bioreactor may also be named a chemostat, when operating under certain conditions. The fresh medium is continuously added to the reactor, and the volume is kept constant by removal from the reactor at the same rate of the input of medium. This rate is the flow rate (Q) and along with the reactor

Table 2.5 – Biofilm reactors grouped according to the flow characteristics (based on [210])

Batch reactor	PFR	CFSTR
Microtiter plate	Modified Robbins device	Chemostat
Biofilm Ring Test®	Drip flow reactor	CDC reactor
Calgary biofilm device		Rotating cylinder reactor
Chamber slide		Rotating annular reactor
		Rotating disc reactor
		Propella®
		Conical Taylor-Couette reactor
		Concentric cylinder reactor
		Flow-cell [1]

[1] The flow cell can work both as a PFR as a CFSTR, however, it is most commonly found operating in the CFSTR mode (described in more detail in section 2.6.1 to 2.6.10).

volume (V) permits the calculation of the residence time (RT), which is the time it takes to entirely exchange the volume of the reactor. Another important parameter in a chemostat is the dilution rate (D), the ratio between the flow rate and the reactor volume. By adjusting the flow rate of the medium in the chemostat it is possible to control microbial growth, the steady state being the point where the specific growth rate (SGR) is equal to the dilution rate. Increasing the flow rate, the substrate concentration also increases and the microbial growth will reach the exponential phase. If this increase is such that the dilution rate is superior to the specific growth rate of the microorganism, washout occurs, i.e., the planktonic cells are removed with the effluent, and adhered cells remain in the reactor. At this point, the system is operating as a biofilm reactor, where the cells will only remain in the reactor if they are adhered on a surface.

Batch reactors

The main batch bioreactor is the microtiter plate, which is a flat plate with multiple wells arranged in a rectangular array with a 2:3 ratio thus resulting in 6, 12, 24, 48, 96 or 384 wells. A single plate provides a large number of similar miniaturized reactors [214], that are easy to handle using robotics systems and multi-channel micropipettes, allowing the fast development of independent samples of biofilm. Rapid and inexpensive techniques have been developed for quantifying biofilm formation and its bioactivity, such as crystal violet staining for determining biomass [215, 216], or the alamarBlue® technique to the determine cell metabolic activity [217, 218]. The most common model used for biofilm tests is the 96-well plate with a work volume of 200-250 µL per well, saving reagents and appearing as an economic platforms for screening

assays [219]. There is also the possibility of using the 6, 12, 24 or 48-well plates to assess the biofilm formation on the air-liquid interface [220] and the potential of the adhesion of the bacteria [40, 221-223] by inserting slides in the wells of the microtiter plates so that the biofilm grows in the surface of those coupons. Some clinical tests were also performed with microtiter plates, where the researchers established an association between virulence and biofilm formation [224-226], as well as screening tests for antimicrobial activity against biofilms, either with antibiotics [223, 227-229], antifungals [230, 231], biocides [232-234], phytochemicals [218, 235-239] and quorum-sensing inhibitors [240].

Other batch systems available for biofilms studies were derived from the microplate model, like the Biofilm Ring Test® or the Calgary device. The Biofilm Ring Test® is a technology commercialized by BioFilm Control SAS (France). The method relies on the addition of the paramagnetic beads to the bacterial culture solution before the incubation of the microtiter plates. The plate is placed in a magnetic holder and the beads will rest immobilized (positive result) or migrate radially (no biofilm formed) according to the biofilm formation. This technique can be used to evaluate the early stages of biofilm formation [241-243] including the effect of drug activity on early biofilm formation [244].

The Calgary biofilm device, developed in 1996 at the University of Calgary [245], is commercially available as the Minimal Biofilm Eradication Concentration Assay System (MBEC™) – through Innovotech Inc., Edmonton, Canada. This system is based on a 96-well microplate with downward-pointing depressions (pegs) attached to the lid. The aim is for the biofilms to develop on the surface of the pegs so the inoculation follows the same procedure as in any biofilm microtiter assay. After biofilm formation, the lid is transferred to other plates for further steps of the protocol and quantification methods in order to quantify the biofilm mass and number of viable cells and thus determine the MBEC (defined as the minimal concentration of antibiotic required to eradicate the biofilm). This method has been used for evaluating the efficacy of antimicrobial agents [246-248]. It is also possible to remove the pegs individually for further observations of the biofilm in scanning electron microscopy (SEM) [249, 250] and confocal laser scanning microscopy (CLSM) [251], after the appropriate treatment. There is also the possibility of coating the surface with a number of materials to facilitate the growth of fastidious microorganisms. Harrison et al. [251] described protocols for the study of *Candida* spp. biofilms in the Calgary Biofilm Device where the pegs had been coated with a solution of 1.0% L-lysine.

Chamber slides are focused for microscopy of *in situ* tissue culture and are commercially available as the Lab-Tek ® II Chamber Slide™ System, property of Nunc (Thermo Fisher Scientific

Inc.). This device is composed of a standard glass microscope slide with an attached growth chamber, which is removable and may be individual or may have 2-, 4- 8- or 16-well configurations. Biofilm tests may be performed in the chambers following the microtiter plate's protocols, and the biofilm is formed preferentially on the slide. Different tests may be performed as well, namely antimicrobial treatments, and then the chamber can be removed so that the slide is used to observe the biofilm structure with microscopic methods. [252]. This method has been used for analysis of the biofilm architecture using CLSM [251].

Plug-flow biofilm reactors

2.6.1. Modified Robbins device

The actual Modified Robbins device (MRD) was adapted from the original Robbins device by Jim Robbins at the University of Calgary [253]. This type of reactor is constituted by a main block, built in stainless steel or acrylic, channelled in a rectangular cross-section along its length. The top is designed with a linear set of sampling ports, where plugs are connected in the inner surface, with the coupons of the testing material (Fig. 2.3). The first MDR was presented by Nickel et al. [253] and is now commercially available from BioSurface Technologies or Tyler Research Corporation. Dimensions of the device vary depending on the number of ports. The commercial versions can withstand low to high pressures and may have 10 to 25 ports for the sampling plugs, generally with a surface area of 50 mm^2. Alternatively there are cassette-type low pressure MDR devices that hold 10 rectangular coupons (38mm x 19mm, 5 per cassette) of different materials.

The nutrient medium and other desired fluids like the microbial bacterial culture or antimicrobials are pumped through the MDR. Regarding the inoculation of the system, it may be inoculated in an inverted position during an initial period of time, to promote the bacterial adhesion to the slides, or there may be a chemostat assembled before the inlet of the MDR, providing a continuous inoculum [254]. The main application of the MDR is the assessment of the effect of diverse materials on biofilm prevention and control [255-257], as well as testing antimicrobials and phytochemicals with the aim of inhibiting biofilm formation [258, 259]. As this configuration has flexibility in terms of the setup, it allows the formation of biofilms in the

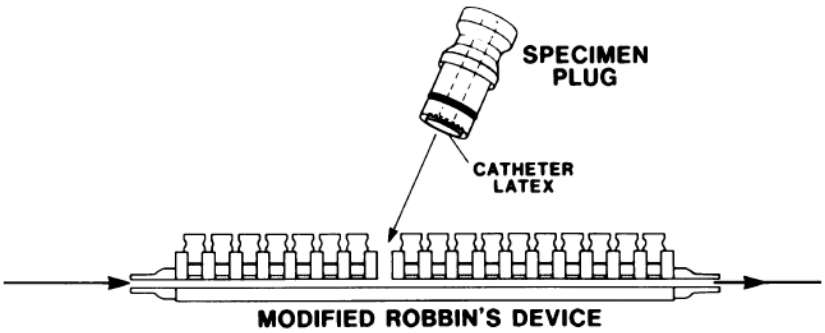

Fig. 2.3 – Schematic representation of the MDR (adapted from Nickel et al. [253]).

absence of flow to simulate an artificial throat for studies of biofilm formation on shunt prostheses [260, 261].

2.6.2. Drip flow reactor

The drip flow reactor (DFR) is characterized by having coupons in an inclined plan, continuously irrigated by nutrient medium. The medium is dripped onto the coupons at typically low flow rates (0.8 mL/min) [262], thus resulting in mild shear environments where biofilms are formed near to the air-liquid interface. The atmosphere inside the reactor can be altered in order to grow anaerobic biofilms [262]. The experimental setup of this reactor is simple (Fig. 2.4). The DFR is commercially available from BioSurface Technologies. This configuration allows around 4 coupons with dimensions generally similar to the ones of microscope slides (2.5 x 7.5 cm).

Several materials can be used as adhesion surface for biofilm formation, and many techniques can be further used to analyses the biofilm, including plate counting and microscopy methods preceded or not by cryosectioning. [54, 263]. Due to the properties of the biofilms formed in this system, it has been used for studies of spatial physiology of biofilms [263, 264], as well as to mimic biofilm formation in catheters by *Staphylococcus epidermidis* [265] and assess the efficacy of powered brushing on the removal of *Streptococcus mutans* biofilms [266]. It has also been used for biofilm susceptibility tests to disinfection procedures [54, 267, 268].

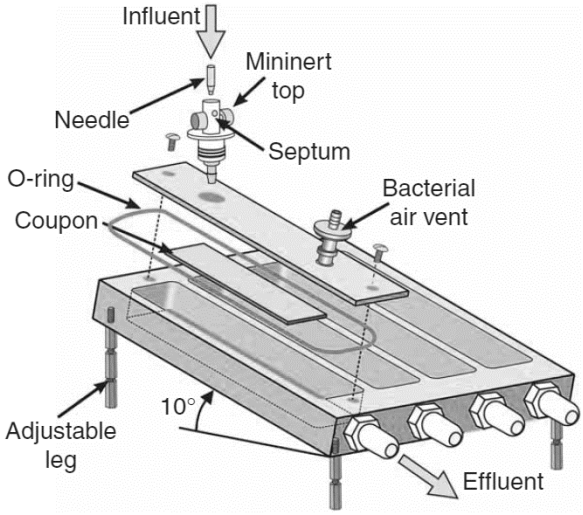

Fig. 2.4 – Schematic representation of the DFR (adapted from Goeres et al. [262]).

Continuous biofilm reactors

2.6.3. Chemostat

The chemostat operating as a biofilm reactor consists in a vessel, with continuous medium input and waste output (Fig. 2.5). Aeration is provided by input of sterile air and generally a magnetic stirrer is used for agitation. The chemostat may be either inoculated with a bacterial culture in the beginning of the experiment or it may be continuously inoculated by a bacterial culture of planktonic cells growing in another upstream chemostat of smaller volume. This smaller chemostat must have the growth conditions adjusted to guarantee a permanent bacterial culture in the exponential phase of growth. In the main chemostat the biofilm is formed on slides that may have different shapes (square or circular) and may be manufactured from a wide range of materials. A vertical support is used to hold the slides so that they can easily be removed after the appropriated period for biofilm formation. The volume of the tank may vary between 3-5L and the volume of the chemostat is 0.5 L.

The biofilm formation in the chemostat is caused mainly by the increased dilution rate due to the high flow rate of nutrient medium. The main advantages of this reactor are the high number of samples and versatility of materials that may be used for the slides, but on the other

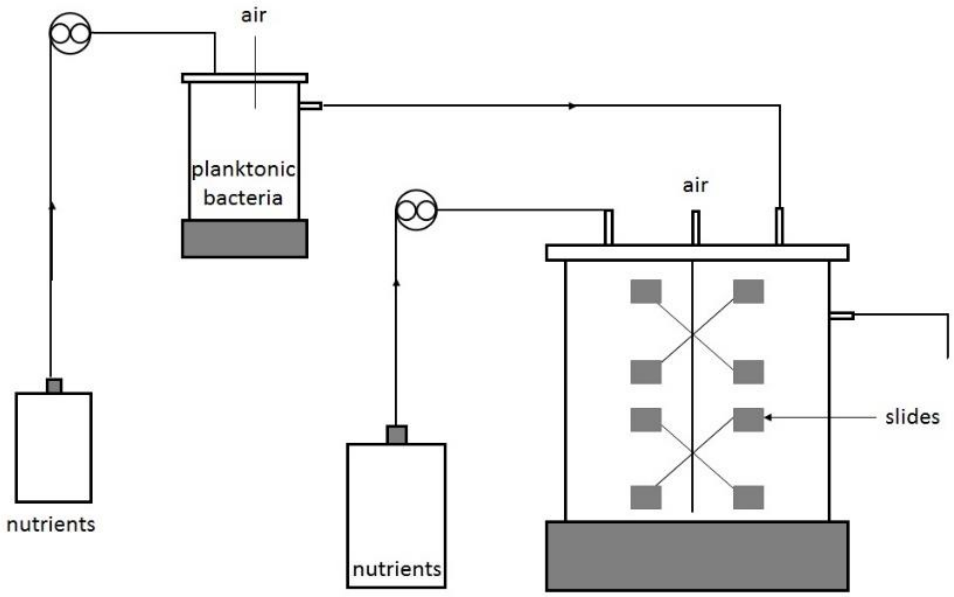

Fig. 2.5 – Schematic representation of the experimental setup for the chemostat biofilm reactor, including the smaller chemostat for pre-inoculation (left) and the chemostat for biofilm formation (right) (adapted from Simões et al. [160]).

hand they are exposed to very low shear stress conditions. The chemostat has been used for biofilm formation control studies, with single species biofilms [269], dual-species biofilms [160], drinking water biofilms [48], and also for assessing the effect of surface pre-conditioning in the antimicrobial action of biocides [270].

2.6.4. Centers for Disease Control (CDC) reactor

The CDC biofilm reactor is commercially available from BioSurface Technologies. This reactor is constituted by a glass vessel with a volume of 1L and an effluent spout on the side. The total liquid volume is approximately 350 ml. It has a special lid made of ultra-high-molecular-weight polyethylene, which supports eight polypropylene rods, accommodating three 12.7 mm diameter coupons each (Fig. 2.6). The bulk fluid is mixed by a baffled stir bar that is magnetically driven therefore the coupons where cells adhere are exposed to equivalent shear stress forces [271, 272].

This configuration is a well suited *in vitro* biofilm model for applications that include growing biofilms on test surfaces as it supports 24 coupons, available in a wide variety of

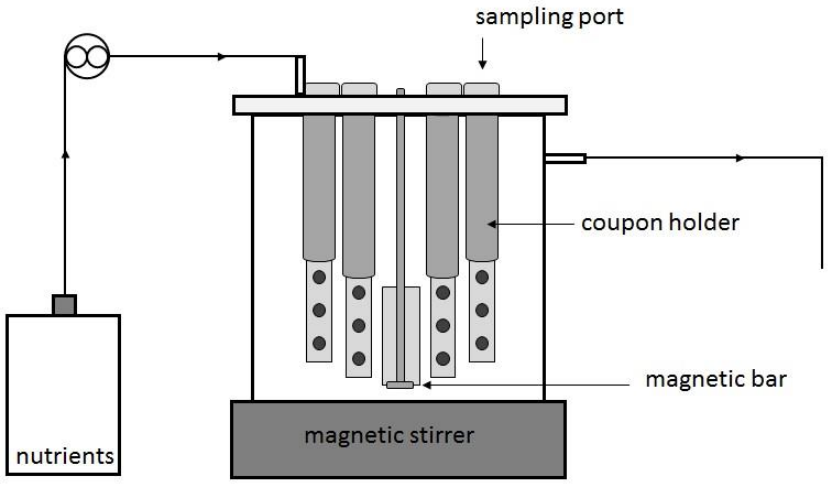

Fig. 2.6 – Schematic representation of the CDC biofilm (adapted from Williams et al. [273]).

materials [273]. Each rod can be removed individually, allowing the sampling of coupons in different moments along the experiment [274]. The CDC biofilm reactor is part of the ASTM Standard Method E2562-07: Standard Test Method for Quantification of *Pseudomonas aeruginosa* Biofilm Grown with High Shear and Continuous Flow using CDC Biofilm Reactor, and is used in for antimicrobial testing and assessment of disinfection and cleaning measures with clinical biofilms [268, 275, 276]. As it provides continuous flow conditions, Nailis et al. [277] grew *C. albicans* biofilms in a CDC reactor to be used to analyse the kinetics of *ALS1* and *ALS3* gene expression. More recently biofilm grown using the CDC biofilm was analysed through different SEM methods, for the purpose of observing the biofilm matrix of *Staphylococcus epidermidis* [272]. These results showed that after 48 h of growth the biofilms formed on the CDC reactor produce EPS matrix with mushroom or pillar-like structures with signs of water channels, indicating mature biofilm development.

2.6.5. Rotating annular reactor – Rototorque reactor

The biofilm rotating annular reactor (RAR), also known as the Rototorque reactor [278], commercially available from BioSurface Technologies, is constituted by a vessel with a rotating inner cylinder, in a configuration similar to a Taylor-Couette reactor [279]. The removable slides are attached to the inner cylinder, which is powered by an external electric motor. The vessel wall is considered the stationary outer cylinder and the biological fluid is circulated in the annulus between the two cylinders (Fig. 2.7). The reactor's volume is 1L.

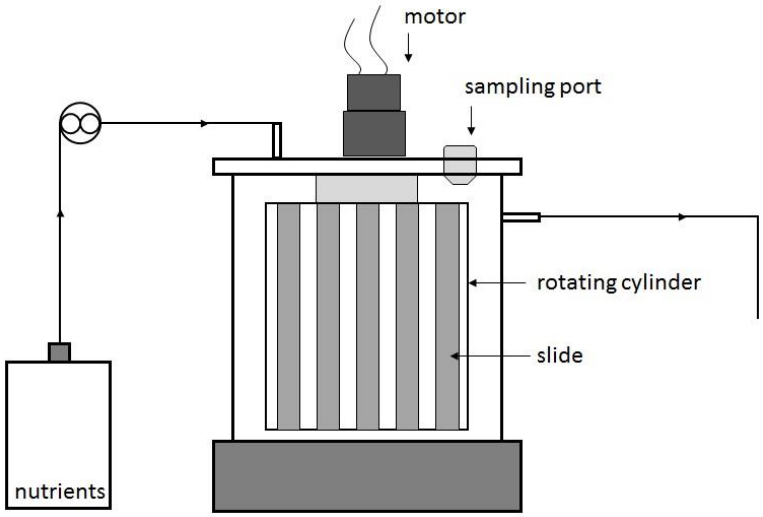

Fig. 2.7 – Schematic representation of the RAR (adapted from Lawrence et al. [280]).

This reactor supports a large number of slides (around 22) and has ports on the top that allow the access to those slides in any moment. The experimental setup of this type of reactor is similar to the previous described (chemostat, CDC reactor), requiring a pre-inoculum from a chemostat. This reactor reproduces conditions observed in drinking water systems [188, 210]. There is also the option of controlling the temperature using a jacketed model that allows circulation of heating or cooling fluids. This is an advantage that was used in disinfection studies for drinking water systems, to mimic the seasonal variations of temperatures and assess the different needs for residual disinfectants to control the biofilms [281, 282]. Moreover, the annular reactor has been used for assays with environmental biofilms [188, 283], including the effect of temperature on their formation along with microscopy techniques like CLSM [284] or fluorescent *in-situ* hybridization (FISH) [285].

2.6.6. Conical Couette-Taylor Reactor

The conical Couette-Taylor reactor (CCTR) is a variation of the annular reactor designed to simulate different shear stress conditions in a single device. The configuration consists of two concentric parallel cones: a rotating inner cone placed inside a stationary outer cone. As the two cones have the same apex angle the gap between them is constant in the vertical direction (Fig. 2.8). This reactor follows the Taylor-Couette flow, i.e., the wall shear stress is dependent on the gap between the two cylinders, the radius of the inner cylinder and the rotating velocity. As the gap is constant the wall shear stress is distributed along the height of the inner cone [286].

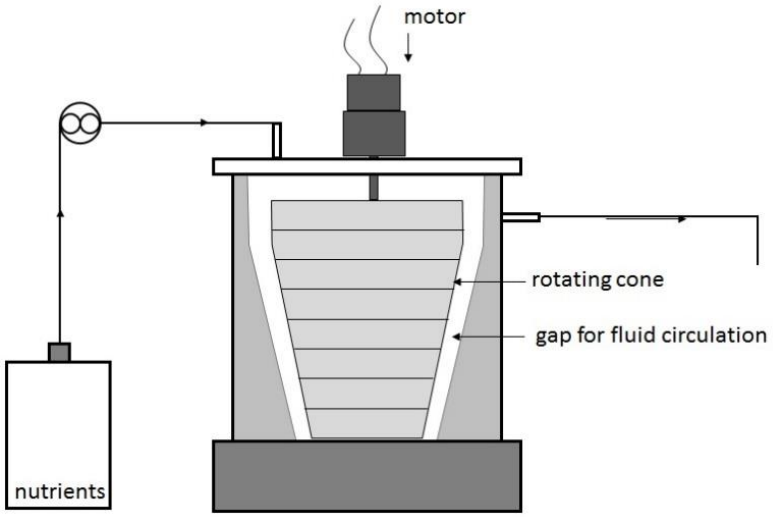

Fig. 2.8 – Schematic representation of the CCTR (adapted from Rochex et al. [13]).

The model presented by Rochex et al. [13] allows shear stress distribution of 0.055 to 0.27 Pa, from the bottom to the top of the reactor and was used to show the effect of shear stress the composition biofilm of bacterial communities.

2.6.7. Concentric cylinder reactor

The concentric cylinder reactor (CCR) consists in four cylinders of increasing radius supported by a plate in a vertical concentric manner. The bottom has four concentric chambers that are stationary and have inlet and outlet ports as well as sampling ports (Fig. 2.9). As the cylinders rotate at different speeds and have different radius, the rotating surfaces will experience different wall shear stresses. Starting from the same inoculum, each chamber can be fed independently and at different flow rates, being their volume maintained constant by means of pumping the overflow. The evaluation of the biofilm formed implies dismantling the reactor and removing the biofilm from the surfaces by means of a scrapper or a swab, therefore the possibilities in terms of analysis are reduced when compared with other systems with smaller coupons. Willcock et al. [287] presented this configuration to investigate the influence of shear rate on biofilm formation and mimic cleaning-in-place cycles. Rickard et al. [64] also used the CCR to investigate the influence of shear rates on the diversity of freshwater biofilm, with focus on the proportions of aggregating bacteria.

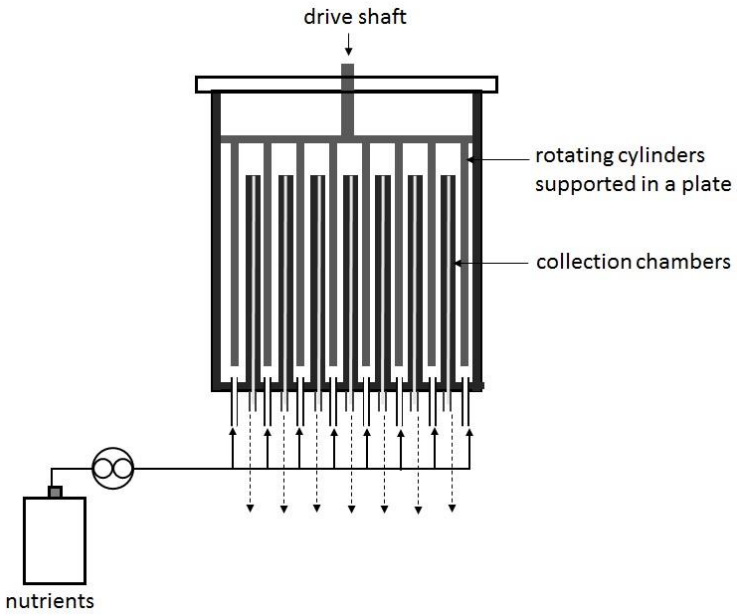

Fig. 2.9 – Schematic representation of the CCR (adapted from Willcock et al. [287]).

2.6.8. Rotating disc reactor

The rotating disc reactor (RDR) is commercially available from BioSurface Technologies. It is composed by a glass vessel (1L) with an effluent side spout and a disc made of Teflon™ and Viton® with recesses for six circular coupons (1.25 cm of diameter). This disc has a magnet incorporated, so that it is stirred by a magnetic external stirrer, causing rotational fluid motion and therefore surface shear on the coupons (Fig. 2.10). These removable coupons may be manufactured in a large diversity of materials, as in the case of the CDC reactor. The operation mode is similar to the CDC reactor, both regarding the sampling methods as the further analysis to be performed to the removed coupons. However, due to its arrangement, this system is more adequate for growing biofilm under moderate shear conditions [288].

The RDR is included in the ASTM Standard Method: ASTM E2196-07 Standard Test Method for Quantification of a *Pseudomonas aeruginosa* Biofilm Grown with Shear and Continuous Flow Using a Rotating Disc Reactor. It has been used for studies of biofilm resistance [289-291], multispecies biofilms [292, 293] and evaluation of antimicrobials and disinfection procedures [268, 275].

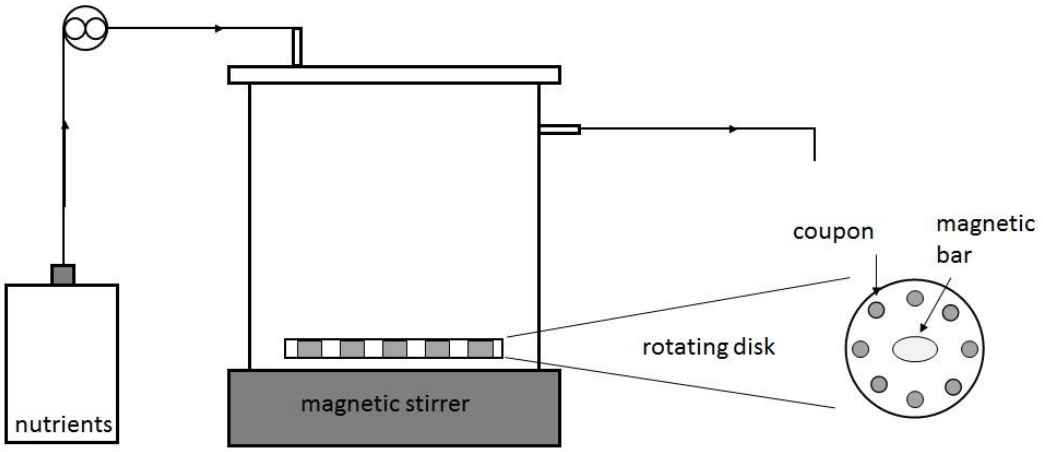

Fig. 2.10 – Schematic representation of the RDR (adapted from Murga et al. [293]).

2.6.9. Propella®

The Propella® reactor is a complex system, constituted by two concentrically aligned pipes, being the outer pipe equipped with coupons slides for biofilm sampling. Inside the inner pipe there is a propulsive propeller which rotation at high velocities causes the fluid motion down the inner pipe an upwards the annular space between the two pipe (Fig. 2.11). Controlling the rotation speed of the propeller, it is possible to define the Reynolds number and thus the hydraulic regime in the reactor. This type of reactor supports a large number of coupons, which may be manufactured in any type of machinable material.

The system used by Manuel et al. [48] had an internal volume of 2.23 L and supports 20 coupons of 2.0 cm^2 each.

The main advantages of this reactor are similar to those of the Rototorque, particularly the possibility to simultaneously control temperature and flow velocity, hydraulic residence time and Reynolds number [294]. The Propella® has been used mainly for studies evolving drinking water biofilms [48, 295-298].

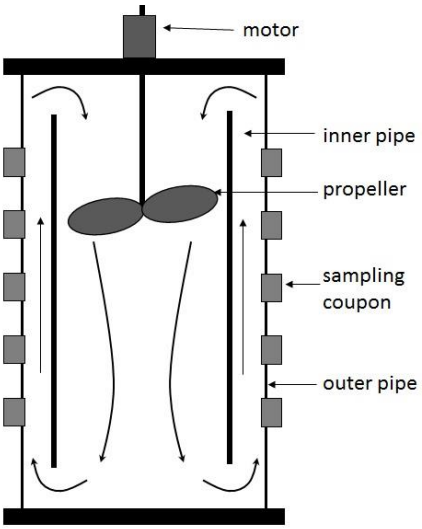

Fig. 2.11 – Schematic representation of the Propella® reactor (adapted from Manuel [299]).

2.6.10. Flow-cell

The flow-cell reactor design is based on the Modified Robbins device (section 2.6.1), however, it is usually placed in a vertical position. It is composed by a PMMA block with semi-circular inner section. Several sampling coupons which can be periodically removed without stopping the flow inside the reactor. The dimensions of this cell may vary between around 30 to 100 cm, and the number of dimensions of coupons vary as well. On these coupons, flat slides of the testing surface materials are attached so they are in contact with the fluid circulating inside the flow-cell. Despite some flow cell configurations work with continuous flow and therefore may be are considerate PFR, generally the flow cell operates with continuous recirculation of the fluid provided by centrifuge pumps, thus the typical residence time distributions approximate this reactor type to a CFSTR [300]. The recirculation tank operates as a chemostat where the growth conditions are kept constant, including feeding, temperature control through a recirculating water bath, pH monitoring, and sterile aeration. This tank, with variable volume (from 1 to 5 L) may be either inoculated in the beginning of the experiment or continuously inoculated by another smaller chemostat where the microbial culture is growing at the exponential phase of growth. This reactor configuration is ideal for biofilm monitoring during time as it allows the sampling of individual coupons with no disturbance of the flow. There are outlet ports in the opposite face of the flow cell to that which has the coupons so that it is possible to deviate the circulating flow in the immediate point before the coupon to be removed (Fig. 2.12).

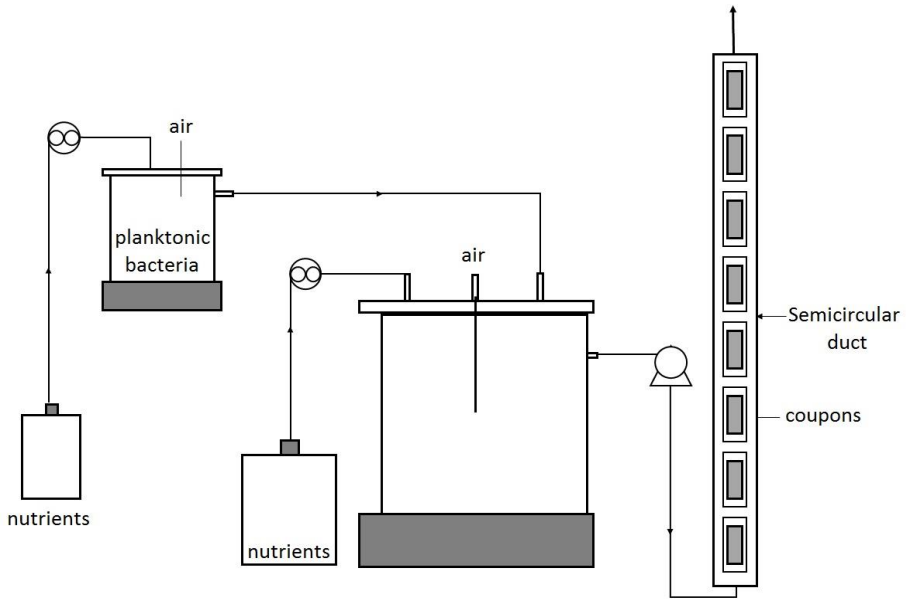

Fig. 2.12 – Schematic representation of the experimental setup for the flow-cell (adapted from Teodósio et al. [301]).

A wide range of materials may be used as surface for biofilm formation. Frequently the experimental setup includes two parallel flow-cell reactors operating with recirculation from the same tank. It is possible to control the flow rate in each of those cells and therefore the Reynolds number, thus having different hydraulic regimes on each flow cell [302]. This system is highly adaptable and has been used for laboratory scale recreation of industrial scenarios where biofilm is common [301], from studies of influence of hydrodynamic conditions on the biofilm formation [48, 58, 84, 302-304], to the evaluation of the action of biocides in biofilms formed under different flow regimes [183, 201, 305, 306].

2.7. Biofilm reactor selection

The selection of the reactor must take in consideration mainly the environment of the biofilm formation, as well as the further analyses to be performed. As the nutritional conditions are easily controlled, as well as the temperature, the reactor selection should take in consideration the desired hydrodynamic conditions (Table 2.6) to produce the biofilm. Hence, the reactors described previously may be categorized according to the shear stress imposed to the microbial cells.

Table 2.6 – Bioreactor categorization based on the magnitude of shear stress.

Low shear	Moderate to high shear	High shear
Microtiter plate	Modified Robbins device	CDC reactor
Chamber slide	Rotating disk reactor	Conical Couette-Taylor reactor
Biofilm Ring test	Rototorque	Concentric cylinder reactor
Calgary device	Conical Couette-Taylor reactor	Propella®
Drip flow reactor	Concentric cylinder reactor	Flow cell
Chemostat		

There are also a lot of sampling and analysing techniques, that may be performed when the biofilm is still attached to the coupon, like thickness measuring or microscopy observations, with epifluorescence microscopy, CLSM, SEM, etc. Other techniques from the fields of microbiology as well as molecular biology require the scrapping of the biofilm from the surface of the coupon, or sonication in the case of microtiter plates and the Calgary devices, allowing the use of further methods to characterize the biofilm [307]

The laboratory biofilm reactors allow studies where the biofilm processes are controlled and are ideal for screening and initial tests, where those processes are quantified. The biofilm reactors' configuration should reproduce as much as possible the real environment where biofilms are encountered: there is no universal system suitable to study all the possible variables. The reproducibility in the tests obtained in biofilm reactors will depend on the hypothesis being studied and consequently on the controlled variables. Some variables may not be controlled at the same extent for all the experiments. An example would be the amount of signalling molecules secreted by cells or the pH in the boundary layers near the biofilm. These variables may be measured but not controlled: the operator can guarantee the reproducibility of the experimental conditions and measurements but he cannot guarantee reproducible results [211, 308]. As new and more efficient biofilm control strategies are required, it is expected that the biofilm reactors keep evolving to more controlled and robotized systems, with the tendency to get more focused to specialized areas, either in the industrial or biomedical fields.

CHAPTER 3

Materials and methods

3. Materials and Methods

3.1. Bacteria and culture conditions

Two model bacteria, the Gram-positive *Bacillus cereus* and the Gram-negative *Pseudomonas fluorescens* were selected as they are commonly contaminants encountered in industrial biofilms [309-311]. The bacterial strains used in this work were *P. fluorescens* ATCC 13525^T and a *B. cereus* strain isolated from a disinfectant solution and identified by 16S rRNA gene sequencing, according to Simões et al. [312]. Bacterial growth conditions were 27 $\pm$ 2 °C and pH 7, with agitation at 120 rpm in an orbital incubator (AGITORB 200, Aralab, Portugal) [313].

Chromobacterium violaceum CV12472 was also used to determine quorum sensing inhibition (QSI). This strain was kindly provided by Professor Robert McLean from Texas University, USA. This bacterium was grown aerobically at 27 ± 2 °C with agitation at 150 rpm in a shaking incubator (AGITORB 200, Aralab, Portugal).

3.2. Nutrient Media

Both *B. cereus* and *P. fluorescens* cells were routinely cultured aerobically in a sterile (autoclaved at 121 °C for 20 min) concentrated nutrient medium (CNM) consisting of 5 g glucose/L, 2.5 g peptone/L and 1.25 g yeast extract/L, in 0.2 M phosphate buffer (KH_2PO_4; Na_2HPO_4) (PB). All the components were obtained from Merck (VWR, Portugal).

C. violaceum CV12472 was routinely cultured aerobically in Lysogeny-broth (LB; Liofilchen, Italy) with the Lennox formulation (5g/L NaCl).

For biofilm formation in the biofilm reactor, a sterile diluted nutrient medium (DNM) was used. The DNM was a 1:100 dilution of the CNM in 0.2 M PB.

Stock cultures of all the bacterial species were cryopreserved in vials with 70% of the respective culture media and 30% of glycerol, at -80 °C. To activate the bacteria, 10 µL of cryopreserved suspension was stroked on plate-count agar (PCA, Merck) and incubated during 24 h at 27 ± 2 °C in an incubator (AGITORB 200, Aralab, Portugal).

3.3. Chemicals tested

Two phytochemicals that belong to the group pf the phenolic acids were tested, ferulic acid (FA) and salicylic acid (SA) (Sigma-Aldrich, Portugal) (Fig. 3.1 *a* and *b*). Due to their low solubility in water, FA and SA were prepared in dimethyl sulfoxide (DMSO) (Sigma-Aldrich). The tests were performed in the presence of FA, SA and a combination (1:1) of FA and SA (FSA). Phytochemicals are routinely classified as antimicrobials on the basis of susceptibility tests that produce inhibitory concentrations in the range of 100 to 1000 µg/mL [314], which was the range of concentrations tested.

A cationic surfactant, benzyldimethyldodecyl ammonium chloride (BDMDAC, Fig. 3.1*c*) (Sigma-Aldrich) was also used as antimicrobial agent. Solutions of different concentrations (5 to 500 µg/mL) were prepared in sterile ultrapure water.

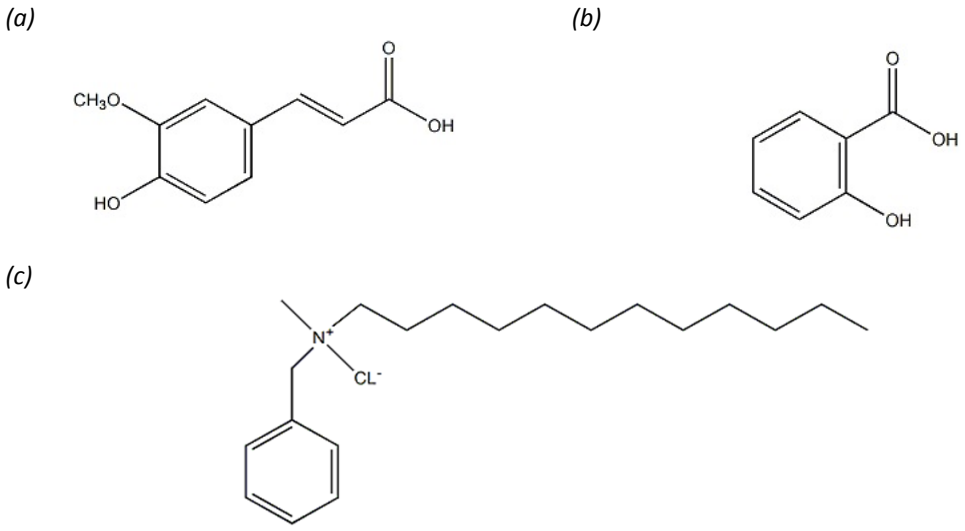

Fig. 3.1 – Chemical structures of FA (a) and SA (b) and BDMDAC (c).

3.4. Surfaces

The materials tested along this work were:

- AISI316 stainless steel (SS)
- High-density polyethylene (HDPE)
- Polymethyl methacrylate (PMMA)
- Polystyrene (PS)

The surfaces used (Neves & Neves, Muro, Portugal) were flat slides of either 3 cm^2 for contact angle measurements or 1 cm^2 for the adhesion assays, and with thicknesses of approximately 1 mm (SS) to 1.5 mm (HDPE, PMMA and PS). The surfaces were cleaned by immersion in a solution of commercial detergent (Sonasol Pril, Henkel Ibérica S. A.) in ultrapure water for 30 min. After rising with ultrapure water, surfaces were immersed in ethanol at 70% (v/v) (SS for 30 min; HDPE, PMMA and PS for 1 min). The surfaces were rinsed three times with ultrapure water and dried at 65 ºC for 3 h. In the Rotating Cylinder Reactor (RCR), biofilms were grown in cylinders of PMMA, SS or HDPE with length = 5.0 cm and diameter of 2.2-2.8 cm (depending on the material as indicated in the corresponding chapter). The cylinders were cleaned as described above and placed in the reactor. The RCR was sterilized with the cylinders mounted in place, by recirculating a solution of 15% (v/v) of sodium hypochlorite (Sigma-Aldrich, Portugal) during 12 h. After the sterilization, the system was rinsed twice with sterile distilled water to remove the residual sodium hypochlorite.

3.5. Growth inhibitory activity – minimum inhibitory concentration

To determine whether the presence of the selected chemicals had some effect on the bacterial growth in liquid medium, the minimum inhibitory concentration (MIC), considered the lowest concentration of an antimicrobial that will inhibit the visible growth of a microorganism after incubation, was determined using a microtiter-plate-based assay [315]. Several concentrations of the selected chemicals were prepared by diluting the stock solutions in the appropriated solvent (sterile distilled water or DMSO). Overnight grown cultures were diluted with fresh CNM in order to set the optical density, at 610 nm (OD_{610}), to 0.4 ± 0.02 for *P. fluorescens* and 0.8 ± 0.02 for *B. cereus*, corresponding approximately to 1×10^8 cells/mL. A sterile 96-wells microtiter plate (Orange Scientific) was inoculated with fresh sterile growth medium, the bacterial suspension, and the chemicals at different concentrations. The bacterial suspension and growth medium complete 90% of the well working volume (200 µL). The volume of chemical added was always ≤ 10% of the total working volume. After incubation in an orbital shaker (24 h, 120 rpm, 27 ± 2 ° C), the OD_{610} in the microtiter plate was measured using an Absorbance Microplate Reader (Spectramax M2e). The lowest concentration of chemical molecule where no growth was detected was considered the MIC of the molecule.

3.6. Motility assays

Swimming and swarming motilities were assessed in the presence of selected chemical molecules. For this assay the solid growth medium was composed of 1% (w/w) tryptone, 0.25% (w/w) NaCl and agar at different concentrations (w/w): 0.3% for swimming and 0.7% for swarming assays [235, 316].The characterization of different types of bacterial motility is based on the use of different concentrations of agar, which originates different levels of porosity of the medium, therefore allowing different levels of bacterial diffusion [235]. All the components were obtained from Merck (VWR, Portugal). The chemicals were incorporated in the growth medium (tempered at 45 °C). A sub-inhibitory concentration (1/5 of the MIC) was used to ensure that the effects on motility inhibition were not due to antimicrobial activity. Overnight grown cultures were washed three times (3777 g, 5 min) with PB and ressuspended in PB to a final concentration of 1×10^8 cells/mL. Aliquots of 15 µL of these cultures were applied in the centre of plates, which produced an 8 mm halo (defined as the baseline). The motility halos were measured at 12, 24, and 48 h. Three plates were used to evaluate the motility of each bacterium and three independent experiments were performed.

3.7. Bacterial surface free energy

The bacterial surface free energy was determined by the sessile drop contact angle measurement on cell layers according to Busscher et al. [317]. Contact angles of the bacteria non-exposed and exposed to the selected chemicals, for 30 min, and of the adhesion surfaces were determined automatically using an OCA 15 Plus (DATAPHYSICS, Germany) video-based optical measuring instrument, allowing image acquisition and data analysis, and ≥ 25 contact angle measurements (per liquid and sample) were carried out according to Simões et al. [318]. The surface energy components of bacteria and adhesion surfaces were obtained by measuring the contact angles with three pure liquids: water, formamide and α-bromonaphthalene (Sigma, Portugal). Reference values for these liquids' surface tension components were obtained from the literature [319]. The approach developed by van Oss (1987, 1988, 1989) was used to determine the hydrophobicity after contact angle measurement. As stated by this approach, the degree of hydrophobicity of a given material (1) is expressed as the free energy of interaction between two entities of that material, when immersed in water (w) [ΔG_{1w1} (mJ/m^2)]. If the interaction between the two entities is stronger than the interaction of each entity with water, $\Delta G_{iwi} < 0$ and the material is considered hydrophobic. Conversely, if $\Delta G_{1w1} > 0$ the material is

hydrophilic. ΔG_{1w1} can be calculated through the surface tension components of the interacting entities, according to equation 3.1:

$$\Delta G = -2\left(\sqrt{\gamma_1^{LW}}-\sqrt{\gamma_w^{LW}}\right)^2 + 4\left(\sqrt{\gamma_1^+\gamma_w^-}+\sqrt{\gamma_1^-\gamma_w^+}-\sqrt{\gamma_1^+\gamma_1^-}-\sqrt{\gamma_w^+\gamma_w^-}\right) \quad (3.1)$$

where γ^{LW} is the Lifshitz-van der Waals component of the surface free energy, and γ^+ and $\gamma^-$are, respectively, the electron acceptor and electron donor parameters of the Lewis acid-base component(γ^{AB}), where $\gamma^{AB} = 2\sqrt{\gamma^+\gamma^-}$.

The surface energy components of a surface (s) (bacterium or substratum), were obtained by measuring the contact angles of the three pure liquids (l) with known surface tension components, followed by the simultaneous resolution of three equations (one for each liquid) of the form:

$$(1+\cos\psi)\gamma_1^{Tot} = 2\left(\sqrt{\gamma_s^{LW}\gamma_l^{LW}}+\sqrt{\gamma_s^+\gamma_l^-}-\sqrt{\gamma_s^-\gamma_l^+}\right) \quad (3.2)$$

where ψ is the contact angle and $\gamma^{Tot} = \gamma^{LW} + \gamma^{AB}$.

3.8. Free energy of adhesion

The free energy of adhesion between the bacteria and the adhesion surfaces was assessed according to Simões et al. [323].When studying the interaction between substances 1 and 2 that are immersed or dissolved in water, the total interaction energy, ΔG_{1w2}^{Tot}, can be expressed as :

$$\Delta G_{1w2}^{Tot} = \gamma_{12}^{LW} - \gamma_{1w}^{LW} - \gamma_{2w}^{LW} + 2\left[\gamma_w^+\left(\sqrt{\gamma_1^-}+\sqrt{\gamma_2^-}-\sqrt{\gamma_w^-}\right)+\sqrt{\gamma_w^-}\left(\sqrt{\gamma_1^+}+\sqrt{\gamma_2^+}-\sqrt{\gamma_w^+}\right)-\sqrt{\gamma_1^+\gamma_2^-}-\sqrt{\gamma_1^-\gamma_2^+}\right]$$

(3.3)

Thermodynamically, if $\Delta G_{1w2}^{Tot} < 0$, adhesion is favoured, whereas adhesion is not expected to occur if $\Delta G_{1w2}^{Tot} > 0$ mJ/m².

3.9. Bacterial surface charge - zeta potential

The electrostatic component surface potential is commonly described using the zeta (ζ) potential, which is a measurement of electrical surface charge. The zeta potential of bacterial suspensions, before and after treatment with the selected chemicals, was determined using a Nano Zetasizer (Malvern Instruments, UK). Cell suspensions in ultrapure water (pH 6), without chemicals, were used as controls. The zeta potential was measured by applying an electric field across the bacterial suspensions. Bacteria in the aqueous dispersion with non-zero zeta potential migrated towards the electrode of opposite charge, with a velocity proportional to the magnitude of the zeta potential.

3.10. Bioassay for detection of quorum sensing inhibition

A standard disc diffusion assay [324] was performed with biosensor strain *C. violaceum* CV12472 to detect quorum sensing inhibition (QSI) activity of the selected phytochemicals according to McLean et al. [325]. Briefly, plates of solid LB (13 g/L agar) were inoculated with 100 µL (1.4×10^8 CFU/mL) of overnight cultures of *C. violaceum* CV12472. Afterwards, sterile paper disks (6 mm in diameter) (Oxoid, Spain) were placed over the plates and were loaded with 15 µL of different concentrations of each phytochemical. DMSO and LB broth were used as controls. Plates were incubated for 24 h at 30 °C to check the inhibition of pigment production around the disc (a ring of colourless but viable cells). Antimicrobial activity is indicated by lack of microbial growth. Bacterial growth inhibition was measured as diameter (d1) in mm while cases showing both inhibition of growth and inhibition of production of pigment were measured as diameter (d2) in mm. QSI, assessed by pigment inhibition, was determined by subtracting bacterial growth inhibition diameter (d1) from the total diameter (d2): QSI = (d2-d1), according to Zahin et al. [326].

3.11. Biofilm formation in microtiter plate

Biofilms were developed according to a modified microtiter plate test proposed previously [215]. Single and dual-species 24 h old biofilms were grown in sterile 96-wells flat bottomed PS tissue culture microtiter plates (Orange Scientific, USA). The microtiter plates were inoculated with 180 µL of fresh CNM and 20 µL of a bacterial suspension with a cell density of

1×10^8 cells/mL. Dual-species biofilms were formed with a mixture of equal volumes of *P. fluorescens* and *B. cereus*, with the same cell density as described for single species biofilms [221]. The microtiter plates were incubated for 24 h in an orbital shaker (120 rpm, 27 ± 2 °C) and the biofilms formed were used to assess their cellular density and the effects of the selected chemicals on biofilm control (inactivation and biofilm reduction). Negative controls, where no bacterial growth was expected, were obtained by incubating the wells only with growth medium without adding any bacteria.

3.12. Biofilm cellular density

Single and dual-species biofilms were grown in 96-wells microtiter plates as described in the previous sub-section. After 24 h of incubation, the content of each well was discarded and the biofilm was gently washed with sterile PB to remove loosely attached microorganisms. A volume of 200 µL of PB was added to the wells and the biofilm was scraped with a stainless steel scraper as described by Simões et al. [327]. The ressuspended cells were used to assess total counts. After dilution, a volume (up to 3 mL as a function of the bacterial concentration) was filtered through a black Nucleopore™ polycarbonate membrane with diameter of 25 mm and pore size of 0.2 µm (Whatman, UK). After filtration, cells on the membrane were stained with 400 µL of 4,6-diamino-2-phenylindole (DAPI) (Sigma) at 0.5 µg/mL and left in the dark for 5 min [58]. Cells were visualized under an epifluorescence microscope (LEICA DMLB2 with a mercury lamp HBO/100W/3) incorporating a CCD camera to acquire images using IM50 software (LEICA), using a ×100 oil immersion fluorescence objective, and a filter sensitive to DAPI fluorescence (359 nm excitation filter in combination with a 461 nm emission filter). A total of 20 fields were counted and at least three independent membranes were used to calculate total cells per cm^2 of biofilm.

3.13. Adhesion assays

In vitro initial adhesion was assessed on the flat coupons of the selected surfaces (1 cm^2 slide) inserted in 48-well microtiter plates (Nunc, Denmark). The coupons were inserted vertically in the wells of the plates, which had a working volume of 1.2 mL. Each well was inoculated with fresh sterile growth medium and a bacterial suspension with a cell density of

1×10^8 cells/mL, in the same proportion as described for the biofilm formation in microtiter plates (sub-section 3.11). The microtiter plates were incubated for 2 h in an orbital shaker (120 rpm, 27 ± 2 °C) to allow initial adhesion. Afterwards, the content of each well was discarded and the coupons were washed with sterile PB to remove loosely attached cells. In some cases, treatment with chemical was followed for 30 min. Control experiments were performed with PB. At the end of the chemical treatment each well was washed twice with PB in order to neutralize the biocide to sub-lethal levels [328]. Total bacterial counts were obtained by directly staining the cells in coupons with DAPI (Sigma, Portugal) as described previously [329]. The slides were examined using epifluorescence microscopy (LEICA DMLB2) as described in sub-section 3.12.

3.14. Microtiter-plate test for biofilm prevention and effects of a second dose of phenolic acids

Single- and dual-species biofilms were grown in the presence of the selected chemicals. Microtiter plates where inoculated with a bacterial suspension with a cell density of 1×10^8 cells/mL, fresh CNM and the chemicals so that the bulk volume (200 µL) presented the desired concentration for the test. After 24 h incubation in an orbital shaker (120 rpm, 27 ± 2 °C), the biofilms were used to assess the preventive effects of the selected chemicals on biofilm formation. With this purpose, the biomass and activity of biofilms formed in the presence of the selected chemicals was compared with those formed only with growth medium (the presence of DMSO caused no effects on biofilm formation). Final results are presented as percentage of biofilm reduction and inactivation.

Those biofilms formed in the presence of the selected chemicals were also used to assess their presumptive adaptation to the chemicals by exposing the biofilms to a second dose of the product. After 1 h exposure to the selected chemicals, the biofilms were analysed in terms of biomass and activity and the final results are presented as percentage of biofilm reduction and inactivation.

3.15. Microtiter plate test for biofilm control

To determine whether the selected chemicals had effect on biofilm control, microtiter plates with single and dual-species biofilms were exposed to the desired concentrations of those chemicals, according to Simões et al. [327]. One hour after exposure, the biofilms were analysed in terms of biomass and metabolic activity and the results are presented as percentage of biofilm reduction and inactivation. The biofilm control effects of the phenolic acids were classified according to the following scheme (I – inactivation; R - removal): low efficacy - I or R < 25%; moderate efficacy – 25% ≤ I or R < 60%; high efficacy - 60% ≤ I or R < 90% and excellent efficacy - 90% ≤ I or R ≤ 100%.

3.16. Microtiter plate test for biomass quantification

The biofilm mass was quantified using crystal violet staining according to Stepanović et al. [215]. For the procedure, the biofilms in the microtiter plates were washed with sterile PB and fixed with 250 µL /well of 99% ethanol (Merck) for 15 min. The plates were emptied and left to dry. Then, the fixed bacteria were stained for 5 min with 200 µL/well of crystal violet (Gram colour-staining set for microscopy; Merck). The plate was drained after the staining period, and placed on filter paper, to absorb the excess stain. Afterwards the dye bound to the adherent cells was resolubilized by 200 µL/well of 33% (vol/vol) glacial acetic acid (Merck). The amount of biomass produced is proportional to the absorbance, which was measured at 570 nm using an Absorbance Microplate Reader (Spectramax M2e, Molecular Devices, Inc.).

This method was used to compare quantitatively the reduction of biofilm mass obtained during or/and after antimicrobial treatment. The percentage of reduction was assessed based on the following equation:

$$\text{Percentage of reduction} = \frac{[C - T]}{C} \times 100\% \qquad (3.4)$$

C denotes the absorbance for control wells (absence of antimicrobial), and T is the absorbance for biofilms exposed to the selected antimicrobials.

3.17. Microtiter plate test for biofilm activity

To assess the bacteria viability, a modified alamarBlue® microtiter plate assay was used according to previous works [235, 330]. Pettit et al. [217] reported this staining method as a reliable and reproducible method to assess biofilm susceptibility. The indicator resazurin (7-hydroxy-3H-phenoxazin-3-one-10-oxide) is a blue non-fluorescent redox dye that can be reduced by the cellular metabolic activity to the highly fluorescent pink resorufin [331]. For the procedure, the biofilms in the microtiter plates were washed with sterile PB. A ratio of 190 µL/well fresh CNM and 10 µL/well of resazurin solution were added to each well so that there was a final concentration of 20µM resazurin. Plates were incubated for 20 min in darkness at room temperature. The fluorescence intensity was measured at an emission wave length of 570 nm and an excitation wave length of 590 nm using an Absorbance Microplate Reader (Spectramax M2e, Molecular Devices, Inc.).

This method was used to compare quantitatively the inactivation of the biofilm cells during or/and after antimicrobial treatment. The percentage of inactivation was calculated from the fluorescence of the control samples and the biofilms treated with antimicrobial:

$$\text{Percentage of inactivation} = \frac{[C-T]}{C} \times 100\% \qquad (3.5)$$

C denotes the fluorescence for the biofilm control and T denotes the fluorescence for the biofilm exposed to the selected chemicals.

3.18. Biofilm formation - rotating cylinder reactor

Mature biofilms were formed by *B. cereus* and *P. fluorescens* (single or combined to form dual-species biofilms) using the RCR shown in Fig. 3.2. The RCR is an aerobic biofilm reactor which operates in steady state: three test cylinders are rotated at the same, fixed speed with their axes vertical. This system consists of a main reactor (operating volume 5 L) and a chemostat (operating volume 0.4 L). The bacterial growth conditions were as described in the sub-section 3.1 , 27 ± 2 °C, pH 7 [332].

The chemostat continuously supplied the bioreactor with a planktonic culture of *B. cereus* or *P. fluorescens*, at a constant flow rate, set by gravity. It was fed with a stream of CNM (described in sub-section 3.2) at a flow rate of 10 mL/h via a peristaltic pump. This chemostat

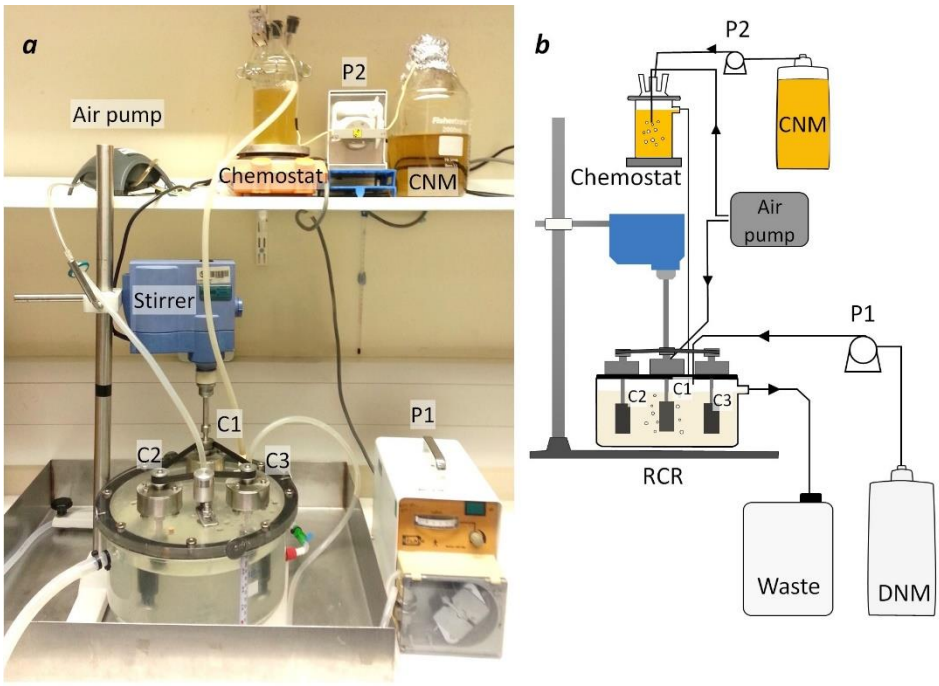

Fig. 3.2 – Photograph (a) and schematic (b) of the rotating fluid reactor apparatus.
RCR – rotating cylinder reactor; CNM – concentrated nutrient medium; DNM – dilute nutrient medium, P1 and P2 – peristaltic pumps; C1, C2 and C3 – test cylinders 1, 2 and 3 connected via the synchronizing belt and driven by the stirrer.

was agitated by a magnetic stirrer and fed the RCR at a steady flow rate, set by gravity. Those reactors were used alone or simultaneously to provide single or dual-species biofilms, respectively. The bioreactor was fed with DNM (described in sub-section 3.2) via a peristaltic pump, at a constant rate of 0.8 L/h in the case of single species biofilms or at 1.6 L/h for dual-species biofilms in order to establish the same dilution rate as for the previous scenario. Sterile aeration via a cellulose acetate syringe filter with pore size of 0.22 µm (Whatman, VWR, Portugal) was provided to the RCR and to the chemostat.

The bioreactor is a cylindrical tank with 28 cm of external diameter, 16 cm of height and 0.40 cm of wall's thickness. On the outside there is an effluent port at a height of 10.00 cm, so that the reactor biological volume is 5 L and there is 3 L left for aeration. A PMMA cover with 32 cm of diameter and 1.40 cm of thickness fits the vessel and supports for the fixed triple shaft system that transmits the power to the cylinders. The main shafts are inserted in the lid in a triangular configuration so that they are distanced by each other in 12 cm and around 6 cm distanced to the wall. There is a tensioner that applies a tensioning force to the timing belt, adjustable accordingly to the desired velocity of the cylinders. An overhead stirrer (IKA-Werke

GmbH & Co. KG, Germany) with speed range from 50 to 2000 rpm provided the simultaneous rotation of the cylinders as they are connected by a synchronous belt. The cylinders rotate at controlled speed, and the corresponding Reynolds number of agitation Re_{A} can be determined accordingly to the following equation [333]:

$$Re_{\mathrm{A}} = \frac{\mathrm{D_a^2 N}\rho}{\mu} \quad (3.6)$$

where $\mathrm{D_a}$ is the diameter of the cylinder; N is the rotation speed, ρ is the fluid density and μ is the fluid viscosity.

Considering that agitation flow in the tank is laminar for Re_{A}< 10 and turbulent for Re_{A}> 10^4, in this study, the biofilms were formed under transitional agitation flow at the cylinders and laminar in the remote parts of the tank [333]. In order to obtain steady-state biofilms, the biofilms grew for 7 days [332].

For a Newtonian fluid, the Fanning friction factor establishes the relation between the τ_{w} and the velocity of the flow kinetic energy given by the fluid density ρ and its velocity v, and is defined by [334]:

$$f = \frac{2\,\tau_{\mathrm{w}}}{\rho\, v^2} \quad (3.7)$$

For the RCR, the relationship between the f and the Re_{A} for a rotating electrode under turbulent flow conditions (the critical Re_A is 200) by Gabe and Walsh [335] was used:

$$f = 0.158 Re_{\mathrm{A}}^{-0.3} \quad (3.8)$$

3.19. Biofilm sampling for characterization

The cylinders were removed from the reactor and the biofilm wet biomass and thickness were measured. The biofilm (chemically untreated) was then removed using a stainless steel scraper, ressuspended in 10 mL of PB, and homogenized by vortexing (Heidolph, model Reax top) for 30 s at 100% power input. After homogenization, the biofilm suspensions were characterized in terms of total and matrix content (proteins and polysaccharides), biomass amount and cell density. Three independent biofilm formation experiments were performed for each case studied.

3.19.1. Thickness

The thickness of biofilms developed in the RCR was determined using a digital micrometer (VS-30H, Mitsubishi Kasei Corporation) according to Teodósio et al. [304], for the studies presented in chapters 5 and 7.

3.19.2. Biofilm mass quantification

For the determination of the wet mass, the cylinders were removed from the RCR and the biofilm accumulated on the top and bottom surfaces was discarded. The cylinders were then weighed and the wet mass obtained by subtracting the mass of the clean cylinders (without biofilm). The dry mass of the biofilms was assessed by the determination of the total volatile solids (TVS) of the homogenized biofilm suspensions according to standard methods (American Public Health Association [APHA], American Water Works Association [AWWA], Water Pollution Control Federation [WPCF]).

The water content was estimated as the difference between the wet mass and the dry mass. The biofilm density was calculated using biofilm dry mass and the volume of the biofilm, estimated from its thickness and the adhesion surface area [337].

3.19.3. Cellular density

For the enumeration of the total cell density, an aliquot of the homogenized biofilm suspension was microfiltered through a 0.22 µm Nucleopore® (Whatman, Middlesex, UK) black polycarbonate membrane. The membrane was stained with DAPI (VWR, Portugal). 0.5 µg/mL and left in the dark for 5 min [58]. After incubation the total cell counts were assessed using epifluorescence microscopy (LEICA DMLB2) as described in the sub-section 3.13. *B. cereus* spore numbers were assessed by surface plating (300 mL sample) after biofilm suspension heat treatment (80 °C, 5 min). The plates of solid CNM (13 g/L agar) were incubated at 27 °C for 72 h.

3.19.4. Protein and polysaccharide quantification

Biofilm EPS extraction was performed according to a previously described method [338]. The procedure used for total (before EPS extraction) and extracellular biofilm protein quantification was the Lowry et al. [339] method as modified by Peterson [340], using the Total Protein Kit, Micro Lowry, Peterson's Modification (Sigma, Portugal), with bovine serum albumin as standard. The total and extracellular polysaccharides were quantified through the phenol-sulphuric acid method of Dubois et al. [341], with glucose as standard.

3.20. Biofilm chemical treatment

The cylinders from the RCR with biofilm were removed from the 5 L reactor, and then immersed vertically in 250 mL glass beakers (diameter: 6.8 cm) containing 200 mL of BDMDAC solution. The exposure to the biocide was carried out for 30 min, under the same Re_{A} used for biofilm formation. After biofilm chemical exposure, a neutralization step was performed to dilute the biocide to residual levels, as described by Johnston et al. [328]. The wet weight of the cylinders plus biofilm attached was determined before and after the exposure. The wet mass of the biofilm that was removed from the surface area of each cylinder, was expressed in terms of percentage of biofilm removal, as defined by equation 3.9.

$$\text{Biofilm removal } (\%) = \frac{X}{X_{\text{biofilm}}} \times 100 \qquad (3.9)$$

where X_{biofilm} is the wet mass of the biofilm before biocide exposure and X is the wet mass of the biofilm that was removed due to biocide exposure.

3.21. Biofilm removal by hydrodynamic stress

The biofilm removal by hydrodynamic stress was assessed according to the method described by Simões et al. [332]. Biofilm layers were removed by submitting the biofilms submerged in PB to 30 s pulse exposure to increasing Re_{A} (from 4000 to 16100). The wet weight of the cylinders plus biofilm attached was determined before and after exposure to the hydrodynamic stress. Additionally, the residual biofilms, covering the cylinders, were entirely removed with a stainless steel scraper and then the weight of cylinders without biofilm was determined, to quantify the remaining biofilm after the hydrodynamic treatment. The same

procedure was followed with the control assay, i.e., with the cylinder plus biofilm non-exposed to biocide.

The amount of biofilm that remained adhered after exposure to the complete series of Re_{A} was expressed as percentage of biofilm remaining, according to equation 3.10.

$$\text{Biofilm remaining (\%)} = \frac{X_{\mathrm{remaining}}}{X_{\mathrm{biofilm}}} \times 100 \qquad (3.10)$$

where X_{biofilm} is the wet mass of the biofilm non-exposed to the series of increasing Re_{A} and $X_{\mathrm{remaining}}$ is the wet mass of the biofilm remaining adhered to the cylinder surface after the exposure to the series of increasing Re_{A}.

3.22. Cylindrical zero-discharge FDG

The FDG technique was invented in 2000 at the University of Cambridge by Tuladhar et al. [342] and relates the pressure drop across a nozzle to the distance between the nozzle and surface that is being gauged. A key feature is that the nozzle does not contact the surface. The cylindrical zero-discharge FDG (czFDG) was designed so that it could perform measurements in curved surfaces with no net change of liquid volume due to zero net discharge of liquid from the system. This new FDG device was also constructed at the University of Cambridge, in 2014. In addition to the author of this thesis, Professor Ian Wilson, Mr Shiyao Wang and Dr Akin Ali were also co-authors involved in its proof of concept.

Fig. 3.3 shows a photograph and schematic of the czFDG apparatus. An aluminium frame holds the motorized linear drive and the reservoir (R). The test cylinder is located on a stainless steel shaft, so that its axis is collinear with that of the reservoir. Rotational and vertical movements of the sample are controlled manually, with 12 azimuthal positions (labelled by roman numerals I-XII) at 5 heights (labelled A-E), giving 60 different measuring locations. The gauging tube was moved via a motorized linear slide (Zaber Technologies, T-LSR075B, UK), manipulated via LabVIEW™ software (version 2013), with an accuracy of ± 15 µm. Pressure was measured using a piezo pressure transducer (Honeywell 24PCEFA6G, UK) relative to atmospheric pressure. The stated accuracy of the pressure transducer was ±5 Pa. The analogue signal from the pressure transducer was converted to digital via a DAQ device (National Instruments, USB-6009). Data were collected on a laptop using the LabVIEW™ software. The flow of the liquid through the nozzle was set by a syringe pump (Cole-Parmer, EW-74900-20):

the accuracy was determined by separate tests as ± 0.45%. An electrical circuit was used to determine the point of zero clearance. A digital microscope (Maplin, UK) provided images of the gauged area with 400× magnification. Fig. 3.4 shows the details of the nozzle and its dimensions.

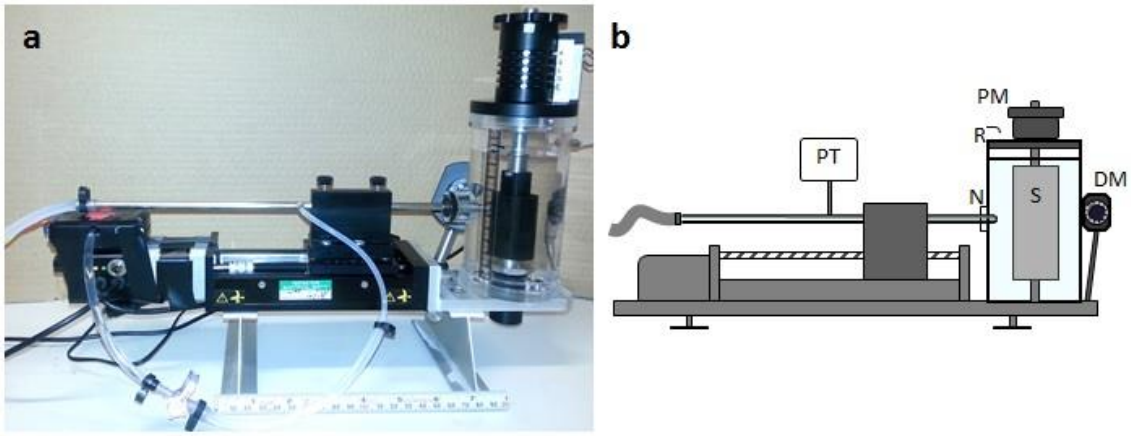

Fig. 3.3 – Photograph (a) and schematic (b) of the fluid dynamic gauging apparatus.
DM - digital microscope; N - nozzle; PM - positioning mechanism; PT – pressure transducer; R - reservoir; S - sample.

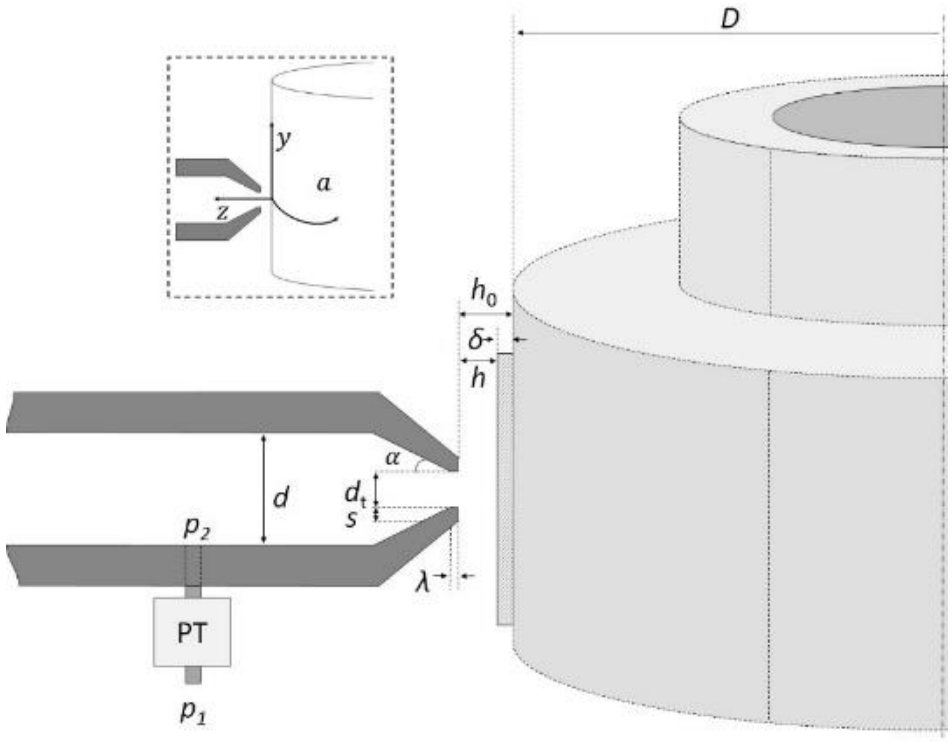

Fig. 3.4 – Detailed schematic of the gauging nozzle.
Dimensions: inner diameter of gauging tube, $d_t = 1$ mm; inner diameter of gauging tube, d = 3.8 mm; nozzle entry length; nozzle entry length, $\lambda = 0.2$ mm; nozzle lip width, $s = 0.4$. The internal divergent angle, α, is 45°. PT - pressure transducer, δ – deposit thickness; h_0 is the distance between the nozzle and the substrate; h is the clearance measured by FDG; pi is the pressure at station i.

The device used here operates in pressure mode. The mass flow rate through the nozzle, $\dot{m}$, depends on the pressure drop across the nozzle, ΔP_{12}, and the distance between the nozzle and the surface (the clearance), h. At small values of h, $\dot{m}$ is very sensitive to ΔP_{12} and *vice versa*. The mass flow rate is maintained constant, using the syringe pump, and ΔP is measured as the nozzle is moved towards the surface. The ($\dot{m}$, ΔP) data are used to calculate the discharge coefficient, C_d, which is the ratio between the measured $\dot{m}$ and the ideal mass flowrate through the nozzle, [342]:

$$C_{\mathrm{d}} = \frac{\dot{m}}{\pi/_4 \, d_{\mathrm{t}}^2 \sqrt{2\rho\Delta P_{12}}} \qquad (3.11)$$

where ρ is the density of the gauging liquid and d_{t} is the diameter of the nozzle throat (see Fig. 3.4). Knowledge of C_d allows h to be estimated from calibration plots. The FDG technique relies on the finding that C_d is usefully sensitive to h/d_{t} when h/d_{t} < 0.3. Examples of the calibration plots are presented further in Fig. 8.4*b*.

In practice, after determination of the reference point (*e.g.* using the metal strip on non-conductive cylinders), the nozzle location relative to the substrate, h_0, is known and controlled by the movement of linear slide in pre-determined steps. Liquid is either sucked into or ejected from the nozzle at a set flow rate and ΔP_{12} is measured, allowing C_d to be calculated and h then estimated from the C_d - h/d_{t} relationship. The thickness of any layer present, δ, is calculated from:

$$\delta = h_0 - h \qquad (3.12)$$

Estimates of δ can be made with the nozzle at different locations, for instance as the nozzle is moved towards the surface. The pressure drop (and accuracy of the measurement) increases as the nozzle approaches the surface, but the shear stress imposed by the gauging flow also increases, which could cause the deposit to deform.

In FDG measurements the gauging fluid through the nozzle is in the laminar or inertial regime so the C_d - h/d_{t} relationship is sensitive to the Reynolds number, Re_{t}, which is conventionally based on the nozzle throat diameter, d_{t}:

$$Re_{\mathrm{t}} = 4\dot{m}/\pi\mu d_{\mathrm{t}} \qquad (3.13)$$

where μ is the kinematic viscosity of the gauging liquid.

For calibration tests, both ejection and suction modes were performed with fixed flow rates of 0.066 g/s ($Re_t = 84$) and 0.050 g/s ($Re_t = 63$). The nozzle is moved to a known location relative to the surface and the syringe pump set to eject or withdraw liquid at a constant rate. The pressure drop ΔP_{12} is measured before, during, and after the pumping period in order to determine the hydrostatic and dynamic pressure drops. A differential pressure transducer of sufficient accuracy in both modes was not available so gauge pressures were measured and the hydrostatic contribution accounted for. The nozzle is then moved to give another clearance value and the measurement repeated. This process was automated and took approximately 60 s. Afterwards, while the nozzle was moved away from the surface, the position of the sample was adjusted manually (to the pre-determined positions) in order to measure at another point on the surface.

Biofilms measurements were performed at room temperature, using PB as the gauging fluid, in order to maintain the physiological conditions similar to that in the RCR. Low gauging flow rates, of 0.066 g/s and 0.050 g/s, were used to prevent disruption of the biofilm layers. The alignment of the cylinder was first checked using the calibration procedure on cleaned regions at three different heights and two diametrically opposed locations on the azimuth plane. Variation in alignment arose from small differences in machining and assembling the cylinders, as well as mechanical slack in the mounting. The above procedure overcame this issue.

3.23. Statistical analysis

The experimental data was analysed using the statistical program SPSS version 20.0 (Statistical Package for the Social Sciences). The mean and standard deviation within samples were calculated for all cases. At least three independent experiments were performed for each conditions tested. Data were analysed by the application of the non-parametric tests like the Kruskal-Wallis test or Mann-Whitney test (confidence level ≥ 95%).

CHAPTER 4

The effects of ferulic and salicylic acids on *Bacillus cereus* and *Pseudomonas fluorescens* single and dual-species biofilms - biocide selection for biofilm control

4. The effects of ferulic and salicylic acids on *Bacillus cereus* and *Pseudomonas fluorescens* single and dual-species biofilms - biocide selection for biofilm control

Abstract

Biofilms are a problem to food industries as they can cause equipment damage, food spoilage, increase energy costs and are a potential harbour for pathogenic microorganisms. Their extreme antimicrobial resistance proposes that novel control strategies are necessary. Plant secondary metabolites (phytochemicals) already demonstrated promising antimicrobial properties when applied against planktonic cells and biofilms. The aim of this study was to test the effectiveness of two phenolic acids: ferulic (FA) and salicylic (SA), alone and in combination (FSA) on the prevention and control of *B. cereus* and *P. fluorescens* biofilms. The antimicrobial activity of FA and SA was compared with a selected quaternary ammonium compound (BDMDAC). Additionally, several tests were performed to predict the adhesion ability of bacteria, namely, motility assays, bacterial surface characterization (hydrophobicity and surface charge) and the detection of quorum sensing inhibition (QSI) with the phenolic acids. The effects of a concentration two times the minimum inhibitory concentration (500 µg/mL) were assessed on single and dual-species biofilms. The results demonstrated that only swimming was affected by FA and SA and no clear relationship was obtained between the effects of phenolic acids on motility and biofilm prevention. The bacterial potential of adhesion was affected by the phenolic acids, as well as the surface charge. Only SA and FSA demonstrated capacity for QSI. Both bacteria were able to form single and dual-species biofilms in the presence of the phenolic acids. The application of FA and SA (single and combined) to biofilms caused low to moderate inactivation and removal. However, dual-species biofilms formed in the presence of phenolic acids were highly susceptible to a second exposure to the chemicals. The continuous exposure of dual-species biofilms to the phenolic acids decreased their resilience and resistance to inactivation and removal. The overall study clarifies the role of FA and SA on the prevention and control of biofilms formed by two important food spoilage bacteria. Moreover, it demonstrates their reduced antimicrobial activity compared to BDMDAC.

Keywords: antimicrobial resistance; biofilm control; motility; ferulic acid; salicylic acid; dual-species biofilms

4.1. Introduction

The evolution of microbial resistance mechanisms is related to the biofilm phenotype, and emergent strategies are required for their control. In fact, biofilm cells are more resistant to antimicrobial products than their planktonic counterparts [221, 343]. Therefore, new antimicrobial products need to be identified and their antimicrobial action against biofilms must be assessed. The lack of new antibacterial products for biofilm control has been recognized as a major unmet industrial and biomedical need. Plant secondary metabolites (phytochemicals) can provide interesting solutions for biofilm control [238, 314, 344]. Natural antimicrobial products can be attractive to the food industry in that they control natural spoilage microorganisms [345]. Previous studies [346, 347] have demonstrated that essential oils from selected plants inhibited the growth of four pathogenic bacteria (*E. coli* O157:H7, *L. monocytogenes*, *S. enterica* Typhimurium, and *S. aureus*) and reduced the metabolic activity of *L. monocytogenes* biofilms.

Phenolic substances, including simple phenols and phenolic acids, are a major class of phytochemicals that have already demonstrated significant antimicrobial properties [314, 348, 349]. Their mechanism of action may include enzyme inhibition by the oxidized products and consequent disruption of energy production [181, 235, 314]. Phenolic acids have a carboxylic acid functionality and in the realm of plant metabolites they constitute a distinct group of organic acids, divided into two characteristic constitutive carbon frameworks: the hydroxycinnamic and hydroxybenzoic structures [350]. Chemically, their basic structure is similar, but the position and number of the hydroxyl groups on the aromatic ring defines the difference between the molecules. Phenolic acids are commonly used as preservatives in food applications, due to their antioxidant and antimicrobial activities [350]. However, diverse phenolic acids, including ferulic and salicylic acids, are promising candidates for cleaning and disinfection due to their antimicrobial properties and low cutaneous toxicity [235, 351-354].

The main purpose of this work was to study the action of two selected phenolic acids—ferulic acid, a hydroxycinnamic acid; and salicylic acid, a hydroxybenzoic acid, against *B. cereus* and *P. fluorescens* single and dual-species biofilms. Positive controls were performed using BDMDAC, a biocide commonly used in disinfection products for domestic and clinic purposes and food industries [170, 187, 269]. The mechanism of action on bacteria of this quaternary ammonium compound was previously studied by Ferreira et al. [355], who also proved its efficiency in the inactivation of *P. fluorescens* biofilms [269]. The effects of phenolic acids were assessed on biofilm formation/prevention and control. Additional tests on bacterial motility,

quorum sensing inhibition (QSI), and cell surface physicochemical properties and charge were performed in order to assess potential mechanisms of action of the selected products.

4.2. Materials and Methods

The work described in this section was performed using *B. cereus* and *P. fluorescens* cultures as described in sub-section 3.1 and cultivated in CNM according to sub-section 3.2. *C. violaceum* CV12472 was used to determine QSI according to sub-sections 3.1 and 3.2. Two phenolic acids were tested: ferulic acid (FA) and salicylic acid (SA) (Sigma-Aldrich, Portugal), as well as a combination (1:1) of FA and SA (FSA) as described in sub-section 3.3. To determine whether the presence of the FA and SA had some effects on the bacterial growth in liquid medium, the MIC (sub-section 3.6). For positive control in MIC determination a quaternary ammonium compound—BDMDAC (sub-section 3.3) was selected. Swimming and swarming motilities were also measured in the presence of FA, SA (sub-section 3.6), as well as the QSI activity (sub-section 3.10). The physicochemical properties of the bacterial surfaces, namely hydrophobicity and surface charge were assessed before and after exposure to FA, SA and FSA at 100, 500 and 1000 µg/mL for 1 h (following the methods described in the sub-sections 3.7 and 3.9, respectively). As the physicochemical properties of the PS surfaces were also determined, it was possible to estimate the predicted free energy of adhesion of both species to PS according to sub-section 3.8. Additionally, the phenolics were used for screening tests in biofilms formed in microtiter plates for 24 hours (sub-section 3.11) to assess their cellular density (sub-section 3.12); their preventive effects (when biofilms were formed in the presence of the biocide) including the effects of exposure to a second dose (sub-section 3.14) and their effects on biofilm control (sub-section 3.15). The concentration of the phytochemicals used in these tests was 1000 µg/mL, as they are routinely classified as antimicrobials on the basis of susceptibility tests that produce inhibitory concentrations in the range of 100 to 1000 µg/mL [314]. For this purpose, a biomass quantification method using crystal violet (sub-section 3.16) and a modified alamarBlue® test (sub-section 3.17) were used to determine the percentage of biofilm removal and inactivation, respectively.

4.3. Results and discussion

Interest in the use of phytochemicals as an alternative to conventional antimicrobials has been increasing significantly in recent years [181, 314, 356]. These molecules can act on multiple biochemical targets of the cell, preventing the emergence of antimicrobial resistance events [314, 357]. In the present work, the *in-vitro* activity of two phenolic acids was assessed, as single compounds – FA and SA, and in combination – FSA, against single and dual-species biofilms formed by *B. cereus* and *P. fluorescens*. Those bacteria are ubiquitous in industrial systems, and are particularly problematic in food processing plants [343]. Both FA and SA had inhibitory effects on the growth of the tested bacteria. The MIC of the phenolic acids was 500 µg/mL for both bacteria. The phenolic acids (single and in combination) at twice the MIC had low effects on the inactivation of single and dual-species biofilms of *B. cereus* and *P. fluorescens*. BDMDAC also inhibited the growth of the bacteria. Its MIC was 5 µg/mL for *B. cereus* was and 15µg/mL for *P. fluorescens.* Ferreira et al. [358] had already proved the biocidal effectiveness of BDMDAC against a *P. fluorescens* strain isolated from a drinking water distribution system, and established that it follows a mechanisms that includes ionic and hydrophobic interactions with the cell membrane, causing changes in membrane properties and function, and resulting in cellular disruption and loss of membrane integrity with consequent leakage of essential intracellular constituents. This is probably the cause of the higher growth inhibitory effects of BDMDAC compare to FA and SA.

There are studies on the inhibition of planktonic cell growth with phenolic products [179, 181, 359, 360]. However, studies on their biofilm control potential are scarce [235, 238, 344, 351]. Furiga et al. [344] tested compounds from red wine, grape marc, and pine bark, and demonstrated interesting anti-plaque activity *in-vitro* against *Streptococcus mutans*. Jagani et al. [238] verified that phenol and natural phenolic compounds showed a significant reduction in biofilm formation by *P. aeruginosa*. Ergün et al. [351] evaluated the antimicrobial properties of aromatic ester derivatives of ferulic acid, which showed significant biofilm eradication potential, comparable to their MIC for planktonic cultures against Gram-positive bacteria and fungi. It seems fundamental to understand the role of phytochemicals as a source of new antimicrobial products for biofilm prevention and control.

In order to ascertain putative aspects involved in the behaviour of *B. cereus* and *P. fluorescens* single and dual-species biofilms, studies on the effects of FA and SA on bacterial motility, surface physicochemical properties, and charge and QSI activity were performed.

Bacterial motility and biofilm formation are manifestations of functional responses to surface colonization. It is believed that motility may be implicated in the stabilization of cell-surface and cell-to-cell interactions [361]. Swimming and swarming motilities are flagella-mediated. However, swimming is considered to be individual motility in liquid medium, while swarming is a social movement of a group of bacteria, and permits rapid migration over a surface [362]. It is accepted that biofilm formation is enhanced by cell motility, particularly when it is mediated by flagella. This occurs because bacteria overcome the long-range repulsive forces that facilitate close approach to the surfaces, enabling accelerated surface adhesion [363]. In this study, the effects of phenolic acids were tested on swimming and swarming motilities of *B. cereus* and *P. fluorescens*. Swimming and swarming motilities increased over time in the absence of phenolic acids, for both bacteria (Table 4.1). However, this increase was only significant for swimming motility ($P < 0.05$). In the presence of the phenolic acids the swimming motility of *B. cereus* and *P. fluorescens* was significantly reduced when compared with the control experiments ($P < 0.05$). No significant changes over time were detected for the swimming motility of both bacteria when they were exposed to FA or SA ($P > 0.05$).

The swarming motility of *P. fluorescens* and *B. cereus* was not significantly affected by FA or SA ($P > 0.05$). There are no statistical significant differences ($P > 0.05$) when comparing the action of the two phenolic acids on swimming and swarming motilities of *B. cereus* and

Table 4.1 – Swimming and swarming motilities (mm) of *B. cereus* and *P. fluorescens* in the absence (control) and presence of FA and SA.
The means ± standard deviation SD for at least three replicates are given. The 15 µL of bacterial culture produced an 8-mm (baseline) spot on the agar.

	B. cereus			*P. fluorescens*		
	24 h	48 h	72 h	24 h	48 h	72 h
Swimming						
Control	3.67 ± 0.6	7.33 ± 0.5	12.3 ± 1.5	13.3 ± 2.3	19.3 ± 2.5	24.7 ± 3.1
FA	1.00 ± 0.2	1.00 ± 0.0	1.00 ± 0.0	1.00 ± 0.0	1.00 ± 0.0	1.00 ± 0.5
SA	1.00 ± 0.0	1.00 ± 0.3	1.00 ± 0.0	1.67 ± 1.1	2.00 ± 0.4	2.00 ± 0.0
Swarming						
Control	4.00 ± 0.0	5.00 ± 0.0	6.67 ± 0.6	3.00 ± 1.0	3.67 ± 1.2	4.67 ± 0.6
FA	3.00 ± 0.0	3.00 ± 0.8	3.00 ± 1.9	2.33 ± 0.5	3.33 ± 0.6	3.33 ± 1.1
SA	3.33 ± 0.6	3.33 ± 0.6	3.33 ± 1.6	3.33 ± 0.6	3.67 ± 0.8	3.33 ± 0.8

P. fluorescens. Houry et al. [364] reported the importance of motility in *B. cereus* biofilm formation in microtiter plates. In a previous study, Muller et al. [365] found that the inclusion of 5 mM of SA in medium inhibited both growth and biofilm production by *Staphylococcus epidermidis* by up to 55%. Farber and Wolff [366] found that SA prevented the adhesion of bacteria (*P. aeruginosa*, *E. aerogenes*, *K. pneumoniae*, and *Enterococcus faecalis*) and yeast (*Candida albicans*) to silastic catheters. Borges et al. [235] found that gallic and ferulic acids had potential to inhibit motility and to prevent biofilms of four important human pathogenic bacteria (*E. coli*, *L. monocytogenes*, *P. aeruginosa*, and *S. aureus*). Those results clearly demonstrate that the action of FA and SA in motility and further biofilm prevention is strongly dependent on the bacterial species used. In this work, the assays of biofilm prevention showed low to moderate effects of FA, SA, and FSA on the inhibition of single and dual-species biofilm formation, indicating that the effects of phytochemicals on bacterial motility were not significant on biofilm prevention. Therefore, it was important to understand other factors involved in biofilm formation and development, particularly the aspects involved in the initial adhesion processes.

Adhesion is a complex process that is affected by many aspects, such as the physicochemical characteristics of bacteria, the material surface properties, and the environmental factors [367, 368]. It is commonly observed that cell surface hydrophobicity can affect bacterial adhesion to different types of substrata, including hydrophobic surfaces, such as PS (Pang et al., 2005). *B. cereus* and *P. fluorescens* cells untreated and phenolic acids-treated cells were analysed in order to determine their surface tension parameters and hydrophobicity (Table 4.2). Both *B. cereus* and *P. fluorescens* cells are naturally hydrophilic, as their $\Delta G_{1w1} > 0$ mJ/m^2, with this characteristic more pronounced for *B. cereus* ($P < 0.05$). The exposure to the phenolic acids caused a significant increase on ΔG_{1w1} ($P < 0.05$) for the *B. cereus* cells when they were exposed to FSA at 100 µg/mL and SA at 100 µg/mL. For *P. fluorescens*, the value of this component increased significantly ($P < 0.05$), namely after exposure to the highest concentrations of all the phenolic acids. The Lifshitz-van der Waals component γ^{LW} and the Lewis acid–base component, γ^{AB}, indicate the apolar or polar surface properties of the bacterial cell, respectively. Regarding the *B. cereus* cells, the exposure to the phenolic acids had no significant effect on the γ^{LW} ($P > 0.05$). The γ^{LW} was significantly increased by both the phenolic acids ($P < 0.05$) for *P. fluorescens* cells, with the smaller difference caused by the FA at 100 µg/mL and the most significant increase observed with SA at 100 µg/mL. Moreover, in the case of *B. cereus*, the γ^{AB} component was significantly affected by all the phenolic acids ($P < 0.05$),

Table 4.2 – Surface tension parameters and hydrophobicity (ΔG_{1w1}) of the untreated (control) and phenolic acids-treated cells.
The means ± SD for at least three replicates are given.

		Conc. (μg/mL)	Surface tension parameters (mJ/m^2)				(ΔG_{1w1}) (mJ/m^2)
			γ^{LW}	γ^{AB}	γ^+	γ^-	
Control			37.9 ± 2.5	15.9 ± 3.5	1.2 ± 0.4	47.4 ± 7.5	29.5 ± 6.0
B. cereus	FA	100	39.0 ± 0.3	11.8 ± 1.0	0.7 ± 0.1	52.4 ± 1.7	32.2 ± 2.3
		500	39.1 ± 1.2	9.4 ± 2.2	0.4 ± 0.1	51.0 ± 6.0	34.1 ± 6.5
		1000	38.9 ± 0.9	12.6 ± 1.6	0.8 ± 0.2	50.5 ± 2.3	29.4 ± 3.2
	SA	100	41.2 ± 0.9	0.0 ± 0.0	0.0 ± 0.0	75.8 ± 17.9	69.2 ± 15.8
		500	37.8 ± 0.3	11.9 ± 1.1	0.7 ± 0.2	56.2 ± 3.9	38.2 ± 6.6
		1000	38.7 ± 1.2	12.2 ± 2.0	0.8 ± 0.2	53.5 ± 4.5	33.3 ± 6.4
	FSA	100	36.7 ± 0.5	0.0 ± 0.0	0.0 ± 0.0	73.2 ± 16.7	76.5 ± 14.5
		500	36.0 ± 1.9	12.7 ± 3.1	1.2 ± 0.2	54.5 ± 3.4	34.8 ± 6.1
		1000	38.1 ± 1.0	0.0 ± 0.0	0.0 ± 0.0	67.9 ± 8.7	56.8 ± 14.1
Control			18.0 ± 0.9	9.6 ± 1.0	9.6 ± 1.0	48.9 ± 2.3	14.8 ± 2.2
P. fluorescens	FA	100	30.3 ± 0.6	15.5 ± 2.6	1.5 ± 0.4	44.0 ± 6.2	19.6 ± 3.6
		500	35.7 ± 1.6	15.1 ± 3.7	0.3 ± 0.3	54.6 ± 8.6	39.0 ± 14.8
		1000	35.7 ± 0.4	0.0 ± 0.0	0.0 ± 0.0	68.0 ± 8.4	60.7 ± 10.7
	SA	100	37.0 ± 0.5	10.1 ± 3.0	0.7 ± 0.4	47.9 ± 8.0	22.3 ± 5.3
		500	35.9 ± 0.4	9.4 ± 3.2	0.0 ± 0.0	46.2 ± 8.5	41.2 ± 5.4
		1000	33.9 ± 2.0	3.0 ± 0.7	0.0 ± 0.0	64.2 ± 7.9	54.1 ± 11.6
	FSA	100	35.8 ± 1.3	14.3 ± 2.9	1.2 ± 0.4	40.8 ± 10.5	13.3 ± 3.5
		500	34.2 ± 1.5	14.4 ± 2.4	1.5 ± 0.3	38.7 ± 3.3	15.1 ± 3.1
		1000	36.3 ± 1.2	9.8 ± 1.3	0.6 ± 0.1	46.5 ± 5.0	24.8 ± 1.5

except for FA at 1000 μg/mL, FSA at 500 μg/mL and SA at 500 μg/mL. For *P. fluorescens* the magnitude of this parameter decreased significantly ($P < 0.05$) for all the conditions tested, with the minimum value being observed with FA at 1000 μg/mL and the maximum with FA at 100 μg/mL. The γ^+ and γ^- values indicate if the cells have more ability to accept or donate electrons, respectively. The electron donor component of *B. cereus* cell surfaces increased significantly after treatment with FSA at 100 μg/mL and SA at 100 μg/mL ($P < 0.05$). The electron acceptor ability of *B. cereus* cell surfaces increased after treatment with FA at 500 μg/mL and SA at 100 μg/mL ($P > 0.05$). The γ^- of *P. fluorescens* cell surfaces increased significantly ($P < 0.05$)

with exposure to FA at 1000 µg/mL and SA at 1000 µg/mL ($P < 0.05$). The γ^+component of *P. fluorescens* cell surfaces decreased significantly with exposure to the phenolic acids and with an increase of concentration ($P < 0.05$).

The surface tension values allowed the assessment of the free energy of adhesion between the bacterial surfaces and the substratum PS (Table 4.3). *B. cereus* untreated cells had a ΔG_{1w2}^{Tot}= -1.80 mJ/m^2. After exposure to the phenolic acids there was an increase of the free energy of adhesion for all the conditions. The maximum value of ΔG_{1w2}^{Tot}= 12.18 mJ/m^2 was observed for the treatment with SA at 100 µg/mL. In the case of *P. fluorescens* the untreated cells had a ΔG_{1w2}^{Tot}= 13.51 mJ/m^2. The exposure to the phenolic acids caused a decrease in the free energy of adhesion, for all the conditions. The minimum value of ΔG_{1w2}^{Tot}= -5.62 mJ/m^2 was observed after exposure to FSA at 500 µg/mL. Comparing the thermodynamic capability for adhesion between the bacteria and PS, the results obtained shown that the exposure to the phenolic acids works against the adhesion of *B. cereus* to PS but favours *P. fluorescens*. These results based on thermodynamic analysis indicate that FA and SA may prevent *B. cereus* biofilm formation. The effects of phytochemicals on the prevention of biofilm formation by *E. coli*, *P. aeruginosa*, *S. aureus,* and *L. monocytogenes* was also demonstrated by Borges et al. [235] using microtiter plate tests.

Table 4.3– Free energy of adhesion (ΔG_{1w2}^{Tot}) between *B.cereus* and *P. fluorescens* untreated (control) and phenolic acids-treated cells to PS.

Phenolic acid	Conc.(µg/mL)	*B. cereus*	*P. fluorescens*
Control		-1.80	13.51
FA	100	1.04	-1.25
	500	-0.69	2.42
	1000	0.08	8.91
SA	100	12.18	-1.70
	500	3.90	-5.74
	1000	2.13	7.21
FSA	100	11.82	-5.62
	500	4.27	-6.40
	1000	8.26	-2.69

The surface charge of the cell was also assessed to provide information on the potential electrostatic repulsive/attractive events between the bacterial cell surfaces and PS. The bacteria tested have a negative cellular surface charge: -19.07 mV (*B. cereus)* and -9.07 mV (*P. fluorescens).* The zeta potential values (Fig. 4.1) of both bacteria after exposure to the phenolic acids were significantly different from the control ($P < 0.05$).

It was observed that under physiologically conditions the bacteria have negative surface charges. When exposed to phenolic acids the surface charge of the bacteria increased significantly. The surface charge of *P. fluorescens* became less negative with increasing phenolic acid concentration, for all compounds ($P < 0.05$). Also, the surface charge changes were concentration-dependent. The same behaviour was observed for *B. cereus* with FSA ($P < 0.05$). Exposure of *B. cereus* to SA and FA also increased significantly the surface charge ($P < 0.05$), however, this change was not concentration dependent ($P > 0.05$).

This effect seems to increase the interaction between the bacterial surfaces and PS and may help in understanding the failure of FA and SA (single and combined) to prevent biofilm formation. In fact, PS has a zeta potential of -32 mV [221]. Quorum sensing, a form of cell-to-cell communication in bacteria, is an important regulatory mechanism in biofilm formation and

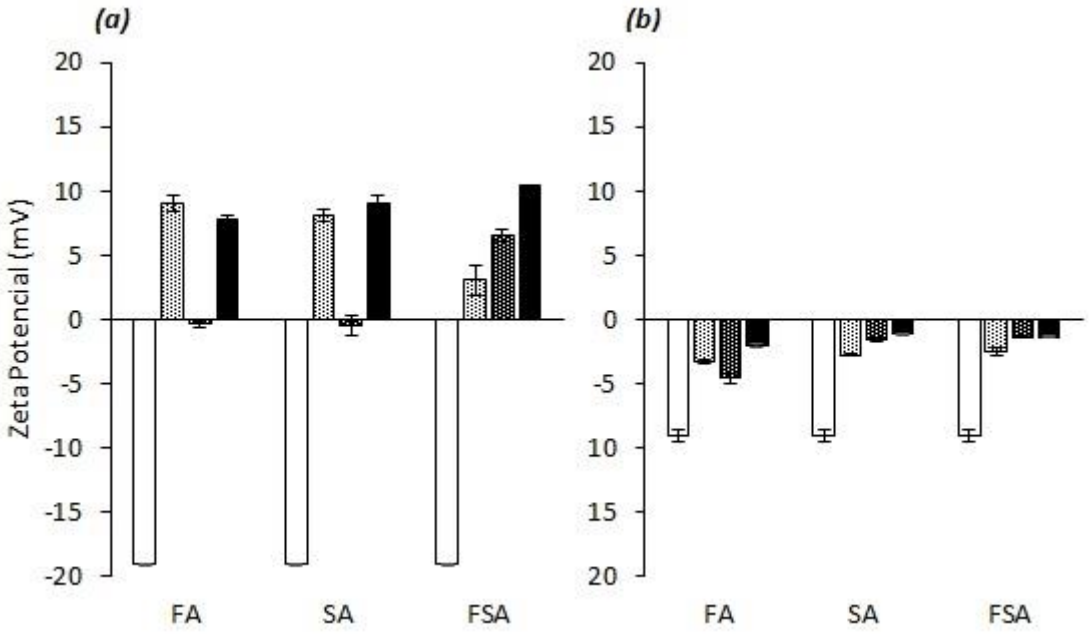

Fig. 4.1 – Zeta potential values (mV) of suspensions of *B. cereus* (*a*) and *P. fluorescens* (*b*) when exposed to different concentrations of FA, SA and FSA: 0 (☐), 100 (▨), 500 (▩) and 1000 (■) µg/mL) for 1h. The means ± SD for at least three replicates are given.

differentiation. Interference with quorum sensing can affect the biofilm development and make the bacteria more susceptible to antimicrobials [369]. Data provided by some studies showed that mutants with lack of quorum sensing form biofilms that are more unstructured, and susceptible to chemical agents compared to wild types [9, 370]. A disc diffusion assay was performed for QSI screening using *C. violaceum* CV12472. Diverse concentrations of the phenolic acids were tested, in order to ascertain if the halos produced around the biosensor strain were due to bacterial growth inhibition and/or QSI (Table 4.4). Hence, loss of purple pigment by *C. violaceum* CV12472 was indicative of QSI by phytochemicals.

No pigment inhibition was observed with FA at the concentrations tested. However, growth inhibition halos between 6.5 and 9.6 mm were detected. Inhibition of pigment production was observed for SA and FSA at 500 and 1000 µg/mL. SA caused a higher inhibition halo than FSA and that effect was also concentration dependent. For these cases, the white zones of inhibition were opaque and not transparent, indicating that the halo around the disks

Table 4.4 – Screening for the QSI effects and antimicrobial activity (AM) of FA, SA and FSA against *C. violaceum* CV12472.
The halos are present as the total final halo minus the diameter of the disk (6mm).

	Concentration (µg/mL)	Pigment production [a]	AM [b] (mm)	QSI [c] (mm)
	100	+	Y (6.5)	N
FA	500	+	Y (8.5)	N
	1000	+	Y (9.6)	N
	100	+	Y (6.9)	N
SA	500	+/-	Y (9.9)	Y (4.9)
	1000	+/-	Y (13.3)	Y (7.9)
	100	+	Y (6.7)	N
FSA	500	+/-	Y (9.9)	Y (2.4)
	1000	+/-	Y (12.5)	Y (4.3)
DMSO	LB	+	N	N
		+	N	N

[a] (+) Indicates visualization of pigment; (-) Indicates absence of purple pigment colors; (+/-) Indicates partial visualization of purple pigment

[b] Y – Antimicrobial activity observed as a clear halo; absence of antimicrobial activity. Diameter of zone of inhibition in mm in parentheses.

[c] Y – QSI observed as colourless halo of viable cells; N absence of QSI. Diameter of QSI in mm in parentheses.

was caused by inhibition of violacein production, and not due to the inhibition of cell growth. Antimicrobial activity, in addition to QSI, was also observed for SA and FSA. The results obtained in this study demonstrated that SA had potential for QSI, despite the small size of halos produced. Moreover, SA had antimicrobial activity in addition to QSI. This effect of SA on QSI can help in understanding the results obtained with biofilms, particularly the behaviour of dual-species biofilms after a second exposure to phytochemicals. However, the QSI activity verified with this phenolic acid needs to be further characterized, particularly in relation to the mechanisms involved in the inhibition process. In fact, it is probable that FA may have QSI activity, not detectable by the method used [325].

The single and dual-species biofilms were characterized in terms of total cell numbers. *B. cereus* biofilms had total cell counts of 6.49 ± 0.16 log cells/cm^2, whereas *P. fluorescens* had 6.64 ± 0.13 log cells/cm^2. Dual-species biofilms presented higher values of total cells (6.77 ± 0.23 log cells/cm^2), although this result was not statistically different from the cell densities of single species biofilms ($P > 0.05$). These 24 h old biofilms had statistically comparable cell densities and they were similar to those of biofilms formed by other bacteria on 96-well PS microtiter plates [327]. It is conceivable that the small differences in cell density of *P. fluorescens* and *B. cereus* single and dual-species biofilms were not the reason for the distinct susceptibility and behaviour to phytochemical exposure.

The preventive action of FA, SA, and FSA on biofilm formation at twice the MIC (1000 µg/mL) was assessed by developing *B. cereus* and *P. fluorescens* single and dual-species biofilms in the presence of these chemicals (Fig. 4.2). In terms of inactivation (Fig. 4.2*a*), dual-species biofilms were equally affected in terms of reduction of biofilm activity by FSA and SA ($P > 0.05$), whereas a significantly lower percentage was found for FA ($P < 0.05$). *P. fluorescens* biofilms had the highest percentage of inactivation with FSA, compared with FA and SA. However, the inactivation percentages were statistically similar ($P > 0.05$). The SA had low effects on *B. cereus* biofilm inactivation. The effects of FSA were more pronounced than those of FA on *B. cereus* biofilms ($P < 0.05$).

The reduction on *P. fluorescens* biofilm formation (Fig. 4.2*b*) was similar ($P > 0.05$) for FSA and FA, and showed a moderate decrease ($P < 0.05$) for SA. In the case of *B. cereus* biofilms, FA had the most significant preventive action ($P < 0.05$) when it was compared with FSA and SA ($P > 0.05$). The highest preventive effects were observed with FA and FSA ($P < 0.05$) for the dual-species biofilms.

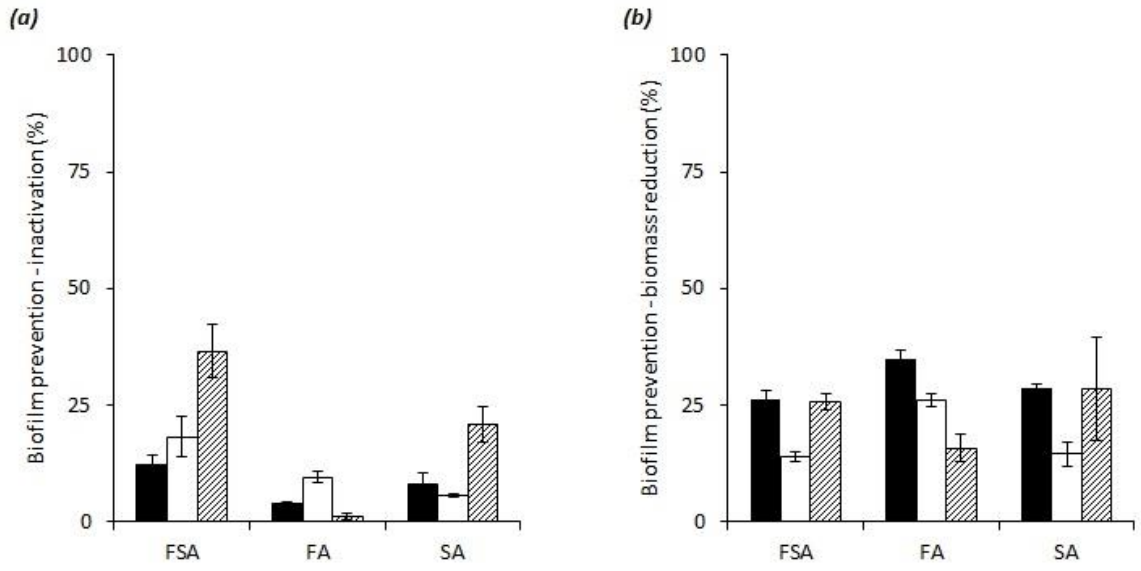

Fig. 4.2 – Preventive action (24 h old biofilms formed in the presence of phenolic acids) of FSA, SA, and SA on the activity *(a)* and biomass formation *(b)* of *P. fluorescens* (■) and *B. cereus* (□) single and dual- (▨) species biofilms.
Mean values ± SD for at least three replicates are illustrated.

For *P. fluorescens* biofilms, no correlation was verified between the thermodynamic adhesion and biofilm prevention tests. This result indicates that the surface physicochemical properties are not the main factor regulating the initial adhesion process. Moreover, in these conditions biofilm prevention was not achieved. This indicates that initial adhesion did not predict the ability of the tested bacteria to form a biofilm, suggesting that other events such as phenotypic and genetic switching during biofilm development and the production of extracellular polymeric substances, may play a significant role in biofilm formation and differentiation [221].

The phenolic acids were applied to 24 h old biofilms and their effects were assessed on inactivation (Fig. 4.3*a*) and biomass removal (Fig. 4.3*b*). The phenolic acids had low effects on the inactivation (< 25%) of single and dual-species biofilms of *B. cereus* and *P. fluorescens*. Despite the lower percentage (< 20%), FSA promoted the most significant inactivation for *P. fluorescens* and *B. cereus* single and dual-species biofilms ($P < 0.05$).

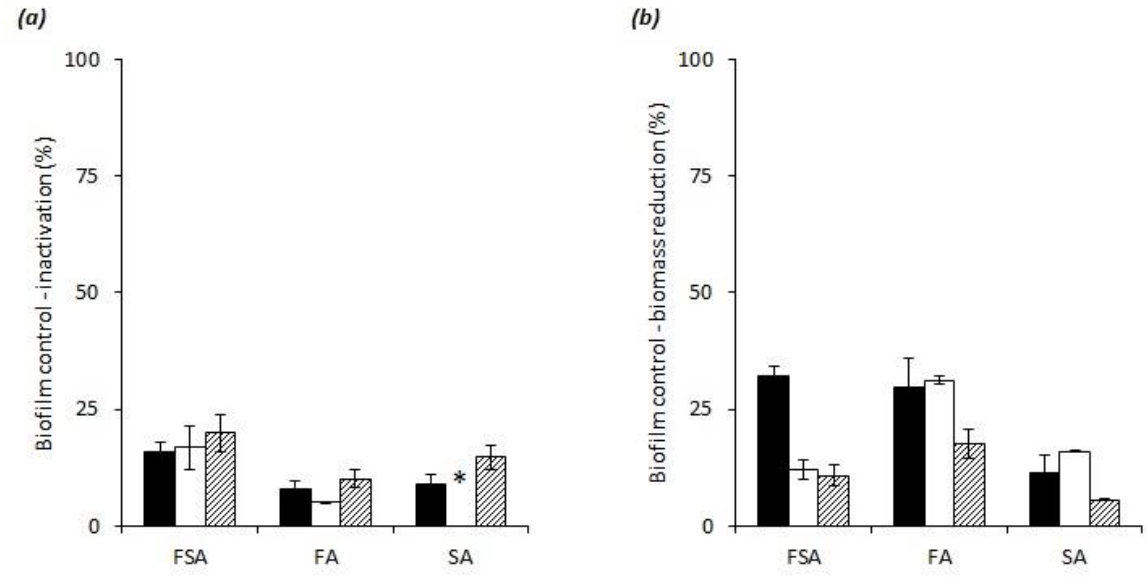

Fig. 4.3 – Percentage of inactivation (a) and reduction (b) of *P. fluorescens* (■) and *B. cereus* (□) single and dual-species (▨) biofilms treated with FSA, FA, and SA for 1 h.
* no inactivation was found.
Mean values ± SD for at least three replicates are illustrated.

In the case of *P. fluorescens* biofilms, SA was more effective than FA ($P < 0.05$), while the opposite occurred for *B. cereus* biofilms ($P < 0.05$). The FA and SA had similar ($P > 0.05$) effects on the inactivation of dual-species biofilms. In terms of biofilm removal, a moderate action (removal > 25%) was found for *P. fluorescens* biofilms treated with FSA and FA and for *B. cereus* biofilms exposed to FA. The remaining treatments had low effects in terms of biofilm removal. The biomass reduction of *P. fluorescens* and *B. cereus* single biofilms (Fig. 4.3*b*) was similar ($P > 0.05$) for FA and SA. For the dual-species biofilm, the biomass reduction was low and statistically similar for the diverse treatments ($P > 0.05$).

Comparing the effects of FA or SA on biofilm control (inactivation and removal), no significant differences were obtained. Also, their combination (FSA) was not always more effective than the individual chemicals. The comparison of the results from this study with previous reports clearly demonstrates that different bacterial species display distinct antimicrobial susceptibilities. A study with hydroxycinnamic and hydroxybenzoic acids demonstrated that those hydroxycinnamics cause higher inhibition of a strain of *Oenococcus oeni* in planktonic state [371]. Borges et al. [235] found that both gallic and ferulic acids had strong potential to inactivate and remove biofilms of *E. coli*, *L. monocytogenes*, *P. aeruginosa,* and *S. aureus*. Prithiviraj et al. [372], using the *Arabidopsis thaliana – P. aeruginosa* pathosystem, gathered evidence that suggests that SA, besides triggering defence responses, could also act

on *P. aeruginosa* by disruption of biofilm formation on biotic and abiotic surfaces and by repression of a number of virulence factors. Other authors [373, 374] found that salicylic-acid-based and releasing polymers significantly reduced biofilm formation by *S. enterica* Typhimurium and *E coli*. Ergün et al. [351] demonstrated that simple aromatic esters of FA inhibited biofilm formation by *S. aureus* at a concentration below 8 μg/mL. In terms of biofilm removal, moderate efficacy was only detected for FSA (*P. fluorescens* single biofilms) and FA (*B. cereus* and *P. fluorescens* single biofilms). These results are in accordance with the findings of Jagani et al. [238]. These authors compared the effects of various natural phenolic compounds on *P. aeruginosa* biofilm removal, showing that SA caused a moderate reduction (45%) when compared to other molecules. Saavedra et al. [181], in studies with planktonic bacteria (*E. coli*, *P. aeruginosa*, *L. monocytogenes*, and *S. aureus*) found low levels of inhibitory effects of hydroxycinnamic acids (ferulic and caffeic acids) and a hydroxybenzoic acid (gallic acid), when compared to selected antibiotics (gentamicin, ciprofloxacin, and streptomycin). It is assumed that hydroxycinnamic and hydroxybenzoic acids have similar antibacterial action mechanisms, promoting enzyme inhibition, possibly through reaction with sulfhydryl groups or through nonspecific interactions such as the reversible or irreversible reaction of quinonic compounds with amino acids or with peptides [356, 375].

The effects of a second exposure to phytochemicals were assessed on single and dual-species biofilms formed in the presence of phenolic acids (Fig. 4.1). The exposure of presumptively adapted biofilms to the phytochemicals promoted a high inactivation (> 80%) of dual-species biofilms, with FSA, FA, and SA showing similar effects ($P > 0.05$). The metabolic activity of single species biofilms was affected to a low extent and the inactivation promoted by the phenolic acids was similar when comparing both *B. cereus* and *P. fluorescens* single species biofilms ($P > 0.05$). The action of phenolic acids on the removal of presumptively adapted biofilms was moderate (removal > 25%) for all conditions analysed. The application of FA, SA, and FSA caused similar removal of *B. cereus* and *P. fluorescens* single species biofilms ($P > 0.05$). The dual-species biofilms were the most significantly affected by the chemicals, with FA and SA promoting the higher removal percentages ($P < 0.05$).

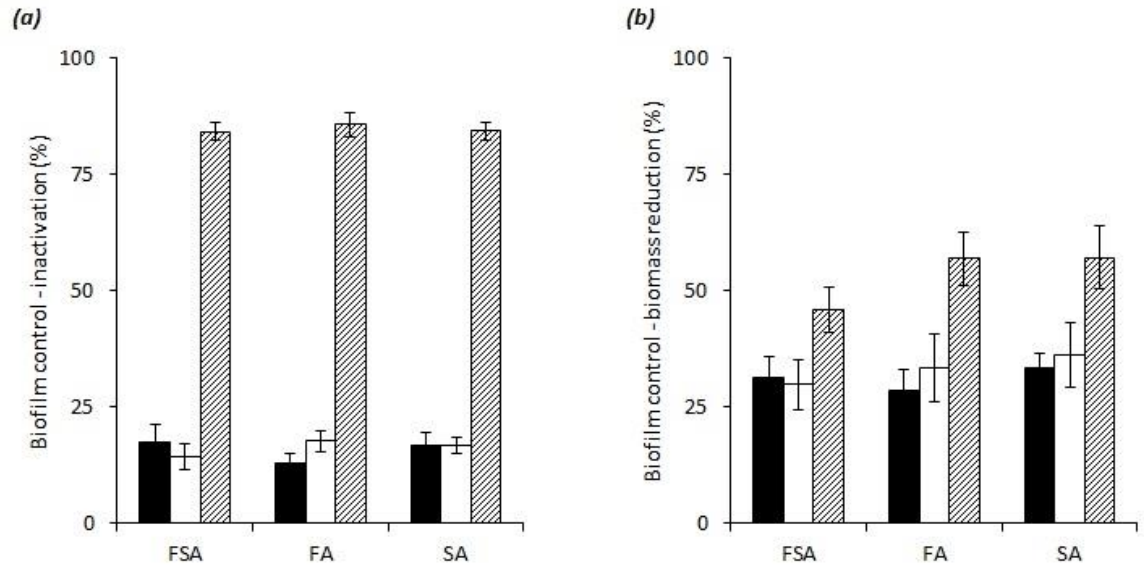

Fig. 4.4 – Percentage of inactivation (a) and reduction (b) of *P. fluorescens* (■) and *B. cereus* (□) single and dual-species (▨) biofilms formed in the presence of FSA, FA, and SA for 24 h and subsequently exposed to the phenolic acids for 1 h.
Mean values ± SD for at least three replicates are illustrated.

This is a surprising result as in previous studies [160, 312] it was found that the *B. cereus – P. fluorescens* association increased resistance to antimicrobial products (an aldehyde-based biocide and a quaternary ammonium compound) comparatively to their single species biofilms. This study demonstrates that dual-species biofilm formation in the presence of FA, SA, or FSA will increase their susceptibility to a second exposure to the chemicals. This is a new finding and indicates that the interactions established by *B. cereus* and *P. fluorescens* in the formation of dual-species biofilms seem to be affected by the presence of FA, SA, or FSA. In fact, single species biofilms were almost unaffected by the second exposure to the phenolic acids. Houry et al. [364] demonstrated that the infiltration of *Bacillus thuringiensis* into a *Staphylococcus aureus* biofilm promotes the penetration of macromolecules, such as antimicrobials, into the biofilm. The authors suggested that these tunnelling bacteria can be used to increase the efficacy of biocides in both industrial abiotic surface disinfection and human infections. This is one of the probable aspects that might be involved in the increased susceptibility of the dual-species biofilms to the phytochemicals tested.

4.4. Conclusion

In conclusion, FA and SA can significantly reduce bacterial swimming motility, increase the surface charge value, and promote changes in the physicochemical surface properties of both *B. cereus* and *P. fluorescens*. SA demonstrated potential for QSI. Their distinct chemical structure does not seem to cause differences in the biofilm control activity, when the molecules were applied individually (FA and SA) and in combination (FSA). This result reinforces the inadequacy of planktonic tests to the design of disinfection procedures to be applied to control biofilms. The development of biofilms in the presence of phenolic acids increased the susceptibility of dual-species biofilms to a second exposure to the chemicals, arguably due to an interference with the interactions involved in *B. cereus – P. fluorescens* biofilm formation and structure. For both bacteria, the MIC of BDMDAC was significantly lower than the MIC of the phenolic acids, and therefore the biocide was selected for further studies regarding biofilm control. This option is based on the use of more economic and sustainable control strategies, since smaller amounts of the compound would be needed to achieve the same growth inhibitory results, when compared to the phytochemicals.

Chapter 5

The effects of surface type on the removal of *Bacillus cereus* and *Pseudomonas fluorescens* single and dual-species biofilms

5. The effects of surface type on the removal of *Bacillus cereus* and *Pseudomonas fluorescens* single and dual-species biofilms

Abstract

The aim of this work was to assess the effectiveness of the biocide BDMDAC on the removal of single and dual-species biofilms of *B. cereus* and *P. fluorescens* formed in a RCR, using SS and PMMA as adhesion surfaces. Additional tests were performed to understand the adhesion of *B. cereus* and *P. fluorescens* to the selected surfaces. Predictions of the adhesion potential according to a thermodynamic theory showed more favourable adhesion on SS than on PMMA, for both species. Thermodynamically, adhesion was more favourable for *B. cereus*. After BDMDAC treatment, thermodynamic adhesion ability was favoured for *P. fluorescens* and decreased for *B. cereus*, mainly on PMMA. Both bacteria had negative surface charge and the exposure to BDMDAC increased the charge to less negative values. *In vitro* adhesion results were, for most cases, contradictory to those predicted by the thermodynamic theory. Single and dual-species biofilms were formed in the RCR for 7 days. The phenotypes of biofilms formed on the two materials were evaluated. PMMA favoured the production of extracellular proteins in the case of dual-species biofilms and extracellular polysaccharides in the case of *B. cereus* single species biofilms. *P. fluorescens* biofilms presented the highest amount of extracellular proteins and polysaccharides when formed on SS. Afterwards, the biofilms were exposed to the chemical (use of BDMDAC) and to hydrodynamic stresses (use of increasing Reynolds number of agitation), alone and combined. The applications of BDMDAC or hydrodynamic stress, when applied alone, were insufficient to remove the biofilms from the surfaces. The combined effects of BDMDAC with a series of increasing Reynolds number of agitation promoted additional biofilm removal. This effect was dependent on the surface used. For PMMA, the hydrodynamic stress was more effective on the removal of BDMDAC-treated dual-species biofilms. For SS, the synergy of the chemical and hydrodynamic stresses removed more *B. cereus* and dual-species biofilms. The overall results demonstrate that the species association was not advantageous in biofilm resistance to removal when compared with the single species biofilms, particularly those of *P. fluorescens*. In general, removal by hydrodynamic stress, alone and preceded by the BDMDAC treatment, was higher for biofilms formed on SS. However, even the combined action of BDMDAC with the exposure to a series of increasing Reynolds number of agitation were not effective to obtain biofilm-free surfaces.

5.1. Introduction

Food industries face costly losses due to food spoilage and contamination with pathogenic microorganisms that often survive as biofilms [150], which are highly resistant to antimicrobials [376, 377]. Conventional strategies for disinfection leave residual microorganisms on the equipment surfaces, allowing the biofilm re-establishment [75, 149]. An effective biofilm control strategy must include the combination of disinfection with a mechanical removal step [332, 378]. Previous works using similar strategies have been done, though using only one material as adhesion surface and mostly one bacterium for biofilm formation [302, 312, 332, 379]. However, the biofilm formation process can be affected by the type of adhesion surface [30], and further evidences are needed on the practical influence of this aspect on surface cleaning.

In this study, the RCR was used for biofilm formation on SS and PMMA surfaces, providing hydrodynamic conditions similar to those found in industrial plants [312]. SS is the most common material used in industrial processes [380]. PMMA is widely used in laboratory-scale bioreactors [48, 269, 381, 382]. To understand the microbial behaviour in the first steps of the biofilm formation process, the effects of the surface type and the exposure to BDMDAC were assessed on the bacterial physicochemical surface properties and on the initial adhesion to the selected surfaces.

5.2. Materials and Methods

The work described in this section was performed using *B. cereus* and *P. fluorescens* cultures described in sub-section 3.1 and cultivated using the media and the conditions described in the sub-section 3.2. The materials tested were AISI316 SS and PMMA prepared according to sub-section 3.4. The physicochemical properties of the bacterial surfaces (before and after exposure to BDMDAC at 300 µg/mL for 30 min) and materials, namely hydrophobicity and surface charge were assessed following the methods described in the sub-sections 3.7 and 3.9, respectively. Additionally *in-vitro* adhesion assays (sub-section 3.13) were performed in 1 cm^2 slides of both materials to assess the initial adhesion of single and dual-species cultures. The RCR was used to grow biofilms on cylinders of PMMA with a surface area of 44.0 cm^2 (diameter = 2.8 cm, length = 5.0 cm) or SS with a surface area of 34.6 cm^2 (diameter = 2.2 cm, length = 5.0 cm) using the method described in sub-section 3.18. The biofilms obtained were

characterized in terms of major structural aspects as described in the sub-section 3.19. The biofilm removal was assess after treatment with BDMDAC at 300 µg/mL for 30 min (sub-section 3.20) and with hydrodynamic stresses by means of increasing Reynolds number of agitation (sub-section 3.21). Results are presented in terms of percentage of biomass removed after each treatment and after the combination of both chemical and mechanical treatments

5.3. Results and Discussion

Initial tests regarding the hydrophobicity of the cells and the selected surfaces were performed in order to estimate the effects of BDMDAC on bacteria-surface interaction, according to the thermodynamic theory of adhesion [320-322]. The results for the untreated *B. cereus* and *P. fluorescens* cells were already presented and discussed in Chapter 4. Therefore, Table 5.1 presents only the results of the surface tension parameters and hydrophobicity for the cells treated with BDMDAC, and for PMMA and SS surfaces.

P. fluorescens cell surfaces became even more hydrophilic after the exposure to BDMDAC, whereas in the case of *B. cereus* no significant effect was observed. The treatment of *P. fluorescens* with BDMDAC increased significantly ($P < 0.05$) its apolar properties (indicated by the Lifshitz-van der Waals component) and decreased significantly ($P < 0.05$) its polar properties (indicated by the Lewis acid-base component). Again, no significant effects occurred in these parameters after exposure of *B. cereus* to BDMDAC ($P > 0.05$). The surfaces of both cells were predominantly electron donors. This ability increased significantly due to BDMDAC exposure ($P < 0.05$). The electron accepting capacity of *P. fluorescens* ($P < 0.05$) decreased after biocide

Table 5.1 – Surface tension parameters and hydrophobicity (ΔG_{1w1}) of the BDMDAC-treated cells, and for PMMA and SS surfaces.
The means ± SD for at least three replicates are given

	Surface energy parameters (mJ/m^2)				ΔG_{1w1} (mJ/m^2)
	γ^{LW}	γ^{AB}	γ^{+}	γ^{-}	
B. cereus	37.7 ± 1.2	14.3 ± 2.2	1.0 ± 0.2	57.7 ±1.9	37.5 ± 3.2
P. fluorescens	39.5 ± 1.7	9.3 ± 2.5	0.3 ± 0.1	64.2 ± 3.9	49.3 ± 7.2
PMMA	40.9 ± 0.9	4.2 ± 1.0	1.5 ± 0.4	2.4 ± 0.5	-58.4 ± 7.3
SS	37.6 ± 1.1	4.0 ± 0.4	0.6 ± 0.1	5.9 ± 1.3	-44.8 ± 7.9

exposure, but the same did not occur for *B. cereus* ($P > 0.05$). PMMA and SS are hydrophobic surfaces. However, PMMA is more hydrophobic and its apolar properties (γ^{LW}) were higher than for SS. Nevertheless, the ability to donate electrons (γ^{-}) was higher for SS ($P < 0.05$). The results obtained for the SS hydrophobicity are similar to previous observations [40]. The water contact angles of PMMA are also in agreement with earlier studies [383, 384].

The results on the free energy of adhesion (Table 5.2) between the bacteria and the selected surfaces showed that adhesion was thermodynamically more favourable on PMMA than on SS, for both species. Before the chemical treatment, *P. fluorescens* adhesion seems to be less favourable than for *B. cereus*. The bacterial exposure to BDMDAC disfavoured the adhesion of *B. cereus,* particularly on PMMA. An opposite effect was observed for *P. fluorescens*.

The cell surface charge was determined in order to assess the influence of BDMDAC on this cell property (Table 5.3). Under physiological conditions *B. cereus* and *P. fluorescens* had negative surface charges. The treatment with BDMDAC increased the bacterial cell charge to less negative values. This effect is probably a result of the cationic nature of BDMDAC [355].

Table 5.2 – Free energy of adhesion (ΔG_{1w2}^{TOT} – mJ/m^2) between the untreated (control) and BDMDAC-treated *B. cereus* and *P. fluorescens* cells and PMMA and SS surfaces.
The means for at least three replicates are given.

	B. cereus		*P. fluorescens*	
	Control	BDMDAC	Control	BDMDAC
PMMA	-19.0	-14.2	2.6	-14.6
SS	-9.3	-3.7	7.7	-2.9

Table 5.3 – Zeta potential values (mV) of the untreated (control) and BDMDAC-treated *B. cereus* and *P. fluorescens*, PMMA and SS.
The means ± SD for at least three replicates are given

	Control	BDMDAC
Bacteria		
B. cereus	-18.7 ± 0.9	-15.6 ± 2.0
P. fluorescens	-9.8 ± 0.5	-4.1 ± 0.1
Materials		
PMMA	-1.7 ± 0.3	
SS	-2.1 ± 0.3	

The mechanism of initial bacterial adhesion to surfaces has been studied by many researchers and was proposed to depend on both long-range forces like electrostatic and thermodynamic forces and short-range forces like van der Waals attraction [385, 386]. In addition to thermodynamics, the cell surface charge was found to influence bacterial adhesion to surfaces through attractive or repulsive electrostatic forces [387, 388]. Bellon-Fontaine et al. [389] stated that prediction of bacterial adhesion to surfaces was found to be made accurately when electrostatic forces were considered in addition to thermodynamic properties of the cell surface. However, the *in vitro* adhesion results (Fig. 5.1) do not provide clear evidences on the role of thermodynamic aspects and surface charge on bacterial adhesion. Even if *B. cereus* was thermodynamically more prone to adhere to the surfaces, higher numbers of *P. fluorescens* cells adhered to the surfaces, being the number of adhered cells similar on PMMA and SS ($P > 0.05$). The number of adhered cells for the combination of *B. cereus* and *P. fluorescens* is apparently an average of the numbers obtained with the single species. *In vitro* tests also indicated that BDMDAC decreased the numbers of adhered cells, being this effect stronger for *B. cereus* ($P < 0.05$) than for *P. fluorescens* ($P > 0.05$). The higher number of *P. fluorescens* remaining adhered, after BDMDAC exposure, might be due to the fact that Gram-negative bacteria have a cell envelope/outer membrane which regulates the passage of substances to the periplasmic space and the cytoplasm. This fact may contribute to a higher intrinsic resistance of *P. fluorescens* to biocides than the Gram positive *B. cereus* [390].

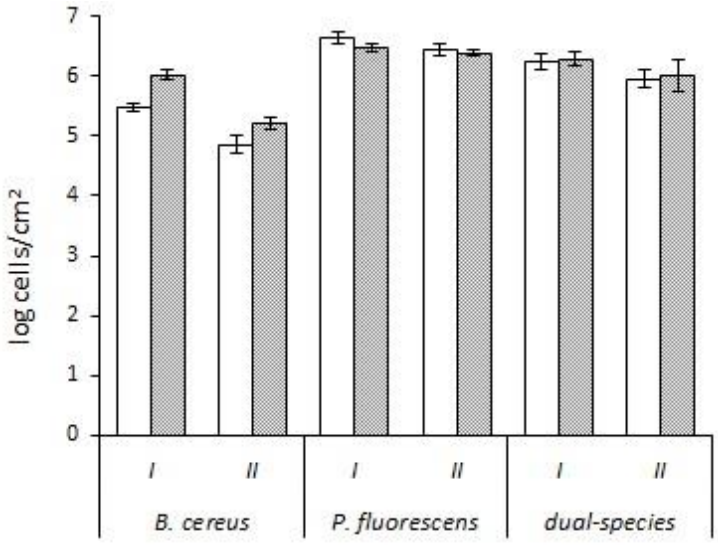

Fig. 5.1 – Numbers of *B. cereus* and *P. fluorescens* single and dual-species cells previously adhered for 2h on PMMA (☐) and SS (▨) surfaces, before *(I)* and after a 30 min treatment with BDMDAC *(II).*
The means ± SD for at least three replicates are given.

The disagreement between the thermodynamic study and *in vitro* adhesion results is arguably due to the limitations of the thermodynamic theory. This theory of adhesion may predict some outcomes of the bacterial adhesion. However, accurate values for bacterial surface free energies are very difficult to obtain as cells are living organisms, with complex chemistry and hydration processes. Moreover, this theory implies an equilibrium model and a closed system, where there are no energy exchanges with the outside [391]. Bacterial cells are metabolically active, and energy consuming physiological mechanisms like the synthesis of EPS, may be influencing the adhesion events [392]. In fact, Simões et al. [221] had also found similar results studying the initial adhesion of drinking water-isolated bacteria. These findings underscore that despite the physicochemical surface properties of both the bacterium and substratum being crucial for the adhesion phenomena, other biological aspects such as phenotypic and genetic switching, and the production of EPS, may play a significant role on biofilm formation and differentiation. Motility processes ruled by extracellular appendages (pili, flagella, fimbriae), the presence of outer membrane proteins and quorum sensing mechanisms also play an important role in the attachment to surfaces [8, 393, 394].

The 7 days old biofilms (shown in Fig. 5.2 prior to the treatments) were exposed to BDMDAC under the same hydrodynamic conditions used for its formation.

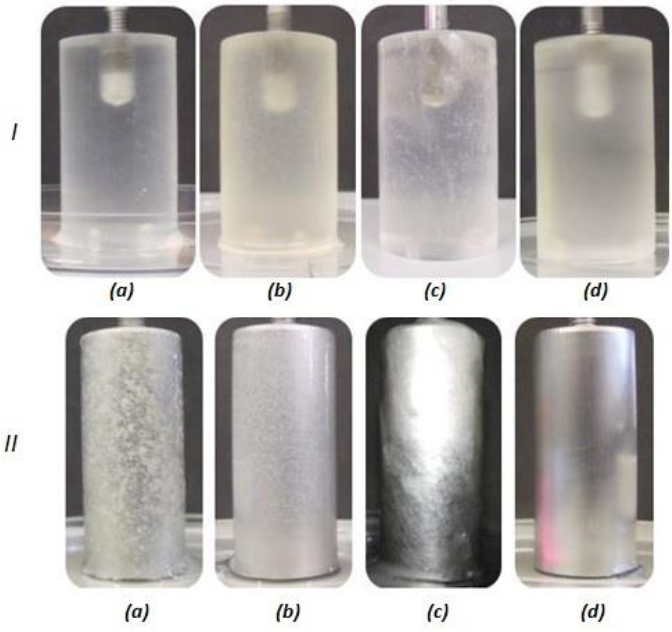

Fig. 5.2 – Photographs of the cylinders of PMMA *(I)* and SS *(II)* covered with *B. cereus (a)*, *P. fluorescens (b)* single and dual-species *(c)* biofilms, before any treatment.
For both materials, the photograph of a clean cylinder *(d)* is shown for comparison.

Biofilms formed on PMMA and SS cylinders were characterized in order to infer on the influence of some structural aspects on their resistance to removal. The results obtained (Table 5.4) demonstrated that both species formed biofilms with distinct characteristics, dependent on the species association and on the adhesion surface used. *P. fluorescens* and *B. cereus* single and dual-species biofilms differed in terms of thickness and biofilm dry mass. These differences are also dependent on the substratum, although the same patterns can be observed in the case of thickness and biofilm mass, which were both higher for the dual-species biofilms, followed by the *P. fluorescens* and *B. cereus* single species biofilms. Overall the biofilms formed on PMMA presented higher values of dry mass than those formed on SS. Dual-species biofilms presented higher cellular density when formed on PMMA, and were always predominantly colonized by *B. cereus*. Again, these results are not in agreement with the thermodynamic prediction of adhesion, which was globally more favourable in the case of *P. fluorescens*, when compared to

Table 5.4 – Characteristics of *B. cereus* and *P. fluorescens* single and dual-species biofilms formed on PMMA and SS cylinders.
The means ± SDs for at least three replicates are given.

	B. cereus	*P. fluorescens*	Dual-species
	PMMA		
Biofilm thickness (μm)	59 ± 20	255 ± 8	329 ± 9
Dry biofilm mass (mg/cm^2)	0.258 ± 0.06	0.295 ± 0.02	0.324 ± 0.05
Log cell density (cells/cm^2)	6.78 ± 0.31	6.81 ± 0.14	7.66 ± 0.08[a]
Matrix polysaccharides (% of the total polysaccharides)	80.8 ± 10.8	62.0 ± 0.4	11.9 ± 1.4
Matrix proteins (% of the total proteins)	78.1 ± 4.4	39.8 ± 7.9	94.9 ± 5.1
	SS		
Biofilm thickness (μm)	75 ± 4	262 ± 42	484 ± 163
Dry biofilm mass (mg/cm^2)	0.197 ± 0.03	0.258 ± 0.05	0.272 ± 0.05
Log cell density (cells/cm^2)	6.44 ± 0.10	7.15 ± 0.16	6.66 ± 0.02[b]
Matrix polysaccharides (% of the total polysaccharides)	59.5 ± 6.3	82.8 ± 0.4	61.0 ± 2.9
Matrix proteins (% of the total proteins)	45.5 ± 1.3	72.3 ± 0.1	57.2 ± 1.4

a – 7.47 (± 0.06) of *B. cereus* and 7.18 (± 0.13) of *P. fluorescens*

b – 6.44 (± 0.08) of *B. cereus* and 6.24 (± 0.08) of *P. fluorescens*

B. cereus. The present results for the composition of the EPS in terms of polysaccharides and proteins were dependent on the nature of the surface and the microorganism [395, 396]. The type of microbial population, being a single or dual-species culture is the main factor influencing the differences in the structural characteristics [10].

When formed on PMMA, the biofilms with highest amount of extracellular proteins were the dual-species (94.9%), whereas biofilms with highest amount of extracellular polysaccharides were those of *B. cereus (*80.8%). On the other hand, when formed on SS, the *P. fluorescens* biofilms had the highest amount of extracellular proteins and extracellular polysaccharides (72.3% and 82.8%, respectively).

The percentage of the remaining biofilm on PMMA and SS cylinders was determined for the following scenarios (Fig. 5.3): after the action of BDMDAC alone, for 30 min; after the exposure to increasing Re_A; and after applying the two treatments combined (BDMDAC exposure followed by hydrodynamic stress). The percentage of biofilm removed after exposure to BDMDAC was significantly higher for *B. cereus* and dual-species biofilms than for the *P. fluorescens* single species adhered on PMMA. Conversely, when the biofilms were formed on SS, *P. fluorescens* biofilms were more susceptible to this treatment, followed by the dual-species and the *B. cereus* single species biofilms. The latter results contradict those found by Simões et al. [312], who observed that *P. fluorescens* biofilms formed on SS surfaces were the most

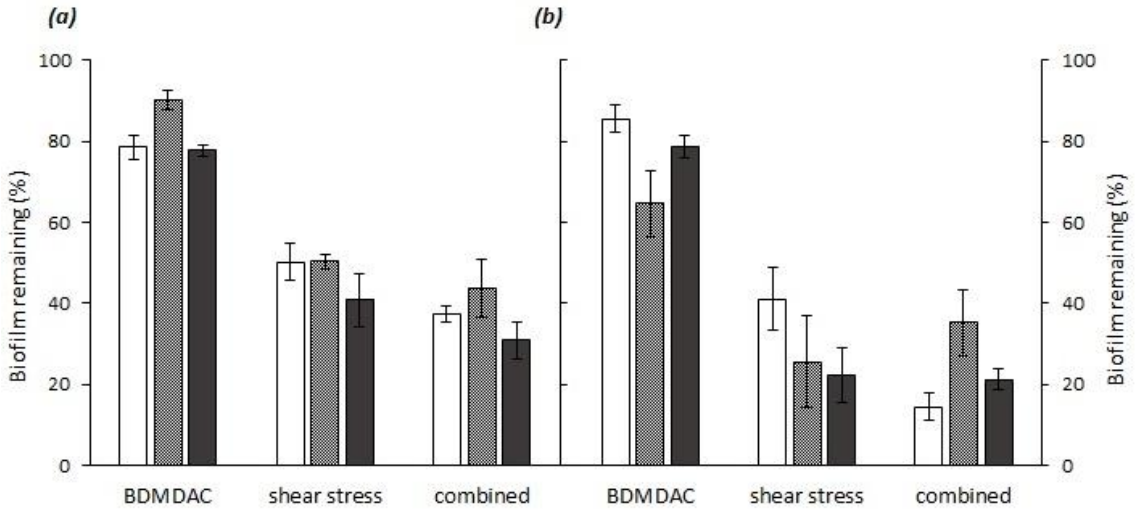

Fig. 5.3 – Biofilm remaining (%) after submitting the biofilms to BDMDAC treatment alone, to the complete series of hydrodynamic stresses and to combination of both treatments. *B. cereus* (□), *P. fluorescens* (▩) single and dual-species (■) biofilms formed on PMMA *(a)* and on SS *(b).*
The means ± SDs for at least three replicates are given.

resistant to the chemical treatment with the biocides glutaraldehyde and cetyl trimethyl ammonium bromide (CTAB). These differences are likely due to distinct chemicals used, proposing that no general conclusion on a biofilm control strategy can be withdrawn from experiments based on a single antimicrobial agent, even if they share the same chemical nature as occurs for BDMADC and CTAB (both are quaternary ammonium compounds). Moreover, the amounts of removal caused by the chemical treatment and the different structure characteristics presented by the biofilms are not correlated. This suggests that other parameters of the physical structure of the biofilm, like porosity, might have influenced the diffusivity of the BDMDAC molecules within the biofilm and consequently the disintegration of the matrix [397].

After the chemical treatments, the biofilms were subjected to a hydrodynamic stress caused by increased Re_{A} (Fig. 5.3). Control tests were performed subjecting untreated biofilms to the same hydrodynamic stress. The results shown that the aim of obtaining biofilm-free surfaces was not achieved, for all conditions tested. In fact, after the hydrodynamic stress tests, significant amounts of *B. cereus, P. fluorescens* and dual-species biofilms remained on the PMMA (37%, 44% and 31%, respectively) and the SS cylinders (14%, 35% and 21%, respectively). However, the removal values were higher than those achieved with only mechanical action, with the exception of *P. fluorescens* biofilms formed on SS, where no significant difference was observed ($P > 0.05$). *P. fluorescens* biofilms were the most resistant to the combined treatment, especially when formed on PMMA. BDMDAC is a quaternary ammonium compound (QAC) and therefore acts by destabilizing the cell membranes, causing rapid cell lysis [157]. Its action against bacteria was described by Ferreira et al. [355], including its efficacy in the inactivation of biofilms [269]. No reports are available on the mode of action and/or resistance of BDMDAC on biofilms. A study performed with two quaternary ammonium compounds (benzalkonium chloride and CTAB) demonstrated the reduction of their antimicrobial effects against *B. cereus* and *P. fluorescens* due to interaction with biofilm components [398]. Campanac et al. [399] found that resistance of the Gram negative bacterium *P. aeruginosa* biofilms to diverse QAC`s was due to the involvement of the negatively charged EPS produced by the bacterium and the reduce diffusion of antimicrobials through the biofilm. In the case of the Gram positive bacterium *Staphylococcus aureus,* the role of the three-dimensional structure was limited and drastic physiological changes in the biofilm cells were the most important aspect implicated in resistance. It is recognized that the EPS matrix can cause mass transfer limitations, and that interactions between their molecules and the biocide may occur, reducing its availability to interact with the biofilm cells [66, 397, 400]. A previous report [40] described that the *B. cereus* strain used in the present study is a low biofilm EPS producer compared to the *P. fluorescens*

biofilms. This high EPS content of *P. fluorescens* biofilms can help to explain their higher resistance to removal. Actually, when the substrate used was SS, the fact that *P. fluorescens* biofilms presented the highest amounts of extracellular polysaccharides and proteins (82.8% and 72.3%) was probably the cause of its highest resistance to the overall treatment. In fact, one of the most important functions of EPS is supposed to be their role as fundamental structural elements of the biofilm matrix determining the mechanical stability of biofilms, mediated by non-covalent interactions either directly between the polymeric chains or indirectly via multivalent cation bridges [401, 402].

The species association was not advantageous in forming biofilm resistant to removal. The biofilm remaining on the surfaces after the chemical and hydrodynamic stresses, alone and/or combined, was, for most of the cases, lower for the dual-species biofilms. This result contradicts previous studies, where species association increased biofilm resistance [16, 403, 404]. However, in those studies, the biofilms were challenged with antimicrobial chemicals and the viability of the biofilm cells was analysed. In the present study, the outcomes of the chemical and/or hydrodynamic stresses were only assessed in terms of biofilm removal. It is likely that the bacteria in the dual-species biofilms had higher resistance to killing but a decreased resistance to removal, compared with the single species biofilms, particularly those formed by *P. fluorescens*. In fact, the killing and the removal of a biofilm are distinct processes [405, 406] and it is possible to kill a biofilm without promoting its removal from the surface [312].

Although total removal of the biofilm was not achieved, the overall results underscore that SS should be preferred to other materials as it facilitates the sanitization procedures, reinforcing previous findings [34, 407].

5.4. Conclusions

Biofilm formation on SS and PMMA surfaces was monitored on a RCR. This bioreactor proved to be a versatile tool to ascertain the effectiveness of the biocide BDMDAC to be used in the removal of biofilms. The thermodynamic approach was not reliable in the prediction of bacterial initial adhesion to the selected surfaces. Laboratorial adhesion assays demonstrated that *P. fluorescens* had the highest ability to adhere on PMMA and SS surfaces, while *B. cereus* had the lowest ability. The number of adhered cells for the combination of *B. cereus* and *P. fluorescens* was apparently an average of the numbers obtained with the single species. BDMDAC decreased moderately the numbers of adhered cells, being this effect stronger for

B. cereus single cells than for *P. fluorescens* single cells and combined. Using the RCR, neither the application of BDMDAC nor the increasing series of Re_A, when applied alone or combined with the chemical, were able to totally remove the biofilms from the surfaces. Biofilm removal was dependent on the adhesion surface and on the microbial species. *P. fluorescens* biofilms were the most resistant to removal, while dual-species biofilms had the lowest mechanical stability, for most of the cases. No advantage in biofilm resistance to removal was found for the dual-species biofilms. SS was the surface for which biofilm removal by the hydrodynamic stress, alone and preceded by the BDMDAC treatment, was higher. However, even if additional removal was achieved by the combination of both treatments, total removal was not achieved, regardless the biofilm forming species and the surface material used.

CHAPTER 6

The effects of shear stress on the formation and removal of *Bacillus* biofilms

6. The effect of shear stress on the formation and removal of *Bacillus cereus* biofilms

Abstract

The influence of the shear stress (τ_w) under which biofilms were formed was assessed on their susceptibility to removal when exposed to chemical and mechanical stresses. A rotating cylinder reactor was used to form biofilms, allowing the simulation of τ_w conditions similar to those found in industrial settings, particularly in areas with low τ_w like elbows, corners, valves and dead zones. *B. cereus* was used as a model bacterium for biofilm formation. Biofilms were formed on SS cylinders under different τ_w (estimated at 0.20, 1.46 and 2.14 Pa) for 7 days. Some biofilm phenotypic characteristics, including thickness, biomass production, cellular density and extracellular proteins and polysaccharides content were assessed. Biofilm density was found to increase significantly with τ_w while the thickness decreased. Also, biofilms formed at 0.20 Pa had lowest biomass content, cell density and extracellular polysaccharide content. Those characteristics were not statistically different for the biofilms formed under 1.46 and 2.14 Pa. *Ex situ* tests were performed by treating the biofilms with the biocide BDMDAC, followed by exposure to increasing τ_w conditions, up to 22.84 Pa (whereas the maximum τ_w used during growth was 2.14 Pa). The biofilms formed under low τ_w were more resistant to removal caused by the BDMDAC action alone. Those formed under higher τ_w were more resistant to the mechanical and the combined chemical and mechanical treatments. The amount of biofilm remaining on the cylinders, after both treatments was statistically similar for biofilms formed under 1.46 and 2.14 Pa. The resistance of biofilms to removal by mechanical treatment (alone and combined with BDMDAC) was related to the amount of matrix polysaccharides. However, none of the methods investigated were able to remove all the biofilm from the cylinders.

6.1. Introduction

In the biofilm formation process, the hydrodynamic conditions define the transport of the cells, oxygen and nutrients from the bulk fluid to the microbial film [57-59]. Diverse studies have demonstrated the influence of hydrodynamic conditions on biofilm behaviour. Douterelo et al. [189] examined biofilms from DWDS and found that the hydraulic regime influenced the bacterial composition and community structure. They also observed that flushing (sudden flow of fluid at high τ_w inside the system) did not succeed in total biofilm removal but altered the

biofilm microbial community. Paul et al. [191] studied the influence of the substrate and hydrodynamic conditions on biofilm formation and erosion, measuring biofilm thickness and density. Their results showed that increasing the τ_w experienced during growth resulted in biofilms with lower thickness and mass and higher volumetric density, compared with low τ_w conditions. The authors also found that the biofilms presented stratified cohesion: exposure to $\tau_w \leq 2$ Pa caused detachment while $\tau_w > 2$ Pa caused compression of the biofilm. The effect of environmental conditions on biofilm formation, their structure, composition and physical properties have been reported by Cloete et al. [408]; Derlon et al. [409] and Rochex et al. [13].

The aim of this study was to investigate the influence of the τ_w under which biofilms were formed on their resistance to removal by chemical and mechanical treatments. The rotating cylinder reactor was used to form biofilms on stainless steel cylinders at low τ_w, mimicking conditions found in engineered systems. The low τ_w simulated with this reactor are often found in elbows, valves and dead zones in corners and in sudden pipe expansions [190, 410]. Also, typical τ_w values found in drinking water distribution systems (e.g., 0.25 Pa in a 100 mm diameter pipe) are in the range of those used in this study [411]. The combined mechanical action and chemical treatment was used to challenge biofilms formed by *B. cereus*. This bacterium is an industrial contaminant and a public health hazard widespread in nature and frequently isolated from dairy products and equipment [168, 311, 407, 412, 413].

6.2. Materials and Methods

The work described in this section was performed using the *B. cereus* culture described in sub-section 3.1, cultivated using the media and the conditions described in sub-section 3.2. Biofilms were grown on cylinders of AISI316 SS (sub-section 3.4) using the RCR described in the sub-section 3.18, under different τ_w values presented in Table 6.1 (estimated for each rotation speed selected in the overhead stirrer).

Table 6.1 – Estimated values for τ_w and Re_A at the rotation speeds N used in this study.

N (s^{-1})	Re_A	τ_w (Pa)
2.1	1000	0.20
6.6	3200	1.46
8.3	4000	2.14

The cylinders were removed from the RCR and phenotypic characteristics were assessed (sub-section 3.19), namely thickness, dry mass, volumetric density, cellular density, water content, and amount of extracellular proteins and polysaccharides. A chemical treatment was performed (sub-section 3.20) by exposing the biofilms formed under the different τ_w to BDMDAC at 300 μg/mL for 30 min under the same τ_w of formation. These tests were followed by exposure to increasing τ_w conditions (sub-section 3.21) to assess the removal by hydrodynamic stress both alone along with in combination with previous chemical treatment. The amount of biofilm removed for all the conditions, (chemical or mechanical treatments alone or combination of both) is presented in terms of dry mass (mg/cm^2).

6.3. Results and Discussion

The biofilm structure is determined essentially by the nature of the microorganisms and by the environmental conditions under which they are formed [337, 414]. In this study, *B. cereus* biofilms were formed under different τ_w (0.20, 1.46 and 2.14 Pa), over 7 days, using the RCR with constant nutrient loading rate, temperature and pH. The biofilms presented different characteristics (Table 6.2). Only the water content was statistically similar for the three biofilms ($P > 0.05$). These biofilms were mostly composed of water (> 93% of the total mass). Higher τ_w applied during formation resulted in lower biofilm thickness ($P < 0.05$). The thickness of a biofilm grown under 0.20 Pa was about three times higher than those formed under 2.14 Pa. The biofilms formed under 1.46 Pa were twice as thick as those formed under 2.14 Pa. On the other hand, increasing τ_w caused an increase ($P < 0.05$) in the biofilm mass, volumetric density and cell density ($P < 0.05$). Previous works showed similar trends regarding the effects of hydrodynamic conditions on biofilm thickness, volumetric density and cell density [58, 191, 337, 415]. It is known that the flow velocity affects the transport of substrate to the surface of the biofilm, influencing microbial metabolism and growth [58, 416]. The main reasons for the distinct structure, physiological composition and metabolic characteristics of biofilms formed under distinct hydrodynamic conditions are attributed to the different transport rates of oxygen, nutrients and cells from the fluid to the biofilm, the effect of flow conditions on the structural plasticity of biofilms (mass transfer limitations) and the cellular induced reactions, acting as single or concomitant factors [25, 417, 418]. The influence of hydrodynamic conditions on biofilm formation and characteristics might help to explain the increase in the dry mass and cell density and decrease in the biofilm thickness, with increasing τ_w.

Table 6.2— Characteristics of *B. cereus* biofilms formed under different τ_w. These are the characteristics of the biofilms before any chemical or mechanical treatment.
The means ± SD for at least three replicates are given.

τ_w (Pa)	0.20	1.46	2.14
Thickness (μm)	298 ± 17	220 ± 10	108 ± 20
Dry mass (mg/cm^2)	0.382 ± 0.03	0.621 ± 0.02	0.694 ± 0.05
Volumetric density (mg/cm^3)	12.9 ± 0.7	28.4 ± 1.3	66.8 ± 12.1
Cellular density ($\log_{10}$ cells/cm^2)	7.60 ± 0.58	8.13 ± 0.09	8.37 ± 0.52
Water content (% of total biofilm mass)	97.0 ± 0.03	93.9 ± 0.37	95.1 ± 0.35
Extracellular polysaccharides (% of total biofilm polysaccharides)	31.5 ± 6.7	50.5 ± 0.7	40.4 ± 10.7
Extracellular proteins (% of total biofilm proteins)	29.5 ± 4.6	41.9 ± 1.6	22.7 ± 0.4

The differences in biofilm characteristics are more significant when comparing the biofilms formed under 0.20 Pa with those formed under higher τ_w. The biofilm mass and cell density were not significantly different when the biofilms were formed under 1.46 and 2.14 Pa ($P > 0.05$). A previous study [419] with different strains of *P. fluorescens* (the type strain ATCC 13525 and two strains, D3-348 and D3-350, isolated from an industrial processing plant) demonstrated the presence of higher cell counts for turbulent flow-generated biofilms than for those formed under laminar flow. However, those biofilms were formed in a flow cell reactor, where the hydrodynamic regimes were laminar flow (Re = 2000, corresponding to a linear velocity of $v = 0.20$ m/s) and transition/turbulent flow (Re = 4200, $v = 0.53$ m/s), whereas in this work the Re_a was essentially turbulent (above 100) and the maximum linear velocity used (for the highest Re_A) was 0.51 m/s[1].

The numbers of spores were negligible (always lower than 2.2 $\log_{10}$ cells.cm^{-2}) comparatively to the numbers of vegetative cells, for the three biofilms. This result corroborates previous findings where *B. cereus* biofilms had residual numbers of spores comparatively to the numbers of vegetative cells [379, 420]. However, Faille et al. [412] found that sporulation occurred in biofilms formed by *Bacillus* strains and suggested that biofilms would be a significant source of food contamination with spores. It is possible that the presence of spores in the biofilm

may depend on the microbial strain and on the process conditions used, including the type and mode of operation of the bioreactor used for biofilm formation.

The biofilms presented different amounts of matrix proteins and polysaccharides (Table 6.2). The percentage of matrix polysaccharides was higher for the biofilms formed under 1.46 and 2.14 Pa. It has been proposed [421-423] that high detachment forces can induce the biofilms to secrete more EPS. However, there was no relationship apparent between the percentage of matrix proteins and polysaccharides τ_w increased. In fact, the biofilms formed at 1.46 Pa presented the highest percentage of both proteins and polysaccharides.

A combined strategy of chemical and mechanical stress was applied to the *B. cereus* biofilms formed in the RCR in order to promote biofilm removal. This was performed by exposing the biofilms to BDMDAC at the same τ_w used for its formation. This process was followed by exposing the biofilm to a series of increasing τ_w values. The amount of biofilm mass removed with the chemical treatment is presented in Fig. 6.1.The highest amount of biomass removed was observed for the biofilms formed under 2.14 Pa while those formed at 0.20 Pa were the least affected by BDMDAC. In terms of percentage of the initial biofilm that was removed the highest percentage was observed for biofilms formed at 2.14 Pa and the lowest percentage was obtained for biofilms formed at 1.46 Pa.

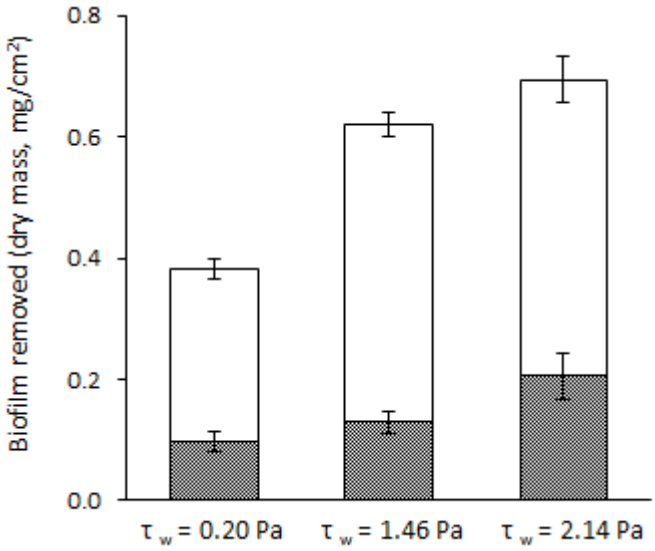

Fig. 6.1 – Biofilm removed (■) after submitting the biofilms to BDMDAC treatment for 30 min. The white bar (□) represents the amount of biofilm remaining after the treatment and the complete bar represents the amount of biofilm formed, over 7 days. The means ± SD for at least three replicates are given.

Quaternary ammonium compounds have demonstrated their potential to remove biofilms [311, 424, 425]. It was found that BDMDAC only induced modest biofilm removal, being the amount of biomass removed lower for the biofilms formed under lower τ_w. In fact, the use of high τ_w during biofilm formation causes the compression of the matrix and facilitate the mass transfer of the biocides, allowing the complete penetration of the microbial layers [414]. Therefore, it is not surprising that the amount of biomass removed due to BDMDAC was higher for those biofilms formed under 2.14 Pa, being followed by those formed under 1.46 Pa.

The amount of biofilm remaining on the cylinders surface after the mechanical treatment and the synergic chemical and mechanical treatments is presented In Fig. 6.2. The application of increasing τ_w was not sufficient to remove all the biofilm from the surfaces, neither was its synergy with BDMDAC. The biofilms formed under 0.20 Pa were the least resistant to both mechanical and combined chemical and mechanical treatments ($P < 0.05$). The amount of biomass remaining on the cylinders was higher for the biofilms formed at 1.46 and 2.14 Pa, after biofilm exposure to the mechanical treatment alone and combined with BDMDAC. The amount of biofilm remaining was statistically similar for both biofilms ($P > 0.05$).

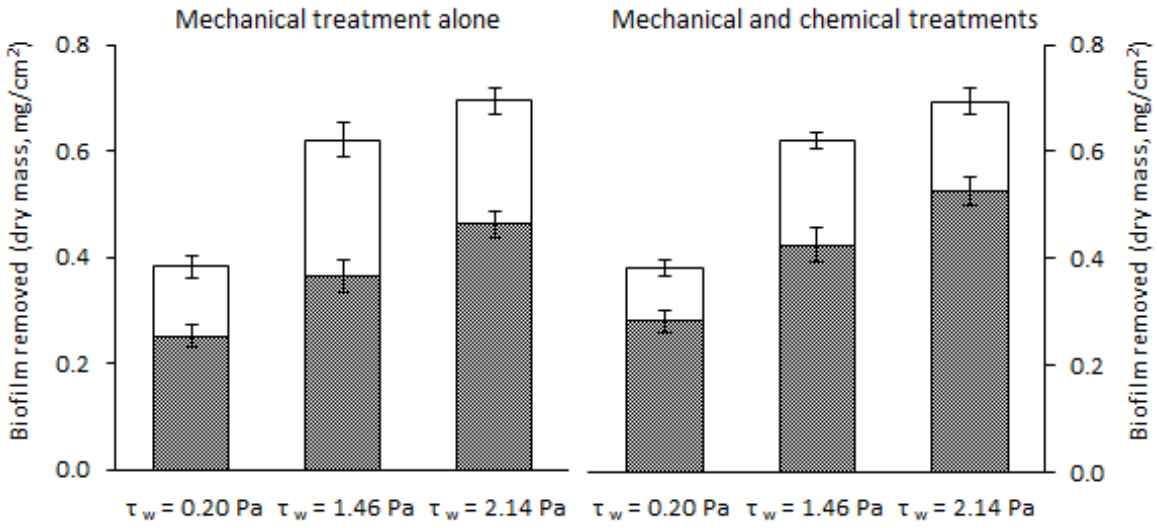

Fig. 6.2 – Biofilm removed (■) after submitting the biofilms to the mechanical treatment alone and to the combination of mechanical and chemical treatments.
The white bar (□) represents the amount of biofilm remaining after the treatment and the complete bar represents the amount of biofilm formed, over 7 days. The means ± SD for at least three replicates are given.

For the three conditions, the synergy between the chemical and mechanical treatments removed an additional fraction of biofilm ($P < 0.05$), when compared with the mechanical treatment alone. This effect was more significant for those biofilms formed under higher τ_w ($P < 0.05$).

Comparing the results from Fig. 6.1 and Fig. 6.2 it can be seen that biofilm formation under the lowest τ_w increased biofilm removal due to combined treatment (on an absolute mass basis). However, the biofilms formed at the intermediate τ_w (1.46 Pa) were more resistant to removal due to the mechanical treatment alone and the combined with BDMDAC, as a higher amount of biomass remained adhered to the surface. The results also showed that the susceptibility to mechanical and the combined chemical and mechanical treatments was similar for the biofilms formed under 1.46 and 2.14 Pa ($P > 0.05$), even if the highest amounts of biofilm remaining were found for those biofilms formed under 1.46 Pa.

The resistance of biofilms was correlated with the percentage of matrix polysaccharides, when mechanical stress was used. The biofilms formed at 1.46 Pa demonstrated the highest resilience to mechanical stress (alone and combined with BDMDAC). These biofilms had the highest percentages of matrix polysaccharides and proteins. EPS is known to strengthen the cohesive forces within the biofilm, thereby contributing to an enhanced inherent biofilm mechanical stability [426].

For all conditions tested, a layer of residual biofilm was found on the cylinder surface. It is interesting to note that even after the combined treatment with both chemical and mechanical actions there was always a layer of about 25% of the total biofilm mass that was still attached to the cylinders surface, for the three biofilms tested. Coufort et al. [415] stated that whatever the environmental conditions are used during formation, biofilms will present a stratified structure where layers present different cohesion from the top to the bottom (close to the substratum). Later, Paul et al. [191] also proposed the existence of a stratified structure of mature biofilms, with a strongly cohesive and dense basal layer. The results obtained in this study also indicate that the *B. cereus* biofilms had a basal layer strongly resistant to removal by chemical and mechanical action, regardless of the τ_w value under which the biofilms were formed. Even if the biofilms were treated with a biocide with recognized antimicrobial efficacy [269, 355], BDMDAC only promoted modest biofilm removal. In real process conditions, this result means that the sanitation strategy was not effective, and that this basal layer will help reseeding a new biofilm possibly with higher resistant and resilient properties than its predecessor.

6.4. Conclusions

The RCR allowed the formation of *B. cereus* biofilms under different hydrodynamic conditions. Increasing the τ_w experienced during biofilm formation resulted in biofilms with lower thickness, higher dry mass, and higher volumetric and cell densities. The biofilms formed under low τ_w were more resistant to removal due to BDMDAC action alone since the low amounts of biomass were removed from the surface. However, the biofilms formed under higher τ_w were more resistant to the mechanical and the combined chemical and mechanical treatments. The amount of biofilm remaining after mechanical or combined chemical and mechanical treatments was similar for both biofilms formed under 1.46 and 2.14 Pa. The combined action of BDMDAC and mechanical treatment provided additional biofilm removal when compared with the single chemical or mechanical treatments. However, total biofilm removal was not achieved, neither by the use of mechanical treatment alone, neither with its combination with BDMDAC. All the biofilms had a basal layer (about 25% of the initial biofilm mass) strongly resistant to removal by chemical and mechanical actions, which may promote the reseed of the biofilm after sanitation.

Chapter 7

The effects of benzyldimethyldodecyl ammonium chloride on the removal of *Bacillus cereus* and *Pseudomonas fluorescens* single and dual-species biofilms formed on high density polyethylene

7. The effects of benzyldimethyldodecyl ammonium chloride on the removal of *Bacillus cereus* and *Pseudomonas fluorescens* single and dual-species biofilms formed on high density polyethylene

Abstract

The complex physical structure of biofilms contributes to its resilience and resistance to cleaning and disinfection methods. In this work, single and dual-species biofilms of *B. cereus* and *P. fluorescens* were formed on high-density polyethylene (HDPE) surfaces using the rotating cylinder reactor (RCR). The biofilms were treated with BDMDAC to assess the removal achieved. In combination with this treatment or separately, the mechanical stability of the biofilms was assessed during exposure to increasing shear stress conditions (τ_w). Additional tests were performed to assess the effects of BDMDAC on the bacterial surface properties (physicochemical properties and surface charge) and on the initial adhesion ability to HDPE. The predictions of the free energy of adhesion indicated a more favourable adhesion of *B. cereus* to HDPE compared with *P. fluorescens.* The treatment with BDMDAC decreased the thermodynamic ability of *B. cereus* to adhere on HDPE but had the opposite effect for *P. fluorescens*. This treatment also modified the surface charge of both bacteria to less negative values. *In vitro* adhesion in HDPE slides was assessed for both single and dual-species cultures, showing that *B. cereus* was the worst surface colonizer. Steady-state biofilms formed in the RCR presented distinct characteristics and behaviour when facing mechanical and chemical stresses. Dual-species biofilms were the thickest while *P. fluorescens* biofilms had the highest volumetric density (13.1 ± 1.9 mg/cm^3). Dual-species biofilms were the most affected by the BDMDAC pre-treatment, with more than 50% of biofilm mass being removed. The combination of chemical and mechanical stresses caused significant additional biomass removal. However, even an exposure of the biofilms to τ_w of 17.7 Pa, after treatment with BDMDAC, was insufficient to totally remove the biofilms. The overall results reinforce the resistance and resilience of biofilms to control procedures, even when combining chemical and mechanical actions.

7.1. Introduction

Food industries and drinking water systems have more strict cleaning standards than other industries as they must control microorganisms relevant for the public health. Current practices on food industries use CIP protocols which are highly based in strong chemical agents namely caustic detergents, followed by acids (to clean mineral deposits), intercalated by rinses with water at high flow rates. General design principles for CIP circuits recommend the usage of AISI316 or AISI304 SS with electropolished surface finish and a flow with minimum Reynolds number of 10000 [427]. Hydrodynamic removal is also used in drinking water systems, by means of water flushing to promote the biofilm removal [65]. However, due to the viscoelastic properties of the biofilms, it is impossible to obtain completely cleaned surfaces [189].

The type of material used for industrial equipment and piping systems may also influence biofilm inactivation and removal. SS has been a classical material choice in industries especially where cleanability is critical. However, polymeric materials are also frequently used at moderate temperatures due to their flexible use, resistance to corrosion and usually lower cost. In this work, HDPE was selected as surface for biofilm formation as this material is currently used in water systems, particularly for drinking water supply and in food industries, offering high mechanical performance [428, 429].

The success of a cleaning strategy in the elimination of the biofilms will depend on the combination of the inactivation of the microorganisms with the removal of the biopellicle from the surfaces. Therefore, the effects of the hydrodynamic stress during the cleaning step should be closely investigated. This is of particular importance when the aim is to design sustainable control strategies: it is important to assess and optimize the amount of biofilm removed for different flow conditions, in order to save water and energy. Previous works regarding the influence of τ_w on biofilm detachment were already reported: Ochoa et al. [279] used a Taylor-Couette reactor to study the non-uniform distribution of local τ_w on aerobic biofilms formed previously on flat surfaces in a low τ_w reactor, and noticed different patterns of erosion according to the τ_w values under which the biofilm was exposed. Mathieu et al. [430] also assessed the effects of hydrodynamics conditions on the erosion of drinking water biofilms formed on HDPE, in combination with chlorination to chemically stress the cells. The biocide used in this study was BDMDAC, a QAC that already demonstrated a good efficiency in killing biofilms of *P. fluorescens* [269], but not studied regarding its potential to remove biofilms from surfaces. In this work, a rotating cylinder reactor was used to characterize the phenotype of single and dual-species biofilms and their behaviour when exposed to chemical and mechanical

stresses. The mechanical resistance of single and dual-species biofilms of *B. cereus* and *P. fluorescens* before and after exposure to the selected biocide was determined. Moreover, the surface properties (charge and hydrophobicity) and initial adhesion of both bacteria to HDPE were characterized in order to ascertain if those aspects influence biofilm formation and behaviour.

7.2. Materials and Methods

The work described in this section was performed using *B. cereus* and *P. fluorescens* cultures described in sub-section 3.1 and cultivated using the medium and the conditions of sub-section 3.2. The biocide tested was BDMDAC at 300 µg/mL for 30 min (sub-section 3.3). *In-vitro* adhesion assays (sub-section 3.13) were performed in 1 cm^2 slides of HDPE (sub-section 3.4) to assess the initial adhesion of single and dual-species biofilms of *B. cereus* and *P. fluorescens.* The physicochemical properties of the bacterial surfaces, namely hydrophobicity and surface charge were assessed before and after exposure to BDMDAC (following the methods described in the sub-sections 3.7 and 3.9, respectively). Steady-state single and dual-species biofilms of *B. cereus* and *P. fluorescens* were formed in the RCR (sub-section 3.19) on HDPE (sub-section 3.4) and characterized in terms of some phenotypical aspects as described in sub-section 3.19. Table.7.1 presents the Re_{A} and the τ_w values estimated at each rotation speeds used in this study. The mechanical stability of these biofilms was studied after either exposure to BDMDAC (sub-section 3.20) or after a series of increasing τ_{w} as well as a combination of both treatments (sub-section 3.21), being the amount of biofilm removed presented in terms of percentage.

Table.7.1 – Estimated values for τ_{w} and Re_{A} at the rotation speeds N used in this study

N (s^{-1})	Re_{A}	τ_w (Pa)
3.84	2400	0.70
6.40	4000	1.66
13.0	8100	5.50
19.4	12100	10.9
25.8	16000	17.7

7.3. Results and discussion

The results for the untreated and BDMDAC-treated *B. cereus* and *P. fluorescens* cells were already presented and discussed in chapters 4 and 5. Therefore, Table 7.2 presents only the results of the surface tension parameters and hydrophobicity for HDPE.

HDPE is a hydrophobic surface (ΔG_{1w1}= -63.8 ± 13 mJ/m^2) with an electron donating character. Simões et al. [40] performed similar tests with polyethylene (PE) and found that it also has an electron donating character, however, with higher hydrophobicity (ΔG_{1w1}=-90.3 mJ/m^2). PE is available in several formulations such as HDPE, medium-density polyethylene (MDPE) or low-density polyethylene (LDPE), among others. These materials differ in terms of their chemical and mechanical properties, which define the density and branching of the material [431, 432]. Therefore, the fact that surface properties vary with the type of polymer may be the reason for the differences between the values reported by Simões et al. [40] and those obtained in the present study.

The surface tension values allowed the assessment of the free energy of adhesion between the bacterial surfaces and HPDE (Table 7.3). The results for the thermodynamic adhesion potential showed favourable adhesion of *B. cereus* to HDPE compared to *P. fluorescens.* BDMDAC treatment decreased the adhesion ability of *B. cereus* to HDPE. Conversely, BDMDAC favoured the thermodynamic adhesion potential of *P. fluorescens*.

Table 7.2 – Surface tension parameters and hydrophobicity (ΔG_{iwi}) of HDPE.
The means ± SD for at least three replicates are given

	Surface energy parameters (mJ/m^2)				ΔG_{1w1} (mJ/m^2)
	γ^{LW}	γ^{AB}	γ^{+}	γ^{-}	
HDPE	39.6 ± 0.6	0.0 ± 0.0	0.0 ± 0.0	2.9 ± 1.7	-63.8 ± 13

Table 7.3 – Free energy of adhesion (ΔG_{1w2}^{TOT} – mJ/m^2) between *B. cereus* or *P. fluorescens*, untreated (control) and BDMDAC-treated cells, and HDPE.
The means for at least three replicates are given

	B. cereus		*P. fluorescens*	
	Control	BDMDAC	Control	BDMDAC
HDPE	-13.1	-6.5	7.8	-5.8

The electrostatic repulsive/attractive forces that may exist between the bacterial cell surface and the substratum are significant in initial adhesion (Busscher et al. 2010, Marshall 1986). The surface charge of the cell and surface was determined in order to obtain information on these events. HDPE surface presents negative surface with zeta potential value of -1.0 ± 0.9 mV. As previously described in chapter 5, the bacteria had negative surface charge in the absence of BDMDAC. Treatment with the biocide increased the bacterial surface charge to less negative values. This effect was also observed by Ferreira et al. [355] when exposing a *P. fluorescens* strain isolated from drinking water to this biocide and this effect is apparently due to the cationic nature of BDMDAC.

Adhesion assays on HDPE were performed to ascertain the reliability of the thermodynamic analysis of bacterial adhesion to HDPE (Table 7.4). The results of the adhesion assays show that both bacteria, single and dual cultures, adhered on HDPE. The adhesion of *B. cereus* happened in a lower extent when compared to *P. fluorescens* and the dual culture (difference of 1.1 $\log_{10}/cm^2$). The exposure of adhered cells to BDMDAC caused a decrease in the number of adhered cells of 0.1 $\log_{10}$ /cm^2 (dual culture and *P. fluorescens*) and 0.2 $\log_{10}$ /cm^2 (*B. cereus*). The analysis of bacteria in the dual culture adhered cells shows that *P. fluorescens* was the dominant species in both control (0.9 ($\log_{10}/cm^2$ higher) and BDMDAC (1.5 $\log_{10}/cm^2$ higher) assays.

These assays showed that the numbers of *B. cereus* cells adhered on HDPE were the lowest compared to *P. fluorescens* or the bacterial co-culture. This result contradicts the thermodynamic analysis (Table 7.3). Moreover, BDMDAC caused low to modest removal of adhered cells, being *B. cereus* affected in a higher extent. The number of *P. fluorescens* adhered cells in the co-culture was significantly higher than that of *B. cereus.* This difference is pronounced after the chemical treatment. It is known that Gram-negative bacteria have high

Table 7.4 – Numbers of *B. cereus* and *P. fluorescens* single and dual-species cells ($\log_{10}$ cells/cm^2) adhered for 2h on HDPE, before (control) and after treatment with BDMDAC
The means ± SD for at least three replicates are given

	Control	BDMDAC
B. cereus	5.35 ± 0.10	5.18 ± 0.10
P. fluorescens	6.44 ± 0.09	6.32 ± 0.08
Dual-species	6.42 ± 0.07 [a]	6.30 ± 0.08 [b]

[a] 5.46 ± 0.11 of *B. cereus* and 6.37 ± 0.08 of *P. fluorescens*.
[b] 4.75 ± 0.14 of *B. cereus* and 6.29 ± 0.08 of *P. fluorescens*.

intrinsic resistance to biocides due to their cell envelope which regulates the passage of substances through the cell membrane [433]. Gram-positive bacteria do not possess specific receptor molecules or permeases that can hinder the biocide penetration, and therefore may be more easily affected [390].

In general, the results from the thermodynamic analysis of adhesion did not fit those obtained with the in vitro adhesion assays. This is usually attributed to the existence of other mechanisms involved in the initial adhesion rather than just hydrophobic and electrostatic interactions. Actually, extracellular appendages and proteins, like pili, flagella, fimbriae and outer membrane proteins play an important role in cellular motility and attachment to surfaces [393, 394]. Other factors also have influence on bacterial adhesion including the substratum surface properties (surface charge and roughness) and environmental process conditions (temperature, pH, bacterial concentration, time of contact, chemical treatment or the fluid flow conditions) [74, 367, 434].

Biofilms attached on HDPE were developed in the RCR for 7 days and their characteristics are depicted in Table 7.5. Dual-species biofilms were the thickest, followed by *P. fluorescens* and *B. cereus* single biofilms ($P < 0.05$). *P. fluorescens* had the highest productivity in terms of dry mass, followed by the dual-species biofilms ($P < 0.05$). From the wet and dry biomass values it was possible to determine the amount (%) of water in the biofilms which did not presented significant differences ($P > 0.05$), oscillating between 95.0% and 99.3% higher in the dual-species biofilms, followed by *B. cereus* and *P. fluorescens* single biofilms. The biofilm volumetric density (determined as the ratio between the biofilm dry mass and the wet thickness) of *P. fluorescens* single biofilms was higher (13.1 mg/cm^3) than that of *B. cereus* biofilms and dual-species biofilms, which had similar values: 3.6 and 3.7 mg/cm^3, respectively ($P < 0.05$).

These results were different from the data obtained with SS and PMMA surfaces as adhesion surface (chapter 5). These differences in biofilm formation and characteristics may be explained based on the different physicochemical characteristics of HDPE and SS.

The dual-species biofilms formed on HDPE were predominantly colonized by *B. cereus*. This is contradictory to the adhesion results, emphasizing that one should not predict the evolution of a mature biofilm only through its first stages of development. In fact, understanding the relationship between adhesion and biofilm formation can be useful to understand the role that microorganisms may play in the system and to develop reliable preventive and control

Table 7.5— Characteristics of *B. cereus* and *P. fluorescens* single and dual-species biofilms formed on HDPE.
The means ± SD for at least three replicates are given.

	B. cereus	*P. fluorescens*	Dual-species
Thickness (μm)	526 ± 8	278 ± 71	880 ± 90
Dry mass (mg/cm^2)	0.191 ± 0.02	0.365 ± 0.07	0.324 ± 0.09
Volumetric density (mg/cm^3)	3.6 ± 0.3	13.1 ± 1.9	3.7 ± 1.1
Cellular density (log_{10} cells/cm^2)	6.67 ± 0.11	6.94 ± 0.20	6.90 ± 0.04*
Water content (% of total biofilm mass)	97.9 ± 0.7	95.0 ± 3.1	99.3 ± 2.5
Extracellular polysaccharides (% of total biofilm polysaccharides)	72.1 ± 1.5	69.8 ± 2.1	59.4 ± 0.7
Extracellular proteins (% of total biofilm proteins)	50.9 ± 0.5	34.3 ± 0.6	72.0 ± 4.5

* 6.75 (± 0.03)/81.9% of *B. cereus* and 6.33 (± 0.21)/18.1% of *P. fluorescens*.

strategies efficient in the early stages of biofilm development. However, the initial stages of biofilm formation do not provide reliable information on the characteristics and behaviour of mature biofilms.

The cell densities of the three biofilms were similar. Their composition in terms of polysaccharides and proteins was statistically different in both total and extracellular concentrations ($P < 0.05$). The production of extracellular polysaccharides was favoured for *B. cereus* and *P. fluorescens* single biofilms, whereas dual-species biofilms produced more extracellular proteins ($P < 0.05$)

The single and dual-species biofilms were exposed to BDMDAC at the same τ_w used for biofilm formation and the effects of the chemical on biofilm removal were assessed (Fig. 7.1). The percentage of biofilm removed after biocide exposure was significantly higher ($P < 0.05$) for the dual biofilms (53%) than for the single species (16% of *B. cereus* and 12% of *P. fluorescens* single species biofilms). In fact, this particular species association increased the susceptibility of the biofilms formed on HDPE to removal by BDMDAC. This result contradicts the previous finding of Simões et al. [312] using AISI316 SS as adhesion surface and the biocides glutaraldehyde and cetyl trimethyl ammonium bromide for biofilm control. In this study, *P. fluorescens* biofilms were

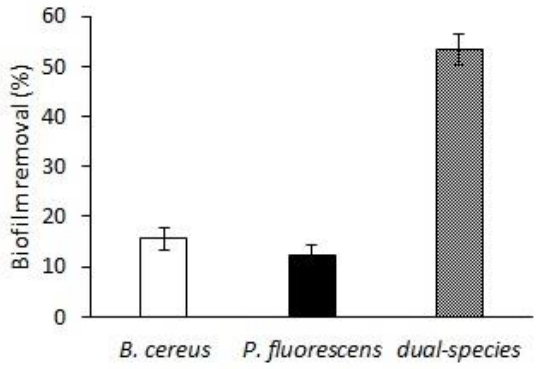

Fig. 7.1 – Biofilm removal after submitting the *B. cereus* (□), *P. fluorescens* (■) single and dual-species (▩) biofilms to BDMDAC for 30 min at τ_w = 0.04 Pa.
The means ± SD for at least three replicates are given.

the most resistant to the chemical treatment. This is apparently due to their higher amount of extracellular polysaccharides and higher volumetric mass density when compared to the other biofilms. In fact, the EPS matrix can cause mass transfer limitations, and their molecules may interact with the biocide, reducing their availability to interact with the biofilm cells [26, 397, 435].

The control of industrial biofilms often involves the use of biocides [203]. Nevertheless, chemical treatments alone have already proved to be insufficient to remove and inactivate biofilms [332, 406]. The limited effects of chemical treatments in biofilm control are of great concern. The residual microorganisms left on equipment surfaces after biocide treatment can promote the rapid re-establishment of biofilms, usually showing a decreased susceptibility to biocides. Therefore the biofilms remaining from the chemical stress were challenged by a sequential increase of τ_w (Fig. 7.2). The τ_w = 1.66 Pa caused the most significant biofilm removal, and this effect was more pronounced in the BDMDAC treated biofilms (Fig. 7.2*b*). Here, biofilm removal was statistically higher for dual-species biofilms, followed by *B. cereus* and *P. fluorescens* single biofilms ($P < 0.05$). However, this first step of mechanical stress did not cause such removal of non-treated biofilms of *B. cereus* and dual-species biofilms, as it did for *P. fluorescens* biofilms. The next condition, τ_w = 5.50 Pa, did not remove as much biofilm as the first one, indicating that there was a possible compression of the biofilm. Paul et al. [191] also verified that during erosion tests under τ_w < 2 Pa detachment occurred, however, above that value compression mechanisms influenced more the physical stability of the biofilm. As biofilms get progressively compressed by the τ_w forces, variations in the biofilm porosity caused by

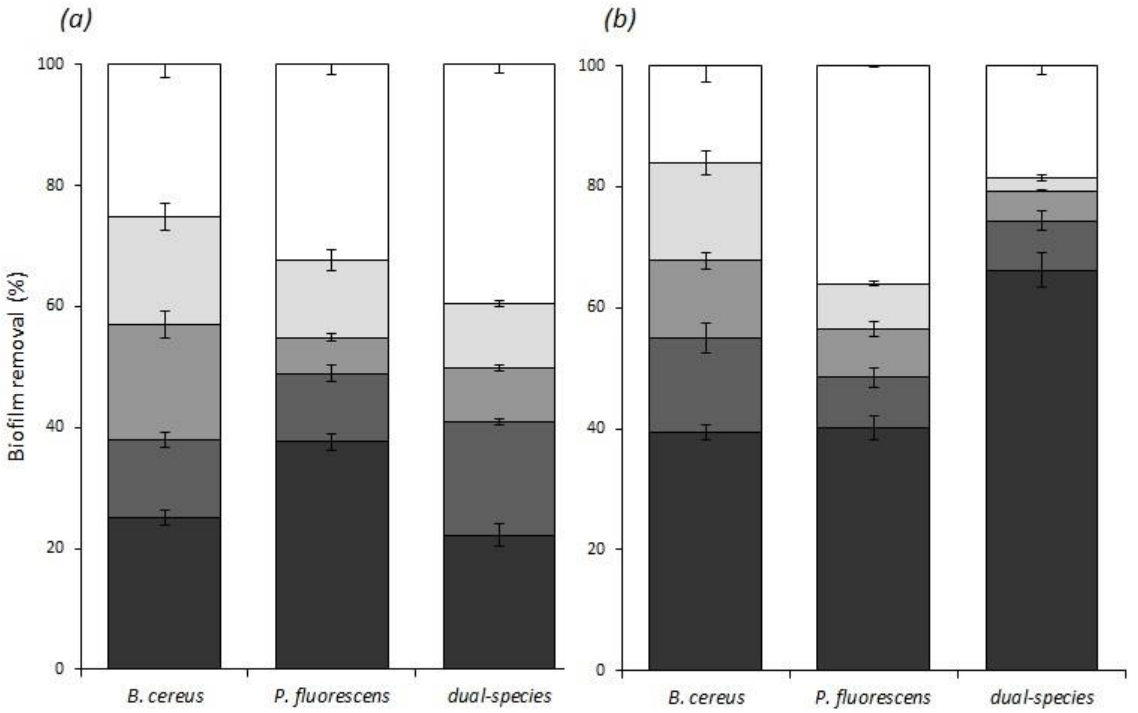

Fig. 7.2 – Biofilm removal after submitting the non-treated *(a)* and BDMDAC treated biofilms *(b)* to increasing τ_w values (■ – 1.66 Pa, ■ – 5.50 Pa, ■ – 10.9 Pa, ■ – 17.7 Pa).
The white bar (□) represents the amount of biofilm remaining after the treatment. The means ± SD for at least three replicates are given.

external agents will affect the mechanical stability and therefore the detachment processes. According to Hornemann et al. [436], the QACs effect on EPS leads to the elimination of the diffusive restrictions of biomacromolecules in the biofilm. This mechanisms suggests that some physical alterations also occur which may be explain the higher removal obtained for the BDMDAC treated biofilms when exposed to the higher τ_w conditions.

The complete series of τ_w was not sufficient to remove the biofilms, both untreated and BDMDAC-treated. Even after the combined chemical and mechanical treatments, there was still 16%, 36% and 19% of biofilm mass covering the HDPE cylinders, for *B. cereus, P. fluorescens* and the dual-species biofilms, respectively. The biofilms formed by *P. fluorescens* showed a higher resistance to chemical stress when compared to those of *B. cereus*, as previously shown in studies performed with cetyl trimethyl ammonium bromide [312]. Pechaud et al. [378] used a combination of mechanical and enzymatic treatments to control multispecies biofilms and observed that hydrodynamic treatments caused both detachment and compaction of biofilms. The enzymatic treatments applied alone were not effective in biofilm removal, but the combined treatments resulted in up to 90% biomass removal. In this study, the treatment of the biofilms with BDMDAC in addition to the mechanical stress induced modest

biofilm removal of *B. cereus* and dual-species biofilms, compared with the mechanical stress alone. For *P. fluorescens* biofilms, the previous exposure to the biocide was apparently indifferent in reducing its mechanical stability. This result proposes that a universal biofilm control strategy, valid for broad range of microbial species, will hardly be achieved.

7.4. Conclusions

The RCR proved to be a versatile tool to investigate the efficacy of a combined strategy using BDMDAC treatment and mechanical removal for the control of single and dual-species biofilms of *B. cereus* and *P. fluorescens* formed on HDPE. Predictions provided by the thermodynamic theory of adhesion failed to confirm the in vitro assays on HDPE which indicated that *P. fluorescens* adhered in higher number than *B. cereus*. BDMDAC treatment decreased the number of cells adhered on HDPE more extensively for *B. cereus* than for *P. fluorescens* and dual-species culture. *B. cereus* and *P. fluorescens* formed distinct biofilms on HDPE, both single and dual-species, with different phenotypic characteristics and behaviour to chemical and mechanical stresses. The treatment of 7-days old single and dual-species biofilms with BDMDAC was inadequate to totally remove the biofilms. *P. fluorescens* biofilms were the most resistant to the biocide and those formed by both species were the most susceptible. The application of distinct τ_w emphasized the inherent mechanical stability of the single and dual-species biofilms. The overall results indicate a stratified structure of the biofilm in terms of cohesive properties. Low τ_w values (1.56 Pa) caused higher erosion of the biofilm whereas the higher τ_w values seem to cause a compression of the biofilm indicated by smaller amounts of biofilm removed from the surfaces. The combination of BDMDAC with the exposure to a series of increasing τ_w enhanced biofilm removal, for every condition tested. However, even with the synergistic chemical and mechanical treatment, total biofilm eradication was not achieved for *B. cereus* and *P. fluorescens* single and dual-species biofilms formed on HDPE.

CHAPTER 8

A fluid dynamic gauging device for measuring biofilm thickness on cylindrical surfaces

8. A fluid dynamic gauging device for measuring biofilm thickness on cylindrical surfaces

Abstract

Many industrial processes are susceptible to biofouling. The thickness and structure of such biofilms are key factors in the design of effective cleaning strategies. A novel method based on fluid dynamic gauging has been developed for measuring the thickness and the shear stress needed for removal of the biofilms formed on cylindrical surfaces. The device operates with the test cylinder immersed in liquid: liquid is withdrawn or ejected from a nozzle located near the biofilm surface. There is no net change of liquid volume, making it ideal for sterile and aseptic operation and for studies using valuable liquids. Biofilm removal may also be tested by using appropriate hydrodynamic conditions. Calibration tests using ejection and suction flows indicated a measurement accuracy of $\pm$19 μm and showed good agreement with computational fluid dynamics simulations. The device was commissioned in tests on *P. fluorescens* biofilms formed on HDPE and SS cylinders under conditions of mild shear stress. The biofilm thickness was not uniform: measurements made over the surface of the test cylinders confirmed this: layer thicknesses ranged from effectively zero to 300 μm. The biofilms formed on HDPE were thicker than those formed on SS.

8.1. Introduction

A wide range of biofilm reactors have been employed to study biofilms. Mature biofilms can be formed in systems like the rotating cylinder reactor (RCR), the Centre for Disease Control (CDC) reactor, the rotating annular reactor, the rotating disc reactor, the Propella® system, the constant depth film fermenter or the flow-cell [138, 191, 273, 291, 437, 438]. There are also many techniques for sampling and analysis that may be performed directly on test coupons, including thickness measuring or microscopy observations assisted by epifluorescence microscopy, confocal laser scanning microscopy (CLSM) [251], and scanning electron microscopy (SEM) [250]. However these methods generally require the removal of the substrate from the bulk fluid and some treatments, to fix the cells or stain the structures that involve removing part of the water content from the sample. This dehydrating treatments compromise significantly the biofilms' structure as their composition is essentially water (at least 90%) [138]. Methods to study biofilms *in situ* that minimize the manipulation of the samples are required, and

particularly ones which allow the biofilm response to biocides and other agents to be monitored. This work reports the development of a variant of the fluid dynamic gauging (FDG) technique for measuring the thickness – and change of thickness in response to biocide application – of biofilms prepared on cylindrical surfaces. The biofilms studied were formed using the RCR, as it mimics industrial conditions, with rotation speed manipulated to promote growth conditions with low to moderate wall shear stress. In this work, biofilms were prepared using the bacterium *P. fluorescens,* and grown on cylinders of HDPE, a polymer regularly used for drinking water pipes [380, 439], and AISI316 SS.

FDG is a non-contact technique developed for measuring the thickness of soft deposits *in situ* and in real time. Since its introduction by Tuladhar et al. [342] its functionality has been extended to study the strength of soft solid layers using computational fluid dynamics (CFD) to evaluate the stresses that the gauging fluid imposes on the surface being studied [440]. FDG has been used previously to study biofilms, including different natures like algal – *Chlorella* spp*.,* [441], cyanobacterial – *Synechococcus* sp. WH 5701, [442], and bacterial – *E. coli* and *P. aeruginosa* [443], all prepared on flat plates. The device presented here employs a curved surface and also employs the zero discharge mode introduced by Yang et al. [444], in which alternate ejection and suction stages mean that the total liquid volume does not change over the course of a test. This has particular advantages for aseptic operation or when liquid consumption is to be minimized.

8.2. Materials and Methods

P. fluorescens cultures were used with the culture conditions and nutrient media described in sub-sections 3.1 and 3.2. Biofilms were grown in the RCR described in sub-section 3.18 using samples of HDPE and AISI316 SS (sub-section 3.4)

A czFDG device was designed, commissioned and used to assess the thickness of those biofilms. Calibration tests were performed simultaneously with all the measurements. For each sample, 12 of 60 possible locations were gauged (sub-section 3.22).

Numerical simulations were performed by Mr Shiyao Wang (PhD candidate in the University of Cambridge – Department of Chemical Engineering and Biotechnology), to support this work. Because these simulations are fundamental for the description of this work, they are described in the sub-section 8.3., with Mr Wang's permission.

8.3. Numerical Simulations

Three dimensional computational fluid dynamics simulations were performed using the COMSOL Multiphysics® software (version 4.1, Chemical Engineering module) on a desktop PC using technique described in detail by Chew et al. [440] for flat substrates and by Gu et al. [445] for annular geometries similar to the czFDG. These earlier studies had only considered suction configurations, where liquid leaves the reservoir via the nozzle. Flow in the tube is assumed to be laminar, steady state and fully established. The gauging liquid is Newtonian and the flow is isothermal. The Navier-Stokes and continuity equations are solved for a set flow rate into or out of the nozzle (for suction and ejection, respectively). The pressure field solution gives an estimate of $\Delta \mathrm{P}$, and thus C_{d}, for comparison with experimental data. The geometry of the model and coordinate system are presented in Fig. 8.1. The two projections employed in presenting the results are shown in the Fig. 8.3*c*. Tags A-D label boundaries in the simulation with the following boundary conditions (further details are provided by Chew et al. [440]:

A. Axis of symmetry:
There was no flow across symmetry planes, *i.e.* $\mathbf{n} \cdot \mathbf{v} = 0$, where $\mathbf{n}$ is the vector normal to the relevant plane and ***v*** is the velocity vector.

B. Gauging tube: inlet (ejection flow) or outlet (suction flow)

Flow is assumed to be fully developed, giving the Hagen-Poiseuille velocity profile, i.e. $v_{\mathrm{y}} = 0$ and

$$v_{\mathrm{z}} = v_{\mathrm{max}}\left(1 - \frac{4y^2}{d^2}\right) \qquad (8.1)$$

where v_{max} is the centreline velocity, v_{y} is the velocity in the y-direction and v_{z} is the velocity in the *z*-direction.

C. Walls

These is no slip and they are impermeable, *e.g*. for the cylinder wall in Fig. 8.1, $v_{\mathrm{y}} = 0$ and $v_{\mathrm{z}} = 0$.

D. Bulk liquid in reservoir: outlet (ejection) or inlet (suction)

The distance of this boundary to the axis of symmetry was set to be much larger than the radius of the gauging tube ($d/2$). This guarantees that the streamlines are parallel and normal to the boundary surface [440].

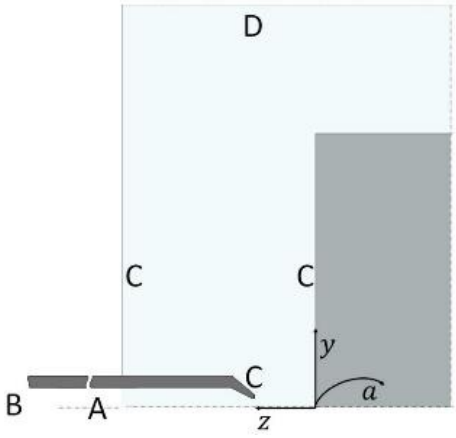

Fig. 8.1 – Simulation geometry.

Co-ordinates: z – horizontal axis (gauging tube), y – vertical axis (reservoir height) and a – arc length, along the cylinder surface.

COMSOL employs the finite element method (FEM) code. The domain was modelled using a 3-D mesh of tetrahedral elements (Fig. 8.2), constructed with the software's built-in mesh generator. There were 376806 mesh elements within the fluid domain, comprising half of the gauging tube and one eighth of the reservoir. The mesh density is higher under the nozzle rim and along the lip, where the largest pressure and velocity gradients were found. The effect of the number of mesh elements, N_e, on the simulation results is reported in Table 8.1 for a representative case. The values for C_d differ for suction and ejection modes. Above a certain value of N_e, there is incremental change in C_d.

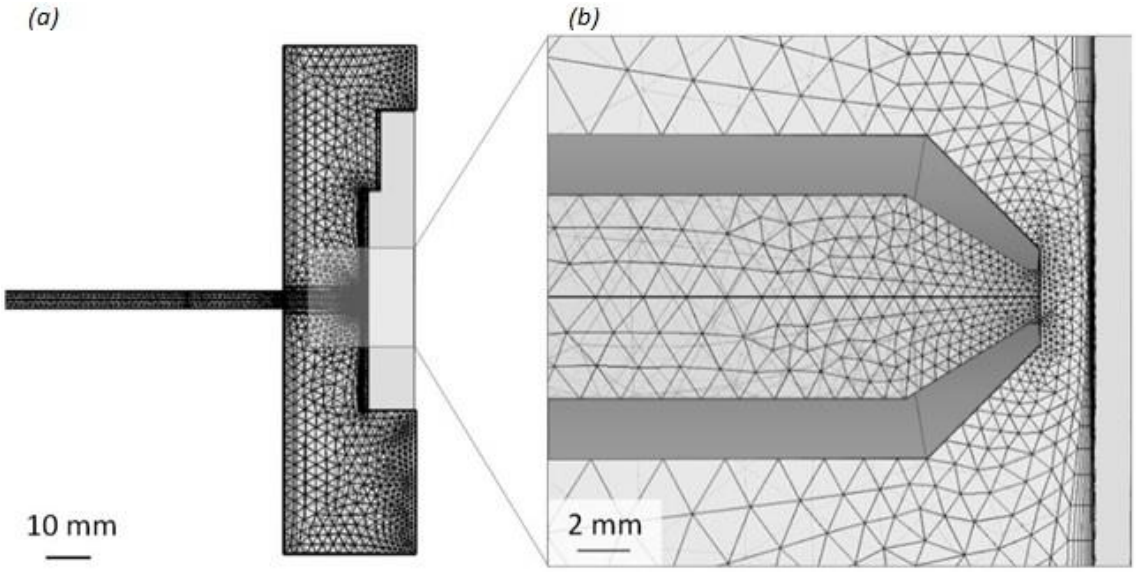

Fig. 8.2 – Simulation mesh, tetrahedral elements.

(a) whole system, 2-D slice; *(b)* detailed illustration of the region beneath the nozzle rim.

Table 8.1 – Effect of mesh refinement on solution accuracy for the case Re_t=84, h/d_t=0.074.

N_e	Ejection mode		Suction mode	
	C_d	solution time (s)	C_d	solution time (s)
80669	0.127	293	0.121	381
84288	0.126	303	0.121	400
136422	0.126	519	0.121	673
248736	0.125	836	0.121	1089
787334	0.121	2253	0.118	2869
3572597	0.120	17635	0.117	20697

The mesh density affected the numerical performance, *e.g*. time to converge, but the mass balance was closed with accuracy similar to earlier studies [440], for even the smallest N_e values.

8.4. Results and discussion

8.4.1. CFD and calibrations

As stated previously, the numerical simulations were performed by Mr Shiyao Wang to support this work. The discussion of the results is presented here as it was considered fundamental for the complete discussion and description of this work, as in the correspondent publication.

Fig. 8.3 presents velocity distributions within the nozzle for (a) ejection and (b) suction mode for the same Re_t and h/d_tvalues. The largest velocity gradients are found near the nozzle throat, as reported in previous quasi-static FDG studies [445, 446].

The two flow configurations differ in the existence of large recirculation cells downstream of the nozzle in suction mode, marked by solid boxes in Fig. 8.3(*b*). For ejection mode the flow in this region approximates a radially converging flow. It will be seen in Fig. 8.4 that this gives rise to slightly different C_d behavior in ejection.

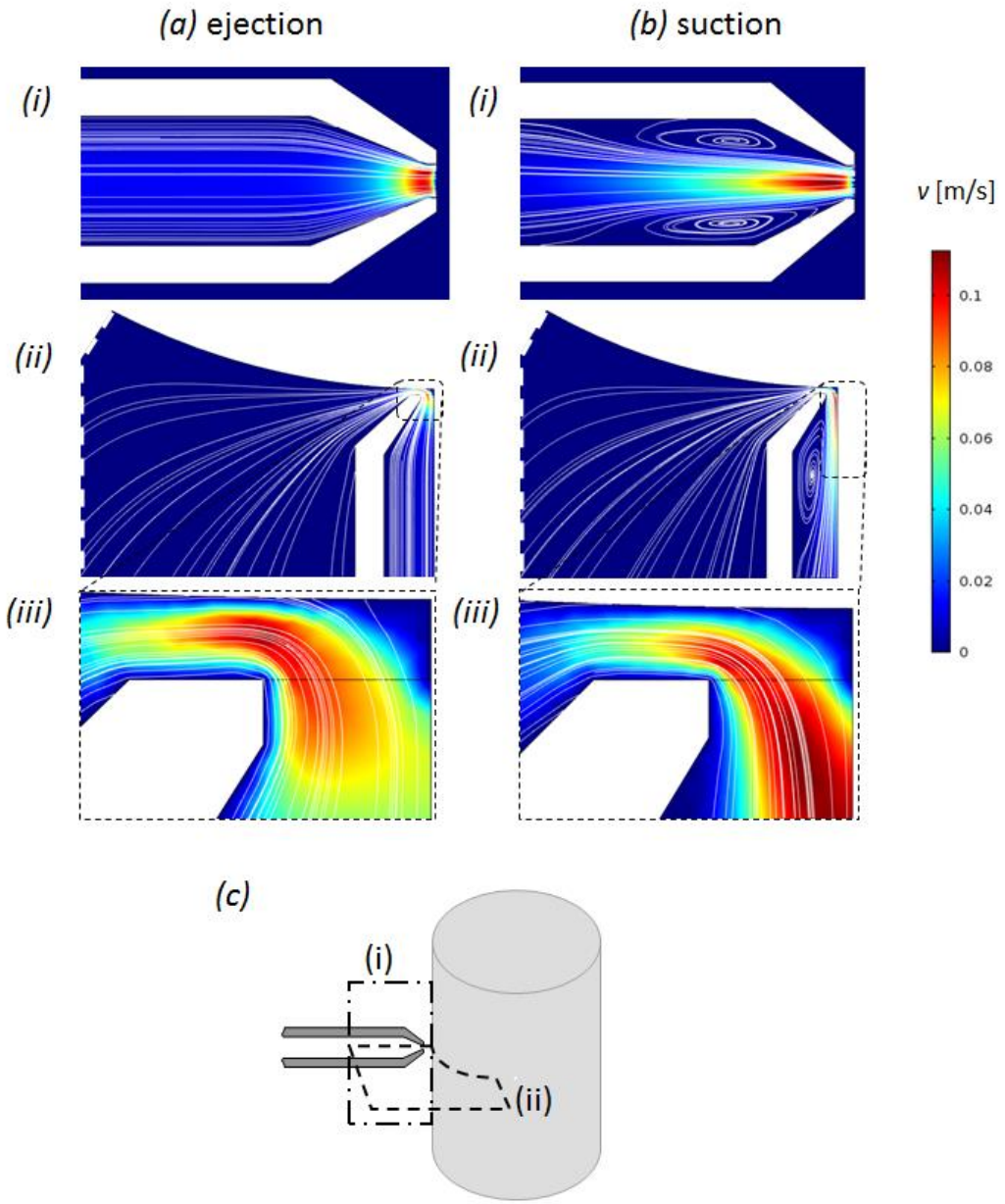

Fig. 8.3 – CFD simulation results for *(a)* ejection and *(b)* suction mode for Re_t= 63, h_0= 0.25 mm (h/d_t = 0.25) for the planes labelled *(i)* and *(ii)* in schematic *(c).*

Colors indicate the local speed, scale on right. White lines indicate streamlines in the flow. The projections of planes in *(ii)* were cropped (indicated by the dashed boundary) to fit the page. The solid boxes in *(b, i)* and *(b, ii)* emphasize the presence or absence of recirculation cells within the conical part of the nozzle. The flow pattern in the region between the nozzle rim and the surface being gauged is enlarged in *(iii)*.

Fig. 8.4 compares the measured pressure drops and the associated C_d values obtained from ejection mode calibration tests using two mass flow rates. Plotted alongside are the results from CFD simulations: each CFD datum required a new simulation. Similar trends, and similarly good agreement between experimental and simulation results, were obtained for suction mode.

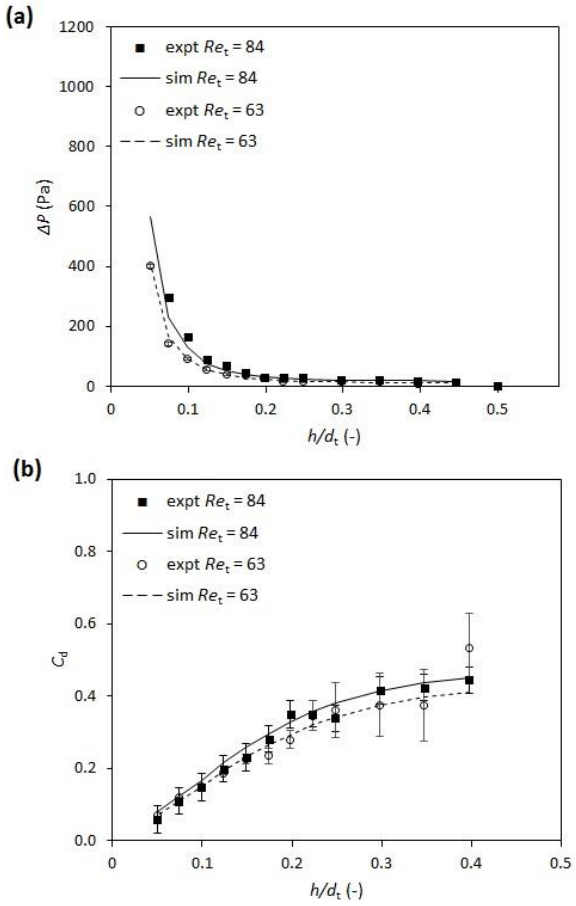

Fig. 8.4 – Comparison of experimental (expt) calibration curves with results obtained by simulation (sim) for ejection mode with Re_{t} = 84 and Re_{t} = 63.

Plots denote *(a)* pressure drop- h/d_{t}profile and *(b)* C_d - h/d_{t} profile. Error bars indicate the uncertainty calculated for each experimental value and are not visible for *(a)* as the error is not significant and is hidden by the symbol.

Ejection mode results are presented here as this was the configuration employed to measure the biofilm thickness. It should be noted that there are no adjustable parameters in the CFD calculations. Table 8.1 shows that the C_{d} value depends on mesh refinement and approaches a limiting value asymptotically. The asymptotic value (at high N_{e}) is compared with the experimental values in Fig. 8.4.

The calibration curves indicate a usefully linear region for the thickness measurements within the interval 0.05 < h/d_{t} < 0.25. For h/d_{t} < 0.05, C_{d} is small but also very sensitive to any misalignment between the nozzle and the cylinder, when the nozzle axis is not collinear with the normal to the cylinder surface. This is nullified by avoiding small clearances. The pressure drop is also large when h/d_{t} is small, requiring a pressure transducer with a large sensitivity range.

Furthermore, the high pressure drop means that the approach to the surface is readily noticed and this can set an alarm in the FDG software. For h/d_t > 0.25, C_d approaches as asymptotic value, and a pressure drop that is no longer a function of h, therefore FDG measurements cannot be performed.

For both modes, the flow in region between the nozzle and the substrate, enlarged in Fig. 8.3 (*iii*), approximates to a radial flow pattern with parallel streamlines. These patterns differed at smaller h/d_t (see [447]): a small recirculation zone attached to the underside of the nozzle is evident in ejection mode and is absent in the suction case. The differences in the flow near the nozzle throat, evident from the streamlines and velocity fields, give rise to different shear stress distributions on the substrate surface in Fig. 8.5.

The shear stress imposed by the gauging flow on the cylinder surface along the line of increasing *y* co-ordinate (parallel to the cylinder axis) is plotted in Fig. 8.5 for both suction and ejection modes. The system is symmetrical about y = 0 in practice so results for ejection are plotted with positive y and suction with negative y. The distribution of shear stress in the azimuthal direction (indicated by co-ordinate 'a' on the cartoons) can also be calculated. These data are not reported here as the shear stress decays more strongly in the azimuthal direction (see below). The Fig. 8.5 shows noticeable differences between the two configurations. There is a noticeably larger peak in the shear stress near the nozzle inlet with ejection mode at Re_t = 84, which results from the difference in flow field near the nozzle exit (see Figure 8.3(*iii*)), increasing the shear rate on the surface and hence the shear stress. This feature is not as marked at the lower flow rate. This behaviour is also evident when the data are compared with the analytical result for the shear stress distribution created by steady, incompressible radial flow of a Newtonian fluid between two parallel discs (see Middleman [448]):

$$\tau = \left(\frac{3\mu\dot{m}}{\rho\pi h^2}\right)\frac{1}{r} \qquad (8.2)$$

Here *r* is the distance from the axis of the discs. Fig. 8.5 shows the shear stress distributions on the cylinder surface where it is bisected by the plane of symmetry (direction *y* in the schematics) obtained from CFD simulations for two values of Re_t, in suction and ejection, alongside those predicted by Equation (8.2). The magnitudes of the simulation results for suction are similar to the predictions, but do not agree exactly.

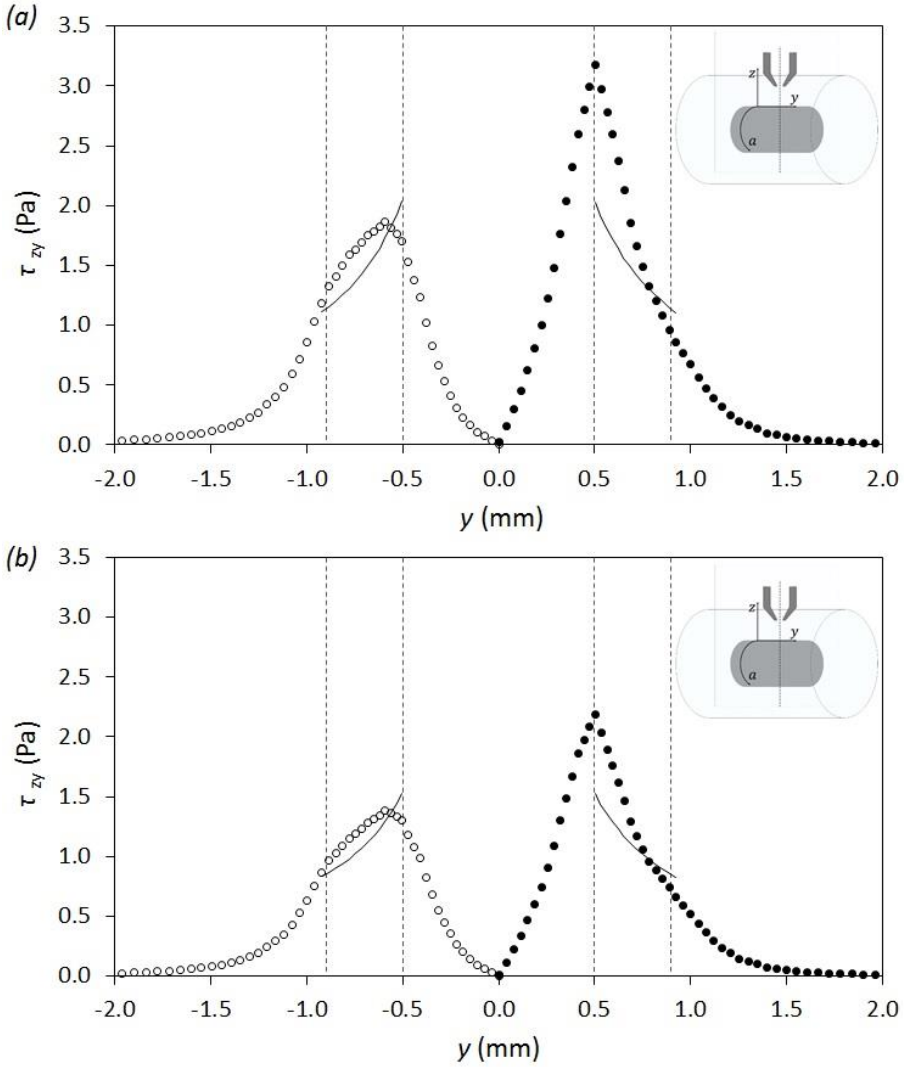

Fig. 8.5 – Shear stresses imposed by the gauging flow on the surface of the cylinder, along the line of increasing y (see insets).
(a) Re_t = 84, *(b)* Re_t = 63, $h/d_t = 0.25$. Solid symbols - ejection mode, open circles - suction mode. Solid line shows analytical result for parallel discs (Equation 8.2). Vertical dashed lines indicate the location of the inner and outer lip of the gauging nozzle.

One of the reasons for this is that the geometry is not one-dimensional: the gap between the nozzle lip and the surface varies with azimuthal angle (it increases steadily in the a direction). As a result the shear stress on the surface decreases more strongly with increasing a than that with y (data not presented). The results in Fig. 8.5 indicate that Equation (8.2) can be used to estimate the largest shear stress imposed on the cylindrical surface or any biofilm growing on it, to one significant figure. Significantly better agreement is obtained for gauging on flat surfaces [444]. Equation (8.2) assumes a steady velocity profile in the gap between the discs, which differs from that predicted by the CFD studies for ejection with Re_t = 84. The simulated shear stress value is larger than that predicted, as expected.

It is noteworthy that the shear stress values imposed by the gauging flow on the surface in the region under the nozzle in Fig. 8.5 range from 1–2 Pa when h/d_t = 0.25. The shear stresses imposed by steady pipe flow are given by $^1/_2 f\rho u_m^2$, where u_m is the mean bulk velocity and the friction factor f is typically around 0.005. This gives $\tau_w \sim$ 2.5 u_m^2, *e.g.* $\tau_w \sim$ 2.5 Pa for u_m = 1 m/s. The gauging flow exhibits pipe flow conditions even at this low mass low rate. The shear stress can be increased by moving the nozzle closer to the surface: equation (8.2) indicates that $\tau \sim h^{-2}$ so at the smallest accessible clearance, *i.e.* h/d_t = 0.05, a shear stress of around 50 Pa can be generated, which corresponds to $u_m \sim$ 4.5 m/s.

The above results demonstrate that zero net flow FDG can be achieved with cylindrical geometries. Measurements of biofilm thickness could be made during an ejection step, a suction step, or both, as the syringe is being filled or emptied, or back and forth with small volume changes and suction steps. In the tests here with biofilms, thickness measurements were made in ejection mode as the biofilms were quite fragile and could be dislodged as clumps which, in suction mode, could block the nozzle. If this did occur in practice, the pressure drop characteristics would change noticeably. Blockage could be countered by withdrawing the nozzle a long distance from the test surface and ejecting a burst of liquid to clear the nozzle.

8.4.2. Measurements on biofilms

The photographs in Fig. 8.6 of biofilms formed on the HDPE and SS cylinders after 7 days of growth show uneven coverage.

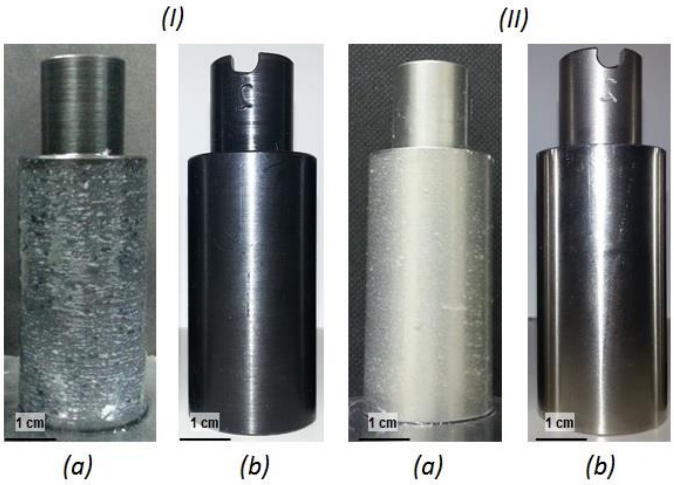

Fig. 8.6 – Cylinders of HDPE *(I)* and SS *(II)* after 7 days of biofilm growth *(a)* versus clean cylinders *(b)*.

The average wet mass on the HDPE cylinders (3 independent measurements) was 20.0 ± 2.2 mg $_{biofilm}$/cm^2. It was not possible to obtain reliable coverage values for the SS cylinders owing to the mass of the metal. Examples of biofilm thickness measurements are presented in Fig. 8.7. Data are plotted for one cylinder (of the three) per test. Appendix Figures A1 and A2 report the complete data sets for the two materials. Measurements were made at 12 positions for each cylinder.

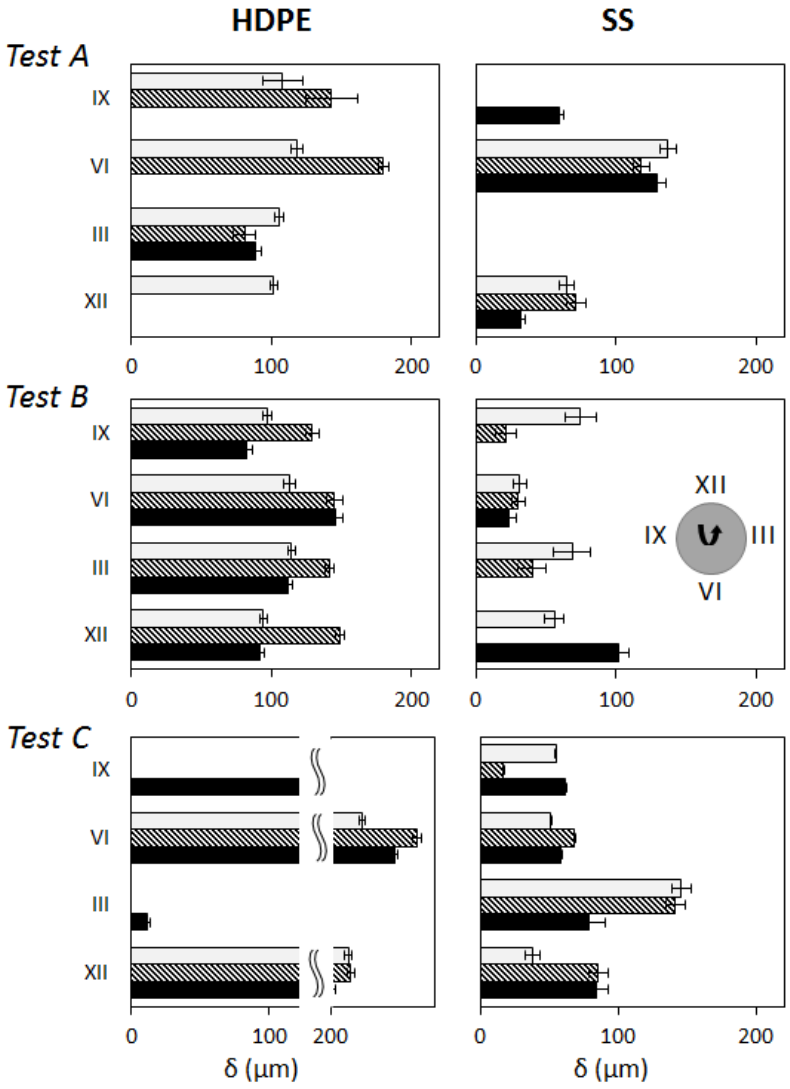

Fig. 8.7 – Biofilm thickness measurements for HDPE and SS cylinders after three independent tests (labelled A, B and C, data presented for one cylinder of the three measured per test).

Measurements performed at 4 different azimuthal positions (indicated in Roman numerals, corresponding to clock positions, see middle plot) and 3 different heights (open bar - highest position, crossed bar - intermediate position, solid bar - lowest position). Error bars indicate the uncertainty calculated for each experimental value.

Measurements were made at 12 positions for each cylinder. There is noticeable variation between cylinders and between tests. There is noticeable variation between cylinders and between tests. The resolution of the czFDG technique is ±19 μm due to the sensibility of the pressure transducer used and of the linear drive.

The pattern obtained for the HDPE cylinder in Tests A and B showed significant similar trends ($P > 0.05$) and was noticeably different to test C ($P < 0.05$). For SS cylinders a similar trend was observed for the three tests ($P > 0.05$). The absence of data on some cylinders does not indicate that there was no layer present: the resolution of ±19 μm is quite large compared to the size of individual *P. fluorescens* cells, which are rod shaped with a typical diameter of 2 μm. The digital microscope confirmed that material was present on the surface, but evidently some factor had prevented the bacteria progressing to the colonization and growth stage. If anything, these results confirm some of the difficulties in working with biofilms: reproducibility is hard to achieve!

The biofilms were formed under the same hydrodynamic conditions, using a metallic and a polymeric substrate. Overall results indicate that biofilms formed on HDPE have an average thickness of (0.104 ± 0.006 mm) significantly superior than the ones formed on SS (0.072 ± 0.006 mm). Previous findings for *P. fluorescens* biofilms formed on SS and PMMA surfaces (described in the chapter 5) showed no significant difference between the numbers of adhered cells on those materials. The HDPE and PMMA substrates have different properties in terms of hydrophobicity: the sample roughness, although not measured, was clearly different and striated patterns were evident on the HDPE samples. These patterns appeared to follow machining marks in the HDPE surface which may have functioned as harbours for initial cell adhesion [33]. The PMMA samples were buffed during manufacture, which is likely to explain the differences.

Augustin et al. [441] reported similar variation in thickness values for *Chlorella* spp. biofilms, measured with scanning FDG operated with under mass flow mode, where the pressure drop is fixed and the mass flow rate varies as the nozzle approaches the surface (as used by Tuladhar et al. [342]). Salley et al. [442] measured the thickness of biofilms formed from *Synechococcus* sp. WH 5701 on different substrates (glass, stainless steel and indium tin oxide), over a period of 4 weeks. They measured thickness at three positions on each substrate and reported variation similar to that on cylinders 1 and 3 in tests A and B. These algal biofilms grew to thicknesses ranging from 100-300 μm after 4 weeks. The variation between measurements decreased with time, as the biofilms became more mature.

Whereas Augustin et al. [33] and Salley et al. [34] used static growth conditions, Peck et al. [443] grew *E. coli* and *P. aeruginosa* on different substrates, placed in petri dishes and cultivated in a rocking incubator with an agitation speed of 70 rpm. These studies also reported noticeable variation in biofilm thickness. All the above studies employed flat substrates: to our knowledge, this is the first work reporting results for steady-state bacterial biofilms formed on curved surfaces, under rotational flow. The ability of the czFDG to scan over the entire cylinder surface also allows meaningful statistics to be collected for each sample. The technique could be employed to study biofilms formed on the external surfaces of pipes or the inner wall of a fermenter, as long as the location of the nozzle relative to the substrate can be determined reliably.

8.5. Conclusions

A novel FDG device for measuring the thickness and the shear stress needed for removal of soft deposits on cylindrical surfaces, with zero net discharge of liquid from the system, has been designed, constructed and commissioned. Calibration tests showed similar trends in both suction and ejection flow modes, with the results being consistent with CFD predictions. The differences between the two modes were consistent with simulations. The accuracy of the measurements in calibration tests was estimated was ±19 μm, with the dominant factor being the accuracy of the linear drive (which can be improved by employing a different drive). *P. fluorescens* biofilms formed under mild shear stress on HDPE and SS cylinders in the RCR were successfully measured with this device, under aseptic conditions. The biofilm thickness varied noticeably over the cylinder surface and this was confirmed by the CZFDG measurements, with measured values ranging from zero (below the resolution of the device) to about 300 μm

CHAPTER 9

General conclusions and Future work

9. General conclusions and Future remarks

9.1. Conclusions

The main conclusions drawn through the work of this thesis are described below.

Ferulic and salicylic acids presented moderate antimicrobial action against *B. cereus* and *P. fluorescens* biofilms. Their use for control of biofilms did not cause significant removal, neither that happened when the phytochemicals were used for biofilm prevention. Significant removal was only observed for the dual-species biofilms, after a second exposure to the phytochemicals. Within this stage BDMDAC was selected as the preferred biocide for further studies, because its MIC was significantly lower than that of phytochemicals. This choice allows the use of smaller amounts of biocide, an important aspect for the design of more economic and sustainable control strategies.

The RCR demonstrated to be a versatile tool to ascertain the effectiveness of BDMDAC on the removal of biofilms. Different surfaces were used for adhesion and several hydrodynamic conditions were tested during the formation of *B. cereus* and *P. fluorescens* single and dual-species biofilms.

When comparing a polymeric (PMMA) with a metallic (SS) surface, the biofilm removal was dependent both on the adhesion surface and on the microbial species. *In-vitro* assays indicated that the numbers of adhered cells decreased moderately after treatment with BDMDAC, essentially in the case of *B. cereus.* The predictions of the thermodynamic theory of adhesion did not agree with the laboratorial adhesion assays, probably because it neglects important biological phenomena like motility and surface sensing mechanisms as well as EPS production.

The biofilms formed in the RCR were treated with BDMDAC, followed by hydrodynamic stress. Even though additional removal was achieved by the combination of both treatments, they failed in the aim of achieving total removal. *P. fluorescens* biofilms were the most resistant to removal. SS was the easiest surface to clean with the hydrodynamic stress, alone and preceded by the BDMDAC treatment.

Using the RCR*, B. cereus* biofilms were formed on SS surfaces under different hydrodynamic conditions. BDMDAC treatment alone was more effective against biofilms formed under low τ_w. Biofilms formed under intermediate and high τ_w presented higher amounts of

extracellular polysaccharides and were more resistant to the combination of chemical and mechanical treatments. A strongly adhered basal layer was present in all biofilms and resisted to removal by chemical and mechanical actions. The existence of this layer is an important fact as it may lead to the growth of recidivist biofilms even after sanitation procedures.

The effect of the hydrodynamic stress was closely investigated in single and dual-species biofilms of *B. cereus* and *P. fluorescens* on HDPE, using the RCR. Again, the predictions provided by the thermodynamic theory of adhesion failed to confirm the *in vitro* assays on HDPE, confirming its inadequacy to indicate the trends of initial adhesion. The biofilms formed on HDPE presented distinct phenotypic characteristics and behaviour to chemical and mechanical stresses. *P. fluorescens* biofilms were the most resistant to the BDMDAC treatment alone. Exposure to increasing shear stresses demonstrated a stratified behaviour of the biofilm in terms of cohesiveness. Low shear stresses led to erosion of the biofilm. A compression of the biofilm happened with exposure to higher shear stress values. The combination of BDMDAC with the hydrodynamic stress enhanced biofilm removal, however, total biofilm eradication was not achieved.

A czFDG was developed. This novel device is able to measure the thickness and the shear stress needed for removal of soft deposits on cylindrical surfaces, with zero net discharge of fluid from the system. The CFD simulations preformed to model the flow in the nozzle showed consistent trends with the experimental results. The czFDG was successfully employed to measure the thickness of *P. fluorescens* biofilms formed on HDPE and SS surfaces using the RCR. The biofilm thickness varied noticeably over the cylinder surface, with measured values ranging from zero (below the resolution of the device) to about 300 μm and thickest biofilms observed formed on HDPE. This system is ideal for work in aseptic conditions and allows measurements *in situ* with minimum manipulation of the biofilm, therefore allowing the conservation of its structural properties.

9.2. Future work

The investigation on complex and highly adaptable systems such as biofilms is relatively recent (40 years) and therefore there is a great deal of unknown territory to explore. Biofilms are not the exception but rather the rule of bacterial growth. It is fascinating to see how the oldest living organisms on the planet can build such complex and resilient structures from unicellular microorganisms.

The scope of this thesis, biofilm control strategies, is an equally complex theme, due to the multitude of factors that can interfere with their success. The contribution presented in this work is only a starting point of a long investigation that should focus all those factors, and the tools presented can also be improved with that goal.

It would be interesting to pursue additional studies in order to ascertain the potential of other phytochemicals to act as synergistic agents with conventional biocides for biofilm control. The aim would be to reduce the strong dependency of disinfection practices on conventional chemicals and gradually move to more sustainable compounds, with reduced ecological impact.

The influence of materials on the control of biofilms is also an aspect deserving more attention. Novel surfaces and coatings are being developed and tested with this focus. The utilization of those modified surfaces in simulated industrial conditions is important for the design of biofilm control strategies. The RCR would be a valuable tool for these studies due to its versatility for adhesion surfaces and environmental conditions. The variation of carbon sources and temperature conditions in the RCR is certainly worth of further investigation, in order to ascertain biofilm formation and behaviour when the nutrients are limited or in refrigerated areas of food industries.

Other hydrodynamic conditions should also be tested, however, the present configuration of the RCR limits the rotation speed imposed to cylinders. In fact, the RCR suffered many improvements during the development of the experiments described in this work. In the present configuration two cylinders are ‘slaves’ of the ‘master’ which is the one connected to the overhead stirrer. This ‘master’ shaft is exposed to additional stress compared to the other two, and even though recently a double homokinetic joint was installed to minimize the effect of possible oscillations of the stirrer, it is expected that its bearings will wear out sooner than the ones correspondent to the ‘slave’ shafts. Therefore, some alterations in the design of the RCR are proposed, utilizing a gear system, with a small motor coupled to a main gear transmitting to smaller gears deriving to the cylinders.

Furthermore, it would also be useful to perform the hydrodynamic study of the RCR. Early steps were made in this direction with the collaboration of Dr Bart Hallmark, from the Cambridge University, which kindly performed some early stage CFD simulations using Polyflow software. A model was made of one third of the reactor, using a tetrahedral mesh with 751 000 elements. Dr Hallmark performed simulations for three different rotational speeds: 1, 11.8 and 25 rpm, however, he could not proceed with higher speeds due to limitations of the software. In fact, he noted that the flow becomes too inertial for a viscous solver approach to handle above 25 rpm and taking the simulation to speeds approaching 300 rpm would require a CFD code that can handle inertia and probably turbulence, so Fluent or CFX could be an option. This would be a project in itself, particularly the selection and tuning of the turbulence model. Important aspects regarding the geometry should be considered, in particular the selection of the boundary conditions and the fact that there are air bubbles injected in the centre of the tank.

The czFDG is in an early stage of development and can equally benefit of some improvements in its design, particularly concerning the alignment of the samples and the calibration methods (location of the sample). The estimate of the shear stress needed to remove the biofilms from the surfaces is one possibility to be explored, as well the advantage of studying the effect of biocides in the structure of biofilm (thickness and cohesive properties) in real time.

Other methodologies could be included to complement these studies. Optical coherence tomography (OCT) can provide three-dimensional images with high-resolution of the structure of biofilms, in real-time [449]. Quantitative studies regarding mesostructured properties of the biofilms (thickness and morphology) can be performed with this method using 2D and 3D image reconstruction *in-situ* and non-destructively [450-452]. The combination of czFDG and OCT could provide a powerful tool pack to investigate the aspects of the biofilm mechanical stability that contribute to its great resistance and resilience.

REFERENCES

References

1. Henrici, A.T., Studies of Freshwater Bacteria: I. A Direct Microscopic Technique. J. Bacteriol., 1933. 25(3): 277-287.

2. Heukelekian, H. and A. Heller, Relation between Food Concentration and Surface for Bacterial Growth. J. Bacteriol., 1940. 40(4): 547-558.

3. Costerton, J.W., Z. Lewandowski, D.E. Caldwell, D.R. Korber, and H.M. Lappin-Scott, Microbial biofilms. Annu. Rev. Microbiol., 1995. 49: 711-745.

4. Watnick, P. and R. Kolter, Biofilm, city of microbes. J. Bacteriol., 2000. 182(10): 2675-2679.

5. Sauer, K., A.H. Rickard and D.G. Davies, Biofilms and biocomplexity. American Society for Microbiology, 2007. 2: 347-353.

6. Van Loosdrecht, M.C.M., J. Lyklema, W. Norde, and A.J.B. Zehnder, Influence of interfaces on microbial activity. Microbiological Reviews, 1990. 54(1): 75-87.

7. Costerton, J.W., Introduction to biofilm. Int. J. Antimicrob. Agents, 1999. 11(3-4): 217-221.

8. Nadell, C.D., J.B. Xavier and K.R. Foster, The sociobiology of biofilms. FEMS Microbiol. Rev., 2009. 33(1): 206-224.

9. Davies, D.G., M.R. Parsek, J.P. Pearson, B.H. Iglewski, J.W. Costerton, and E.P. Greenberg, The involvement of cell-to-cell signals in the development of a bacterial biofilm. Science, 1998. 280(5361): 295-298.

10. Flemming, H.C., The perfect slime. Colloid Surface B, 2011. 86(2): 251-9.

11. Peyton, B.M. and W.G. Characklis, A statistical analysis of the effect of substrate utilization and shear stress on the kinetics of biofilm detachment. Biotechnol. Bioeng., 1993. 41(7): 728-735.

12. Sellam, A., T. Al-Niemi, K. McInnerney, S. Brumfield, A. Nantel, and P. Suci, A *Candida albicans* early stage biofilm detachment event in rich medium. BMC Microbiol., 2009. 9(1): 25.

13. Rochex, A., J.-J. Godon, N. Bernet, and R. Escudié, Role of shear stress on composition, diversity and dynamics of biofilm bacterial communities. Water Res., 2008. 42(20): 4915-4922.

14. Lu, P., C. Chen, Q. Wang, Z. Wang, X. Zhang, and S. Xie, Phylogenetic diversity of microbial communities in real drinking water distribution systems. Biotechnology and Bioprocess Engineering, 2013. 18(1): 119-124.

15. Wang, J., M. Liu, H. Xiao, W. Wu, M. Xie, M. Sun, C. Zhu, and P. Li, Bacterial community structure in cooling water and biofilm in an industrial recirculating cooling water system. Water Sci. Technol., 2013. 68(4): 940-7.

16. Lee, K.W.K., S. Periasamy, M. Mukherjee, C. Xie, S. Kjelleberg, and S.A. Rice, Biofilm development and enhanced stress resistance of a model, mixed-species community biofilm. ISME Journal, 2014. 8(4): 894-907.

17. Kearns, D.B., A field guide to bacterial swarming motility. Nature reviews. Microbiology, 2010. 8(9): 634-644.

18. Nadell, C.D., J.B. Xavier, S.A. Levin, and K.R. Foster, The evolution of quorum sensing in bacterial biofilms. PLoS Biol., 2008. 6(1).

19. Ng, W.L. and B.L. Bassler, Bacterial quorum-sensing network architectures. 2009. p. 197-222.

20. Parsek, M.R. and E.P. Greenberg, Sociomicrobiology: The connections between quorum sensing and biofilms. Trends Microbiol., 2005. 13(1): 27-33.

21. Christensen, B.B., C. Sternberg, J.B. Andersen, L. Eberl, S. Møller, M. Givskov, and S. Molin, Establishment of new genetic traits in a microbial biofilm community. Appl. Environ. Microb., 1998. 64(6): 2247-2255.

22. Fletcher, M., The physiological activity of bacteria attached to solid surfaces. Adv. Microb. Physiol., 1991. 32: 53-85.

23. Flemming, H.C. and J. Wingender, The biofilm matrix. Nature Reviews Microbiology, 2010. 8(9): 623-633.

24. !!! INVALID CITATION !!! [24, 25].

25. Vieira, M.J., L.F. Melo and M.M. Pinheiro, Biofilm formation: Hydrodynamic effects on internal diffusion and structure. Biofouling, 1993. 7(1): 67-80.

26. Stewart, P.S., Diffusion in biofilms. J. Bacteriol., 2003. 185(5): 1485-1491.

27. Murthy, P.S. and R. Venkatesan, Industrial Biofilms and their Control, in *Marine and Industrial Biofouling*, H.-C. Flemming, et al., Editors. 2009, Springer Berlin Heidelberg. p. 65-101.

28. Stewart, P.S. and M.J. Franklin, Physiological heterogeneity in biofilms. Nat. Rev. Microbiol., 2008. 6(3): 199-210.

29. Renner, L.D. and D.B. Weibel, Physicochemical regulation of biofilm formation. MRS Bull., 2011. 36(5): 347-355.

30. Tuson, H.H. and D.B. Weibel, Bacteria-surface interactions. Soft Matter, 2013. 9(17): 4368-4380.

31. van Oss, C.J. and C. Jan, Hydrophobicity and hydrophilicity of biosurfaces. Current Opinion in Colloid & Interface Science, 1997. 2(5): 503-512.

32. Oliveira, R., J. Azeredo, P. Teixeira, and A.P. Fonseca. 2001. The role of hydrophobicity in bacterial adhesion. In: "Biofilm community interactions : chance or necessity?" Contributions made at the Meeting of the Biofilm Club, 5, Powys, UK. P. Gilbert.

33. Whitehead, K.A. and J. Verran, The Effect of Surface Topography on the Retention of Microorganisms. Food Bioprod. Process., 2006. 84(4): 253-259.

34. Allion, A., S. Lassiaz, L. Peguet, P. Boillot, S. Jacques, J. Peultier, and M.C. Bonnet, A long term study on biofilm development in drinking water distribution system: Comparison of stainless steel grades with commonly used materials. Revue de Metallurgie. Cahiers D'Informations Techniques, 2011. 108(4): 259-268.

35. Arnold, J.W., D.H. Boothe, O. Suzuki, and G.W. Bailey, Multiple imaging techniques demonstrate the manipulation of surfaces to reduce bacterial contamination and corrosion. Journal of Microscopy, 2004. 216(3): 215-221.

36. Chia, T.W.R., R.M. Goulter, T. McMeekin, G.A. Dykes, and N. Fegan, Attachment of different *Salmonella* serovars to materials commonly used in a poultry processing plant. Food Microbiol., 2009. 26(8): 853-859.

37. Jang, H.J., Y.J. Choi and J.O. Ka, Effects of diverse water pipe materials on bacterial communities and water quality in the annular reactor. J. Microbiol. Biotechnol., 2011. 21(2): 115-23.

38. Storgards, E., H. Simola, A.M. Sjöberg, and G. Wirtanen, Hygiene of Gasket Materials Used in Food Processing Equipment Part 1: New Materials. Food Bioprod. Process., 1999. 77(2): 137-145.

39. V.O. Adetunji, T.O.I., Crystal violet binding assay for assessment of biofilm formation by *Listeria monocytogenes* and *Listeria* spp on wood, steel and glass surfaces. Global Veterinarian, 2011. 6(1): 6-10.

40. Simões, L.C., M. Simões, R. Oliveira, and M.J. Vieira, Potential of the adhesion of bacteria isolated from drinking water to materials. J. Basic Microb., 2007. 47(2): 174-183.

41. Waines, P.L., R. Moate, A.J. Moody, M. Allen, and G. Bradley, The effect of material choice on biofilm formation in a model warm water distribution system. Biofouling, 2011. 27(10): 1161-1174.

42. Kerr, C.J., K.S. Osborn, G.D. Robson, and P.S. Handley, The relationship between pipe material and biofilm formation in a laboratory model system. J. App. Microbiol. Symposium Supplement, 1999. 85(28): 29S-38S.

43. Lehtola, M.J., I.T. Miettinen, T. Lampola, A. Hirvonen, T. Vartiainen, and P.J. Martikainen, Pipeline materials modify the effectiveness of disinfectants in drinking water distribution systems. Water Res., 2005. 39(10): 1962-1971.

44. Yu, J., D. Kim and T. Lee, Microbial diversity in biofilms on water distribution pipes of different materials. Water Sci. Technol., 2010. 61(1): 163-71.

45. Chang, Y.C. and K. Jung, Effect of distribution system materials and water quality on heterotrophic plate counts and biofilm proliferation. J. Microbiol. Biotechnol., 2004. 14(6): 1114-1119.

46. Lee, D.G., S.J. Park and S.J. Kim, Influence of pipe materials and VBNC cells on culturable bacteria in a chlorinated drinking water model system. J. Microbiol. Biotechnol., 2007. 17(9): 1558-1562.

47. Niquette, P., P. Servais and R. Savoir, Impacts of pipe materials on densities of fixed bacterial biomass in a drinking water distribution system. Water Res., 2000. 34(6): 1952-1956.

48. Manuel, C.M., O.C. Nunes and L.F. Melo, Dynamics of drinking water biofilm in flow/non-flow conditions. Water Res., 2007. 41(3): 551-562.

49. Jun, W., M.S. Kim, B.-K. Cho, P.D. Millner, K. Chao, and D.E. Chan, Microbial biofilm detection on food contact surfaces by macro-scale fluorescence imaging. J. Food Eng., 2010. 99(3): 314-322.

50. Oliveira, R., L. Melo, A. Oliveira, and R. Salgueiro, Polysaccharide production and biofilm formation by *Pseudomonas fluorescens*: effects of pH and surface material. Colloids Surf. B. Biointerfaces, 1994. 2(1–3): 41-46.

51. Bendinger, B., H.H.M. Rijnaarts, K. Altendorf, and A.J.B. Zehnder, Physicochemical cell surface and adhesive properties of coryneform bacteria related to the presence and chain length of mycolic acids. Appl. Environ. Microb., 1993. 59(11): 3973-3977.

52. Chmielewski, R.A.N. and J.F. Frank, A predictive model for heat inactivation of *Listeria monocytogenes* biofilm on buna-N rubber. LWT - Food Sci. Technol., 2006. 39(1): 11-19.

53. Chaturongkasumrit, Y., H. Takahashi, S. Keeratipibul, T. Kuda, and B. Kimura, The effect of polyesterurethane belt surface roughness on *Listeria monocytogenes* biofilm formation and its cleaning efficiency. Food Control, 2011. 22(12): 1893-1899.

54. Xu, K.D., G.A. McFeters and P.S. Stewart, Biofilm resistance to antimicrobial agents. Microbiology, 2000. 146(3): 547-549.

55. Klapper, I., C.J. Rupp, R. Cargo, B. Purvedorj, and P. Stoodley, Viscoelastic fluid description of bacterial biofilm material properties. Biotechnol. Bioeng., 2002. 80(3): 289-296.

56. Butler, C.S. and J.P. Boltz, Biofilm Processes and Control in Water and Wastewater Treatment, in *Comprehensive Water Quality and Purification*. 2013. p. 90-107.

57. Stoodley, P., I. Dodds, J.D. Boyle, and H.M. Lappin-Scott, Influence of hydrodynamics and nutrients on biofilm structure. J. Appl. Microbiol., 1999. 85 Suppl 1: 19s-28s.

58. Simões, M., M.O. Pereira, S. Sillankorva, J. Azeredo, and M.J. Vieira, The effect of hydrodynamic conditions on the phenotype of *Pseudomonas fluorescens* biofilms. Biofouling, 2007. 23(4): 249-258.

59. Bryers, J. and W. Characklis, Early fouling biofilm formation in a turbulent flow system: Overall kinetics. Water Res., 1981. 15(4): 483-491.

60. Pereira, M.O., M. Kuehn, S. Wuertz, T. Neu, and L.F. Melo, Effect of flow regime on the architecture of a *Pseudomonas fluorescens* biofilm. Biotechnol. Bioeng., 2002. 78(2): 164-171.

61. Stoodley, P., J.D. Boyle, D. Debeer, and H.M. Lappin-Scott, Evolving perspectives of biofilm structure. Biofouling, 1999. 14(1): 75-90.

62. Kirisits, M.J., J.J. Margolis, B.L. Purevdorj-Gage, B. Vaughan, D.L. Chopp, P. Stoodley, and M.R. Parsek, Influence of the hydrodynamic environment on quorum sensing in *Pseudomonas aeruginosa* biofilms. J. Bacteriol., 2007. 189(22): 8357-60.

63. Stewart, P.S. and M.J. Franklin, Physiological heterogeneity in biofilms. Nat. Rev. Microbiol., 2008. 6(3): 199-210.

64. Rickard, A.H., A.J. McBain, A.T. Stead, and P. Gilbert, Shear Rate Moderates Community Diversity in Freshwater Biofilms. Appl. Environ. Microb., 2004. 70(12): 7426-7435.

65. Abe, Y., S. Skali-Lami, J.-C. Block, and G. Francius, Cohesiveness and hydrodynamic properties of young drinking water biofilms. Water Res., 2012. 46(4): 1155-1166.

66. Peyton, B.M., Effects of shear stress and substrate loading rate on *Pseudomonas aeruginosa* biofilm thickness and density. Water Res., 1996. 30(1): 29-36.

67. Cao, Y.S. and G.J. Alaerts, Influence of reactor type and shear stress on aerobic biofilm morphology, population and kinetics. Water Res., 1995. 29(1): 107-118.

68. Vieira, M.J. and L.F. Melo, Intrinsic kinetics of biofilms formed under turbulent flow and low substrate concentrations. Bioprocess. Eng., 1999. 20(4): 369-375.

69. Bott, T.R., Industrial Biofouling. 2011: Elsevier.

70. Dourou, D., C.S. Beauchamp, Y. Yoon, I. Geornaras, K.E. Belk, G.C. Smith, G.J.E. Nychas, and J.N. Sofos, Attachment and biofilm formation by *Escherichia coli* O157:H7 at different temperatures, on various food-contact surfaces encountered in beef processing. Int. J. Food Microbiol., 2011. 149(3): 262-268.

71. Meira, Q.G.D., I.D. Barbos, A.J.A.A. Athayde, J.P. de Siqueira, and E.L. de Souza, Influence of temperature and surface kind on biofilm formation by *Staphylococcus aureus* from food-contact surfaces and sensitivity to sanitizers. Food Control, 2012. 25(2): 469-475.

72. Sharma, M. and S.K. Anand, Characterization of constitutive microflora of biofilms in dairy processing lines. Food Microbiol., 2002. 19(6): 627-636.

73. Patil, S.A., F. Harnisch, C. Koch, T. Hübschmann, I. Fetzer, A.A. Carmona-Martínez, S. Müller, and U. Schröder, Electroactive mixed culture derived biofilms in microbial bioelectrochemical systems: The role of pH on biofilm formation, performance and composition. Bioresour. Technol., 2011. 102(20): 9683-9690.

74. Garrett, T.R., M. Bhakoo and Z. Zhang, Bacterial adhesion and biofilms on surfaces. Prog. Nat. Sci., 2008. 18(9): 1049-1056.

75. Fletcher, M., Bacterial biofilms and biofouling. Curr. Opin. Biotech., 1994. 5(3): 302-306.

76. Hall-Stoodley, L., J.W. Costerton and P. Stoodley, Bacterial biofilms: From the natural environment to infectious diseases. Nature Reviews Microbiology, 2004. 2(2): 95-108.

77. Kriwy, P. and S. Uthicke, Microbial diversity in marine biofilms along a water quality gradient on the Great Barrier Reef. Syst. Appl. Microbiol., 2011. 34(2): 116-126.

78. Taylor, C.D., C.O. Wirsen and F. Gaill, Rapid Microbial Production of Filamentous Sulfur Mats at Hydrothermal Vents. Appl. Environ. Microb., 1999. 65(5): 2253-2255.

79. Reysenbach, A.-L. and S.L. Cady, Microbiology of ancient and modern hydrothermal systems. Trends Microbiol., 2001. 9(2): 79-86.

80. Westall, F., M.J. de Wit, J. Dann, S. van der Gaast, C.E.J. de Ronde, and D. Gerneke, Early Archean fossil bacteria and biofilms in hydrothermally-influenced sediments from the Barberton greenstone belt, South Africa. Precambrian Res., 2001. 106(1–2): 93-116.

81. Simões, L.C. and M. Simões, Biofilms in drinking water: problems and solutions. RSC Adv., 2013. 3(8): 2520-2533.

82. Farkas, A., M. Dragan-Bularda, V. Muntean, D. Ciataras, and S. Tigan, Microbial activity in drinking water-associated biofilms. Central European Journal of Biology, 2013. 8(2): 201-214.

83. Zacheus, O.M., M.J. Lehtola, L.K. Korhonen, and P.J. Martikainen, Soft deposits, the key site for microbial growth in drinking water distribution networks. Water Res., 2001. 35(7): 1757-1765.

84. Manuel, C.M., O.C. Nunes and L.F. Melo, Unsteady state flow and stagnation in distribution systems affect the biological stability of drinking water. Biofouling, 2010. 26(2): 129-139.

85. Barker, J. and S.F. Bloomfield, Survival of *Salmonella* in bathrooms and toilets in domestic homes following salmonellosis. J. Appl. Microbiol., 2000. 89(1): 137-144.

86. Lin, W., Z. Yu, X. Chen, R. Liu, and H. Zhang, Molecular characterization of natural biofilms from household taps with different materials: PVC, stainless steel, and cast iron in drinking water distribution system. Appl. Microbiol. Biotechnol., 2013. 97(18): 8393-401.

87. Eboigbodin, K.E., A. Seth and C.A. Biggs, A review of biofilms in domestic plumbing. Journal / American Water Works Association, 2008. 100(10): 131-138+12.

88. Rayner, J., R. Veeh and J. Flood, Prevalence of microbial biofilms on selected fresh produce and household surfaces. Int. J. Food Microbiol., 2004. 95(1): 29-39.

89. Ak, N.O., D.O. Cliver and C.W. Kaspar, Decontamination of plastic and wooden cutting boards for kitchen use. J. Food Protect., 1994. 57(1): 23-30.

90. Schaule, G., S. Schulte and H.C. Flemming, Biofilms on aged materials in household installation systems. GWF, Wasser - Abwasser, 2010. 151(Special Issue): 71-73.

91. Beumer, R.R., M.C. te Giffel, E. Spoorenberg, and F.M. Rombouts, *Listeria* species in domestic environments. Epidemiol. Infect., 1996. 117(3): 437-442.

92. Carter, G., M. Wu, D.C. Drummond, and L.E. Bermudez, Characterization of biofilm formation by clinical isolates of *Mycobacterium avium.* J. Med. Microbiol., 2003. 52(9): 747-752.

93. Hull, N.M., A.L. Reens, C.E. Robertson, L.F. Stanish, J.K. Harris, M.J. Stevens, D.N. Frank, C. Kotter, and N.R. Pace, Molecular analysis of single room humidifier bacteriology. Water Res., 2015. 69: 318-327.

94. Kelley, S.T., U. Theisen, L.T. Angenent, A. St. Amand, and N.R. Pace, Molecular analysis of shower curtain biofilm microbes. Appl. Environ. Microb., 2004. 70(7): 4187-4192.

95. Liguori, G., V. Di Onofrio, F. Gallè, R. Liguori, R.A. Nastro, and M. Guida, Occurrence of *Legionella* spp. in thermal environments: virulence factors and biofilm formation in isolates from a spa. Microchem. J., 2014. 112: 109-112.

96. Timke, M., N.Q. Wang-Lieu, K. Altendorf, and A. Lipski, Fatty acid analysis and spoilage potential of biofilms from two breweries. J. Appl. Microbiol., 2005. 99(5): 1108-1122.

97. Joseph, C.M.L., G. Kumar, E. Su, and L.F. Bisson, Adhesion and Biofilm Production by Wine Isolates of *Brettanomyces bruxellensis.* American Journal of Enology and Viticulture, 2007. 58(3): 373-378.

98. Maifreni, M., F. Frigo, I. Bartolomeoli, S. Buiatti, S. Picon, and M. Marino, Bacterial biofilm as a possible source of contamination in the microbrewery environment. Food Control, 2015. 50: 809-814.

99. Bergsveinson, J., N. Baecker, V. Pittet, and B. Ziola, Role of Plasmids in *Lactobacillus brevis* BSO 464 Hop Tolerance and Beer Spoilage. Appl. Environ. Microb., 2015. 81(4): 1234-1241.

100. Goode, K.R., K. Asteriadou, P.T. Robbins, and P.J. Fryer, Fouling and Cleaning Studies in the Food and Beverage Industry Classified by Cleaning Type. Comprehensive Reviews in Food Science and Food Safety, 2013. 12(2): 121-143.

101. Waak, E., W. Tham and M.L. Danielsson-Tham, Prevalence and fingerprinting of *Listeria monocytogenes* strains isolated from raw whole milk in farm bulk tanks and in dairy plant receiving tanks. Appl. Environ. Microb., 2002. 68(7): 3366-3370.

102. Sharma, M. and S.K. Anand, Biofilms evaluation as an essential component of HACCP for food/dairy processing industry – a case. Food Control, 2002. 13(6–7): 469-477.

103. Zottola, E.A. and K.C. Sasahara, Microbial biofilms in the food processing industry — Should they be a concern? Int. J. Food Microbiol., 1994. 23(2): 125-148.

104. Latorre, A.A., J.S. Van Kessel, J.S. Karns, M.J. Zurakowski, A.K. Pradhan, K.J. Boor, B.M. Jayarao, B.A. Houser, C.S. Daugherty, and Y.H. Schukken, Biofilm in milking equipment on a dairy farm as a potential source of bulk tank milk contamination with *Listeria monocytogenes.* J. Dairy Sci., 2010. 93(6): 2792-2802.

105. Faruque, S.M., K. Biswas, S.M. Nashir Udden, Q.S. Ahmad, D.A. Sack, and G. Balakrish Nair, Transmissibility of cholera: In vivo-formed biofilms and their relationship to infectivity and persistence in the environment. Proceedings of the National Academy of Sciences of the United States of America, 2006. 103(16): 6350-6355.

106. Enos-Berlage, J.L., Z.T. Guvener, C.E. Keenan, and L.L. McCarter, Genetic determinants of biofilm development of opaque and translucent *Vibrio parahaemolyticus.* Mol. Microbiol., 2005. 55(4): 1160-1182.

107. Kogure, K., E. Ikemoto and H. Morisaki, Attachment of *Vibrio alginolyticus* to glass surfaces is dependent on swimming speed. J. Bacteriol., 1998. 180(4): 932-937.

108. Guðbjörnsdóttir, B., H. Einarsson and G. Thorkelsson, Microbial Adhesion to Processing Lines for Fish Fillets and Cooked Shrimp: Influence of Stainless Steel Surface Finish and Presence of Gram-Negative Bacteria on the Attachment of *Listeria monocytogenes.* Food Technol. Biotechnol., 2004. 43(1): 55-61.

109. Bagge-Ravn, D., Y. Ng, M. Hjelm, J.N. Christiansen, C. Johansen, and L. Gram, The microbial ecology of processing equipment in different fish industries - Analysis of the microflora during processing and following cleaning and disinfection. Int. J. Food Microbiol., 2003. 87(3): 239-250.

110. Marouani-Gadri, N., G. Augier and B. Carpentier, Characterization of bacterial strains isolated from a beef-processing plant following cleaning and disinfection - Influence of isolated strains on biofilm formation by Sakaï and EDL 933 *E. coli* O157:H7. Int. J. Food Microbiol., 2009. 133(1-2): 62-67.

111. Habimana, O., E. Heir, S. Langsrud, A.W. Åsli, and T. Møretrø, Enhanced surface colonization by *Escherichia coli* 0157:H7 in biofilms formed by an *Acinetobacter calcoaceticus* isolate from meat-processing environments. Appl. Environ. Microb., 2010. 76(13): 4557-4559.

112. Thévenot, D., M.L. Delignette-Muller, S. Christieans, and C. Vernozy-Rozand, Fate of *Listeria monocytogenes* in experimentally contaminated French sausages. Int. J. Food Microbiol., 2005. 101(2): 189-200.

113. Jessen, B. and L. Lammert, Biofilm and disinfection in meat processing plants. Int. Biodeter. Biodegr., 2003. 51(4): 265-269.

114. Park, S.H., R. Jarquin, I. Hanning, G. Almeida, and S.C. Ricke, Detection of *Salmonella* spp. survival and virulence in poultry feed by targeting the *hilA* gene. J. Appl. Microbiol., 2011. 111(2): 426-432.

115. Marin, C., A. Hernandiz and M. Lainez, Biofilm development capacity of *Salmonella* strains isolated in poultry risk factors and their resistance against disinfectants. Poultry Science, 2009. 88(2): 424-431.

116. Deming, M.S., R.V. Tauxe, P.A. Blake, S.E. Dixon, B.S. Fowler, T.S. Jones, E.A. Lockamy, C.M. Patton, and R.O. Sikes, *Campylobacter enteritis* at a university: Transmission from eating chicken and from cats. Am. J. Epidemiol., 1987. 126(3): 526-534.

117. Harris, N.V., N.S. Weiss and C.M. Nolan, The role of poultry and meats in the etiology of *Campylobacter jejuni/coli enteritis.* Am. J. Public Health, 1986. 76(4): 407-411.

118. Patel, J. and M. Sharma, Differences in attachment of *Salmonella enterica* serovars to cabbage and lettuce leaves. Int. J. Food Microbiol., 2010. 139(1–2): 41-47.

119. Keskinen, L.A. and B.A. Annous, Efficacy of adding detergents to sanitizer solutions for inactivation of *Escherichia coli* O157:H7 on Romaine lettuce. Int. J. Food Microbiol., 2011. 147(3): 157-161.

120. Ölmez, H. and S.D. Temur, Effects of different sanitizing treatments on biofilms and attachment of *Escherichia coli* and *Listeria monocytogenes* on green leaf lettuce. LWT - Food Sci. Technol., 2010. 43(6): 964-970.

121. Gil, M.I., M.V. Selma, F. López-Gálvez, and A. Allende, Fresh-cut product sanitation and wash water disinfection: Problems and solutions. Int. J. Food Microbiol., 2009. 134(1–2): 37-45.

122. Liu, Y., W. Zhang, T. Sileika, R. Warta, N.P. Cianciotto, and A. Packman, Role of bacterial adhesion in the microbial ecology of biofilms in cooling tower systems. Biofouling, 2009. 25(3): 241-253.

123. Balamurugan, P., M. Hiren Joshi and T.S. Rao, Microbial fouling community analysis of the cooling water system of a nuclear test reactor with emphasis on sulphate reducing bacteria. Biofouling, 2011. 27(9): 967-978.

124. Liu, H., B. Zheng, D. Xu, C. Fu, and Y. Luo, Effect of sulfate-reducing bacteria and iron-oxidizing bacteria on the rate of corrosion of an aluminum alloy in a central air-conditioning cooling water system. Industrial & Engineering Chemistry Research, 2014. 53(19): 7840-7846.

125. Moreno, D.A., J.R. Ibars, J.L. Polo, and J.M. Bastidas, EIS monitoring study of the early microbiologically influenced corrosion of AISI 304L stainless steel condenser tubes in freshwater. J. Solid State Electrochem., 2014. 18(2): 377-388.

126. Cloete, T.E., Biofouling control in industrial water systems: What we know and what we need to know. Mater. Corros., 2003. 54(7): 520-526.

127. Eckford, R.E. and P.M. Fedorak, Chemical and microbiological changes in laboratory incubations of nitrate amendment “sour” produced waters from three western Canadian oil fields. J. Ind. Microbiol. Biotechnol., 2002. 29(5): 243-254.

128. Howsam, P., Microbiology in Civil Engineering: Proceedings of the Federation of European Microbiological Societies Symposium held at Cranfield Institute of Technology, UK. 2003: Taylor & Francis.

129. Sanders, P.F. and P.J. Sturman, Biofouling in the Oil Industry, in *Petroleum Microbiology*. 2005, American Society of Microbiology.

130. Alabbas, F.M., C. Williamson, S.M. Bhola, J.R. Spear, D.L. Olson, B. Mishra, and A.E. Kakpovbia, Microbial corrosion in linepipe steel under the influence of a sulfate-reducing consortium isolated from an oil field. J. Mater. Eng. Perform., 2013. 22(11): 3517-3529.

131. Qiu, L.N., Y.N. Mao, A.J. Gong, L. Tong, and Y.Q. Cao, Inhibition effect of *thiobacillus denitrificans* on the corrosion of X70 pipeline steel caused by sulfate-reducing bacteria in crude petroleum. Mater. Corros., 2015. 66(6): 588-593.

132. Mori, K., H. Tsurumaru and S. Harayama, Iron corrosion activity of anaerobic hydrogen-consuming microorganisms isolated from oil facilities. J. Biosci. Bioeng., 2010. 110(4): 426-430.

133. Flemming, H.-C., Microbial Biofouling: Unsolved Problems, Insufficient Approaches, and Possible Solutions, in *Biofilm Highlights*, H.-C. Flemming, J. Wingender, and U. Szewzyk, Editors. 2011, Springer - Verlag Berlin Heidelberg p. 81-109.

134. Carpentier, B. and O. Cerf, Biofilms and their consequences, with particular reference to hygiene in the food industry. J. Appl. Microbiol., 1993. 75(6): 499-511.

135. Beech, I.B. and J. Sunner, Biocorrosion: towards understanding interactions between biofilms and metals. Curr. Opin. Biotech., 2004. 15(3): 181-186.

136. Cloete, T.E., Resistance mechanisms of bacteria to antimicrobial compounds. International Biodeterioration and Biodegradation, 2003. 51(4): 277-282.

137. Lewis, K., Persister cells, dormancy and infectious disease. Nat. Rev. Microbiol., 2007. 5(1): 48-56.

138. Lemos, M., F. Mergulhão, L. Melo, and M. Simões, The effect of shear stress on the formation and removal of *Bacillus cereus* biofilms. Food Bioprod. Process., 2015. 93(0): 242-248.

139. Simões, L.C., M. Lemos, A.M. Pereira, A.C. Abreu, M.J. Saavedra, and M. Simões, Persister cells in a biofilm treated with a biocide. Biofouling, 2011. 27(4): 403 — 411.

140. Srey, S., I.K. Jahid and S.-D. Ha, Biofilm formation in food industries: A food safety concern. Food Control, 2013. 31(2): 572-585.

141. Ludensky, M., Control and monitoring of biofilms in industrial applications. Int. Biodeter. Biodegr., 2003. 51(4): 255-263.

142. Costerton, J.W., P.S. Stewart and E.P. Greenberg, Bacterial biofilms: A common cause of persistent infections. Science, 1999. 284(5418): 1318-1322.

143. Müller-Steinhagen, H., Handbook of Heat Exchanger Fouling: Mitigation and Cleaning Technologies. 2000: IChemE.

144. Melo, L. and H.C. Flemming, Mechanistic Aspects of Heat Exchanger and Membrane Biofouling and Prevention, in *The Science and Technology of Industrial Water Treatment*. 2010, Taylor and Francis Group: Boca Raton, Fla, USA. p. 365-380.

145. Rao, T.S., A.J. Kora, P. Chandramohan, B.S. Panigrahi, and S.V. Narasimhan, Biofouling and microbial corrosion problem in the thermo-fluid heat exchanger and cooling water system of a nuclear test reactor. Biofouling, 2009. 25(7): 581-591.

146. Müller-Steinhagen, H., M.R. Malayeri and A.P. Watkinson, Heat Exchanger Fouling: Mitigation and Cleaning Strategies. Heat Transfer Eng, 2011. 32(3-4): 189-196.

147. Hood, S.K. and E.A. Zottola, Biofilms in food processing. Food Control, 1995. 6(1): 9-18.

148. Teixeira, P., Silva, S., Araújo, F., Azeredo, J., Oliveira, R., Bacterial adhesion to food contacting surfaces, in *Communicating Current Research and Educational Topics and Trends in Applied Microbiology*. 2007.

149. Verran, J., Biofouling in food processing: Biofilm or biotransfer potential? Food and Bioproducts Processing: Transactions of the Institution of of Chemical Engineers, Part C, 2002. 80(4): 292-298.

150. Brooks, J.D. and S.H. Flint, Biofilms in the food industry: problems and potential solutions. Int. J. Food Sci. Tech., 2008. 43(12): 2163-2176.

151. Klahre, J. and H.C. Flemming, Monitoring of biofouling in papermill process waters. Water Res., 2000. 34(14): 3657-3665.

152. Flemming, H.-C., M. Meier and T. Schild, Mini-review: microbial problems in paper production. Biofouling, 2013. 29(6): 683-696.

153. Directive 98/8/EC of the European Parliament and of the Council of 16 February 1998 concerning the placing of biocidal products on the market

154. Denyer, S.P. and G.S.A.B. Stewart, Mechanisms of action of disinfectants. International Biodeterioration and Biodegradation, 1998. 41(3-4): 261-268.

155. Moore, S.L. and D.N. Payne, Types of Antimicrobial Agents, in *Russell, Hugo & Ayliffe's Principles and Practice of Disinfection, Preservation & Sterilization*, J.-Y.M. Adam P. Fraise, Syed Sattar Editor. 2008, Blackwell Publishing Ltd. p. 8-97.

156. Uhr, H., B. Mielke, O. Exner, K.R. Payne, and E. Hill, Biocides, in *Ullmann's Encyclopedia of Industrial Chemistry*. 2000, Wiley-VCH Verlag GmbH & Co. KGaA.

157. Chapman, J.S., Biocide resistance mechanisms. Int. Biodeter. Biodegr., 2003. 51(2): 133-138.

158. Walsh, S.E., J.Y. Maillard and A.D. Russell, *Ortho*-phthalaldehyde: A possible alternative to glutaraldehyde for high level disinfection. J. Appl. Microbiol., 1999. 86(6): 1039-1046.

159. Pereira, M.O. and M.J. Vieira, Effects of the interactions between glutaraldehyde and the polymeric matrix on the efficacy of the biocide against *Pseudomonas fluorescens* biofilms. Biofouling, 2001. 17(2): 93-101.

160. Simões, L.C., M. Lemos, P. Araújo, A.M. Pereira, and M. Simões, The effects of glutaraldehyde on the control of single and dual biofilms of *Bacillus cereus* and *Pseudomonas fluorescens.* Biofouling, 2011. 27(3): 337-346.

161. Walsh, S.E., J.Y. Maillard, A.D. Russell, and A.C. Hann, Possible mechanisms for the relative efficacies of *ortho*-phthalaldehyde and glutaraldehyde against glutaraldehyde-resistant *Mycobacterium chelonae.* J. Appl. Microbiol., 2001. 91(1): 80-92.

162. Simons, C., S.E. Walsh, J.Y. Maillard, and A.D. Russell, A NOTE: *Ortho*-Phthalaldehyde: proposed mechanism of action of a new antimicrobial agent. Lett. Appl. Microbiol., 2000. 31(4): 299-302.

163. Walsh, S.E., J.Y. Maillard, C. Simons, and A.D. Russell, Studies on the mechanisms of the antibacterial action of *ortho*-phthalaldehyde. J. Appl. Microbiol., 1999. 87(5): 702-710.

164. Armon, R., T. Arbel and M. Green, A quantitative and qualitative study of biofilm disinfection on glass, metal and PVC surfaces by chlorine, bromine and bromochloro-5,5 dimethylhydantoin (BCDMH). Water Sci. Technol., 1998. 38(12): 175-179.

165. Yoffe, D., R. Frim, S.D. Ukeles, M.J. Dagani, H.J. Barda, T.J. Benya, and D.C. Sanders, Bromine Compounds, in *Ullmann's Encyclopedia of Industrial Chemistry*. 2000, Wiley-VCH Verlag GmbH & Co. KGaA.

166. Kramer, J.F. 2001. Biofilm Control with Bromo-chloro-dimethyl-hydantoin. In: CORROSION 2001. NACE International.

167. Mayack, L.A., R.J. Soracco, E.W. Wilde, and D.H. Pope, Comparative effectiveness of chlorine and chlorine dioxide biocide regimes for biofouling control. Water Res., 1984. 18(5): 593-599.

168. Nam, H., H.-S. Seo, J. Bang, H. Kim, L.R. Beuchat, and J.-H. Ryu, Efficacy of gaseous chlorine dioxide in inactivating *Bacillus cereus* spores attached to and in a biofilm on stainless steel. Int. J. Food Microbiol., 2014. 188(0): 122-127.

169. Bhawana, J.M. Stubblefield, A.L. Newsome, and A.B. Cahoon, Surface decontamination of plant tissue explants with chlorine dioxide gas. In Vitro Cell. Dev. Biol. Plant, 2015. 51(2): 214-219.

170. Vaerewijck, M.J.M., K. Sabbe, J. Bare, H.P. Spengler, H.W. Favoreel, and K. Houf, Assessment of the efficacy of benzalkonium chloride and sodium hypochlorite against *Acanthamoeba polyphaga* and *Tetrahymena* spp. J. Food Protect., 2012. 75(3): 541-546.

171. Fransisca, L., B. Zhou, H. Park, and H. Feng, The Effect of Calcinated Calcium and Chlorine Treatments on *Escherichia coli* O157:H7 87-23 Population Reduction in Radish Sprouts. J. Food Sci., 2011. 76(6): M404-M412.

172. Lagrange, F., W. Reiprich and M. Hoffmann, CIP-cleaning and desinfection with ozoned water. Fleischwirtschaft, 2004. 84(2): 112-114.

173. Pascual, A., I. Llorca and A. Canut, Use of ozone in food industries for reducing the environmental impact of cleaning and disinfection activities. Trends in Food Science and Technology, 2007. 18(SUPPL. 1): S29-S35.

174. Sapers, G.M. and J.E. Sites, Efficacy of 1% hydrogen peroxide wash in decontaminating apples and cantaloupe melons. J. Food Sci., 2003. 68(5): 1793-1797.

175. Elkins, J.G., D.J. Hassett, P.S. Stewart, H.P. Schweizer, and T.R. McDermott, Protective Role of Catalase in *Pseudomonas aeruginosa* Biofilm Resistance to Hydrogen Peroxide. Appl. Environ. Microb., 1999. 65(10): 4594-4600.

176. Ibusquiza, P.S., J.J.R. Herrera and M.L. Cabo, Resistance to benzalkonium chloride, peracetic acid and nisin during formation of mature biofilms by Listeria monocytogenes. Food Microbiol., 2011. 28(3): 418-425.

177. Bridier, A., R. Briandet, V. Thomas, and F. Dubois-Brissonnet, Comparative biocidal activity of peracetic acid, benzalkonium chloride and *ortho*-phthalaldehyde on 77 bacterial strains. J. Hosp. Infect., 2011. 78(3): 208-213.

178. Yoon, D.Y. and D.S. Kim, Molecular design of anti-biofouling materials from natural phenolic compounds. Korean J. Chem. Eng., 2009. 26(2): 433-437.

179. Cueva, C., M.V. Moreno-Arribas, P.J. Martín-Álvarez, G. Bills, M.F. Vicente, A. Basilio, C.L. Rivas, T. Requena, J.M. Rodríguez, and B. Bartolomé, Antimicrobial activity of phenolic acids against commensal, probiotic and pathogenic bacteria. Res. Microbiol., 2010. 161(5): 372-382.

180. Maddox, C.E., L.M. Laur and L. Tian, Antibacterial activity of phenolic compounds against the phytopathogen *Xylella fastidiosa.* Curr. Microbiol., 2010. 60(1): 53-58.

181. Saavedra, M.J., A. Borges, C. Dias, A. Aires, R.N. Bennett, E.S. Rosa, and M. Simões, Antimicrobial activity of phenolics and glucosinolate hydrolysis products and their synergy with streptomycin against pathogenic bacteria. 2010. 6(3): 174-83.

182. Leopoldini, M., N. Russo and M. Toscano, The molecular basis of working mechanism of natural polyphenolic antioxidants. Food Chem., 2011. 125(2): 288-306.

183. Simões, M., L.C. Simões, M.O. Pereira, and M.J. Vieira, Sodium dodecyl sulfate allows the persistence and recovery of biofilms of *Pseudomonas fluorescens* formed under different hydrodynamic conditions. Biofouling, 2008. 24(1): 35-44.

184. Copello, G.J., S. Teves, J. Degrossi, M. D'Aquino, M.F. Desimone, and L.E. Diaz, Proving the antimicrobial spectrum of an amphoteric surfactant-sol-gel coating: a food-borne pathogen study. J. Ind. Microbiol. Biotechnol., 2008. 35(9): 1041-6.

185. Gerba, C.P., Quaternary Ammonium Biocides: Efficacy in Application. Appl. Environ. Microb., 2015. 81(2): 464-469.

186. Fazlara, A. and M. Ekhtelat, The disinfectant effects of benzalkonium chloride on some important foodborne pathogens. American-Eurasian Journal of Agricultural & Environmental Sciences, 2012. 12(1): 23-29.

187. Jaramillo, D.E., A. Arriola, K. Safavi, and L.E.C. de Paz, Decreased bacterial adherence and biofilm growth on surfaces coated with a solution of benzalkonium chloride. J. Endodont., 2012. 38(6): 821-825.

188. Batté, M., B. Koudjonou, P. Laurent, L. Mathieu, J. Coallier, and M. Prévost, Biofilm responses to ageing and to a high phosphate load in a bench-scale drinking water system. Water Res., 2003. 37(6): 1351-1361.

189. Douterelo, I., R.L. Sharpe and J.B. Boxall, Influence of hydraulic regimes on bacterial community structure and composition in an experimental drinking water distribution system. Water Res., 2013. 47(2): 503-516.

190. Lelièvre, C., P. Legentilhomme, C. Gaucher, J. Legrand, C. Faille, and T. Bénézech, Cleaning in place: effect of local wall shear stress variation on bacterial removal from stainless steel equipment. Chem. Eng. Sci., 2002. 57(8): 1287-1297.

191. Paul, E., J.C. Ochoa, Y. Pechaud, Y. Liu, and A. Liné, Effect of shear stress and growth conditions on detachment and physical properties of biofilms. Water Res., 2012. 46(17): 5499-5508.

192. Chemat, F., E.H. Zill and M.K. Khan, Applications of ultrasound in food technology: Processing, preservation and extraction. Ultrason. Sonochem., 2011. 18(4): 813-835.

193. Piyasena, P., E. Mohareb and R.C. McKellar, Inactivation of microbes using ultrasound: a review. Int. J. Food Microbiol., 2003. 87(3): 207-216.

194. Oulahal-Lagsir, N., A. Martial-Gros, E. Boistier, L.J. Blum, and M. Bonneau, The development of an ultrasonic apparatus for the non-invasive and repeatable removal of fouling in food processing equipment. Lett. Appl. Microbiol., 2000. 30(1): 47-52.

195. Bott, T.R., Biofouling Control with Ultrasound. Heat Transfer Eng, 2000. 21(3): 43-49.

196. Bott, T.R., Techniques for reducing the amount of biocide necessary to counteract the effects of biofilm growth in cooling water systems. Appl. Therm. Eng., 1998. 18(11): 1059-1066.

197. Quarini, J., Ice-pigging to reduce and remove fouling and to achieve clean-in-place. Appl. Therm. Eng., 2002. 22(7): 747-753.

198. Ainslie, E.A., G.L. Quarini, D.G. Ash, T.J. Deans, M. Herbert, and T.D.L. Rhys. 2009. Heat exchanger cleaning using ice pigging. In: Proceedings of International Conference Heat Exchanger Fouling and Cleaning VIII H. Muller-Steinhagen, M.R. Malayeri, and A.P. Watkinson. Schladmig, Austria 433 - 438.

199. Cornelissen, E.R., L. Rebour, D. van der Kooij, and L.P. Wessels, Optimization of air/water cleaning (AWC) in spiral wound elements. Desalination, 2009. 236(1–3): 266-272.

200. Meyer, B., Approaches to prevention, removal and killing of biofilms. International Biodeterioration and Biodegradation, 2003. 51(4): 249-253.

201. Simões, M., L.C. Simões, I. Machado, M.O. Pereira, and M.J. Vieira, Control of flow-generated biofilms with surfactants: Evidence of resistance and recovery. Food Bioprod. Process., 2006. 84(4 C): 338-345.

202. Gilbert, P. and A.J. McBain, Potential impact of increased use of biocides in consumer products on prevalence of antibiotic resistance. Clin. Microbiol. Rev., 2003. 16(2): 189-208.

203. Cloete, T.E., L. Jacobs and V.S. Brözel, The chemical control of biofouling in industrial water systems. Biodegradation, 1998. 9(1): 23-37.

204. Regulation (EC) 852/2004 of the European Parliament and the Council of 29 April 2004, on the hygiene of foodstuffs,.

205. Regulation (EC) No 853/2004 of the European Parliament and of the Council of 29 April 2004 laying down specific hygiene rules for food of animal origin.

206. Cloete, T.E. and M.R. Maluleke, The use of the Rotoscope as an online, real-time, non-destructive biofilm monitor. Water Sci. Technol., 2005. 52(7): 211-216.

207. Pereira, A., J. Mendes and L.F. Melo, Using nanovibrations to monitor biofouling. Biotechnol. Bioeng., 2008. 99(6): 1407-1415.

208. Flemming, H.-C., A. Tamachkiarowa, J. Klahre, and J. Schmitt, Monitoring of fouling and biofouling in technical systems. Water Sci. Technol., 1998. 38(8–9): 291-298.

209. Hoskins, B.C., L. Fevang, P.D. Majors, M.M. Sharma, and G. Georgiou, Selective imaging of biofilms in porous media by NMR relaxation. J. Magn. Reson., 1999. 139(1): 67-73.

210. Characklis, W.G. and K.C. Marshall, Biofilms. 1990, New York: John Wiley and Son, Inc.

211. Lewandowski, Z. and H. Beyenal, Fundamentals of Biofilm Research, Second Edition. 2013: CRC Press.

212. Flemming, H.C., U. Szewzyk and T. Griebe, Biofilms: Investigative Methods and Applications. 2000: Taylor & Francis.

213. Melo, L., Biorreatores - Caracterização e modos de operação. 2012. Faculdade de Engenharia da Universidade do Porto.

214. Kumar, S., C. Wittmann and E. Heinzle, Minibioreactors. Biotechnol. Lett, 2004. 26(1): 1-10.

215. Stepanović, S., D. Vukovic, I. Dakic, B. Savic, and M. Svabic-Vlahovic, A modified microtiter-plate test for quantification of staphylococcal biofilm formation. J. Microbiol. Methods, 2000. 40(2): 175-179.

216. Peeters, E., H.J. Nelis and T. Coenye, Comparison of multiple methods for quantification of microbial biofilms grown in microtiter plates. J. Microbiol. Methods, 2008. 72(2): 157-165.

217. Pettit, R.K., C.A. Weber, M.J. Kean, H. Hoffmann, G.R. Pettit, R. Tan, K.S. Franks, and M.L. Horton, Microplate alamar blue assay for *Staphylococcus epidermidis* biofilm susceptibility testing. Antimicrob. Agents Ch., 2005. 49(7): 2612-2617.

218. Sarker, S.D., L. Nahar and Y. Kumarasamy, Microtitre plate-based antibacterial assay incorporating resazurin as an indicator of cell growth, and its application in the in vitro antibacterial screening of phytochemicals. Methods, 2007. 42(4): 321-324.

219. Nakayama, G.R., Microplate assays for high-throughput screening. Current Opinion in Drug Discovery and Development, 1998. 1(1): 85-91.

220. Wijman, J.G., P.P. de Leeuw, R. Moezelaar, M.H. Zwietering, and T. Abee, Air-liquid interface biofilms of *Bacillus cereus*: formation, sporulation, and dispersion. Appl. Environ. Microb., 2007. 73(5): 1481-8.

221. Simões, L.C., M. Simões and M.J. Vieira, Adhesion and biofilm formation on polystyrene by drinking water-isolated bacteria. Antonie van Leeuwenhoek, 2010. 98(3): 317-329.

222. Christensen, G.D., W.A. Simpson, J.J. Younger, L.M. Baddour, F.F. Barrett, D.M. Melton, and E.H. Beachey, Adherence of coagulase-negative staphylococci to plastic tissue culture plates: A quantitative model for the adherence of staphylococci to medical devices. J. Clin. Microbiol., 1985. 22(6): 996-1006.

223. Cerca, N., S. Martins, G.B. Pier, R. Oliveira, and J. Azeredo, The relationship between inhibition of bacterial adhesion to a solid surface by sub-MICs of antibiotics and subsequent development of a biofilm. Res. Microbiol., 2005. 156(5–6): 650-655.

224. Lizcano, A., T. Chin, K. Sauer, E.I. Tuomanen, and C.J. Orihuela, Early biofilm formation on microtiter plates is not correlated with the invasive disease potential of *Streptococcus pneumoniae*. Microb. Pathog., 2010. 48(3-4): 124-130.

225. Deighton, M.A. and B. Balkau, Adherence measured by microtiter assay as a virulence marker for *Staphylococcus epidermidis* infections. J. Clin. Microbiol., 1990. 28(11): 2442-2447.

226. Coenye, T., E. Peeters and H.J. Nelis, Biofilm formation by *Propionibacterium acnes* is associated with increased resistance to antimicrobial agents and increased production of putative virulence factors. Res. Microbiol., 2007. 158(4): 386-392.

227. Cerca, N., S. Martins, F. Cerca, K.K. Jefferson, G.B. Pier, R. Oliveira, and J. Azeredo, Comparative assessment of antibiotic susceptibility of coagulase-negative staphylococci in biofilm versus planktonic culture as assessed by bacterial enumeration or rapid XTT colorimetry. J. Antimicrob. Chemoth., 2005. 56(2): 331-336.

228. White, R.L., D.S. Burgess, M. Manduru, and J.A. Bosso, Comparison of three different in vitro methods of detecting synergy: Time-kill, checkerboard, and E test. Antimicrob. Agents Ch., 1996. 40(8): 1914-1918.

229. Smith, K., A. Perez, G. Ramage, C.G. Gemmell, and S. Lang, Comparison of biofilm-associated cell survival following in vitro exposure of meticillin-resistant *Staphylococcus aureus* biofilms to the antibiotics clindamycin, daptomycin, linezolid, tigecycline and vancomycin. Int. J. Antimicrob. Agents, 2009. 33(4): 374-378.

230. Ramage, G., K. Vande Walle, B.L. Wickes, and J.L. López-Ribot, Standardized method for in vitro antifungal susceptibility testing of *Candida albicans* biofilms. Antimicrob. Agents Ch., 2001. 45(9): 2475-2479.

231. Vandenbosch, D., K. Braeckmans, H.J. Nelis, and T. Coenye, Fungicidal activity of miconazole against *Candida* spp. biofilms. J. Antimicrob. Chemoth., 2010. 65(4): 694-700.

232. Pitts, B., M.A. Hamilton, N. Zelver, and P.S. Stewart, A microtiter-plate screening method for biofilm disinfection and removal. J. Microbiol. Methods, 2003. 54(2): 269-276.

233. Shakeri, S., R.K. Kermanshahi, M.M. Moghaddam, and G. Emtiazi, Assessment of biofilm cell removal and killing and biocide efficacy using the microtiter plate test. Biofouling, 2007. 23(2): 79-86.

234. Peeters, E., H.J. Nelis and T. Coenye, Evaluation of the efficacy of disinfection procedures against *Burkholderia cenocepacia* biofilms. J. Hosp. Infect., 2008. 70(4): 361-368.

235. Borges, A., M.J. Saavedra and M. Simões, The activity of ferulic and gallic acids in biofilm prevention and control of pathogenic bacteria. Biofouling, 2012. 28(7): 755-767.

236. Niu, C. and E.S. Gilbert, Colorimetric method for identifying plant essential oil components that affect biofilm formation and structure. Appl. Environ. Microb., 2004. 70(12): 6951-6956.

237. Devienne, K.F. and M.S.G. Raddi, Screening for antimicrobial activity of natural products using a microplate photometer. Braz. J. Microbiol., 2002. 33(2): 166-168.

238. Jagani, S., R. Chelikani and D.S. Kim, Effects of phenol and natural phenolic compounds on biofilm formation by *Pseudomonas aeruginosa.* Biofouling, 2009. 25(4): 321-324.

239. Quave, C.L., L.R.W. Plano, T. Pantuso, and B.C. Bennett, Effects of extracts from Italian medicinal plants on planktonic growth, biofilm formation and adherence of methicillin-resistant *Staphylococcus aureus.* J. Ethnopharmacol., 2008. 118(3): 418-428.

240. Brackman, G., U. Hillaert, S. Van Calenbergh, H.J. Nelis, and T. Coenye, Use of quorum sensing inhibitors to interfere with biofilm formation and development in *Burkholderia multivorans* and *Burkholderia cenocepacia.* Res. Microbiol., 2009. 160(2): 144-151.

241. Nagant, C., M. Tré-Hardy, M. Devleeschouwer, and J.P. Dehaye, Study of the initial phase of biofilm formation using a biofomic approach. J. Microbiol. Methods, 2010. 82(3): 243-248.

242. Crémet, L., S. Corvec, E. Batard, M. Auger, I. Lopez, F. Pagniez, S. Dauvergne, and N. Caroff, Comparison of three methods to study biofilm formation by clinical strains of *Escherichia coli.* Diagn. Microbiol. Infect. Dis., 2012(0).

243. Chavant, P., B. Gaillard-Martinie, R. Talon, M. Hébraud, and T. Bernardi, A new device for rapid evaluation of biofilm formation potential by bacteria. J. Microbiol. Methods, 2007. 68(3): 605-612.

244. Tré-Hardy, M., C. Macé, N. El Manssouri, F. Vanderbist, H. Traore, and M.J. Devleeschouwer, Effect of antibiotic co-administration on young and mature biofilms of cystic fibrosis clinical isolates: the importance of the biofilm model. Int. J. Antimicrob. Agents, 2009. 33(1): 40-45.

245. Ceri, H., M.E. Olson, C. Stremick, R.R. Read, D. Morck, and A. Buret, The Calgary Biofilm Device: New technology for rapid determination of antibiotic susceptibilities of bacterial biofilms. J. Clin. Microbiol., 1999. 37(6): 1771-1776.

246. Ali, L., F. Khambaty and G. Diachenko, Investigating the suitability of the Calgary Biofilm Device for assessing the antimicrobial efficacy of new agents. Bioresour. Technol., 2006. 97(15): 1887-1893.

247. Lewis, K., Riddle of Biofilm Resistance. Antimicrob. Agents Ch., 2001. 45(4): 999-1007.

248. Aaron, S.D., W. Ferris, K. Ramotar, K. Vandemheen, F. Chan, and R. Saginur, Single and combination antibiotic susceptibilities of planktonic adherent, and biofilm-grown *Pseudomonas aeruginosa* isolates cultured from sputa of adults with cystic fibrosis. J. Clin. Microbiol., 2002. 40(11): 4172-4179.

249. Wei, G.X., A.N. Campagna and L.A. Bobek, Effect of MUC7 peptides on the growth of bacteria and on *Streptococcus mutans* biofilm. J. Antimicrob. Chemoth., 2006. 57(6): 1100-1109.

250. Olson, M.E., H. Ceri, D.W. Morck, A.G. Buret, and R.R. Read, Biofilm bacteria: Formation and comparative susceptibility to antibiotics. Can J Vet Res, 2002. 66(2): 86-92.

251. Harrison, J.J., H. Ceri, J. Yerly, C.A. Stremick, Y. Hu, R. Martinuzzi, and R.J. Turner, The use of microscopy and three-dimensional visualization to evaluate the structure of microbial biofilms cultivated in the Calgary biofilm device. Biol Proced Online, 2006. 8(1): 194-213.

252. Jurcisek, J.A., A.C. Dickson, M.E. Bruggeman, and L.O. Bakaletz, In vitro Biofilm Formation in an 8-well Chamber Slide. J Vis Exp, 2011(47): e2481.

253. Nickel, J.C., I. Ruseska, J.B. Wright, and J.W. Costerton, Tobramycin resistance of *Pseudomonas aeruginosa* cells growing as a biofilm on urinary catheter material. Antimicrob. Agents Ch., 1985. 27(4): 619-624.

254. Jass, J., J.W. Costerton and H.M. Lappin-Scott, Assessment of a chemostat-coupled modified Robbins device to study biofilms. J. Ind. Microbiol., 1995. 15(4): 283-289.

255. Ruiz, J.-C., C. Alvarez-Lorenzo, P. Taboada, G. Burillo, E. Bucio, K. De Prijck, H.J. Nelis, T. Coenye, and A. Concheiro, Polypropylene grafted with smart polymers (PNIPAAm/PAAc) for loading and controlled release of vancomycin. European Journal of Pharmaceutics and Biopharmaceutics, 2008. 70(2): 467-477.

256. Nava-Ortiz, C.A.B., G. Burillo, A. Concheiro, E. Bucio, N. Matthijs, H. Nelis, T. Coenye, and C. Alvarez-Lorenzo, Cyclodextrin-functionalized biomaterials loaded with miconazole prevent *Candida albicans* biofilm formation in vitro. Acta Biomater., 2010. 6(4): 1398-1404.

257. Prijck, K., N. Smet, K. Honraet, S. Christiaen, T. Coenye, E. Schacht, and H. Nelis, Inhibition of *Candida albicans* Biofilm Formation by Antimycotics Released from Modified Polydimethyl Siloxane. Mycopathologia, 2010. 169(3): 167-174.

258. Honraet, K. and H.J. Nelis, Use of the modified robbins device and fluorescent staining to screen plant extracts for the inhibition of *S. mutans* biofilm formation. J. Microbiol. Methods, 2006. 64(2): 217-224.

259. Raad, I., H. Hanna, T. Dvorak, G. Chaiban, and R. Hachem, Optimal antimicrobial catheter lock solution, using different combinations of minocycline, EDTA, and 25-percent ethanol, rapidly eradicates organisms embedded in biofilm. Antimicrob. Agents Ch., 2007. 51(1): 78-83.

260. Krom, B.P., K. Buijssen, H.J. Busscher, and H.C. Van Der Mei, *Candida* biofilm analysis in the artificial throat using fisH. 2009. p. 45-54.

261. Oosterhof, J.J.H., K.J.D.A. Buijssen, H.J. Busscher, B.F.A.M. van der Laan, and H.C. van der Mei, Effects of Quaternary Ammonium Silane Coatings on Mixed Fungal and Bacterial Biofilms on Tracheoesophageal Shunt Prostheses. Appl. Environ. Microb., 2006. 72(5): 3673-3677.

262. Goeres, D.M., M.A. Hamilton, N.A. Beck, K. Buckingham-Meyer, J.D. Hilyard, L.R. Loetterle, L.A. Lorenz, D.K. Walker, and P.S. Stewart, A method for growing a biofilm under low

shear at the air-liquid interface using the drip flow biofilm reactor. Nature protocols, 2009. 4(5): 783-788.

263. Xu, K.D., P.S. Stewart, F. Xia, C.T. Huang, and G.A. McFeters, Spatial physiological heterogeneity in *Pseudomonas aeruginosa* biofilm is determined by oxygen availability. Appl. Environ. Microb., 1998. 64(10): 4035-4039.

264. Huang, C.T., K.D. Xu, G.A. McFeters, and P.S. Stewart, Spatial patterns of alkaline phosphatase expression within bacterial colonies and biofilms in response to phosphate starvation. Appl. Environ. Microb., 1998. 64(4): 1526-1531.

265. Curtin, J.J. and R.M. Donlan, Using bacteriophages to reduce formation of catheter-associated biofilms by *Staphylococcus epidermidis.* Antimicrob. Agents Ch., 2006. 50(4): 1268-1275.

266. Adams, H., M.T. Winston, J. Heersink, K.A. Buckingham-Meyer, J.W. Costerton, and P. Stoodley, Development of a laboratory model to assess the removal of biofilm from interproximal spaces by powered tooth brushing. American journal of dentistry, 2002. 15 Spec No: 12B-17B.

267. Stewart, P.S., J. Rayner, F. Roe, and W.M. Rees, Biofilm penetration and disinfection efficacy of alkaline hypochlorite and chlorosulfamates. J. Appl. Microbiol., 2001. 91(3): 525-532.

268. Buckingham-Meyer, K., D.M. Goeres and M.A. Hamilton, Comparative evaluation of biofilm disinfectant efficacy tests. J. Microbiol. Methods, 2007. 70(2): 236-244.

269. Ferreira, C., R. Rosmaninho, M. Simões, M.C. Pereira, M.M.S.M. Bastos, O.C. Nunes, M. Coelho, and L.F. Melo, Biofouling control using microparticles carrying a biocide. Biofouling, 2010. 26(2): 205-212.

270. Pereira, M.O., M. Simões, S.M.O. Machado, and M.J. Vieira. 2006. Role of benzalkonium chloride surface preconditioning in the increased resistance of biofilms to removal and disinfection. In: International Conference Biofilm Systems. M.C.M.v. Loosdrecht, ed. Amsterdam

271. Coenye, T. and H.J. Nelis, In vitro and in vivo model systems to study microbial biofilm formation. J. Microbiol. Methods, 2010. 83(2): 89-105.

272. Williams, D.L. and R.D. Bloebaum, Observing the biofilm matrix of S*taphylococcus epidermidis* ATCC 35984 grown using the CDC biofilm reactor. Microsc. Microanal., 2010. 16(2): 143-152.

273. Williams, D.L., K.L. Woodbury, B.S. Haymond, A.E. Parker, and R.D. Bloebaum, A modified CDC biofilm reactor to produce mature biofilms on the surface of PEEK membranes for an in vivo animal model application. Curr. Microbiol., 2011. 62(6): 1657-1663.

274. Goeres, D.M., L.R. Loetterle, M.A. Hamilton, R. Murga, D.W. Kirby, and R.M. Donlan, Statistical assessment of a laboratory method for growing biofilms. Microbiology, 2005. 151(3): 757-762.

275. Garo, E., G.R. Eldridge, M.G. Goering, E.D. Pulcini, M.A. Hamilton, J.W. Costerton, and G.A. James, Asiatic Acid and Corosolic Acid Enhance the Susceptibility of *Pseudomonas aeruginosa* Biofilms to Tobramycin. Antimicrob. Agents Ch., 2007. 51(5): 1813-1817.

276. Hadi, R., K. Vickery, A. Deva, and T. Charlton, Biofilm removal by medical device cleaners: comparison of two bioreactor detection assays. J. Hosp. Infect., 2010. 74(2): 160-167.

277. Nailis, H., R. Vandenbroucke, K. Tilleman, D. Deforce, H. Nelis, and T. Coenye, Monitoring ALS1 and ALS3 gene expression during in vitro *Candida albicans* biofilm formation under continuous flow conditions. Mycopathologia, 2009. 167(1): 9-17.

278. Gjaltema, A., P.A.M. Arts, M.C.M. Van Loosdrecht, J.G. Kuenen, and J.J. Heijnen, Heterogeneity of biofilms in rotating annular reactors: Occurrence, structure, and consequences. Biotechnol. Bioeng., 1994. 44(2): 194-204.

279. Ochoa, J.-C., C. Coufort, R. Escudié, A. Liné, and E. Paul, Influence of non-uniform distribution of shear stress on aerobic biofilms. Chem. Eng. Sci., 2007. 62(14): 3672-3684.

280. Lawrence, J.R., G.D.W. Swerhone and T.R. Neu, A simple rotating annular reactor for replicated biofilm studies. J. Microbiol. Methods, 2000. 42(3): 215-224.

281. Pintar, K.D.M. and R.M. Slawson, Effect of temperature and disinfection strategies on ammonia-oxidizing bacteria in a bench-scale drinking water distribution system. Water Res., 2003. 37(8): 1805-1817.

282. Ndiongue, S., P.M. Huck and R.M. Slawson, Effects of temperature and biodegradable organic matter on control of biofilms by free chlorine in a model drinking water distribution system. Water Res., 2005. 39(6): 953-964.

283. Szabo, J.G., E.W. Rice and P.L. Bishop, Persistence and Decontamination of *Bacillus atrophaeus* subsp. *globigii* Spores on Corroded Iron in a Model Drinking Water System. Appl. Environ. Microb., 2007. 73(8): 2451-2457.

284. Packroff, G., J.R. Lawrence and T.R. Neu, In situ confocal laser scanning microscopy of protozoans in cultures and complex biofilm communities. Acta Protozool., 2002. 41(3): 245-253.

285. Declerck, P., J. Behets, A. Margineanu, V. van Hoef, B. De Keersmaecker, and F. Ollevier, Replication of *Legionella pneumophila* in biofilms of water distribution pipes. Microbiol. Res., 2009. 164(6): 593-603.

286. Noui-Mehidi, M.N., Transition in the flow between conical cylinders. Exp. Fluids, 2001. 30(1): 84-87.

287. Willcock, L., P. Gilbert, J. Holah, G. Wirtanen, and D.G. Allison, A new technique for the performance evaluation of clean-in-place disinfection of biofilms. J. Ind. Microbiol. Biotechnol., 2000. 25(5): 235-241.

288. Schwartz, K., R. Stephenson, M. Hernandez, N. Jambang, and B.R. Boles, The use of drip flow and rotating disk reactors for *Staphylococcus aureus* biofilm analysis. J Vis Exp, 2010(46).

289. Teitzel, G.M. and M.R. Parsek, Heavy metal resistance of biofilm and planktonic *Pseudomonas aeruginosa.* Appl. Environ. Microb., 2003. 69(4): 2313-2320.

290. Hentzer, M., G.M. Teitzel, G.J. Balzer, A. Heydorn, S. Molin, M. Givskov, and M.R. Parsek, Alginate overproduction affects *Pseudomonas aeruginosa* biofilm structure and function. J. Bacteriol., 2001. 183(18): 5395-5401.

291. Cotter, J.J., J.P. O'Gara, D. Mack, and E. Casey, Oxygen-mediated regulation of biofilm development is controlled by the alternative sigma Factor σB in *Staphylococcus epidermidis.* Appl. Environ. Microb., 2009. 75(1): 261-264.

292. Komlos, J., A.B. Cunningham, A.K. Camper, and R.R. Sharp, Interaction of *Klebsiella oxytoca* and *Burkholderia cepacia* in Dual-Species Batch Cultures and Biofilms as a Function of Growth Rate and Substrate Concentration. Microb. Ecol., 2005. 49(1): 114-125.

293. Murga, R., T.S. Forster, E. Brown, J.M. Pruckler, B.S. Fields, and R.M. Donlan, Role of biofilms in the survival of *Legionella pneumophila* in a model potable-water system. Microbiology, 2001. 147(11): 3121-3126.

294. Batté, M., B.M.R. Appenzeller, D. Grandjean, S. Fass, V. Gauthier, F. Jorand, L. Mathieu, M. Boualam, S. Saby, and J.C. Block, Biofilms in drinking water distribution systems. Reviews in Environmental Science and Biotechnology, 2003. 2(2-4): 147-168.

295. Grandjean, D., S. Fass, D. Tozza, J. Cavard, V. Lahoussine, S. Saby, H. Guilloteau, and J.C. Block, Coliform culturability in over- versus undersaturated drinking waters. Water Res., 2005. 39(9): 1878-1886.

296. Appenzeller, B.M.R., M. Batté, L. Mathieu, J.C. Block, V. Lahoussine, J. Cavard, and D. Gatel, Effect of adding phosphate to drinking water on bacterial growth in slightly and highly corroded pipes. Water Res., 2001. 35(4): 1100-1105.

297. Lehtola, M.J., E. Torvinen, I.T. Miettinen, and C.W. Keevil, Fluorescence in situ hybridization using peptide nucleic acid probes for rapid detection of *Mycobacterium avium* subsp. *avium* and *Mycobacterium avium* subsp. *paratuberculosis* in potable-water biofilms. Appl. Environ. Microb., 2006. 72(1): 848-853.

298. Simões, L.C., M. Simões and M.J. Vieira, A comparative study of drinking water biofilm monitoring with flow cell and Propella™ bioreactors. 2012. p. 334-342.

299. Manuel, C.M.D., Biofilm Dynamics and Drinking Water Stability: Effects of Hydrodynamics and Surface Materials, in Department of Chemical Engineering. 2007. Universidade do Porto - Faculdade de Engenharia.

300. Pereira, M.O., P. Morin, M.J. Vieira, and L.F. Melo, A versatile reactor for continuous monitoring of biofilm properties in laboratory and industrial conditions. Lett. Appl. Microbiol., 2002. 34(1): 22-6.

301. Teodósio, J.S., M. Simões, M.A. Alves, L.F. Melo, and F.J. Mergulhão, Setup and validation of flow cell systems for biofouling simulation in industrial settings. Scientific World Journal, 2012. 2012.

302. Simões, M., L.C. Simões and M.J. Vieira, Physiology and behavior of *Pseudomonas fluorescens* single and dual strain biofilms under diverse hydrodynamics stresses. Int. J. Food Microbiol., 2008. 128(2): 309-316.

303. Simões, L.C., N. Azevedo, A. Pacheco, C.W. Keevil, and M.J. Vieira, Drinking water biofilm assessment of total and culturable bacteria under different operating conditions. Biofouling, 2006. 22(1-2): 91-9.

304. Teodósio, J.S., M. Simões, L.F. Melo, and F.J. Mergulhão, Flow cell hydrodynamics and their effects on *E. coli* biofilm formation under different nutrient conditions and turbulent flow. Biofouling, 2011. 27(1): 1-11.

305. Simões, M., M.O. Pereira and M.J. Vieira, Monitoring the effects of biocide treatment of *Pseudomonas fluorescens* biofilms formed under different flow regimes. 2003. p. 217-223.

306. Simões, M., M.O. Pereira and M.J. Vieira, Action of a cationic surfactant on the activity and removal of bacterial biofilms formed under different flow regimes. Water Research, 2005. 39(2-3): 478-486.

307. Hamilton, M., J. Heersink, K. Buckingham-Meyer, and D. Goeres, The biofilm laboratory: step-by-step protocols for experimental design, analysis, and data interpretation, ed. M. Hamilton, et al. 2003, Bozeman, Montana, USA: Cytergy Publishing.

308. Lewandowski, Z., H. Beyenal and D. Stookey, Reproducibility of biofilm processes and the meaning of steady state in biofilm reactors. Water Sci. Technol., 2004. 49(11-12): 359-364.

309. Dogan, B. and K.J. Boor, Genetic diversity and spoilage potentials among *Pseudomonas* spp. isolated from fluid milk products and dairy processing plants. Appl. Environ. Microb., 2003. 69(1): 130-138.

310. Kreske, A.C., J.H. Ryu, C.A. Pettigrew, and L.R. Beuchat, Lethality of chlorine, chlorine dioxide, and a commercial produce sanitizer to *Bacillus cereus* and *Pseudomonas* in a liquid detergent, on stainless steel, and in biofilm. J. Food Protect., 2006. 69(11): 2621-2634.

311. Peng, J.S., W.C. Tsai and C.C. Chou, Inactivation and removal of *Bacillus cereus* by sanitizer and detergent. Int. J. Food Microbiol., 2002. 77(1-2): 11-18.

312. Simões, M., L.C. Simões and M.J. Vieira, Species association increases biofilm resistance to chemical and mechanical treatments. Water Res., 2009. 43(1): 229-237.

313. Simões, M., M.O. Pereira, I. Machado, L.C. Simões, and M.J. Vieira, Comparative antibacterial potential of selected aldehyde-based biocides and surfactants against planktonic *Pseudomonas fluorescens.* J. Ind. Microbiol. Biotechnol., 2006. 33(9): 741-749.

314. Simões, M., R.N. Bennett and E.A. Rosa, Understanding antimicrobial activities of phytochemicals against multidrug resistant bacteria and biofilms. Natural product reports, 2009. 26(6): 746-757.

315. Casey, J.T., C. O'Cleirigh, P.K. Walsh, and D.G. O'Shea, Development of a robust microtiter plate-based assay method for assessment of bioactivity. J. Microbiol. Methods, 2004. 58(3): 327-334.

316. Sperandio, V., A.G. Torres and J.B. Kaper, Quorum sensing *Escherichia coli* regulators B and C (QseBC): A novel two-component regulatory system involved in the regulation of flagella and motility by quorum sensing in *E. coli.* Mol. Microbiol., 2002. 43(3): 809-821.

317. Busscher, H.J., A.H. Weerkamp and H.C. van Der Mei, Measurement of the surface free energy of bacterial cell surfaces and its relevance for adhesion. Appl. Environ. Microb., 1984. 48(5): 980-983.

318. Simões, M., L.C. Simões, S. Cleto, I. Machado, M.O. Pereira, and M.J. Vieira, Antimicrobial mechanisms of *ortho*-phthalaldehyde action. J. Basic Microb., 2007. 47(3): 230-242.

319. Janczuk, B., E. Chibowski, J.M. Bruque, M.L. Kerkeb, and F.G. Caballero, On the consistency of surface free energy components as calculated from contact angles of different liquids: an application to the cholesterol surface. J. Colloid Interf. Sci., 1993. 159(2): 421-428.

320. van Oss, C.J., M.K. Chaudhury and R.J. Good, Monopolar surfaces. Adv Colloid Interfac, 1987. 28(C): 35-64.

321. van Oss, C.J., M.K. Chaudhury and R.J. Good, Interfacial Lifshitz-van der Waals and polar interactions in macroscopic systems. Chem. Rev., 1988. 88(6): 927-941.

322. van Oss, C.J., L. Ju, M.K. Chaudhury, and R.J. Good, Estimation of the polar parameters of the surface tension of liquids by contact angle measurements on gels. J. Colloid Interf. Sci., 1989. 128(2): 313-319.

323. Simões, M., L.C. Simões, S. Cleto, M.O. Pereira, and M.J. Vieira, The effects of a biocide and a surfactant on the detachment of *Pseudomonas fluorescens* from glass surfaces. Int. J. Food Microbiol., 2008. 121(3): 335-341.

324. Bauer, A.W., W.M. Kirby, J.C. Sherris, and M. Turck, Antibiotic susceptibility testing by a standardized single disk method. Am J Clin Pathol, 1966. 45(4): 493-6.

325. McLean, R.J.C., L.S. Pierson Iii and C. Fuqua, A simple screening protocol for the identification of quorum signal antagonists. J. Microbiol. Methods, 2004. 58(3): 351-360.

326. Zahin, M., S. Hasan, F. Aqil, M.S.A. Khan, F.M. Husain, and I. Ahmad, Screening of certain medicinal plants from India for their anti-quorum sensing activity. Indian J. Exp. Biol., 2010. 48(12): 1219-1224.

327. Simões, L.C., M. Simões and M.J. Vieira, Influence of the diversity of bacterial isolates from drinking water on resistance of biofilms to disinfection. Appl. Environ. Microb., 2010. 76(19): 6673-6679.

328. Johnston, M.D., R.J.W. Lambert, G.W. Hanlon, and S.P. Denyer, A rapid method for assessing the suitability of quenching agents for individual biocides as well as combinations. J. Appl. Microbiol., 2002. 92(4): 784-789.

329. Saby, S., I. Sibille, L. Mathieu, J.L. Paquin, and J.C. Block, Influence of water chlorination on the counting of bacteria with DAPI (4',6-diamidino-2-phenylindole). Appl. Environ. Microb., 1997. 63(4): 1564-9.

330. Sandberg, M.E., D. Schellmann, G. Brunhofer, T. Erker, I. Busygin, R. Leino, P.M. Vuorela, and A. Fallarero, Pros and cons of using resazurin staining for quantification of viable *Staphylococcus aureus* biofilms in a screening assay. J. Microbiol. Methods, 2009. 78(1): 104-106.

331. Guerin, T.F., M. Mondido, B. McClenn, and B. Peasley, Application of resazurin for estimating abundance of contaminant-degrading micro-organisms. Lett. Appl. Microbiol., 2001. 32(5): 340-5.

332. Simões, M., M.O. Pereira and M.J. Vieira, Effect of mechanical stress on biofilms challenged by different chemicals. Water Res., 2005. 39(20): 5142-5152.

333. Geankoplis, C.J., ed. *Transport Processes and Unit Operations*. third ed. ed. 1993, Prentice-Hall International, Inc: New Jersey.

334. Perry, R.H. and D.W. Green, eds. *Perry's Chemical Engineers' Handbook*. 7th ed. 1999, McGraw-Hill Professional Publishing: New York.

335. Gabe, D.R. and F.C. Walsh, The rotating cylinder electrode: a review of development. J. Appl. Electrochem., 1983. 13(1): 3-21.

336. APHA, AWWA and WPCF, Standard Methods for the Examination of Water and Wastewater, 17th ed. 1989. American Public Health Association, Washington, DC.

337. Melo, L.F. and T.R. Bott, Biofouling in water systems. Exp. Therm Fluid Sci., 1997. 14(4): 375-381.

338. Frølund, B., R. Palmgren, K. Keiding, and P.H. Nielsen, Extraction of extracellular polymers from activated sludge using a cation exchange resin. Water Res., 1996. 30(8): 1749-1758.

339. Lowry, O.H., N.J. Rosebrough, A.L. Farr, and R.J. Randall, Protein measurement with the Folin phenol reagent. J. Biol. Chem., 1951. 193(1): 265-275.

340. Peterson, G.L., Review of the Folin phenol protein quantitation method of Lowry, Rosebrough, Farr and Randall. Anal. Biochem., 1979. 100(2): 201-220.

341. Dubois, M., K.A. Gilles, J.K. Hamilton, P.A. Rebers, and F. Smith, Colorimetric method for determination of sugars and related substances. Anal. Chem., 1956. 28(3): 350-356.

342. Tuladhar, T.R., W.R. Paterson, N. Macleod, and D.I. Wilson, Development of a novel non-contact proximity gauge for thickness measurement of soft deposits and its application in fouling studies. Can J Chem Eng, 2000. 78(5): 935-947.

343. Simões, M., L.C. Simões and M.J. Vieira, A review of current and emergent biofilm control strategies. LWT - Food Sci. Technol., 2010. 43(4): 573-583.

344. Furiga, A., A. Lonvaud-Funel, G. Dorignac, and C. Badet, In vitro anti-bacterial and anti-adherence effects of natural polyphenolic compounds on oral bacteria. J. Appl. Microbiol., 2008. 105(5): 1470-1476.

345. Tajkarimi, M.M., S.A. Ibrahim and D.O. Cliver, Antimicrobial herb and spice compounds in food. Food Control, 2010. 21(9): 1199-1218.

346. Oussalah, M., S. Caillet, L. Saucier, and M. Lacroix, Inhibitory effects of selected plant essential oils on the growth of four pathogenic bacteria: *E. coli* O157:H7, *Salmonella Typhimurium*, *Staphylococcus aureus* and *Listeria monocytogenes.* Food Control, 2007. 18(5): 414-420.

347. Sandasi, M., C.M. Leonard and A.M. Viljoen, The effect of five common essential oil components on *Listeria monocytogenes* biofilms. Food Control, 2008. 19(11): 1070-1075.

348. Cushnie, T.P.T. and A.J. Lamb, Antimicrobial activity of flavonoids. Int. J. Antimicrob. Agents, 2005. 26(5): 343-356.

349. Vaquero, M.J.R., M.R. Alberto and M.C.M. de Nadra, Antibacterial effect of phenolic compounds from different wines. Food Control, 2007. 18(2): 93-101.

350. Robbins, R.J., Phenolic acids in foods: An overview of analytical methodology. J. Agric. Food. Chem., 2003. 51(10): 2866-2887.

351. Ergün, B.C., T. Coban, F.K. Onurdag, and E. Banoglu, Synthesis, antioxidant and antimicrobial evaluation of simple aromatic esters of ferulic acid. Arch. Pharmacal Res., 2011. 34(8): 1251-61.

352. Lin, F.H., J.Y. Lin, R.D. Gupta, J.A. Tournas, J.A. Burch, M.A. Selim, N.A. Monteiro-Riviere, J.M. Grichnik, J. Zielinski, and S.R. Pinnell, Ferulic acid stabilizes a solution of vitamins C and E and doubles its photoprotection of skin. The Journal of investigative dermatology, 2005. 125(4): 826-32.

353. Phan, T.T., L. Wang, P. See, R.J. Grayer, S.Y. Chan, and S.T. Lee, Phenolic compounds of *Chromolaena odorata* protect cultured skin cells from oxidative damage: implication for cutaneous wound healing. Biol. Pharm. Bull., 2001. 24(12): 1373-9.

354. Teichberg, S., B.F. Farber, A.G. Wolff, and B. Roberts, Salicylic acid decreases extracellular biofilm production by *Staphylococcus epidermidis*: electron microscopic analysis. The Journal of infectious diseases, 1993. 167(6): 1501-3.

355. Ferreira, C., A.M. Pereira, M.C. Pereira, L.F. Melo, and M. Simões, Physiological changes induced by the quaternary ammonium compound benzyldimethyldodecylammonium chloride on *Pseudomonas fluorescens.* J. Antimicrob. Chemoth., 2011. 66(5): 1036-43.

356. Cowan, M.M., Plant products as antimicrobial agents. Clin. Microbiol. Rev., 1999. 12(4): 564-582.

357. Abreu, A.C., A.J. McBain and M. Simoes, Plants as sources of new antimicrobials and resistance-modifying agents. Natural Product Reports, 2012. 29(9): 1007-1021.

358. Ferreira, C., A.M. Pereira, M.C. Pereira, L.F. Melo, and M. Simoes, Physiological changes induced by the quaternary ammonium compound benzyldimethyldodecylammonium chloride on *Pseudomonas fluorescens.* J Antimicrob Chemother, 2011. 66(5): 1036-43.

359. Fernández, M.A., M.D. García and M.T. Sáenz, Antibacterial activity of the phenolic acids fractions of *Scrophularia frutescens* and *Scrophularia sambucifolia.* J. Ethnopharmacol., 1996. 53(1): 11-14.

360. Puupponen-Pimiä, R., L. Nohynek, C. Meier, M. Kähkönen, M. Heinonen, A. Hopia, and K.M. Oksman-Caldentey, Antimicrobial properties of phenolic compounds from berries. J. Appl. Microbiol., 2001. 90(4): 494-507.

361. Harshey, R.M., Bacterial motility on a surface: many ways to a common goal. 2003. 57: 249-273.

362. Shapiro, J.A., Thinking about bacterial populations as multicellular organisms. Annu. Rev. Microbiol., 1998. 52: 81-104.

363. Karatan, E. and P. Watnick, Signals, regulatory networks, and materials that build and break bacterial biofilms. Microbiol. Mol. Biol. Rev., 2009. 73(2): 310-+.

364. Houry, A., R. Briandet, S. Aymerich, and M. Gohar, Involvement of motility and flagella in *Bacillus cereus* biofilm formation. Microbiology, 2010. 156(4): 1009-1018.

365. Muller, E., J. Al-Attar, A.G. Wolff, and B.F. Farber, Mechanism of salicylate-mediated inhibition of biofilm in *Staphylococcus epidermidis.* J. Infect. Dis., 1998. 177(2): 501-503.

366. Farber, B.F. and A.G. Wolff, Salicylic acid prevents the adherence of bacteria and yeast to silastic catheters. J. Biomed. Mater. Res., 1993. 27(5): 599-602.

367. An, Y.H. and R.J. Friedman, Concise review of mechanisms of bacterial adhesion to biomaterial surfaces. J. Biomed. Mater. Res., 1998. 43(3): 338-348.

368. Machado, I., J. Graca, A.M. Sousa, S.P. Lopes, and M.O. Pereira, Effect of antimicrobial residues on early adhesion and biofilm formation by wild-type and benzalkonium chloride-adapted *Pseudomonas aeruginosa.* Biofouling, 2011. 27(10): 1151-1159.

369. Landini, P., D. Antoniani, J.G. Burgess, and R. Nijland, Molecular mechanisms of compounds affecting bacterial biofilm formation and dispersal. Appl. Microbiol. Biotechnol., 2010. 86(3): 813-23.

370. Bjarnsholt, T., P.O. Jensen, M. Burmolle, M. Hentzer, J.A.J. Haagensen, H.P. Hougen, H. Calum, K.G. Madsen, C. Moser, S. Molin, N. Hoiby, and M. Givskov, *Pseudomonas aeruginosa* tolerance to tobramycin, hydrogen peroxide and polymorphonuclear leukocytes is quorum-sensing dependent. Microbiology, 2005. 151: 373-383.

371. Campos, F.M., J.A. Couto and T.A. Hogg, Influence of phenolic acids on growth and inactivation of *Oenococcus oeni* and *Lactobacillus hilgardii.* J. Appl. Microbiol., 2003. 94(2): 167-174.

372. Prithiviraj, B., H.P. Bais, T. Weir, B. Suresh, E.H. Najarro, B.V. Dayakar, H.P. Schweizer, and J.M. Vivanco, Down regulation of virulence factors of *Pseudomonas aeruginosa* by salicylic acid attenuates its virulence on *Arabidopsis thaliana* and *Caenorhabditis elegans.* Infect. Immun., 2005. 73(9): 5319-5328.

373. Nowatzki, P.J., R.R. Koepsel, P. Stoodley, K. Min, A. Harper, H. Murata, J. Donfack, E.R. Hortelano, G.D. Ehrlich, and A.J. Russell, Salicylic acid-releasing polyurethane acrylate polymers as anti-biofilm urological catheter coatings. Acta Biomater., 2012. 8(5): 1869-80.

374. Rosenberg, L.E., A.L. Carbone, U. Romling, K.E. Uhrich, and M.L. Chikindas, Salicylic acid-based poly(anhydride esters) for control of biofilm formation in *Salmonella enterica* serovar Typhimurium. Lett. Appl. Microbiol., 2008. 46(5): 593-599.

375. Bittner, S., When quinones meet amino acids: Chemical, physical and biological consequences. Amino Acids, 2006. 30(3 SPEC. ISS.): 205-224.

376. Bridier, A., R. Briandet, V. Thomas, and F. Dubois-Brissonnet, Resistance of bacterial biofilms to disinfectants: a review. Biofouling, 2011. 27(9): 1017-1032.

377. Mah, T.F.C. and G.A. O'Toole, Mechanisms of biofilm resistance to antimicrobial agents. Trends Microbiol., 2001. 9(1): 34-39.

378. Pechaud, Y., C.E. Marcato-Romain, E. Girbal-Neuhauser, I. Queinnec, Y. Bessiere, and E. Paul, Combining hydrodynamic and enzymatic treatments to improve multi-species thick biofilm removal. Chem. Eng. Sci., 2012. 80(0): 109-118.

379. Simões, M., L.C. Simoes, M.O. Pereira, and M.J. Vieira, Antagonism between *Bacillus cereus* and *Pseudomonas fluorescens* in planktonic systems and in biofilms. Biofouling, 2008. 24(5): 339-349.

380. Zacheus, O.M., E.K. Iivanainen, T.K. Nissinen, M.J. Lehtola, and P.J. Martikainen, Bacterial biofilm formation on polyvinyl chloride, polyethylene and stainless steel exposed to ozonated water. Water Res., 2000. 34(1): 63-70.

381. Matsuura, K., Y. Asano, A. Yamada, and K. Naruse, Detection of *Micrococcus Luteus* biofilm formation in microfluidic environments by pH measurement using an ion-sensitive field-effect transistor. Sensors (Switzerland), 2013. 13(2): 2484-2493.

382. Reedy, C.R., C.W. Price, J. Sniegowski, J.P. Ferrance, M. Begley, and J.P. Landers, Solid phase extraction of DNA from biological samples in a post-based, high surface area poly(methyl methacrylate) (PMMA) microdevice. Lab on a chip, 2011. 11(9): 1603-11.

383. Gottenbos, B., H.C. van der Mei and H.J. Busscher, Initial adhesion and surface growth of *Staphylococcus epidermidis* and *Pseudomonas aeruginosa* on biomedical polymers. J. Biomed. Mater. Res., 2000. 50(2): 208-214.

384. Bruinsma, G.M., M. Rustema-Abbing, H.C. van der Mei, and H.J. Busscher, Effects of cell surface damage on surface properties and adhesion of *Pseudomonas aeruginosa.* J. Microbiol. Methods, 2001. 45(2): 95-101.

385. Bos, R., H.C. Van Der Mei and H.J. Busscher, Physico-chemistry of initial microbial adhesive interactions - Its mechanisms and methods for study. FEMS Microbiol. Rev., 1999. 23(2): 179-229.

386. Geoghegan, M., J.S. Andrews, C.A. Biggs, K.E. Eboigbodin, D.R. Elliott, S. Rolfe, J. Scholes, J.J. Ojeda, M.E. Romero-González, R.G.J. Edyvean, L. Swanson, R. Rutkaite, R. Fernando, Y. Pen, Z. Zhang, and S.A. Banwart, The polymer physics and chemistry of microbial cell attachment and adhesion. Faraday Discuss., 2008. 139: 85-103.

387. Eboigbodin, K.E., J.J. Odeja and C.A. Biggs, Investigating the surface properties of *Escherichia coli* under glucose controlled conditions and its effect on aggregation. Langmuir, 2007. 23: 6691–6692.

388. van Loosdrecht, M.C., J. Lyklema, W. Norde, G. Schraa, and A.J. Zehnder, The role of bacterial cell wall hydrophobicity in adhesion. Appl. Environ. Microb., 1987. 53(8): 1893-7.

389. Bellon-Fontaine, M.N., N. Mozes, H.C. van der Mei, J. Sjollema, O. Cerf, P.G. Rouxhet, and H.J. Busscher, A comparison of thermodynamic approaches to predict the adhesion of dairy microorganisms to solid substrata. Cell Biophysics, 1990. 17(1): 93-106.

390. Cloete, T.E., Resistance mechanisms of bacteria to antimicrobial compounds. Int. Biodeter. Biodegr., 2003. 51(4): 277-282.

391. Hermansson, M., The DLVO theory in microbial adhesion. Colloids Surf. B. Biointerfaces, 1999. 14(1–4): 105-119.

392. Katsikogianni, M. and Y.F. Missirlis, Concise review of mechanisms of bacterial adhesion to biomaterials and of techniques used in estimating bacteria-material interactions. European Cells and Materials, 2004. 8: 37-57.

393. Bullitt, E. and L. Makowski, Structural polymorphism of bacterial adhesion pili. Nature, 1995. 373(6510): 164-167.

394. Thomas, W.E., L.M. Nilsson, M. Forero, E.V. Sokurenko, and V. Vogel, Shear-dependent 'stick-and-roll' adhesion of type 1 fimbriated *Escherichia coli.* Mol. Microbiol., 2004. 53(5): 1545-1557.

395. Ortega-Morales, B.O., J.L. Santiago-García, M.J. Chan-Bacab, X. Moppert, E. Miranda-Tello, M.L. Fardeau, J.C. Carrero, P. Bartolo-Pérez, A. Valadéz-González, and J. Guezennec, Characterization of extracellular polymers synthesized by tropical intertidal biofilm bacteria. J. Appl. Microbiol., 2007. 102(1): 254-264.

396. Andersson, S., G. Dalhammar and G. Kuttuva Rajarao, Influence of microbial interactions and EPS/polysaccharide composition on nutrient removal activity in biofilms formed by strains found in wastewater treatment systems. Microbiol. Res., 2011. 166(6): 449-457.

397. Melo, L.F., Biofilm physical structure, internal diffusivity and tortuosity. Water Sci. Technol., 2005. 52(7): 77-84.

398. Araújo, P.A., M. Lemos, F. Mergulhão, L. Melo, and M. Simões, The Influence of Interfering Substances on the Antimicrobial Activity of Selected Quaternary Ammonium Compounds. Int. J. Food Sci., 2013. 2013: 9.

399. Campanac, C., L. Pineau, A. Payard, G. Baziard-Mouysset, and C. Roques, Interactions between biocide cationic agents and bacterial biofilms. Antimicrob. Agents Ch., 2002. 46(5): 1469-1474.

400. Zhang, T.C. and P.L. Bishop, Density, porosity, and pore structure of biofilms. Water Res., 1994. 28(11): 2267-2277.

401. Allison, D.G., The biofilm matrix. Biofouling, 2003. 19(2): 139-150.

402. Flemming, H.C., The forces that keep biofilms together. Int. Biodeterior. Biodegrad., 1996. 133: 311–317.

403. Giaouris E, Chorianopoulos N, Doulgeraki A, and N. G-J, Co-culture with *Listeria monocytogenes* within a dual-species biofilm community strongly increases resistance of *Pseudomonas putida* to benzalkonium chloride. PLoS ONE 2013. 8(10): e77276.

404. Lindsay, D., V.S. Brözel, J.F. Mostert, and A. Von Holy, Differential efficacy of a chlorine dioxide-containing sanitizer against single species and binary biofilms of a dairy-associated Bacillus cereus and a Pseudomonas fluorescens isolate. J. Appl. Microbiol., 2002. 92(2): 352-361.

405. Araújo, P.A., F. Mergulhão, L. Melo, and M. Simões, The ability of an antimicrobial agent to penetrate a biofilm is not correlated with its killing or removal efficiency. Biofouling, 2014. 30(6): 675-683.

406. Chen, X. and P.S. Stewart, Biofilm removal caused by chemical treatments. Water Res., 2000. 34(17): 4229-4233.

407. Lee, M.J., J.H. Ha, Y.S. Kim, J.H. Ryu, and S.D. Ha, Reduction of *Bacillus cereus* contamination in biofilms on stainless steel surfaces by application of sanitizers and commercial detergent. J. Korean Soc. Appl. Bi., 2010. 53(1): 89-93.

408. Cloete, T.E., D. Westaard and S.J. Van Vuuren, Dynamic response of biofilm to pipe surface and fluid velocity. Water Sci. Technol., 2003. 47(5): 57-59.

409. Derlon, N., A. Massé, R. Escudié, N. Bernet, and E. Paul, Stratification in the cohesion of biofilms grown under various environmental conditions. Water Res., 2008. 42(8-9): 2102-2110.

410. Jensen, B.B.B. and A. Friis, Predicting the cleanability of mix-proof valves by use of wall shear stress. J. Food Process Eng., 2005. 28(2): 89-106.

411. Gomes, I.B., M. Simões and L.C. Simões, An overview on the reactors to study drinking water biofilms. Water Res., 2014. 62(0): 63-87.

412. Faille, C., T. Bénézech, G. Midelet-Bourdin, Y. Lequette, M. Clarisse, G. Ronse, A. Ronse, and C. Slomianny, Sporulation of *Bacillus* spp. within biofilms: A potential source of contamination in food processing environments. Food Microbiol., 2014. 40(0): 64-74.

413. Blel, W., P. Legentilhomme, J. Legrand, T. Bénézech, and C.L. Gentil-Lelièvre, Hygienic design: Effect of hydrodynamics on the cleanability of a food processing line. AIChE J., 2008. 54(10): 2553-2566.

414. van Loosdrecht, M.C.M., D. Eikelboom, A. Gjaltema, A. Mulder, L. Tijhuis, and J.J. Heijnen, Biofilm structures. Water Sci. Technol., 1995. 32(8): 35-43.

415. Coufort, C., N. Derlon, J. Ochoa-Chaves, A. Liné, and E. Paul, Cohesion and detachment in biofilm systems for different electron acceptor and donors. Water Sci. Technol., 2007. 55(8-9): 421-428.

416. Tsai, Y.-P., Impact of flow velocity on the dynamic behaviour of biofilm bacteria. Biofouling, 2005. 21(5-6): 267-277.

417. Hall-Stoodley, L. and P. Stoodley, Developmental regulation of microbial biofilms. Curr. Opin. Biotech., 2002. 13(3): 228-233.

418. Liu, Y. and J.-H. Tay, Detachment forces and their influence on the structure and metabolic behaviour of biofilms. World J. Microbiol. Biotechnol., 2001. 17(2): 111-117.

419. Simões, M., M.O. Pereira and M.J. Vieira, The role of hydrodynamic stress on the phenotypic characteristics of single and binary biofilms of *Pseudomonas fluorescens.* Water Sci. Technol., 2007. 55(8-9): 437-45.

420. Ryu, J.H. and L.R. Beuchat, Biofilm formation and sporulation by *Bacillus cereus* on a stainless steel surface and subsequent resistance of vegetative cells and spores to chlorine, chlorine dioxide, and a peroxyacetic acid-based sanitizer. J. Food Protect., 2005. 68(12): 2614-2622.

421. Lazarova, V., V. Pierzo, D. Fontvielle, and J. Manem, Integrated approach for biofilm characterisation and biomass activity control. Water Sci. Technol., 1994. 29(7): 345-354.

422. Liu, Y. and J.-H. Tay, The essential role of hydrodynamic shear force in the formation of biofilm and granular sludge. Water Res., 2002. 36(7): 1653-1665.

423. Tay, J.H., Q.S. Liu and Y. Liu, The effects of shear force on the formation, structure and metabolism of aerobic granules. Appl. Microbiol. Biotechnol., 2001. 57(1-2): 227-33.

424. Amalaradjou, M. and K. Venkitanarayanan, Antibiofilm Effect of Octenidine Hydrochloride on *Staphylococcus aureus*, MRSA and VRSA. Pathogens, 2014. 3(2): 404-416.

425. Trueba, A., F.M. Otero, J.A. González, L.M. Vega, and S. García, Study of the activity of quaternary ammonium compounds in the mitigation of biofouling in heat exchangers–condensers cooled by seawater. Biofouling, 2013. 29(9): 1139-1151.

426. Körstgens, V., H.C. Flemming, J. Wingender, and W. Borchard, Uniaxial compression measurement device for investigation of the mechanical stability of biofilms. J. Microbiol. Methods, 2001. 46(1): 9-17.

427. Chisti, Y. and M. Moo-Young, Clean-in-place systems for industrial bioreactors: Design, validation and operation. J. Ind. Microbiol., 1994. 13(4): 201-207.

428. Rodríguez, A. and L.A. McLandsborough, Evaluation of the transfer of *Listeria monocytogenes* from stainless steel and high-density polyethylene to Bologna and American cheese. J. Food Protect., 2007. 70(3): 600-606.

429. Salles, C., Polyethylene for water. Mater. World, 2009. 17(1): 38-39.

430. Mathieu, L., I. Bertrand, Y. Abe, E. Angel, J.C. Block, S. Skali-Lami, and G. Francius, Drinking water biofilm cohesiveness changes under chlorination or hydrodynamic stress. Water Res., 2014. 55(0): 175-184.

431. Dasari, A., J. Rohrmann and R.D.K. Misra, Micro- and nanoscale evaluation of scratch damage in poly(propylene)s. Macromol. Mater. Eng., 2002. 287(12): 889-903.

432. Ebewele, R.O., Polymer Science and Technology. 2000: CRC Press.

433. Denyer, S.P. and J.Y. Maillard, Cellular impermeability and uptake of biocides and antibiotics in Gram-negative bacteria. J. Appl. Microbiol., 2002. 92 Suppl: 35S-45S.

434. Busscher, H.J. and H.C. van Der Mei, Microbial adhesion in flow displacement systems. Clin. Microbiol. Rev., 2006. 19(1): 127-141.

435. Stewart, P.S., Theoretical aspects of antibiotic diffusion into microbial biofilms. Antimicrob. Agents Ch., 1996. 40(11): 2517-2522.

436. Hornemann, J.A., A.A. Lysova, S.L. Codd, J.D. Seymour, S.C. Busse, P.S. Stewart, and J.R. Brown, Biopolymer and water dynamics in microbial biofilm extracellular polymeric substance. Biomacromolecules, 2008. 9(9): 2322-2328.

437. Simões, L.C., M. Simões and M.J. Vieira. 2008. A comparative study of drinking water biofilm monitoring with flow cell and Propella™ bioreactors. In: Proceedings of the 10th International Chemical and Biological Engineering Conference - CHEMPOR 2008 Braga, Portugal. E.C. Ferreira and M. Mota. 334-342

438. Valappil, S.P., M. Coombes, L. Wright, G.J. Owens, R.J.M. Lynch, C.K. Hope, and S.M. Higham, Role of gallium and silver from phosphate-based glasses on in vitro dual species oral biofilm models of *Porphyromonas gingivalis* and *Streptococcus gordonii.* Acta Biomater., 2012. 8(5): 1957-1965.

439. Pelleïeux, S., I. Bertrand, S. Skali-Lami, L. Mathieu, G. Francius, and C. Gantzer, Accumulation of MS2, GA, and Qβ phages on high density polyethylene (HDPE) and drinking water biofilms under flow/non-flow conditions. Water Res., 2012: 1-11.

440. Chew, J.Y.M., S.S.S. Cardoso, W.R. Paterson, and D.I. Wilson, CFD studies of dynamic gauging. Chem. Eng. Sci., 2004. 59(16): 3381-3398.

441. Augustin, W., Y.M.J. Chew, P.W. Gordon, V.Y. Lister, M. Mayer, W.R. Paterson, J.M. Peralta, S. Scholl, and D.I. Wilson, Dynamic gauging of soft fouling layers on solid and porous surfaces. Chem. Ing. Tech., 2012. 84(1-2): 46-53.

442. Salley, B., P.W. Gordon, A.J. McCormick, A.C. Fisher, and D.I. Wilson, Characterising the structure of photosynthetic biofilms using fluid dynamic gauging. Biofouling, 2012. 28(2): 159-173.

443. Peck, O.P.W., Y.M. John Chew, M.R. Bird, and A. Bolhuis, Application of fluid dynamic gauging in the characterization and removal of biofouling deposits. Heat Transfer Eng, 2015. 36(7-8): 685-694.

444. Yang, Q., A. Ali, L. Shi, and D.I. Wilson, Zero discharge fluid dynamic gauging for studying the thickness of soft solid layers. J. Food Eng., 2014. 127(0): 24-33.

445. Gu, T., Y.M.J. Chew, W.R. Paterson, and D.I. Wilson, Experimental and CFD Studies of Fluid Dynamic Gauging in Annular Flows. AlChE J., 2009. 55(8): 1937-1947.

446. Ali, A., G.J. Chapman, Y.M.J. Chew, T. Gu, W.R. Paterson, and D.I. Wilson, A fluid dynamic gauging device for measuring fouling deposit thickness in opaque liquids at elevated temperature and pressure. Exp. Therm Fluid Sci., 2013. 48(0): 19-28.

447. Chew, J.Y.M., W.R. Paterson and D.I. Wilson, Fluid dynamic gauging for measuring the strength of soft deposits. J. Food Eng., 2004. 65(2): 175-187.

448. Middleman, S., An Introduction to Fluid Dynamics: Principles of Analysis and Design. 1998, New York, USA: Academic Press.

449. Xi, C., D. Marks, S. Schlachter, W. Luo, and S.A. Boppart, High-resolution three-dimensional imaging of biofilm development using optical coherence tomography. J Biomed Opt, 2006. 11(3): 34001.

450. Wagner, M., D. Taherzadeh, C. Haisch, and H. Horn, Investigation of the mesoscale structure and volumetric features of biofilms using optical coherence tomography. Biotechnol. Bioeng., 2010. 107(5): 844-53.

451. Dreszer, C., A.D. Wexler, S. Drusová, T. Overdijk, A. Zwijnenburg, H.C. Flemming, J.C. Kruithof, and J.S. Vrouwenvelder, In-situ biofilm characterization in membrane systems using Optical Coherence Tomography: Formation, structure, detachment and impact of flux change. Water Res., 2014. 67: 243-254.

452. Li, C., S. Felz, M. Wagner, S. Lackner, and H. Horn, Investigating biofilm structure developing on carriers from lab-scale moving bed biofilm reactors based on light microscopy and optical coherence tomography. Bioresour. Technol., 2016. 200: 128-136.

Appendix

Appendix

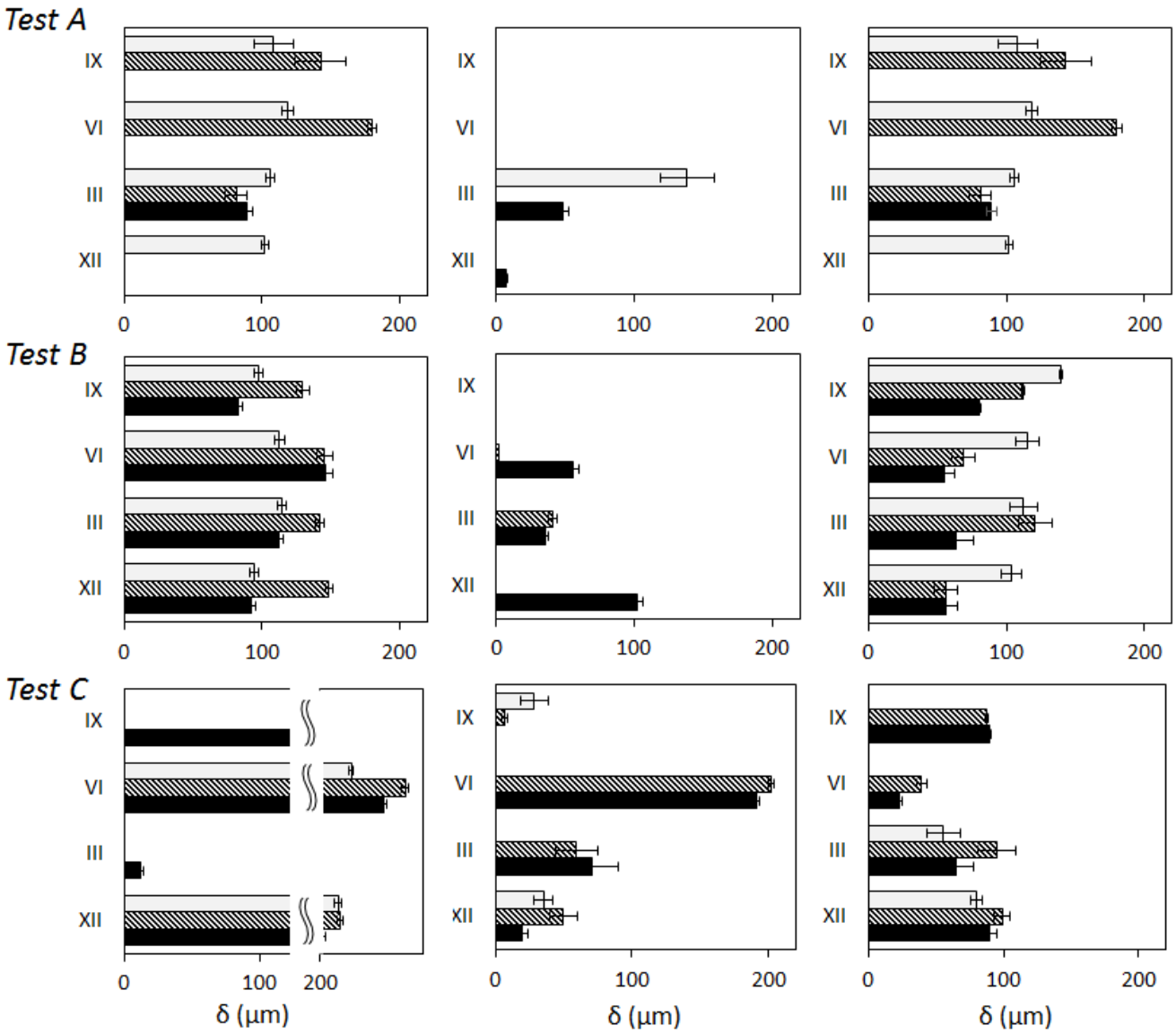

Fig. A 1– Biofilm thickness measurements for the three HDPE cylinders after three independent tests (labelled A, B and C).
Measurements performed at 4 different azimuthal positions (indicated in Roman numerals, corresponding to clock positions, see middle plot) and 3 different heights (open bar - highest position, crossed bar - intermediate position, solid bar - lowest position). Error bars indicate the measurement uncertainty calculated for that location.

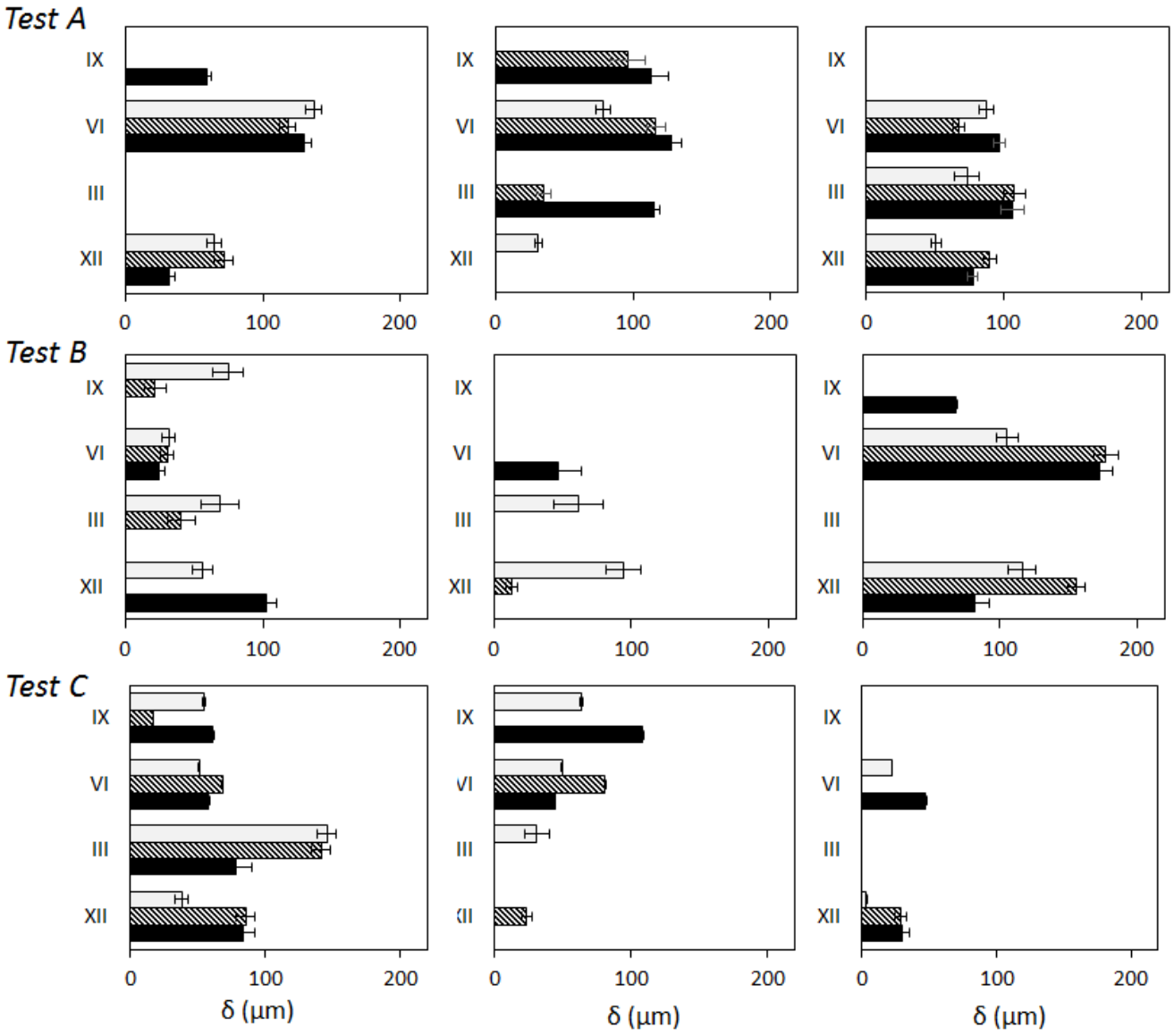

Fig. A 2 – Biofilm thickness measurements for the three SS cylinders after three independent tests (labelled A, B and C).
Measurements performed at 4 different azimuthal positions (indicated in Roman numerals, corresponding to clock positions, see middle plot) and 3 different heights (open bar - highest position, crossed bar - intermediate position, solid bar - lowest position). Error bars indicate the measurement uncertainty calculated for that location.